Redesigning phospho*enol*pyruvate carboxylase for improved catalysis in C_4 photosynthesis

Rowarne Leith

July 2022

A thesis submitted for the degree of Doctor of Philosophy of

The Australian National University

Australian
National
University

Declaration

The research presented in this thesis is my own work unless otherwise stated. This work was carried out at The Australian National University, Research School of Biology. The material presented in this thesis has not been submitted for any other degree.

Rowarne Leith

July 2022

Abstract

C_4 photosynthesis, a carbon concentrating mechanism, evolved as an adaptation to improve photosynthetic CO_2 assimilation in terrestrial plants under conditions of low CO_2, increased temperatures and varying rainfall patterns. Understanding the C_4 photosynthetic cycle could prove invaluable when trying to engineer C_3 crop species with better photosynthetic rates or to improve the photosynthetic rates of C_4 crop species. Phospho*enol*pyruvate carboxylase (PEPC), the primary carboxylase of the C_4 photosynthetic cycle, operates without any oxygenase activity, and at catalytic rates 3-8 times that of Rubisco. PEPC is responsible for catalysing the irreversible β-carboxylation of PEP by HCO_3^- to form oxaloacetate (OAA), which is then converted to a either malate or aspartate, depending on the C_4 photosynthetic subtype to which the plant belongs. Regardless of C_4 subtype, these organic acids contribute to the cytosolic mesophyll environment, where PEPC is located, and are important in driving the carbon flux to the bundle sheath cells (BSC). In this thesis numerous properties of the C_4 PEPC enzyme have been examined and this research has provided valuable insights into avenues for redesigning PEPC for improved catalysis in C_4 photosynthesis.

Firstly, a method of PEPC expression and purification using *Escherichia coli* as an expression system was established and optimised. Establishing and optimising this method showed that PEPC purified from *E. coli* purifies as a dimer and raised questions about whether the tetrameric form of the PEPC enzyme is more prone to dissociation than often presented in the literature.

A C_4 subtype-specific sequence that confers differences in PEPC kinetic properties was identified. This sequence, although not directly involved in allosteric regulator binding, has been shown to affect inhibition of PEPC activity by malate. Purification of C_4 PEPCs and chimera PEPCs expressed in *E. coli*, have allowed for a direct comparison between the kinetic

properties of different PEPC enzymes and the effect of this C_4 subtype-specific sequence. As well as insights into the function of this subtype-specific region, this work also has shown that the *Urochloa panicoides* PEPC enzyme has superior catalytic properties, with V_{max} and k_{cat} values far greater than any of those reported in the literature for PEPC enzymes from C_3 or C_4 plants. This thesis has also shown that oxaloacetate might be a more important C_4 PEPC inhibitor, and aspartate a less important inhibitor, than reported in the literature.

Lastly, an attempt was made to overexpress PEPC in the model plant C_4 grass, *Setaria viridis* and to investigate the effects of expressing a malate-insensitive PEPC enzyme in *S. viridis*. Although the PEPC overexpression experiments were ultimately unsuccessful due to range of unforeseen factors, including cross reactivity of the AcV5 antibody in the MEO34V *S. viridis* ecotype and the large variability in wild-type PEPC activity, this research has provided valuable information on how to redesign this experiment for future PEPC overexpression studies. The attempts to investigate the expressing a malate-insensitive PEPC enzyme in *Setaria viridis* were also unsuccessful for the same reasons. Given the recent success of the CRISPR/Cas9 technology in many plant species, however, revisiting this experiment using the CRISPR/Cas9 technology will allow for a more sophisticated approach.

The overall results of this thesis have shown that there is still more to learn about the regulatory properties of the C_4 PEPC enzyme. This thesis has also highlighted that there are C_4 PEPC enzymes with superior catalytic properties available for transformation into plants. Therefore, increasing photosynthesis through PEPC modification is a prime opportunity and will allow plants to function more efficiently in an increasingly hot, dry climate.

Contents

Acknowledgements

Firstly, I would like to thank my supervisory panel, Susanne von Caemmerer, Robert Sharwood and Maria Ermakova, for their advice, support and patience throughout my PhD. I would especially like to thank Rob for his advice on experiments, his mentorship, and all the time he invested in me and this PhD project. Rob is an amazing researcher and so generous with his knowledge and his time.

I would also like to thank Asaph Cousins and Robert Di Mario for teaching me the MIMS PEPC assay and for collaborating to test my recombinant PEPC protein. Thanks to Simon Williams and Megan Outram for their protein purification advice, for lending me equipment, and for teaching me how to do gel filtration.

I would like to thank Brendon Conlan for the pHUE vector, Hugo Alonso for teaching me how to conduct the C_4 enzyme assays, Masha for teaching me how to do Golden Gate cloning, Loraine Rourke for her advice on restriction enzymes and for letting me use her lab's incubators so many times. I would also like to thank Ben Long and Soumi Bala for all the advice that they gave me on experiments, and Alex Watson-Lazowski for providing PEPC sequences for my experiments. Thanks to everyone in the von Caemmerer and Furbank labs for their help and advice.

I would especially like to thank Anna Flis and Tory Clarke for their friendship. I really valued all of the conversations we had about experiments and just life in general. I am so grateful that we met during my PhD and that we will be friends for many years to come.

A special thanks to Andras Keszei for his advice and the wisdom he shared. I would not have made it to the end of my PhD without the time that you spent calmly advising me. I can’t ever thank you enough.

Finally, I would like to thank my brother, Reuben, and my mum, Jo, for their support throughout my PhD

List of Figures

List of Tables

Abbreviations and Symbols

°C	degrees Celsius
ΔA_{340}	change in absorbance at 340 nm
%	percent
% (v/v)	volume/volume percentage solution
% (w/v)	weight/volume percentage solution; 1% (w/v) = 1 g solute per 100 mL solvent
Γ*	CO_2 compensation point
A	CO_2 assimilation rate
Å	angstrom
α	the efficiency of conversion of captured light into biomass (alpha)
Acetyl-CoA	acetyl coenzyme A
ACi	CO_2 assimilation rate (μmol m^{-2} s^{-1}) vs intercellular CO_2 (μbar)
AlaAT	alanine aminotransferase
ANOVA	analysis of variance
Bicine	*N*,*N*-Bis(2-hydroxyethyl)glycine
bp	base pair
BSA	bovine serum albumin
BSC	bundle sheath cell
CA	carbonic anhydrase
$CaCl_2$	calcium chloride
CAM	crassulacean acid metabolism
CCM	CO_2 concentrating mechanism
Chl	chlorophyll
C_i	CO_2 partial pressure in the intercellular airspace
CIM	callus induction media
cm	centimetre
CO_2	carbon dioxide
CRISPR	clustered regularly interspaced palindromic repeats
DOF	DNA binding with one finger
Da	Dalton
ddH_2O	double deionised water
DNA	deoxyribonucleic acid
DNase	deoxyribonuclease
DTT	dithiothreitol
EDTA	ethylenediamine tetraacetic acid
EPPS	4-(2-hydroxyethyl)-1-piperazinepropanesulfonic acid
ε	the efficiency of conversion of captured light into biomass (epsilon)
FR1	fraction 1
FR2	fraction 2
FR3	fraction 3
FR4	fraction 4
g	gravity
g	grams
G1P	glucose-1-phosphate
G6P	glucose-6-phosphate
Glu	glutamate
Gln	glutamine

h	hour
H^+	hydrogen ion
H_2O	water
H3K4me3	histone H3 lysine 4 tri-methylation
H3K9ac	histone H3 lysine 9 acetylation
H4K5ac	histone H4 lysine 9 acetylation
HCl	hydrochloric acid
HCO_3^-	bicarbonate
HEPES	4-(2-hydroxyethyl)-1-piperazineethanesulfonic acid
HI	harvest index
His	histidine
HRP	horse radish peroxidase
HSD	honestly significant difference
I_{50}; $I_{0.5}$; IC_{50}	inhibitory constant 50%, the required concentration of the inhibitor required to reduced enzyme activity to 50% of uninhibited activity
IMAC	immobilised metal affinity chromatography
IPTG	isopropyl β-D-1-thiogalactopyranoside
I-TASSER	iterative threading assembly refinement
k_{cat}	catalytic turnover rate
k_{cat}^c	carboxylation catalytic turnover rate or Rubisco
kDa	kilodaltons
kg	kilogram
K_i	inhibition constant
K_m	Michaelis-Menten constant, the substrate concentration required for the enzyme to reach a half-maximal rate
$K_mHCO_3^-$	Michaelis-Menten constant for bicarbonate
K_mMg^{2+}	Michaelis-Menten constant for the magnesium ion
K_mPEP	Michaelis-Menten constant for phospho*enol*pyruvate
KOH	potassium hydroxide
L	litres
LB	Luria Bertani
m	metre
M	molar
Mb	megabase
MC	mesophyll cell
MDH	malate dehydrogenase
MEM1	mesophyll expression module 1
MES	2-(N-morpholino)ethanesulfonic acid
mg	milligram
MIMS	membrane inlet mass spectrometry
Mg^{2+}	magnesium ion
$MgCl_2$	magnesium chloride
min	minute
mL	millilitre
mm	millimetre
mM	millimolar
Mn^{2+}	manganese ion
$MnCl_2$	manganese chloride
MOPS	3-(N-morpholino)propanesulfonic acid
MPa	megapascal

MS	Murashige and Skoog
N_2	nitrogen
NaCl	sodium chloride
NAD^+	nicotinamide adenine dinucleotide
NADH	nicotinamide adenine dinucleotide + hydrogen
NAD-ME	NAD-malic enzyme
NADP-ME	NADP-malic enzyme
NaOH	sodium hydroxide
ng	nanograms
NH_3	ammonia
NH_4^+	ammonium ion
Ni^{2+}	nickel ion
Ni-NTA	nickel-nitriloacetic acid
NUE	nitrogen use efficiency
O_2	oxygen
OAA	oxaloacetate
OD	optical density
OD_{600}	optical density measured at a wavelength of 600 nm
PAGE	polyacrylamide gel electrophoresis
PAR	photosynthetically active radiation
PCR	polymerase chain reaction
PEP	phosphoenolpyruvate
PEPC	phosphoenolpyruvate carboxylase
PEPCK	phosphoenolpyruvate carboxykinase
2-PG	2-phosphoglycolate
3-PGA	3-phosphoglycerate
pHUE	histidine-tagged ubiquitin expression plasmid
Pi	inorganic phosphate
PMSF	phenylmethylsulfonyl fluoride
PPDK	pyruvate phosphate dikinase
PRM	plant regeneration media
psi	pounds per square inch
PVPP	polyvinylpolypyrrolidone
RbCl	rubidium chloride
RNA	ribonucleic acid
RNAi	RNA interference
rpm	revolutions per minute
Rubisco	ribulose 1,5-bisphosphate carboxylase/oxygenase
RuBP	ribulose 1,5-bisphospate
s	second
$S_{C/O}$	specificity of Rubisco for CO_2 relative to O_2
SDS	sodium dodecyl sulphate
TAE	tris(hydroxymethyl)aminomethane- acetate-ethylenediamine tetraacetic acid
TBS	tris-buffered saline
TBST	tris-buffered saline + TWEEN 20
TCA	tricarboxylic acid
Tris	tris(hydroxymethyl)aminomethane
U	amount of enzyme that catalyses the conversion of 1 μmol of substrate to product per minute

µg	microgram
µl	microlitre
µM	micromolar
µmol	micromole
USP	Ubiquitin-specific protease
Usp2	mouse deubiquitylating protein
UTR	untranslated region
V	volts
V_{cmax}	the maximum rate of Rubisco carboxylase activity
V_{max}	maximal enzyme velocity
V_{pmax}	the maximum rate of PEPC carboxylase activity
WUE	water use efficiency

Chapter 1: General Introduction

1.1 The need for increased food production

With an estimated global population of 9.7 billion in 2050, it is expected that a 70 – 110% increase in global food production will be required by 2050 to maintain global food security (Long et al., 2006; Tilman et al., 2011; Ray et al., 2013; United Nations, 2019). Current projections for key crop yield in the years leading up to 2050, however, fall far short of required production (Figure 1.1; Ray et al., 2013). Yield increases in key crop plants are insufficient to keep up with our increasing global population and increasing global food demand, especially when it is considered that the current gains in yield of the major crop plants has plateaued (Zhu et al., 2010; Ziska et al., 2012; Long et al., 2015).

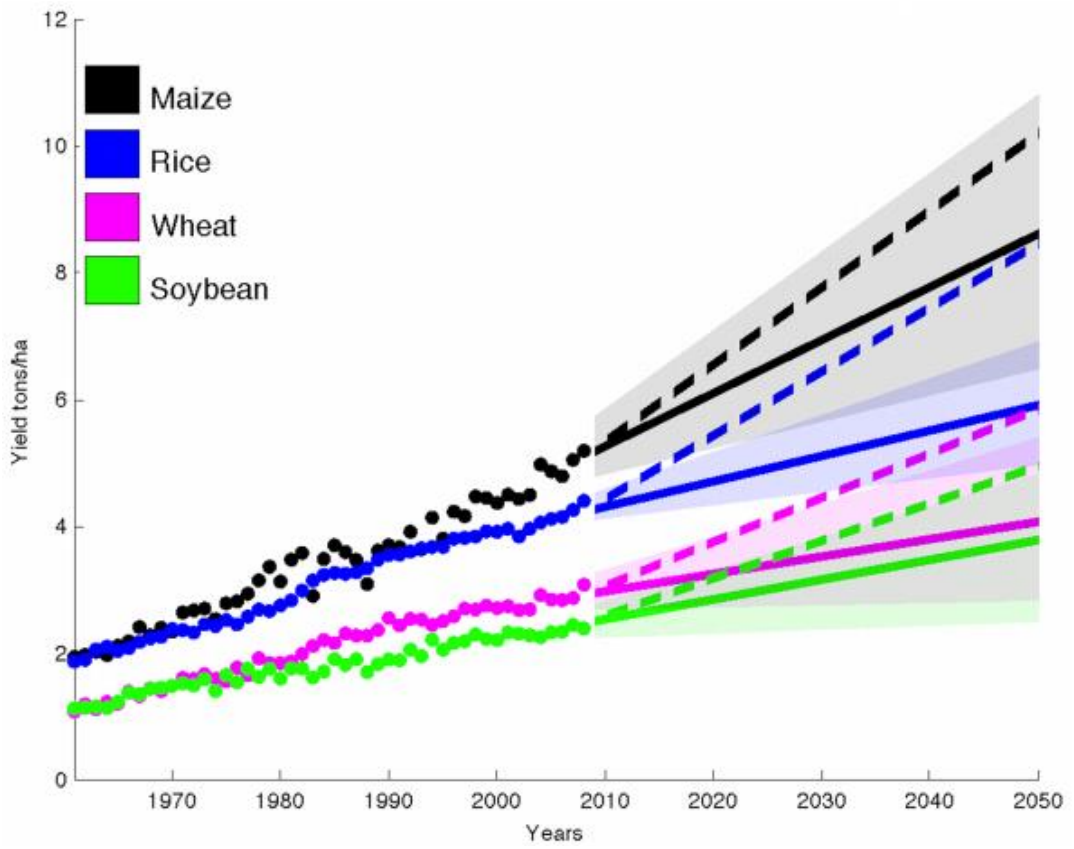

Figure 1.1. Observed global yields, global yield projections and required global yield for four crops. Observed global yield tons/hectare from 1961 – 2008 are shown as circles for maize (black), rice (blue), wheat (pink), and soybean (green). Solid lines show global yield projections from 2010 – 2050 and corresponding dashed lines show global yield required to achieve a doubling in yield without any additional land being recruited for cultivation (Image from Ray et al., 2013).

The yield potential of crops can be defined as:

Yield potential = PAR x α x ε x HI,

determined by the product of parameters of available photosynthetically active radiation available to the crop (PAR), the efficiency of light interception (α), the efficiency of conversion of captured light into biomass (ε), and the proportion of total biomass partitioned into grain (HI) (Long et al., 2006; Long, 2014). The Green Revolution focussed on measures to improve harvest index (HI), and through selective breeding successfully brought HI close to its theoretical biological limits with little possibility for further increases (Zhu et al., 2010; Long, 2014). The huge success realised by Green Revolution, through the implementation of selective breeding and increased fertilisation, saw more than doubling of global crop yields (South et al., 2018; Furbank et al., 2020). As HI nears its theoretical maximum, however, the exhaustion of traditional breeding programs trying to exploit natural variations in HI has become apparent (Long, 2014; Sharwood, 2017; Sharwood et al., 2022). The efficiency of conversion of intercepted light to biomass (ε) is a promising avenue for improving yields of crop plants as it is currently only at one-third of the calculated theoretical maximum (Zhu et al., 2010; Conaty and Constable, 2020). As ε is primarily determined by photosynthetic capacity minus losses from respiration, increasing photosynthetic efficiency should be one of the main focusses of the attempt to increase plant yield (Long et al., 2006; Long et al., 2015; South et al., 2018; Conaty and Constable, 2020).

Increasing nitrogen fertilisation has been shown to increase yield by increasing ε, which contributed to the success of the Green Revolution (Zhu et al., 2010; South et al., 2018). Unfortunately, the application of nitrogen and other chemicals has long reached a maximum. Improvements in nitrogen-use efficiency (NUE) of crop plants would allow more sustainable production, and investigating methods to improve water-use efficiency (WUE) of crops would be beneficial as water availability becomes limiting (Carmo-Silva et al., 2015; Sharwood, 2017). It has been demonstrated, however, that improving photosynthetic efficiency without increasing other factors will still lead to an increase in yield (Long et al., 2006). Ideally, a

combination of improvements in NUE, WUE and photosynthetic efficiency would increase crop production with a more sustainable use of limited resources.

Loss of agricultural land due to urbanisation, soil degradation, and unsustainable irrigation, means that increases in yield must be achieved with reductions in arable land and water availability (Foley et al., 2011; Ziska et al., 2012). Even if we weren't currently at peak agricultural land space, land clearing to achieve such an output would have huge environmental costs in terms of greenhouse gas emissions (Tilman et al., 2011; Sharwood et al., 2022). Agricultural expansion and intensification have had incredible environmental impacts on habitat, biodiversity, pollution, soil conditions and water degradation and disruptions of phosphorus and nitrogen cycles. (Foley et al., 2011; Tilman et al., 2011). It is also a major contributor to climate change, with between 25 – 35% of global greenhouse gas emissions able to be attributed to agricultural activities (Foley et al., 2011; Tilman et al., 2011). Climate change will provide significant challenges for and have huge impacts on crop plant productivity (Carmo-Silva et al., 2015). Increasing atmospheric CO_2 concentrations and the resulting increase in global average ambient air temperatures, will cause more extreme weather and climate events such as heat waves, drought, increases in the frequency of heavy rainfalls and unpredictable rainfall patterns (IPCC, 2012; Sharwood, 2017; IPCC, 2021; BOM and CSIRO, 2022). Average ambient temperatures are modelled to substantially increase by 2 – 5 °C by the late 21st century, with Australia's climate having warmed by 1.47 °C since 1910 and global temperatures gave risen by over 1 °C since 1850 (BOM and CSIRO, 2022). Given these increasing impacts of climate change, a challenge is to increase agricultural output while decreasing the environmental footprint of agricultural activities (Foley et al., 2011).

Therefore, increasing plant yield through improvements to photosynthetic efficiency is one of the few viable methods available to meet the challenge of ensuring food security without the large environmental costs associated with land clearing and increased fertiliser use. Improving photosynthetic efficiency has already shown promising results, with studies by Kromdijk et al.

(2016) and De Souza et al. (2022) reporting 15 % and 33 % increases in plant biomass, respectively, by accelerating responses to changes in light.

1.2 C_4 crop plant productivity

C_4 photosynthetic species make up only 3 % of terrestrial plant species, despite this they are responsible for almost a quarter of global primary productivity (Lloyd and Farquhar, 1994; Sage et al., 1999). The improved water use efficiency (WUE) and nitrogen use efficiency (NUE) of C_4 plants compared to their C_3 counterparts, as well as higher CO_2 assimilation rates above 25 °C, means that in an increasingly hot, dry climate C_4 crop species may become increasingly important in meeting global food demands (Sage and Pearcy, 1987, 1987; Hatch, 1992; Long, 1999; Ghannoum et al., 2011; IPCC, 2012, 2021). Compared with the most productive C_3 species, the most productive C_4 species have yields 40 – 50 % greater (Sage, 2016). C_4 species also have a theoretical maximum of efficiency of conversion of captured light (ε) of 6 % of full spectrum solar radiation or 12.3 % for PAR compared to 4.6 % and 9.4 % for C_3 species (Zhu et al., 2010).

According to crops statistics from the Food and Agriculture Organization of the United Nations (FAO), worldwide four important C_4 grass crops, maize, sorghum, millet and sugar cane account for 12.40 % of total global agricultural production and 4.20 % of total Australian production (Table 1.1, Table 1.2). Five C_3 grass crops important to Australian agriculture, barley, oats, rye, triticale and wheat make up 3.88 % of total global agricultural production and 4.27 % of total Australian production (Table 1.1, Table 1.2; Food and Agriculture Organization of the United Nations (FAO), 2020).

In Australia, the area dedicated to farming these C_3 grass crops (1.80×10^7 hectares) is much greater than the collective area dedicated to farming the C_4 grass crops (1.10×10^6 hectares), for similar production values of 3.41×10^7 tonnes and 3.35×10^7 tonnes for C_3 and C_4 crops, respectively (Table 1.2; Food and Agriculture Organization of the United Nations (FAO), 2020). This raises the question whether Australian farmland could be better utilised farming C_4

grass crops. This appears to be the case when comparing yield between C_3 and C_4 grass species, as all C_4 species bar millet had a greater yield than all of the C_3 grasses (Table 1.2, Figure 1.2; Food and Agriculture Organization of the United Nations (FAO), 2020). This demonstrates, therefore, the potential in Australia for C_4 crops to produce high output for given space of land. Improving C_4 photosynthetic efficiency would further increase plant yield, responsibly utilising the diminishing available agricultural land.

Table 1.1 Yield (tonnes/ha), production (tonnes) and area harvested (ha) for four major C_4 grass crops (maize and maize (green), sorghum, millet and sugar cane) and five major C_3 grass crops (barley, oats, rye, triticale and wheat), in a global context. Data shown are averages from the period between 2008 and 2018 inclusive. The percentages of each individual crop, as well as the sum of groups of the C_3 and C_4 crops, compared to total global crop area harvested, and production are shown. The yield of each crop is compared to the global average yield of all crops across the period between 2008-2018 of 4265.41 tonnes/ha. Table was constructed using crops data sets from the Food and Agriculture Organization of the United Nations (Food and Agriculture Organization of the United Nations (FAO), 2020).

	World (averages from 2008 -2018)					
	Area harvested	% of total global area harvested	Yield	% of global yield of all crops	Production	% of total global production
	hectare		tonne/ha		tonnes	
Maize	1.81×10^{8}	8.08×10^{-1}	6.61	1.27×10^{-1}	9.83×10^{8}	4.21
Maize, green	1.14×10^{6}	5.11×10^{-3}	1.20×10^{1}	2.28×10^{-1}	1.11×10^{7}	4.75×10^{-2}
Millet	3.28×10^{7}	1.47×10^{-1}	1.01	2.06×10^{-2}	2.88×10^{7}	1.23×10^{-1}
Sorghum	4.27×10^{7}	1.91×10^{-1}	3.16	3.36×10^{-2}	6.13×10^{7}	2.63×10^{-1}
Sugar cane	2.57×10^{7}	1.15×10^{-1}	8.07×10^{1}	1.66	1.82×10^{9}	7.79
All above C_4	2.83×10^{8}	1.27	2.07×10^{1}	4.14×10^{-1}	2.90×10^{9}	12.40
Barley	4.99×10^{7}	2.23×10^{-1}	2.09	6.69×10^{-2}	1.42×10^{8}	6.10×10^{-1}
Oats	9.90×10^{6}	4.43×10^{-2}	1.54	5.51×10^{-2}	2.32×10^{7}	9.96×10^{-2}
Rye	5.23×10^{6}	2.34×10^{-2}	6.55×10^{-1}	6.53×10^{-2}	1.45×10^{7}	6.23×10^{-2}
Triticale	2.20×10^{8}	9.82×10^{-1}	1.67	8.62×10^{-2}	1.48×10^{7}	6.35×10^{-2}
Wheat	2.20×10^{8}	9.82×10^{-1}	1.87	7.59×10^{-2}	7.10×10^{8}	3.04
All above C_3	5.04×10^{8}	2.26	1.56	6.99×10^{-2}	9.05×10^{8}	3.88

Table 1.2 Yield (tonnes/ha), production (tonnes) and area harvested (ha) in Australia for four major C_4 grass crops (maize and maize (green), sorghum, millet and sugar cane) and five major C_3 grass crops (barley, oats, rye, triticale and wheat). Data shown are averages from the period between 2008 and 2018 inclusive. The percentages of each individual crop, as well as the sum of groups of the C_3 and C_4 crops, compared to total crop area harvested and production in Australia are also shown. The yield of each crop is compared to the Australian average yield of all crops across the period between 2008-2018 of 16.06 tonnes/ha. Table was constructed using crops data sets from the Food and Agriculture Organization of the United Nations (Food and Agriculture Organization of the United Nations (FAO), 2020).

	Australia (averages from 2008 -2018)					
	Area harvested	% of total Australian area harvested	Yield	% of average Australian yield of all crops	Production	% of total Australian production
	hectare		tonne/ha		tonnes	
Maize	6.25×10^4	3.03×10^{-2}	6.61	41.18	4.10×10^5	5.14×10^{-2}
Maize, green	6.55×10^3	3.18×10^{-3}	11.97	74.50	7.59×10^4	9.52×10^{-3}
Millet	3.58×10^4	1.74×10^{-2}	1.01	6.29	3.62×10^4	4.54×10^{-3}
Sorghum	6.15×10^5	2.98×10^{-1}	3.16	19.67	1.99×10^6	2.50×10^{-1}
Sugar cane	3.85×10^5	1.87×10^{-1}	80.69	502.42	3.10×10^7	3.89
All above C_4	1.10×10^6	5.36×10^{-1}	20.69	128.81	3.35×10^7	4.20
Barley	4.21×10^6	2.04	2.09	13.03	8.75×10^6	1.10
Oats	8.67×10^5	4.20×10^{-1}	1.54	9.56	1.33×10^6	1.66×10^{-1}
Rye	4.82×10^4	2.34×10^{-2}	0.66	4.08	3.13×10^4	3.93×10^{-3}
Triticale	1.60×10^5	7.74×10^{-2}	1.67	10.39	2.43×10^5	3.04×10^{-2}
Wheat	1.27×10^7	6.16	1.87	11.66	2.37×10^7	2.97
All above C_3	1.80×10^7	8.73	1.57	9.74	3.41×10^7	4.27

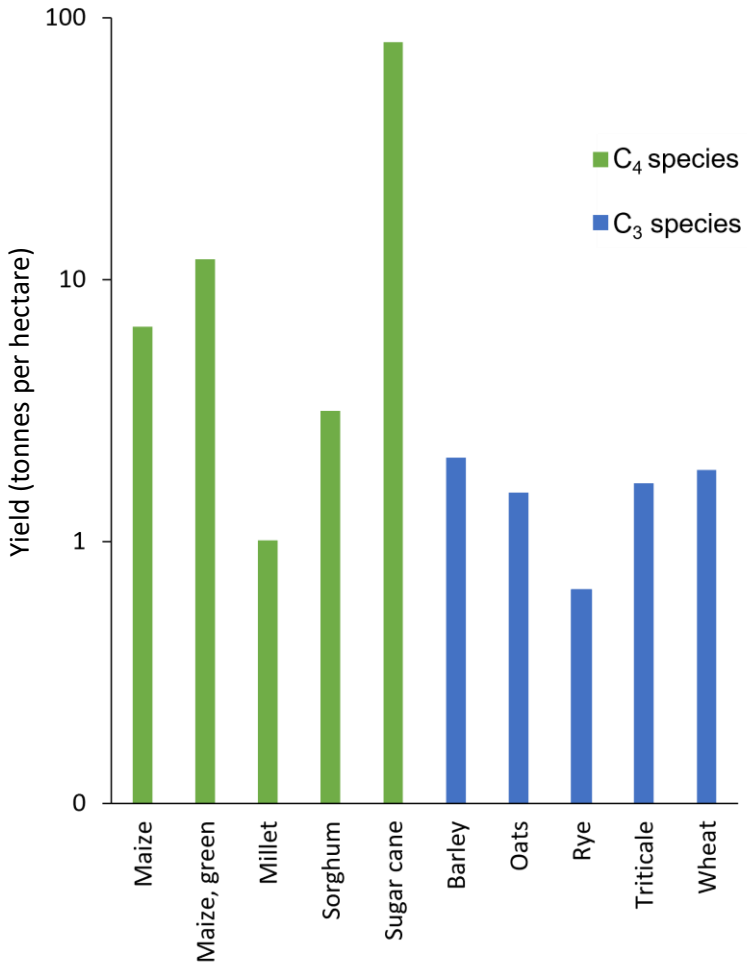

Figure 1.2. The yield (tonnes/hectare) of major C_3 and C_4 crops in Australia. Displayed are data for four major C_4 crops, maize, maize (green), millet, sorghum, and sugar cane and five major C_3 crops, barley, oats, rye, triticale and wheat. Figure was constructed using crops data sets from the Food and Agriculture Organization of the United Nations (Food and Agriculture Organization of the United Nations (FAO), 2020).

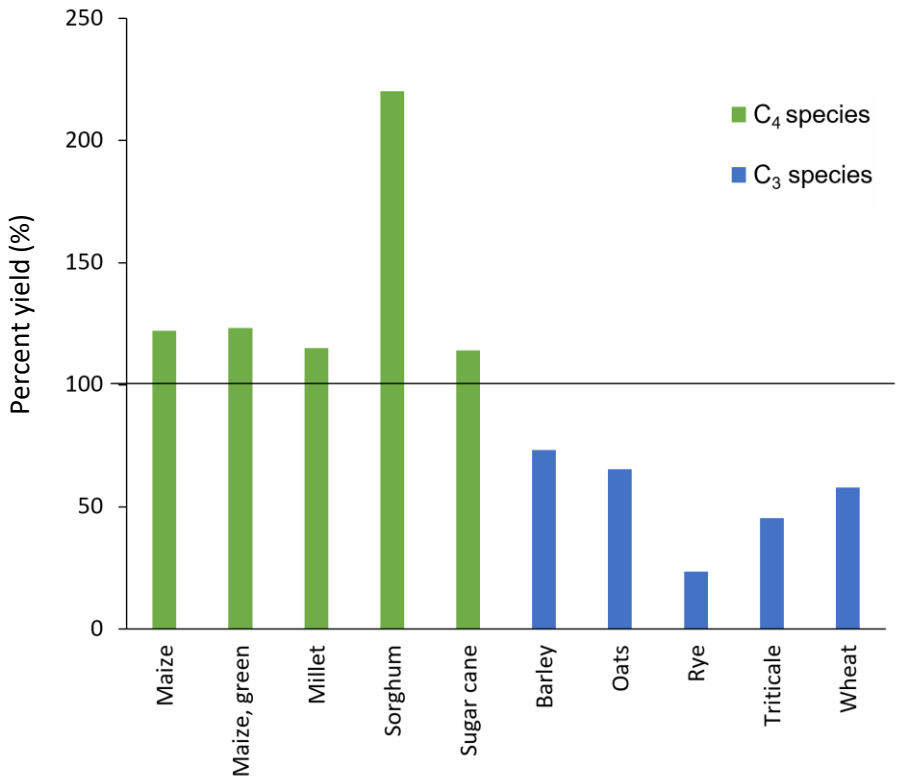

Figure 1.3. The percentage of yield (tonnes/hectare) of each crop in Australia compared to global figures for each of the categories. Displayed are data for four major C_4 crops, maize, maize (green), millet, sorghum, and sugar cane and five major C_3 crops, barley, oats, rye, triticale and wheat. Black line indicates where Australian yield would equal global yield. Figure was constructed using crops data sets from the Food and Agriculture Organization of the United Nations (Food and Agriculture Organization of the United Nations (FAO), 2020).

When comparing yield of these C_4 and C_3 crop grasses in Australia to global yield, in Australia all C_3 species underperform when compared to average yields for their respective species globally (Figure 1.3; Food and Agriculture Organization of the United Nations (FAO), 2020). The Australian yields for all C_4 species outperform the global yield average for their respective species (Figure 1.3; Food and Agriculture Organization of the United Nations (FAO), 2020). This highlights that Australian farmland is used more efficiently to farm C_4 rather than C_3 grass species and that to combat global food shortages, C_4 crops may become more important to the Australian economy. When looking at the average Australian domestic prices per tonne for the five grass crops maize (C_4), sorghum (C_4), wheat (C_3), barley (C_3) and oats (C_3) it is apparent that C_4 crops could become quite lucrative to the Australian economy. The C_4 crop maize has consistently sold for the average highest price per tonne, with only short periods of outperformance by other crops (Figure 1.4; ABARES, 2021). As of the end of the first quarter

(January – March) 2021, both the C_4 crops, sorghum and maize are selling for higher prices per tonne than any of the C_3 crops (Figure 1.4; ABARES, 2021).

Given that C_4 crops have improved water use efficiency (WUE) and nitrogen use efficiency (NUE) compared to C_3 plants, as well as higher CO_2 assimilation in hotter climates, C_4 crops are already more well suited to the unique challenges of a changing Australian climate than C_3 plants. Improving C_4 photosynthesis will improve the future of Australian agriculture, helping to increase the yield of grass crops that already outperform C_3 crops in the Australian climate.

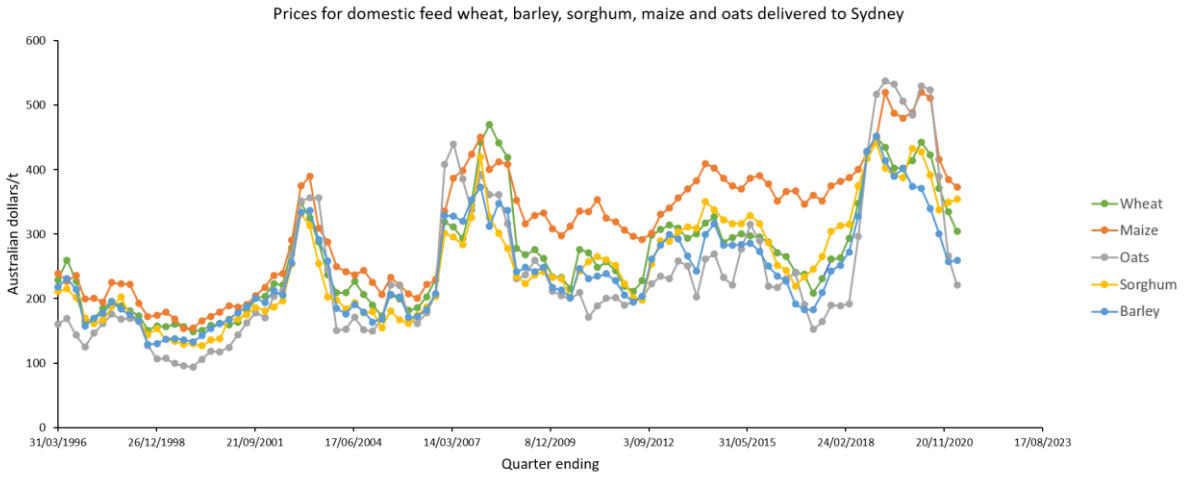

Figure 1.4. Average Australian domestic prices for the crops wheat (C_3), maize, barley (C_3), sorghum (C_4), maize (C_4) and oats (C_3) during the quarters 1 (January-March), 2 (April – June), 3 (July – September), and 4 (October – December). The dates listed on the horizontal axis indicate the final date of the quarter. Prices are shown from Q1 1996 to Q1 2021. Figure was constructed using a subset of data (Table 17 Grain, oilseed and pulse prices) in the Australian crop report: June 2021 No.198, published by the Australian Bureau of Agricultural and Resource Economics and Sciences (ABARES, 2021).

1.3 Photosynthesis

Plants provide the energy on which so much life on earth ultimately relies through the vital process of photosynthesis. Photosynthesis harnesses energy from sunlight and converts it into biochemical energy. There are three main mechanisms of photosynthesis, C_3, C_4 and crassulacean acid metabolism (CAM), however, CAM is beyond the scope of this study (Ehleringer et al., 1991). The C_3 photosynthetic pathway is the most ancestral form of photosynthesis, evolving early in the history of life, at a time where there was high CO_2 concentration in the atmosphere (Sage, 2004). The evolution of C_4 photosynthesis, between 24-35 million years ago, was driven by changing environmental factors, specifically low atmospheric CO_2 concentrations and increased temperatures (Jordan and Ogren, 1984; Ehleringer et al., 1991; Ehleringer et al., 1997; Sage, 2004; Christin et al., 2008; Edwards and Ogburn, 2012; Christin et al., 2013).

1.4 C_3 Photosynthesis and the Limitations of Rubisco

Ribulose 1,5-bisphosphate carboxylase/oxygenase (Rubisco) is the principal enzyme responsible for CO_2 fixation, and the sole enzyme capable of carbon assimilation that leads to carbohydrate production and biomass gain (von Caemmerer and Evans, 2010; Carmo-Silva et al., 2015). Its kinetic properties underpin C_3 photosynthesis, determining the efficiency of CO_2 assimilation, and the efficiency of the use of water, nutrients and light (Farquhar et al., 1980; Whitney et al., 2001). The reactions involved in C_3 photosynthetic mechanism take place in the mesophyll cells of the leaf, where Rubisco is located (Figure 1.5B). Rubisco catalyses the carboxylation of ribulose 1,5-bisphospate (RuBP) by CO_2, producing two molecules of 3-phosphoglycerate (3-PGA) (Figure 1.5A; Bassham and Calvin, 1957). This carboxylation is one of the many reactions in the photosynthetic carbon reduction cycle, which results

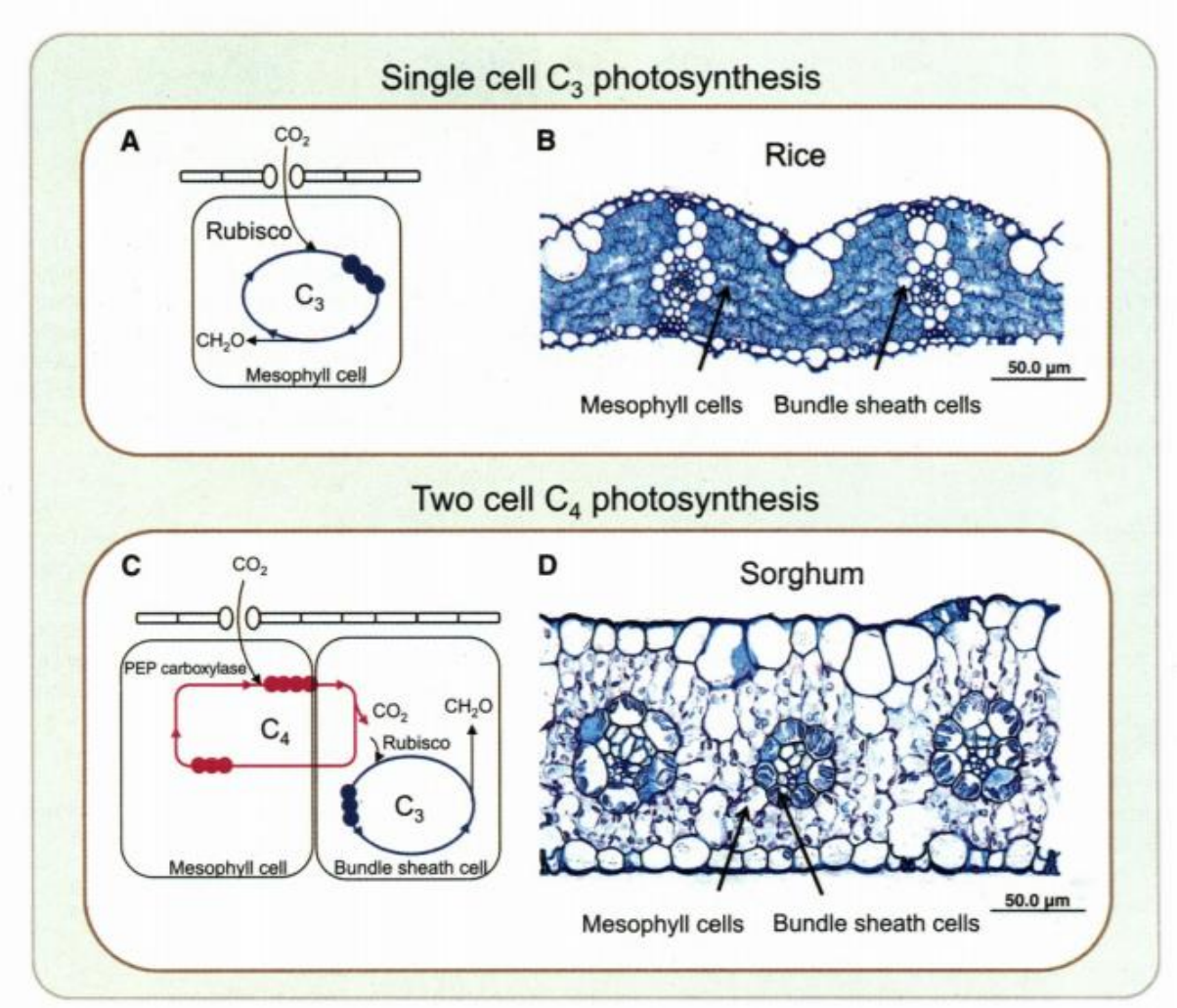

Figure 1.5. The anatomy and biochemistry of plants operating a C_3 and C_4 photosynthetic pathway. A) C_3 photosynthesis involves the fixation of CO_2 by Rubisco in the mesophyll cells to produce carbohydrates. B) Transverse light microscopy image of a rice leaf (C_3). C) C_4 photosynthesis involves two specialised cell types, the mesophyll and the bundle sheath, as well as differential expression of enzymes between the two cell types. The initial fixation of CO_2 by PEPC occurs in the mesophyll cells, creating a 4-carbon organic acid. This 4-carbon organic acid is used to shuttle CO_2 to the bundle sheath cell where Rubisco is located. D) Transverse light microscopy image of a sorghum leaf (C_4). Image from von Caemmerer et al. (2012)

in the assimilation of inorganic atmospheric carbon, producing organic carbon compounds (Bassham and Calvin, 1957; Parry et al., 2007). Photosynthetic inefficiencies stem from the bifunctional nature of the Rubisco enzyme, which has both carboxylase and oxygenase capabilities. Competition of O_2 at the active site of Rubisco can lead to the oxygenation of

RuBP, producing one molecule each of 3-PGA and 2-phosphoglycolate (2-PG) (Figure 1.6; Bowes et al., 1971). The 2-PG produced cannot be used in the PCR_1 cycle, nor can it be directly used in carbohydrate synthesis (Laing et al., 1974; Wingler et al., 2000). The toxic 2-PG must be recycled to 3-PGA via the photorespiratory pathway (Hall et al., 1987; Bauwe et al., 2010). This multi-step pathway requires the coordination of many cellular compartments and results in carbon loss in the form of CO_2, NH_3 release, and the consumption of energy (Tolbert, 1971; Farquhar et al., 1980; Keys, 1986). The carbon lost in the photorespiratory process accounts for between 26 – 30 % of fixed carbon in C_3 plants (Monteith and Moss, 1977; Sharkey, 1988). Excessive photorespiration can, therefore, cause a significant decrease in the photosynthetic efficiency and plant productivity (Zelitch, 1973; Ehleringer and Monson, 1993; Sharwood, 2017). The oxygenase activity of Rubisco is favoured under elevated temperatures as its specificity for CO_2 decreases relative to O_2 and low CO_2 environments. Carboxylase activity decreases with rising temperatures and under water stress due to a decrease stomatal conductance and therefore a decrease in the availability of CO_2 to Rubisco (Figure 1.6; Jolliffe and Tregunna, 1968; Jolliffe and Tregunna, 1973; Laing et al., 1974; Parry et al., 2002; Walker et al., 2016). In such environments the cost of photorespiration becomes more pronounced.

Not only does Rubisco have both carboxylase and oxygenase activity, it has an incredibly slow carboxylation catalytic turnover rate (k_{cat}^c) with an average of two to three turnovers per second in vascular plants. A recent study by Davidi et al. (2020) found a highly active rubisco with a k_{cat}^c value of 22 s^{-1}, however, 95 % of Rubisco k_{cat}^c values falling between 1 s^{-1} and 10 s^{-1} (Bainbridge et al., 1995; Flamholz et al., 2019). This is far below the average catalytic turnover rate (k_{cat}) of 80 s^{-1} of other central metabolic enzymes (Bainbridge et al., 1995; Flamholz et al., 2019). Due to Rubisco's slow k_{cat}^c, large amounts of the enzyme are required in order to achieve sufficient amount of photosynthesis (Mann, 1999). In C_3 leaves, up to 30 % of leaf nitrogen is partitioned into Rubisco, in some cases accounting for up to half the soluble leaf protein (Kung,

1976; Evans and Seemann, 1984; Evans, 1989; Bainbridge et al., 1995; Evans and Clarke, 2019). This huge investment in nitrogen accounts for the low nitrogen use efficiency in C_3 plants.

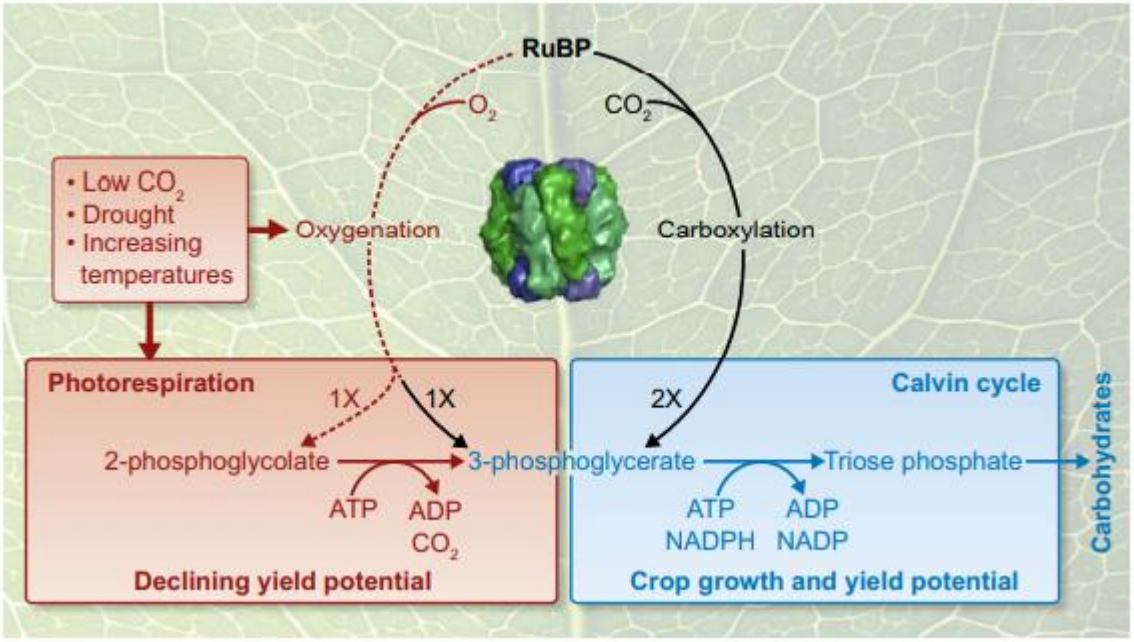

Figure 1.6. The consequences of the bifunctional nature of the Rubisco enzyme. Fixation of CO_2, through the carboxylation action of Rubisco, produces two molecules of 3-phosphoglycerate. The 3- phosphoglycerate enters the photosynthetic carbon reduction cycle, producing carbohydrates necessary for crop growth and yield. Low CO_2, drought and increasing temperatures increase the oxygenation action of Rubisco. The fixation of O_2 rather than CO_2 produces one molecule each of 3-phosphoglycerate and 2-phosphoglycolate. The 2-phosphoglycolate cannot be used to synthesise carbohydrates directly and must be converted to 3-phosphoglycerate through the photorespiratory pathway. This pathway consumes energy and releases CO_2, reducing plant productivity. Image from Sharwood (2017)

Rubisco catalysis is inhibited by a variety of sugar phosphate molecules, including its substrate RuBP, that bind to the catalytic sites of Rubisco not activated with both Mg^{2+} and a non-substrate CO_2 molecule (Lorimer et al., 1976; Jordan and Chollet, 1983; Andrews, 1996). In order to restore catalytic competence and maintain Rubisco activity, an enzyme, Rubisco activase (RCA), is required to remove inhibitory sugar phosphate molecules (Portis et al., 1986).

Overcoming the limitations of Rubisco have long been a focus as a way to improve photosynthesis (Carmo-Silva et al., 2015). In higher plants, Rubisco is comprised of large and small subunits, encoded in the chloroplast and the nucleus, respectively, which has complicated Rubisco engineering attempts (Sharwood, 2017). Engineering attempts have been made to modify Rubisco to increase the k_{cat}^{c}, which would increase the number of CO_2 molecules fixed per Rubisco, and therefore increase photosynthesis (von Caemmerer and Evans, 2010). Another engineering focus has been increasing the specificity of Rubisco for CO_2 relative to O_2 ($S_{C/O}$) to improve carboxylation efficiency. This would increase CO_2 fixation, decrease the oxygenation of RuBP and subsequent photorespiration, and increase photosynthesis when RuBP regeneration is limiting (von Caemmerer and Evans, 2010). It has been widely theorised that there was a trade-off where increasing k_{cat}^{c} leads to a decrease in $S_{C/O}$ and vice versa (Savir et al., 2010). Recent studies, however, have found that a minor catalytic trade-off exists between $S_{C/O}$ and k_{cat}^{c} when surveying Rubisco from a large number of species or when phylogenetic signals are accounted for (Flamholz et al., 2019; Bouvier et al., 2021). Engineering attempts focussing on these targets have had limited success (Carmo-Silva et al., 2015).

Naturally occurring Rubisco with desirable kinetic properties, such as those with better CO_2 specificity relative to O_2 from red algal species, have been identified as prime candidates for transplantation into C_3 crop plants (Whitney et al., 2001; von Caemmerer and Evans, 2010; Zhou and Whitney, 2019). Rubisco requires a suite of chaperone proteins to correctly assemble, including Cpn60/20, Raf1, Raf2, BSDII, and RbcX (Aigner et al., 2017). However, the chaperone suite required to assemble red algal Rubisco has not been elucidated and this impediment prevents red algal Rubisco from assembling in tobacco chloroplasts (Whitney et al., 2001; Sharwood, 2017; Lin et al., 2018). C_4 Rubisco has a higher catalytic turnover rate than C_3 Rubisco, and incorporating C_4 Rubisco into C_3 species could provide significant increases in photosynthesis (von Caemmerer and Evans, 2010). The same chaperone incompatibility exists, however, with the large subunits of monocots, heterologous plants and

cyanobacteria unable to fold and assemble in tobacco chloroplasts (Sharwood et al., 2016; Zhou and Whitney, 2019).

Given the catalytic limitations of Rubisco and the difficulties faced in Rubisco engineering, the CO_2 concentrating mechanism (CCM) of the C_4 photosynthetic pathway provides an efficient solution to the catalytic shortcomings of Rubisco. Research into the C_4 pathway could not be more timely as climate change causes an increasingly hot, dry climate, which will exacerbate many of the issues with Rubisco and therefore the photosynthetic inefficiencies of C_3 photosynthesis (IPCC, 2012, 2021).

1.5 C_4 Photosynthesis

C_4 photosynthesis evolved as an integration of both anatomical and biochemical adaptations to improve photosynthetic CO_2 assimilation in terrestrial plants under conditions of low CO_2 and increased temperatures (Jordan and Ogren, 1984; Ehleringer et al., 1991; Ehleringer et al., 1997; Sage, 2004). C_4 species are also able to grow in environments across a wide gradient of rainfall patterns, and thrive in hot, semi-arid climates (Ellis et al., 1980; Ehleringer and Monson, 1993; Long, 1999; Taub, 2000; Cabido et al., 2008). C_4 plants operate a CO_2 concentrating mechanism that has evolved independently more than 61 times from C_3 ancestors to elevate the CO_2 concentration around the active sites of Rubisco to near saturating levels of CO_2 (von Caemmerer, 2000; Christin et al., 2007; Sage et al., 2012; Sage, 2016). These high levels of CO_2, in some instances up to twenty times greater than in C_3 plants, are achieved by the close collaboration of mesophyll (MC) and bundle-sheath cells (BSC) with cell-specific expression of photosynthetic enzymes, and suppresses photorespiration (Figure 1.5D; Haberlandt, 1914; Hatch et al., 1971; Furbank and Hatch, 1987; Hatch, 1987; Jenkins et al., 1989; Kanai and Edwards, 1999). Photorespiration is a process responsible for the reduction in efficiency of carbon fixation of up to 30 % in C_3 plants (Raines, 2011; Bräutigam and Gowik, 2016).

In most C_4 plants the MC and BSC exhibit a characteristic arrangement, 'Kranz anatomy', with the BSC surrounding the vascular tissue, and the MC radially distributed around the BSC (Figure 1.5B,D; Haberlandt, 1914). C_4 plants also exhibit a redistribution and orientation of chloroplasts and mitochondria between the MC and BSC when compared to C_3 plants, as well as a decrease in leaf interveinal distance (Black and Mollenhauer, 1971; Kawamitsu et al., 1985).

As atmospheric CO_2 diffuses from intercellular airspaces into the MC, it is hydrated by carbonic anhydrase (CA) to produce bicarbonate (HCO_3^-), before being used as a substrate in the carboxylation phosphoenolpyruvate (PEP) in an irreversible reaction catalysed by phospho*enol*pyruvate carboxylase (PEPC) (Hatch et al., 1971; Tashian, 1989). The resulting oxaloacetate (OAA) is then converted into a 4-carbon organic acid (either malate or aspartate), which diffuses down a concentration gradient into the bundle sheath cell (BSC), through the plasmodesmata, which facilitate the connection between the MC and BSC (Kortschak et al., 1965; Hatch and Slack, 1966; Hatch, 1987). Subsequent decarboxylation of this carboxylic acid by a decarboxylase in the BSC releases CO_2, resulting in a high concentration of CO_2 around Rubisco, which is exclusively expressed in the BSC chloroplasts (Link et al., 1978; Furbank and Hatch, 1987; Jenkins et al., 1989; Kanai and Edwards, 1999; von Caemmerer, 2000). The three-carbon organic acid released in the decarboxylation reaction diffuses into the MC, where it is used to regenerate PEP, continuing the cycle (Hatch et al., 1971). C_4 plants can be classified into three subtypes based on the most prevalent decarboxylating enzyme present in the BSC (Kanai and Edwards, 1999). These three subtypes, the NADP-malic enzyme (NADP-ME), NAD-malic enzyme (NAD-ME), and PEP carboxykinase (PEPCK) subtypes are not mutually exclusive, as decarboxylation by the most abundant decarboxylating enzyme does not exclude low-level activity of another (Kanai and Edwards, 1999; Furbank, 2011). The 4-carbon carboxylic acid (malate or aspartate) used to shuttle CO_2 to the BSC varies depending on the subtype, as does the 3-carbon compound released from the decarboxylation reaction (Kanai and Edwards, 1999). This will be discussed in greater depth in Chapter 4 of this thesis.

Due to the elevated concentration of CO_2 around the active site of Rubisco, C_4 plants can commit less soluble protein to Rubisco protein than their C_3 counterparts (Ku et al., 1979). C_4 plants have leaves, therefore, with 3- to 6-fold lower Rubisco concentrations than those in leaves of C_3 plants (Ku et al., 1979). A study by Ghannoum et al. (2005) found that under high nitrogen supply in the soil, plants belonging to the NAD-ME subtype invest on average only 6.1 % of total leaf nitrogen to Rubisco, and plants belonging to the NADP-ME subtype invest even less with Rubisco accounting for an average of only 5.6 % of total leaf nitrogen. This is a vastly reduced commitment of leaf nitrogen to Rubisco when compared to the 30 % investment of leaf nitrogen to Rubisco in C_3 plants (Kung, 1976; Evans and Seemann, 1984; Evans, 1989; Bainbridge et al., 1995; Evans and Clarke, 2019). This is responsible for the increased nitrogen use efficiency (NUE) of C_4 compared to C_3 plants (Sage and Pearcy, 1987, 1987). In light-saturating environments, C_3 photosynthesis is limited by both RuBP regeneration and Rubisco quantity (Long, 1999). Due to the concentration of CO_2 around Rubisco in C_4 plants, higher rates of photosynthesis can be observed when compared to C_3 plants in light-saturating environments (Long, 1999).

1.6 An introduction to phospho*enol*pyruvate carboxylase

PEPC (EC 4.1.1.31) is a ubiquitous enzyme in plants, and can also be found in cyanobacteria, green algae, non-photosynthetic bacteria and archaea (O'Leary, 1982; O'Leary et al., 2011). It catalyses the irreversible β-carboxylation of PEP by HCO_3^-, to form oxaloacetate (OAA) and inorganic phosphate (Pi), requiring either Mg^{2+} or Mn^{2+} as an obligatory cofactor (Hatch et al., 1971). Plant genes encoding PEPC are members of a small multi-gene family and have evolved from a shared ancestral gene, duplications of which have allowed for the evolution of different isoforms (O'Leary et al., 2011; Christin et al., 2014). PEPC is involved in numerous and diverse non-photosynthetic cellular metabolic processes including a contribution to stomatal opening by mediating malate production in the guard cells, anaplerotic replenishment of the

tricarboxylic acid (TCA) cycle, as well as seed development and germination, and fruit ripening (Outlaw et al., 2002; O'Leary et al., 2011). PEPC also provides the malate required by bacteroids in the root nodules of N_2-fixing legumes, supplying the carbon source which allows for the assimilation of NH_4^+ into amino acids (Zhang et al., 1995). In addition to the myriad of non-photosynthetic roles, PEPC is also the primary carboxylase of the C_4 cycle, responsible for the initial fixation of CO_2 in the mesophyll cytosol.

1.6.1 Important residues for a functional phospho*enol*pyruvate carboxylase

Phospho*enol*pyruvate carboxylase exists as a tetramer, comprised of four identical monomers, assembled as a 'dimer-of-dimers' (Figure 1.7; Izui et al., 2004). Salt bridging between E493 and R498 of opposite dimers at the interface of dimer contact establishes tetramer formation (Figure 1.8; Kai et al., 1999). Partial dissociation of the tetramer was demonstrated by R498C site-directed mutagenesis, which disrupted the ion pair (Kai et al., 1999). The overall secondary

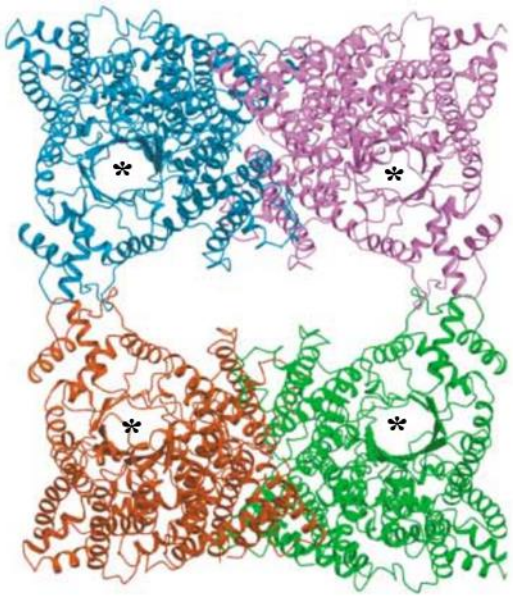

Figure 1.7. Crystal structure of PEPC from *Zea mays*. Asterisks indicate the active site located in the β-barrel of each monomer. Image from Matsumura et al. (2002)

structure of PEPC monomers is highly conserved between maize and *E. coli*, with monomers comprised of 42 alpha-helices and eight β-strands (Matsumura et al., 2002; Izui et al., 2004).

In the tertiary structure, these eight β-strands fold to form a β-barrel, the C-terminal region of which forms the catalytic site (Figure 1.7, Figure 1.9; Izui et al., 2004). The PEPC reactants

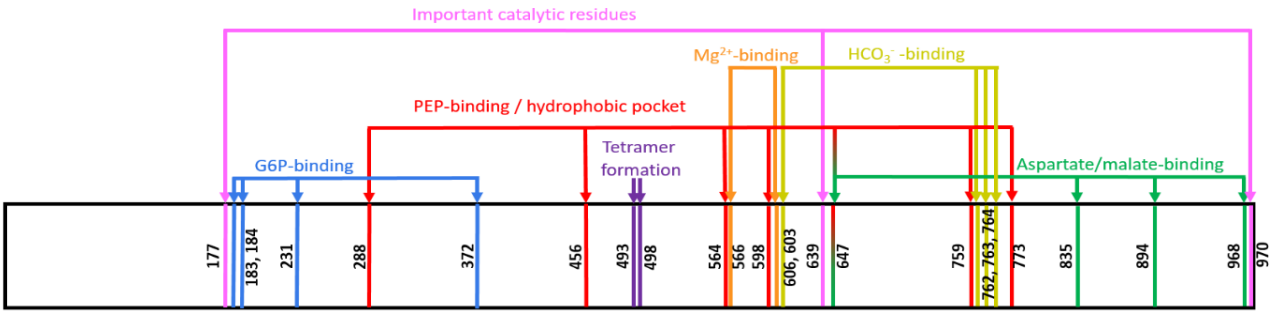

Figure 1.8. Important residues for a functional phospho*enol*pyruvate carboxylase. All numbering shown in the figure corresponds to the C_4 *Zea mays* PEPC monomer. Residues necessary for PEP-binding or creating the hydrophobic pocket are shown in red (288, 456, 564, 598, 647 and 773). Residues required for Mg^{2+}-binding are shown in orange (566, 603) and HCO_3^- -binding residues are indicated in yellow (606, 762, 763, 764). Important catalytic residues are indicated in pink (177, 970), with the two residues involved in tetramer formation indicated in purple (493, 498). Residues in green are necessary for aspartate/malate allosteric inhibitor interactions (647, 835, 894, 968). Residues involved in glucose-6-phospate binding are shown in blue (183, 184, 231, 372).

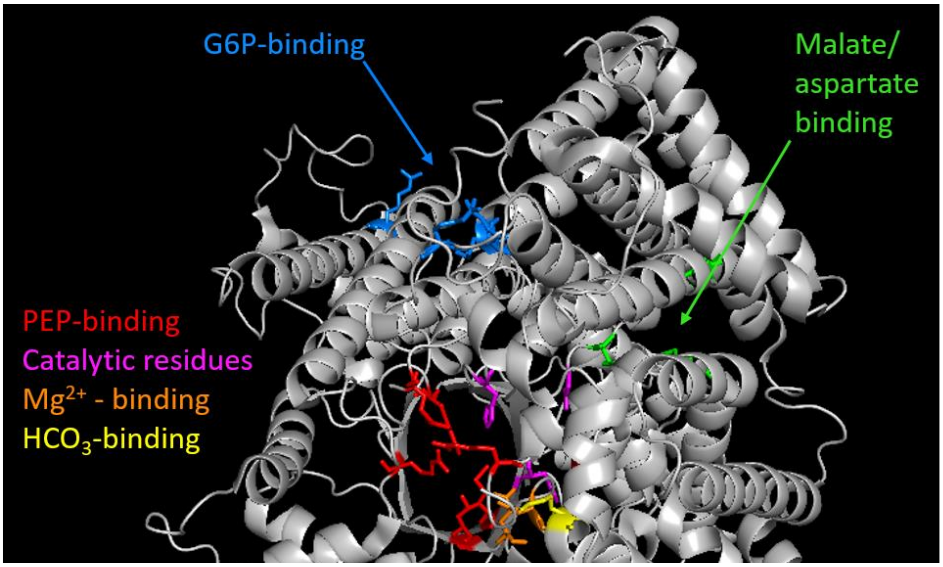

Figure 1.9. Location of PEPC functional residues on the crystal structure of a folded monomer of PEPC. PEP-binding residues are indicated in red, catalytic residues in pink, Mg^{2+}-binding residues in orange, and bicarbonate-binding residues in yellow. Residues involved in binding the allosteric activator, glucose-6-phosphate, are shown in blue, and the malate/aspartate binding residues are shown in green. Crystal structure from Matsumura et al. (2002)(JQ0 on Protein Data Bank)

bind in a sequential manner, with Mg^{2+}/divalent cation binding occurring first, followed by PEP- and finally HCO_3^--binding (Janc et al., 1992). The side-chain carboxylate oxygens of residues E566 and D603 facilitate the binding of the Mg^{2+} cation (Figure 1.8), and thus is co-ordinated to the active site at the C-terminal end of the β-barrel of PEPC (Figure 1.9; Matsumura et al., 1999). Divalent cation binding is essential for catalytic activity, as the conformational changes induced by Mg^{2+}-binding facilitates the interaction of the side chains of R456, R773 and R759, with the phosphoryl group of PEP necessary to accommodate the negatively charged phosphate (Figure 1.8; Bandurski, 1955; Matsumura et al., 1999; Matsumura et al., 2002). The role of R456 and R773 in PEP binding have been confirmed through site-directed mutagenesis studies (Gao and Woo, 1996) . The hydrophobic pocket created by the side chains of residues W288, L564 and M598, surround the methyl group of PEP (Figure 1.8; Matsumura et al., 2002; Kai et al., 2003). This hydrophobic environment is theorised to be vital to the protection of the highly reactive intermediates and sequesters the CO_2 cleaved from the carboxyphosphate, preventing its escape from the catalytic site (Yano et al., 1995; Matsumura et al., 2002). Residues K606, K762, R763, and R764 are involved in binding bicarbonate, and are highly conserved, with residues 762 and 764 conserved as either an arginine or a lysine (Figure 1.8; Kai et al., 1999; Kai et al., 2003). Residues K762, R763 and R764 belong to a flexible loop (residues 761-768; Loop II), both binding HCO_3^-, and subsequently forming a protective lid to the β-barrel, isolating the susceptible catalytic intermediates from surrounding water (Figure 1.8; Kai et al., 1999). Site-directed mutagenesis studies have confirmed the bicarbonate-binding role of K606, R763 and R764 (Gao and Woo, 1995; Kai et al., 1999).

Site-directed mutagenesis studies support H639 being involved in PEP binding, as mutations of the residue cause a drastic increase in K_mPEP of the enzyme, while some percentage of carboxylase activity is retained (Figure 1.8; Terada et al., 1991).

The PEPC reaction mechanism consists of three steps. Firstly, a transfer of phosphate from PEP to HCO_3^- results in the formation of carboxyphosphate and the enolate anion of pyruvate coordinated to the metal cation (Figure 1.10; Chollet et al., 1996; Matsumura et al., 2002; Izui et al., 2004). Secondly, H177, a basic enzyme residue, deprotonates the carboxyl group of carboxyphosphate, which is followed by its cleavage into CO_2 and P_i (Figure 1.8, Figure 1.10; Chollet et al., 1996; Izui et al., 2004). The enolate anion of pyruvate isomerises, bringing CO_2 into close proximity with its carbon 3. CO_2 is then able to electrophillically attack the metal-stabilised enolate to produce oxaloacetate and P_i, which are subsequently released from the enzyme (Figure 1.10; Chollet et al., 1996; Izui et al., 2004). The involvement of H117 in the carboxylation of the enolate form of pyruvate by the carboxyphosphate intermediate was supported by experiments carried out by Terada & Izui in 1991. A H177N mutation resulted in a mutant enzyme with no carboxylase activity, but the enzyme retained the ability to catalyse the bicarbonate-dependent dephosphorylation of PEP (Terada and Izui, 1991). Thus, the conclusion was drawn that H177 is involved in the carboxylation partial reactions.

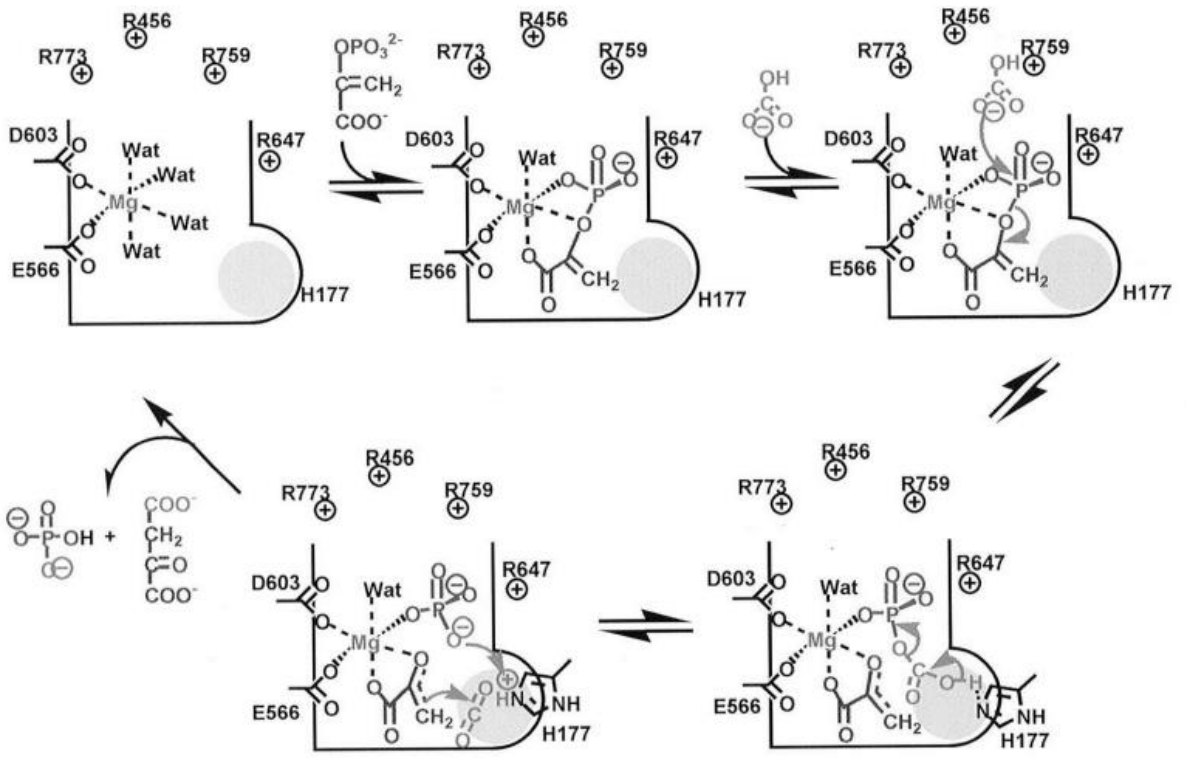

Figure 1.10. Proposed catalytic mechanism of PEPC, including the three-step model. Figure from (Izui et al., 2004)

1.6.2 Post-translational control of PEPC

PEPC is subjected to allosteric control, the molecules involved, however, are dependent on the species to which the organism belongs (Izui et al., 2004). Bacterial PEPC can be subject to activation by numerous molecules depending on the species. Subsets of the molecules acetyl CoA, fructose-1,6,-bisphosphate, 3-phosphoglycerate, glucose-6-phosphate and glucose-1-phosphate, glutamine, long chain fatty acids have been shown to be activators (Izui, 1970; Izui et al., 1981; Chen et al., 2002; Kai et al., 2003). Some bacterial species, such as *Coccochloris peniocystis* and *Thiobacillus thioparus*, have no known activators (Hoban and Lyric, 1975; Owttrim and Colman, 1986). Inhibitors of bacterial PEPC include malate, aspartate, fumarate, cysteine, tartrate, and oxaloacetate (Izui, 1970; Gold and Smith, 1974; Owttrim and Colman, 1986). In higher plants PEPC is activated by glucose-6-phosphate and inhibited by L-malate and, in some plants, aspartate (Andreo et al., 1987; Izui et al., 2004). The C_4 photosynthetic

PEPC isoform from the monocots *Z. mays* and *S. vulgare* have been demonstrated to be activated by glycine, however the C_4 PEPC from dicots and the C_3 PEPC isoform are not activated by glycine (Nishikido and Takanashi, 1973; Uedan and Sugiyama, 1976; Kai et al., 1999; Tovar-Méndez et al., 2000).

Residues K835, R894, N968 and R647 are involved in binding the allosteric inhibitors malate and aspartate (Figure 1.7; Kai et al., 1999). Formation of hydrogen bonds and salt bridges between the main chain of aspartate and R647 and N968 and salt bridge formation between the carboxyl group of aspartate and K835 and R894 accommodate this interaction (Chen et al., 2014). R647 is not only involved in inhibitor binding, but is a catalytically crucial residue. R647 belongs to a mobile loop, and moves the 20 Å between inhibitor-binding and catalytic site depending on the activity status of the enzyme (Matsumura et al., 2002; Izui et al., 2004). In the absence of malate or aspartate, the interaction between the strictly conserved C-terminal G970 carboxyl group and R647, moves R647 to the catalytic site of the enzyme (Dong et al., 1999; Izui et al., 2004). Site-directed mutagenesis studies, changing K835G and R894G result in mutant enzymes with reduced in vitro sensitivity to malate, whilst retaining catalytic activity (Endo et al., 2008).

Residues R183, R184, R231, and R372 form a pocket 15 Å away from the active site, involved in the binding of allosteric activator G6P (Figure 1.7; Matsumura et al., 2002). The region 301-443 (*Zea mays* numbering) has been shown to be important for PEPC activation by G6P, supporting the involvement of R372 in G6P binding (Bläsing et al., 2000; Engelmann et al., 2002). Site-directed mutagenesis studies support the involvement of these four residues in the binding of G6P (Takahashi-Terada et al., 2005). Replacing each arginine residue with a glutamine resulted in complete desensitisation of the PEPC enzyme to G6P in the case of R183Q, R184Q, R183Q/R184Q (double mutant), and R372Q mutations. A significant

desensitisation to G6P was also observed with a R372Q mutation (Takahashi-Terada et al., 2005). Using the kinetic and structural data available, it is hypothesised that the phosphate group of G6P interacts directly with R183 and R231, with R184 and R372 interacting indirectly (Takahashi-Terada et al., 2005).

Regulatory monoubiquitination of PEPC at a conserved lysine residue, K624 (*Sorghum bicolor* numbering), occurs in germinating castor oil (*Ricinus communis*) seeds, germinating sorghum (*Sorghum bicolor*) seeds, and in the developing proteoid roots of *Hakea prostrata* (Uhrig et al., 2008; Shane et al., 2013; Ruiz-Ballesta et al., 2014). This K624 is conserved in all bacterial-type and plant-type PEPCs (O'Leary et al., 2011). Monoubiquitination at this lysine residue reduces PEPC enzymatic activity by increasing the K_m for PEP, as well as increasing sensitivity to allosteric inhibitors (Uhrig et al., 2008; Shane et al., 2013; Ruiz-Ballesta et al., 2014). Subsequent deubiquitination, however, will reverse these changes (Uhrig *et al.* 2008).

1.6.3 C_4 PEPC v C_3 PEPC

In higher plants, photosynthetic C_4 PEPC has different kinetic and regulatory properties when compared to non-photosynthetic C_3 isoforms, including a reduction in sensitivity towards inhibitors, increased activation by G6P, differences in substrate saturation constants. C_4 PEPC also is expressed at greater levels than C_3 isoforms, is expressed in a cell-specific manner and is induced by light (Westhoff and Gowik, 2004; Heimann et al., 2013).

1.6.3.1 Regulation of C_4 phosphoenolpyruvate gene function

While non-photosynthetic PEPC is expressed in a variety of tissues, C_4 PEPC expression is confined to the mesophyll cytosol of the leaf (Hatch, 1987; Svensson et al., 2003). This cell-

specific expression is controlled at both the epigenetic and transcription level through PEPC gene regulation.

Epigenetic regulatory mechanisms have been demonstrated to be involved in both the cell-specific expression of C_4 PEPC and the upregulation of the C_4 PEPC gene in response to illumination (Langdale, 2011; Reeves et al., 2017). Within the promoter regions of the C_4 PEPC gene, histone methylation and acetylation are involved in the regulation of C_4 PEPC gene function. Histone H3 lysine 4 tri-methylation (H3K4me3), associated with actively transcribed genes, has shown to be associated with the mesophyll specific expression of PEPC (Heimann et al., 2013). Enrichment of H3K4me3 of the promoter regions of the C_4 PEPC gene in mesophyll cells when compared with bundle sheath cells has been demonstrated (Heimann et al., 2013). H3K4me3 of the C_4 PEPC gene is controlled by mesophyll specific signals, independent of illumination (Danker et al., 2008; Heimann et al., 2013). Enrichment of histone H3 lysine 9 acetylation (H3K9ac) and histone H4 lysine 9 acetylation (H4K5ac), was shown to be stimulated by illumination and independently of cell-type in the promoter regions of the C_4 PEPC gene (Offermann et al., 2006; Offermann et al., 2008; Heimann et al., 2013). Histone acetylation is highly correlated with gene transcription levels (Heimann et al., 2013). It appears, therefore, that acetylation of histones H3K9 and H4K5 are involved in the activation of C_4 PEPC gene expression in response to light stimuli (Reeves et al., 2017).

There has been much interest locating *cis*-regulatory elements responsible for mesophyll-cell specific expression of C_4 PEPC, but few have been sufficiently proven to be necessary and sufficient for the observed cell-specific expression (Hibberd and Covshoff, 2010; Langdale, 2011; Reeves et al., 2017). *In silico* comparative genetic analyses of promoter regions of genes encoding C_4-associated proteins in maize (C_4) and their orthologues in rice (C_3) identified putative *cis*-regulatory elements recruited to drive mesophyll cell-specific expression of these genes in C_4 plants (Wang et al., 2014). These putative *cis*-regulatory elements have not been tested experimentally. In the genus *Flaveria*, *cis*-regulatory elements vital for the high-level mesophyll cell-specificity of C_4 PEPC have been identified (Gowik et al., 2004; Akyildiz et

al., 2007). The so-called mesophyll expression module 1 (MEM1) of the distal promoter region (-1565 to -2188) is responsible for the mesophyll cell-specific expression of PEPC (Gowik et al., 2004; Akyildiz et al., 2007). The MEM1 element and a proximal promoter region (-570 to -1) act in concert to direct the high levels of expression observed in C_4 species of *Flaveria* (Gowik et al., 2004; Akyildiz et al., 2007; Engelmann et al., 2008).

Putative *trans*-factors regulating cell-specific gene expression and light regulation of the C_4 pepc gene have been identified through *in vitro* experiments (Kano-Murakami et al., 1991; Taniguchi et al., 2000; Windhövel et al., 2001; Reeves et al., 2017). The DOF1 and DOF2 transcription factors, from the DNA binding with one finger (DOF) family, has been proposed to have a role in the regulation expression of the pepc gene in maize in a light-dependent and cell-specific manner (Cavalar et al., 2007; Langdale, 2011). DOF1 is a transcriptional activator, constitutively expressed in maize plant tissue, was shown to bind to the regulatory region of the C_4 pepc gene in *Z. mays*, and activate expression in a light-regulated manner (Yanagisawa and Sheen, 1998). Tissue specificity of C_4 PEPC is achieved by the expression of DOF2, a transcriptional repressor, which binds to the same site as DOF1. DOF2 is expressed in the roots and the stems of maize plants (Yanagisawa and Sheen, 1998). It was later suggested that DOF1 was responsible for transcriptional activation of another C_4 gene, pyruvate phosphate dikinase (PPDK), as well as other non-photosynthetic genes in maize (Yanagisawa, 2000). Using transposon mutagenesis, Cavalar et al. (2007) found that not only was DOF1 unnecessary for light induced expression of PEPC, but five other C_4 photosynthetic genes, including PPDK also do not require DOF1 for expression.

1.6.3.2 C_4 phosphoenolpyruvate carboxylase protein kinetic and regulatory properties

C_3 and C_4 PEPCs have differences in substrate saturation constants (K_m) for both of its substrates, PEP and bicarbonate. C_4 PEPCs have increased K_m for PEP with respect to C_3 PEPC isoforms, usually about 10 times greater than non-photosynthetic isoforms (Ting and Osmond, 1973b; Ting and Osmond, 1973c). In contrast, C_4 PEPC isoforms have a lower K_m for

bicarbonate than C_3 isoforms (Bauwe, 1986; DiMario and Cousins, 2019; DiMario et al., 2021). An invariant mutation at amino acid position 780 (*Zea mays* numbering) from alanine in the C_3 PEPC isoforms to serine in all C_4 isoforms plays an important role in the increased PEP saturation kinetics in the C_4 PEPCs (Bläsing et al., 2000; Christin et al., 2007). In the genus *Flaveria,* site directed mutagenesis studies of this residue, have highlighted the impact of this A780S mutation on the K_m for PEP (Bläsing et al., 2000; Engelmann et al., 2002). Site-directed mutagenesis of the C_4 S780 to an alanine in the otherwise C_4 PEPC of *Flaveria trinervia*, resulted in a substantially decreased K_m for PEP, and this S780A mutation coupled with the addition of a C_3 region 2 (amino acids 296 to 437, *Flaveria numbering*), created a PEPC with a K_m for PEP analogous to C_3 PEPC isoforms. When the C_3 A780 was mutated to a serine in the otherwise C_3 PEPC of *Flaveria pringleii*, the K_m for PEP increased but not to levels equivalent to that of a C_4 isoform. With the A780S mutation coupled with the addition of a C_4 region 2 the K_m for PEP was even lower than with the A780S mutation alone (Engelmann et al., 2002). Therefore, although the C_4 S780 is important for the increase in the K_m for PEP, other residues in the C_4 PEPC sequence must be acting in concert, resulting in the combined increase. The same invariant mutation at amino acid position 780, from alanine in the C_3 PEPC isoforms to serine in all C_4 isoforms, plays a role in the difference in $K_mHCO_3^-$ seen between C_3 and C_4 plants (DiMario and Cousins, 2019). The $K_mHCO_3^-$ was determined for the species *Flaveria trineria* (C_4) and *Flaveria pringleii* (C_3), as well as *Flaveria trineria* (C_4) PEPC with a S780A mutation and *Flaveria pringleii* (C_3) PEPC with a A708S mutation. There was a significant increase in the $K_mHCO_3^-$ of the *Flaveria trineria* (C_4) PEPC when the S780 was mutated to an alanine, from 26.6 µM to 38 µM (DiMario and Cousins, 2019). Given that the $K_mHCO_3^-$ of *Flaveria trineria* (C_4) PEPC with a S780A mutation did not reach the same value of 64 µM recorded for the *Flaveria pringleii* (C_3), it suggests that additional amino acid residues may also be contributing to this change in $KmHCO_3^-$. This is also supported by the

fact that there was no significant change in $K_mHCO_3^-$ of *Flaveria pringleii* (C_3) PEPC when the A780 was mutated to a serine (DiMario and Cousins, 2019). A study by DiMario et al. (2021) substituted the PEPC region contain amino acids 528-880 from *Echinochloa esculenta*, a C_4 plant with a high $K_mHCO_3^-$, with the corresponding region from *Panicum virgatum*, a C_4 plant a low $K_mHCO_3^-$. This substitution increased the affinity of the *E. esculenta* PEPC, reducing the $K_mHCO_3^-$ to a value comparable to that of the *P. virgatum* $K_mHCO_3^-$ (DiMario et al., 2021). Therefore, it appears to be a region, rather than a single amino acid difference that controls the $K_mHCO_3^-$ of PEPC enzymes.

Phylogenetic research investigating grass PEPCs, using only nearly neutral sites, identified twenty-one amino acids thought to have evolved under positive selection in C_4 grasses (Christin et al., 2007). It is hypothesised that individually each of these 21 amino acids would have small effects differences in kinetic properties of PEPC enzyme, but together result in the distinct properties of C_4 isoforms (Christin et al., 2007).

As well as the differences in substrate saturation constants between C_3 and C_4 PEPC isoforms, differences sensitivities to allosteric inhibitors, malate and aspartate, and activators, glucose-6-phosphate (G6P) and glycine, have been demonstrated (Svensson et al., 2003). Photosynthetic C_4 PEPC enzymes generally demonstrate a greater activation by G6P when compared to C_3 isoforms (Ting and Osmond, 1973c; Svensson et al., 2003). C_4 PEPC isoforms have a reduction in sensitivity to malate (Dong et al., 1998; Bläsing et al., 2002; Engelmann et al., 2003; Jacobs et al., 2008). In the genus *Flaveria*, it was demonstrated that this decrease in sensitivity toward malate is the result of a single point mutation resulting in an amino acid change, from arginine (R) at position 884 (R_{884} *Flaveria trinervia* numbering; R_{890} *Zea mays* numbering) in the C_3 isoform, to glycine (G) in the C_4 isoform (Paulus et al., 2013). The C_3 arginine at this position is close to the essential malate binding residues and provides extra

hydrogen bonds with the malate, resulting in strong repressor binding in C_3 PEPCs (Paulus et al., 2013). Removal of the glycine reduces the affinity of the C_4 PEPC isoform for malate (Paulus et al., 2013). Further alignments demonstrated that in C_4 species of the *Poaceae* family, the C_3 R_{884} present in all species examined is replaced with either glycine, serine, glutamine or glutamate (Paulus et al., 2013).

Photosynthetic C_4 PEPC is subject to regulatory phosphorylation in response to photosynthetically active radiation (PAR). Photoactivation of C_4 PEPC, following illumination of leaves, results in a 2- to 3-fold increase in PEPC activity, a reduction in malate inhibition, and an increase in activation of the enzyme by G6P (Huber and Sugiyama, 1986; Nimmo et al., 1987; Jiao and Chollet, 1988; Jiao and Chollet, 1990). This photoactivation, which occurs in many but not all C_4 species, results from the reversible phosphorylation of a conserved N-terminus serine residue (S_{15}, *Zea mays* numbering) catalysed by PEPC protein kinase (Karabourniotis et al., 1983; Jiao and Chollet, 1990). PAR upregulates the activity of the PEPC protein kinase by a complex transduction cascade (McNaughton et al., 1991; Vidal and Chollet, 1997). There is a rapid diurnal turnover of the PEPC protein kinase, with activity levels dropping due to degradation via the ubiquitin-proteosome pathway (Agetsuma et al., 2005). Once levels of PEPC protein kinase have dropped through degradation, the phosphorylation of S15 is reversible by dephosphorylation by a protein phosphatase 2A, which remains at steady levels (Chollet et al., 1996; Agetsuma et al., 2005).

1.7 Thesis Aims

The main aims of this thesis are to:

1. Investigate the catalytic properties of PEPC from different species of the *Paniceae* by recombinant expression in *E. coli*. This aim is addressed in Chapters 3 and 4.

2. Investigate the effects of a PEPCK-specific six amino acid deletion on PEPC enzyme kinetics by recombinant expression in *E. coli*.
3. Modify the PEPC enzyme and investigate *in vivo* effects in the C_4 plant, *Setaria viridis*. This aim is addressed in Chapter 5.
4. Investigate effects of increased PEPC expression in the C_4 plant, *Setaria viridis*. This aim is addressed in Chapter 5.

Chapter 2: General Methods

2.1 Gene synthesis

After preparation for synthesis, sequences were synthesised by GenScript (https://www.genscript.com/gene_synthesis.html?src=pullmenu) and provided in pUC57 vector with ampicillin resistance.

2.2 Production of thermally competent *E. coli* TOP10 competent cells

E. coli TOP10 cells were used to inoculate 3 mL of LB media. The culture was incubated at 37 °C and 220 rpm overnight. 1 mL of the overnight culture was used to inoculate 100 mL of fresh LB media and this was incubated at 37 °C and 220 rpm until an OD_{600} within the range of 0.4-0.6 was reached. The culture was incubated on ice for 5 minutes before the cells were collected by centrifugation for 10 minutes at 5,000 rpm. The supernatant was removed and the pellet was resuspended in filter-sterilised TFBI (30 mM potassium acetate, 100 mM RbCl, 10 mM $CaCl_2$, 50 mM $MnCl_2$, 15 % glycerol, pH 5.8). Cells were collected by centrifugation for 10 minutes at 5,000 rpm, supernatant was removed and cells were resuspended in filter-sterilised TFBII (10 mM MOPS ($C_7H_{15}NO_4S$), 75 mM $CaCl_2$, 10 mM RbCl, 15 % glycerol, pH 6.5). Cells were aliquoted before being immediately frozen in liquid nitrogen.

2.3 Heat shock transformation of *E. coli* TOP10, *E. coli* XL-1 Blue, and *E. coli* BL21 (DE3) competent cells

Competent *E. coli* TOP10 cells (50 µl), *E. coli* XL-1 Blue (200 µl), or *E. coli* BL21 (DE3) (Agilent; 40 µl) were transformed using the heat shock as described by Sambrook et al. (1989). Competent cells were thawed on ice. 1 µl of synthesised or isolated plasmid was added to the competent cells and incubated on ice for 30 minutes. Cells were then heat shocked at 42 °C for 90 seconds and immediately incubated on ice for 5 minutes. LB media was then added to the

cells, followed by incubation at 37 °C and 300 rpm for 60 minutes. After incubation, 50 µl of the culture was plated onto LB-agar plates containing 100 µg/ml of ampicillin and incubated overnight at 37 °C. A single colony from the transformation plate was used to inoculate LB media containing 100 µg/ml of ampicillin and the culture was incubated at 37 °C and 220 rpm overnight.

2.4 Plasmid isolation

Plasmids were isolated using the ISOLATE II Plasmid Mini Kit (Bioline) as per the manufacturer's specifications.

2.5 General protein expression in *E. coli*

Three single colonies from a BL21(DE3) *E. coli* cells (Agilent) transformation plate was used to inoculate a single 5 mL starter culture of LB media containing 100 µg/mL of ampicillin. Three colonies were used in an attempt to reduce any variation in protein production between cultures due to differences in bacterial colony quality. Starter cultures were grown overnight at 37 °C and 160 rpm. The 5 mL starter cultures were then used to inoculate LB media containing 100 µg/mL of ampicillin. The volumes of the LB media for inoculation ranged from 50 mL to 1 L depending on the quantity of protein required. The cultures were then grown at 37 °C and 160 rpm until an OD_{600} of within the range of 0.45-0.65 was reached. Protein expression was induced by the addition of IPTG (final concentration 0.5 mM) and the cultures were incubated overnight at room temperature and 160 rpm.

2.6 SDS-PAGE analysis

Recombinant protein samples, prepared as described in Chapter 3, supplemented with 1 X SDS reducing buffer (10% glycerol, 62.5 mM Tris/HCl, 2 % (w/v) SDS OR 69.35 mM SDS, 0.0025 % (w/v) Bromophenol blue, 0.3575 M β-mercaptoethanol) were boiled for five minutes, and then centrifuged for 5 minutes at 10,000 rpm. Leaf extracts, prepared as described in section 5.2.9, were supplemented with 1 X XT sample buffer (BioRad). Samples were incubated at 65 °C for 10 minutes then centrifuged at 16 000 x *g* for one minute.

10 µl of each sample was loaded onto a NuPAGE 4-12 % Bis-Tris Gel (Invitrogen), with Precision Plus Protein All Blue Standards (BioRad). Gels were run in MES running buffer (50 mM MES, 50 mM Tris base, 3.5 mM SDS, 1 mM EDTA) at 4 °C and 200 V.

SDS-PAGE gels were then fixed using a solution containing 50 % (v/v) methanol, 10 % (v/v) acetic acid and 40% (v/v) H_2O for 45 minutes with continuous, gentle agitation on an orbital shaker (50 rpm). Fixing was followed by three 15-minute wash steps in H_2O, before staining with Gelcode Blue Stain Reagent (Thermo Scientific) and subsequent de-staining in H_2O. Gels were visualised on a ChemiDoc (Bio-Rad).

2.7 Western blot analysis

After separation by SDS-PAGE, as described in section 2.6, proteins were transferred to a nitrocellulose membrane. The gel was placed in between filter paper and pads soaked in transfer buffer (25 mM *N*,*N*-Bis(2-hydroxyethyl)glycine (Bicine), 25 mM Bis-Tris, 1 mM EDTA, 10 % v/v methanol). The transfer was performed in a XCell II™ Blot Module (Thermofisher) and 25 V for 1.5 hours at 4 °C.

The membrane was removed from the apparatus and washed in TBS (20 mM Tris-HCl pH 7.5, 150 mM NaCl) for five minutes on an orbital shaker. The membrane was then blocked in TBS (20 mM Tris-HCl pH 7.5, 150 mM NaCl) supplemented with 10 % (w/v) skim milk powder at 4°C overnight. After blocking, the membrane was washed in TBS (20 mM Tris-HCl pH 7.5, 150 mM NaCl) at room temperature once for ten minutes on an orbital shaker. The membrane was then washed in TBS two more times, each for three minutes on an orbital shaker. Either an anti-PEPC antibody (AS09 458, Agrisera) was diluted 1:10,000 in TBST (20 mM Tris-HCl pH 7.5, 150 mM NaCl , 0.05 % (v/v) TWEEN 20) or an anti-AcV5 tag antibody (ab49581, Abcam) was diluted 1:5,000 (20 mM Tris-HCl pH 7.5, 150 mM NaCl , 0.05 % (v/v) TWEEN 20). The membrane was incubated in the appropriate antibody at room temperature for one hour on an orbital shaker. The membrane was then washed three times for 10 minutes in TBS (20 mM Tris-HCl pH 7.5, 150 mM NaCl). A HRP-conjugated anti-mouse or a HRP-conjugated anti-rabbit secondary antibody diluted 1:10,000 in TBST (20 mM Tris-HCl pH 7.5, 150 mM NaCl , 0.05 % (v/v) TWEEN 20) was used for the anti-AcV5 tag antibody and the anti-PEPC antibody, respectively. The membrane was incubated in the secondary antibody solution for 45 minutes at room temperature on an orbital shaker. The membrane was then washed three times for 10 minutes in TBS (20 mM Tris-HCl pH 7.5, 150 mM NaCl).

Membranes were developed using the Western Lightning Plus-ECL, enhanced chemiluminescence substrate (Perkin Elmer) according to the manufacturer's specifications, and imaged using the ChemiDoc (BioRad).

2.8 PEPC activity assay and data analysis

PEPC activity was assayed at 25 °C following the NADH-coupled spectrophotometric assay as described by Ashton et al. (1990) with the rate of NADH oxidation monitored at 340 nm (one of the absorption maxima for NADH) using a Cary 60 UV-Vis spectrophotometer

(Agilent). The assay buffer contained 50 mM EPPS-NaOH, pH 8, 10 mM $MgCl_2$, 0.5 mM EDTA, 1 mM $NaHCO_3$, 5 mM PEP, 0.2 mM NADH, and 2 U malate dehydrogenase. Glucose-6-phosphate (5 mM) was either present or absent in the buffer. The reaction was initiated with the addition of PEP.

A slope running average was determined using three absorbance data points and the corresponding time points. Using the highest running average points spanning a time of at least 60 seconds, the slope of the change in absorbance vs the change in time was calculated. PEPC activity (µmol CO_2 m^{-2} sec^{-1}) was determined using the following equation:

PEPC activity (µmol CO_2 m^{-2} sec^{-1}) = [($|\Delta OD_{340}|$ × total assay volume × total extract volume)/(6.22×10^{-3} ×volume of leaf extract used ×leaf area)]

Where 6.22×10^{-3} is the extinction coefficient of NADH (6.22×10^{-3} mM^{-1} cm^{-1}) and absolute value of the change in absorbance at 340 nm per second ($|\Delta OD_{340}|$).

2.9 Statistical analysis

Statistical analyses were carried out using Origin software (Version 2020, OriginLab Corporation). One-way and two-way ANOVAs with posthoc Tukey honestly significant difference (HSD) tests were performed to determine statistically significant differences ($P < 0.05$) between the kinetic properties of PEPC (K_mPEP, $K_m HCO_3^-$, k_{cat}, V_{max}). One-way ANOVAs with posthoc Tukey HSD tests were also used to determined statistically significant differences ($P < 0.05$) between wild type and transgenic lines for various parameters (PEPC activity, Rubisco activity, soluble protein, total protein, fresh weight, dry weight, modelled V_{pmax}, modelled V_{cmax}, modelled PEPC activity and modelled Rubisco activity).

2.10 Gas Exchange

Net CO_2 assimilation rate was measured over a range of intercellular CO_2 partial pressure (C_i) values on the uppermost, fully expanded leaf of 14-day old (± 2 days) *Setaria viridis* plants

using a LI-COR 6400XT portable gas exchange system (LI-COR Biosciences). Measurements were made after leaves had equilibrated at 400 µbar, a leaf temperature of 25 °C, an irradiance of 1,800 µmol photons m^{-2} s^{-1}, and a flow rate 500 µmol s^{-1}. CO_2 response curves were measured in a stepwise increase (3-minute intervals) in CO_2 partial pressure as follows: 400, 0, 50, 74, 100, 200, 300, 400, 600, 800, 1000, 1200, 1500, 400 µbar whilst maintaining a leaf temperature of 25 °C and an irradiance of 1,800 µmol photons m^{-2} s^{-1}.

2.11 Protein quantification by Bradford assay

Proteins were quantified by Bradford assay based on Bradford (1976). A bovine serum albumin (BSA) standard was created with BSA concentrations of 0, 5, 10, 15, 20, 26.6 µg/ml. The protein sample/leaf extract was diluted until it was well within the range of the BSA standards. 150 µl of each standard and 150 µl of protein sample or 145 µl of ddH_2O + 5 µl of leaf extract was pipetted into a 96 well microtitre plate in triplicate. 150 µl of Coomassie Plus Assay Reagent (ThermoFisher Scientific) was added to each well. Absorbance of the samples was measured at 595 nm on a BioRad plate reader. The average absorbance of the three readings for each BSA concentration was calculated. Excel was used to fit a linear trendline to the BSA standard curve, and this equation was used to calculate the concentration of the protein sample.

2.12 Protein structure prediction

Predictions for the tertiary structure of various PEPC proteins were obtained using I-TASSER (Iterative Threading ASSEmbly Refinement) (Yang et al., 2015; Yang and Zhang, 2015). PEPC sequences were submitted to I-TASSER at https://zhanggroup.org/I-TASSER/ , and predicted protein structures were obtained for the PEPC proteins. *Panicum coloratum* and *Urochloa panicoides* C_4 PEPC sequences were provided by Alex Watson-Lazowski and the C_4 *S. viridis* PEPC sequence (Sevir.4G143500.1, Phytozome) was obtained from Phytozome (https://phytozome-next.jgi.doe.gov/).

2.13 DNA gel electrophoresis

DNA samples were supplemented with 4X gel loading dye (NEB) to a final concentration of 1X and run at 80 V on a 1 % agarose/ 1X TAE (40 mM trisaminomethane (Tris), 20 mM acetic acid, 1 mM EDTA) gel with 1X SYBR™ Safe DNA Gel Stain (Thermofisher) for visualisation and visualised using a blue light transilluminator or a ChemiDoc (BioRad).

Chapter 3: Establishment and optimisation of PEPC expression and purification using *Escherichia coli* as an expression system

3.1 Introduction

The aim of this chapter is to establish a PEPC expression system in *E. coli* and to optimise the purification of PEPC protein expressed in this system. This will allow PEPC kinetics for different species to be determined *in vitro*, as well as allowing the investigation of the effects of PEPC residues and regions on PEPC kinetics.

3.1.1 Histidine-tagged ubiquitin expression (pHUE) vector for protein expression in *E. coli*

Expression of heterologous proteins in bacterial systems is shown to be enhanced when the protein is expressed as a ubiquitin fusion protein (Baker, 1996). The histidine-tagged ubiquitin expression (pHUE) vector, allows proteins to be expressed in *E. coli* as poly-histidine-tagged ubiquitin fusion proteins, and results in high expression levels associated with ubiquitin fusion proteins (Figure 3.1; Catanzariti et al., 2004). Fusion proteins consist of six N-terminal histidine residues followed by a ubiquitin moiety and then the protein of interest (Catanzariti et al., 2004). The histidine residues allow for purification of the fusion protein using immobilised metal affinity chromatography (IMAC) (Catanzariti et al., 2004). After purification by IMAC, the ubiquitin moiety can be cleaved and removed from the protein by ubiquitin specific proteases (USP), which are advantageous as they exhibit no non-specific cleavage and cleave precisely at the C-terminus of the ubiquitin moiety, leaving no unwanted N-terminal amino acids in the protein of interest (Baker, 1996; Catanzariti et al., 2004; Baker et al., 2005). Cleavage of the ubiquitin moiety also removes the histidine residues at the N-terminus of the fusion protein, leaving just the protein of interest (Catanzariti et al., 2004). A mouse deubiquitylating protein (Usp2) has been engineered to be expressed in *E. coli* as a

polyhistidine-tagged recombinant protein, allowing purification of the Usp2 by IMAC (Baker et al., 2005). The ubiquitin protease can be utilised to cleave the polyhistidine-ubiquitin from the fusion proteins, separating the tag and the protein of interest (Baker et al., 2005). Subsequently, the his-tagged proteins, any uncleaved fusion protein and contaminating *E. coli* proteins that have multiple histidines can be removed from the recombinant protein of interest

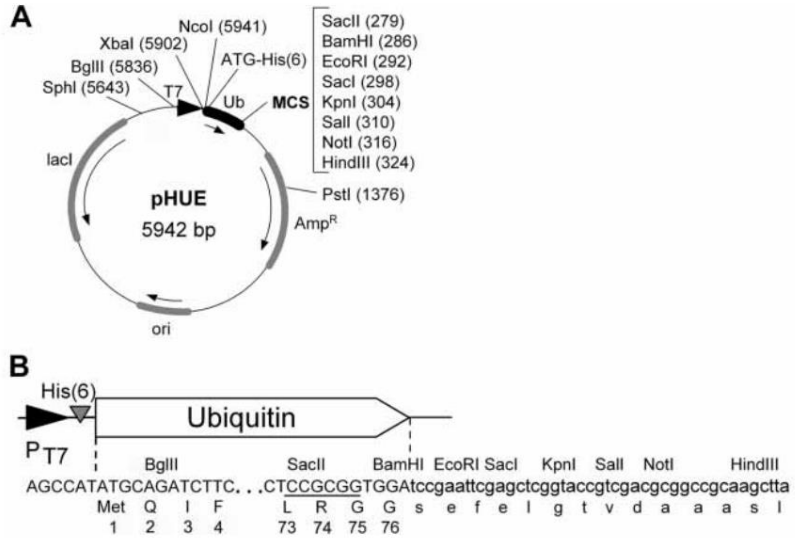

Figure 3.1. The histidine-tagged ubiquitin expression (pHUE) vector. (A) A map of the pHUE vector, with the T7 RNA polymerase promoter (indicated by a black triangle), the poly-histidine tag (ATG-His(6)), the ubiquitin coding sequence (indicated by a black box), the multiple cloning site (MCS), ampicillin resistance gene (Amp^R), the origin of replication (ori) and the lacI repressor gene (lacI). (B) The fusion protein, containing a polyhistidine tag (His(6)), and the ubiquitin moiety. Also featured are the 5' and 3' ends of the DNA sequence encoding the ubiquitin moiety. The SacII restriction enzyme site (CCGCGG) encoded into the 3' end of the ubiquitin coding sequence is underlined. Image from Catanzariti et al. (2004)

by affinity chromatography using Ni-NTA resin (Baker et al., 2005).

Expression of the fusion protein is driven by a T7 RNA polymerase promoter, inducible by IPTG (Figure 3.1; Catanzariti et al., 2004). A multiple cloning site follows the 3' end of the ubiquitin coding region to allow cloning of the protein coding sequence (Figure 3.1). A SacII restriction enzyme site is encoded into the 3' end of the ubiquitin coding sequence (Figure 3.1; Baker et al., 1994; Catanzariti et al., 2004). Utilisation of this SacII restriction enzyme site during cloning ensures that no extra N-terminal residues are left on the protein of interest (Baker et al., 1994; Catanzariti et al., 2004). For this investigation, cloning of PEPC coding sequences was carried out between the SacII and HindII restriction enzyme cloning sites.

The pHUE expression system has been successfully used to purify many proteins, including many found in plants or involved in photosynthesis, including form II Rubisco, rubisco activase, red-type Rubisco activase Cbbx, rubisco-assembly chaperone Raf1, the β-carboxysome scaffolding protein CcmM, and Essential Pyrenoid Component 1 (EPYC1) (Whitney and Sharwood, 2008; Mueller-Cajar et al., 2011; Hauser et al., 2015; Tsai et al., 2015; Peterson-Forbrook et al., 2017; Serban et al., 2018; Wang et al., 2018; Wunder et al., 2018; Wang et al., 2019; He et al., 2020; Zang et al., 2021).

3.1.2 Review of buffers used in previous papers for PEPC purification

From a review of the published literature, a number of buffers have been used to purify PEPC enzymes from *Zea mays* and *Flaveria* species from *E. coli* (Table 3.1). All buffers had a pH between 7.3 – 7.6, and most contained a reducing agent (DTT or β-mercaptoethanol), a protease inhibitor (PMSF or EDTA), and glycerol for protein stabilisation. The EDTA and DTT included in many of the *Flaveria* PEPC extraction buffers are not compatible with IMAC purification. EDTA, a strong chelating agent, is incompatible with nickel-nitriloacetic acid (Ni-NTA) matrices as it binds the nickel ions and strips it from the NTA resin (Novagen; QIAGEN, 2011; Life Technologies Corporation, 2012). DTT, a strong reducing agent, reduces the nickel ions and prevents them from binding polyhistidine-tagged proteins (Novagen; QIAGEN, 2011; Life Technologies Corporation, 2012). Therefore, β-mercaptoethanol and PMSF were selected as the reducing agent and protease inhibitor buffer components for PEPC purification from *E. coli*.

Table 3.1 Buffers used to purify PEPC expressed in *E. coli*. Buffer composition and the role of buffer components are listed. Abbreviations of buffer components are as follows: phenylmethylsulfonyl fluoride (PMSF), dithiothreitol (DTT), and ethylenediamine tetraacetic acid (EDTA).

Buffer composition	Role of buffer component	Reference
100 mM Tris-HCl (pH 7.6), 10% ethylene glycol, 5% glycerol, 1 mM PMSF, 10 mM β -mercaptoethanol.	Buffer Protein stabilisation Protein stabilisation Protease inhibitor Reducing agent	(Dong et al., 1997) (Dong et al., 1998)
100 mM Tris-HCl (pH 7.6), 20% (v/v) glycerol, 1 mM PMSF, 14 mM β -mercaptoethanol	Buffer Protein stabilisation Protease inhibitor Reducing agent	(Takahashi-Terada et al., 2005)
100 mM Tris, (pH 7.6), 10 mM $MgCl_2$, 5 mM DTT, 1 mM EDTA, 20% glycerol	Buffer PEPC cofactor Reducing agent Chelating agent to prevent protease activity Protein stabilisation	(Gao and Woo, 1995)
50mM Tris (pH 7.5), 10mM $MgCl_2$, 150mM NaCl, DNase, lysozyme	Buffer PEPC cofactor Increase ionic strength of buffer Digest DNA Digest cell debris	(Paulus et al., 2013)
100 mM Mops/KOH (pH 7.3) 10 mM $MgCl_2$, 10 mM DTT, 1 mM EDTA, 1 mM PMSF	Buffer PEPC cofactor Reducing agent Chelating agent to prevent protease activity Protease inhibitor	(Svensson et al., 1997) (Bläsing et al., 2002) (Engelmann et al., 2003) (Gowik et al., 2006)
0.5 M $(NH_4)_2SO_4$, 20 mM Tris–HCl (pH 7.5), 0.1 mM DTT, 1 mM EDTA (pH 8.0) 5% (v/v) glycerol, 1 mM PMSF.	 Buffer Reducing agent Chelating agent to prevent protease activity Protein stabilisation Protease inhibitor	(DiMario and Cousins, 2019)

3.1.3 PEPC structure

PEPC has been purified from bacterial, C_3, C_4 and single celled C_4 plant species in the more active tetrameric form, less active dimeric form, and a mixture of the two (Ting and Osmond, 1973c; Miziorko et al., 1974; Nott and Osmond, 1982; Huber et al., 1986; Iglesias et al., 1986; Owttrim and Colman, 1986; Stiborová and Leblová, 1986; Walker et al., 1986; Podesta and Andreo, 1989; Willeford et al., 1990; Arrio-Dupont et al., 1992; Svensson et al., 1997; Takai

et al., 1997; Chen et al., 2002; Lara et al., 2006). It has been suggested that the structure of the PEPC tetramer, with only the salt bridges between the Arg 438 of one subunit and Glu433 of another subunit holding the tetramer together, explains the inherent tendency of the enzyme to dissociate into dimers (Kai et al., 1999). In order to investigate if the purification form of the PEPC enzyme is permanent, or more transient depending on the conditions of the solution in which it is contained, a literature review was conducted.

A number of studies have found that whether the PEPC enzyme is a dimer or a tetramer depends on the conditions of the solution containing the PEPC. Gel filtration has been used to investigate the effect of PEPC protein concentration on the quaternary structure of the enzyme in a number of plant species. High concentrations of PEPC protein loadings (1 mg/ml) result in the elution of the PEPC enzyme as a tetramer. Conversely, low concentrations of PEPC protein loadings of the enzyme result in the elution of the PEPC enzyme as a dimer. This has been observed in a number of plant species including *Bryophyllum fedtschenkoi* (CAM), *Bryophyllum pinnatum* (CAM), and *Zea mays* (C_4, NADP-ME) (Jones et al., 1978; Nott and Osmond, 1982; McNaughton et al., 1989; Wu et al., 1990). Therefore, there appears to be a concentration-dependent dissociation of the PEPC enzyme into dimers at low protein concentration (Jones et al., 1978; Nott and Osmond, 1982; Nimmo et al., 1987; Wu et al., 1990). This concentration-dependent dissociation of the PEPC enzyme into dimers at low protein concentration has also been demonstrated by native-PAGE analysis on the *Crassula argentea* (CAM) PEPC enzyme and dynamic light scattering on the *Zea mays* PEPC enzyme (Willeford et al., 1990; Wu et al., 1990; Meyer et al., 1991; Willeford and Wedding, 1992).

Gel filtration has been used to investigate the effects of the presence of malate on PEPC quaternary structure. It has been found that in the presence of malate, dissociation of the PEPC tetramer to the dimer is induced (Wu and Wedding, 1985; Nimmo et al., 1986; Willeford et al., 1990). This has been observed in a number of plant species including *Bryophyllum fedtschenkoi* (CAM), *Crassula argentea* (CAM), and *Zea mays* (C_4, NADP-ME) (Wu and Wedding, 1985;

Nimmo et al., 1986; Willeford et al., 1990). In addition, incubation of the dimer-tetramer mixture form of the PEPC enzyme with malate has been shown to drive the equilibrium toward the dimeric form of the enzyme (Wu and Wedding, 1987). It has been shown, however, that preincubation of the *Crassula argentea* (CAM) PEPC enzyme with PEP can stop the conversion of the PEPC tetramer into dimers on exposure to 1.5 mM of malate (Wu and Wedding, 1985). Using dynamic laser-light scattering, it has been demonstrated that incubation of the *Crassula argentea* and *Zea mays* PEPC enzyme with malate caused dimer formation (Willeford et al., 1990; Wu et al., 1990; Meyer et al., 1991). Gel filtration has also been used to investigate the effect of the presence of NaCl on PEPC quaternary structure. NaCl has been shown to cause the PEPC tetramer of *Zea mays* to dissociate into dimers (Wagner et al., 1987; McNaughton et al., 1989; Podesta and Andreo, 1989). The extent of dissociation was dependent on protein concentration, with increasing dissociation observed with decreasing PEPC protein concentration (Wagner et al., 1987). The extent of dissociation was also dependent on preincubation time with the NaCl, with increasing in dissociation observed with increasing preincubation time (Wagner et al., 1987).

Gel filtration has also been used to investigate the effect of the presence of Mg^{2+}, PEP, and G6P on PEPC quaternary structure. Incubation of the dimeric form of the PEPC enzyme with Mg^{2+} has been shown to induce the formation of PEPC tetramers (Wu and Wedding, 1985). Incubation of the dimer-tetramer mixture form of the PEPC enzyme with PEP has been shown to drive the equilibrium toward the tetrameric form (Wu and Wedding, 1987). It was shown that preincubation of dilute *Crassula argentea* PEPC enzyme with PEP or G6P resulted in tetramer formation using dynamic laser-light scattering (Meyer et al., 1991). Dynamic laser light scattering in conjunction with gel filtration has shown similar results, with tetramer formation of the *Zea mays* PEPC enzyme being induced in the presence of PEP, Mg^{2+}, a combination of PEP and Mg^{2+}, and interestingly also HCO_3^- (Willeford et al., 1990; Wu et al., 1990; Wedding et al., 1994). Light scattering has also shown that the presence of PEP or G6P

stabilises the *Zea mays* PEPC in tetrameric form, even when the PEPC enzyme is subject to increasing levels of dilution (Willeford and Wedding, 1992).

From the findings of the literature review it was concluded that purification of either the dimeric or tetrameric form of the enzyme was acceptable as the tetrameric form could be induced after purification by altering the components of the solution it was contained in.

3.1.4 Experimental Objectives

The experimental objective is to establish and optimise a PEPC expression and purification method using *E. coli* as an expression system and pHUE as the expression vector.

3.2 Methods

3.2.1 Buffers for PEPC recombinant protein extraction from *E. coli*

3.2.1.1 Expression test extraction buffer

The extraction buffer for the expression test contained 0.1 M Tris-HCl, pH 7.4, 10 % (v/v) glycerol, supplemented with 1 mM PMSF and 10 mM β-mercaptoethanol.

3.2.1.2 Starting buffers for PEPC recombinant protein extraction from E. coli

Given that *Zea mays* and the other C_4 enzymes to be purified were monocots, the starting extraction buffer was chosen to be 0.1 M Tris-HCl, pH 7.4, 10 % (v/v) glycerol, 10 mM imidazole supplemented with 1 mM PMSF and 10 mM β-mercaptoethanol.

The starting elution buffer was 0.1 M Tris-HCl, pH 7.4, 10 % (v/v) glycerol, 300 mM imidazole, the starting equilibration buffer was 50 mM Tris-HCl, pH 8.0, 300 mM NaCl, 10

mM imidazole and the starting wash buffer was 0.1 M Tris-HCl, pH 7.4, 10 % (v/v) glycerol, 10 mM imidazole supplemented with 10 mM β-mercaptoethanol.

3.2.1.3 Optimisation of imidazole concentration in extraction/wash buffer

The extraction buffer was as described in 3.1.1.2 (0.1 M Tris-HCl, pH 7.4, 10 % (v/v) glycerol, 10 mM imidazole supplemented with 1 mM PMSF and 10 mM β-mercaptoethanol), as was the equilibration buffer (50 mM Tris-HCl, pH 8.0, 300 mM NaCl, 10 mM imidazole) and the elution buffer (0.1 M Tris-HCl, pH 7.4, 10 % (v/v) glycerol, 300 mM imidazole). All wash buffers contained 0.1 M Tris-HCl, pH 7.4, 10 % (v/v) glycerol, supplemented with 10 mM β-mercaptoethanol, with either 10 mM, 20 mM, 30 mM, or 40 mM imidazole.

3.2.1.4 Addition of $MgCl_2$ and glucose-6-phosphate to the extraction and wash buffers

$MgCl_2$ can be used in the Ni-NTA affinity chromatography purification process in concentrations up to 4M (QIAGEN, 2011). Given that 10 mM $MgCl_2$ has been used in extraction buffers for the purification of *Flaveria* PEPC proteins, and that the PEPC activity assay protocol (General Methods 2.8) contains 10 mM $MgCl_2$ in the reaction buffer, a concentration of 10 mM $MgCl_2$ was chosen for buffer supplementation (Gao and Woo, 1995; Svensson et al., 1997; Bläsing et al., 2002; Engelmann et al., 2003; Gowik et al., 2006; Paulus et al., 2013). A concentration of 5 mM G6P was chosen for buffer supplementation as this is the concentration used in the PEPC activity assay protocol (General Methods 2.8).

The extraction and wash buffers described in 3.1.1.2 were supplemented with either 10 mM $MgCl_2$, 5 mM G6P, or 10 mM $MgCl_2$ and 5 mM G6P.

The elution buffer was as described in 3.1.1.2 (0.1 M Tris-HCl, pH 7.4, 10 % (v/v) glycerol, 300 mM imidazole), as was the equilibration buffer (50 mM Tris-HCl, pH 8.0, 300 mM NaCl, 10 mM imidazole).

3.2.1.5 Addition of 300 mM NaCl to the extraction and wash buffers

The inclusion of NaCl in buffers prevents non-specific ionic interaction between proteins, preventing copurification, and it is recommended that at least 300 mM NaCl is used for protein purification using Ni-NTA matrices (Novagen; QIAGEN, 2011).

The extraction buffer described in 3.1.1.2 was supplemented with 300 mM NaCl, with the resulting extraction buffer for testing consisting of 0.1 M Tris-HCl, pH 7.4, 10 % (v/v) glycerol, 300 mM NaCl supplemented with 1 mM PMSF and 10 mM β-mercaptoethanol. The wash buffer described in 3.1.1.2 was supplemented with 300 mM NaCl (0.1 M Tris-HCl, pH 7.4, 10 % (v/v) glycerol, 10 mM imidazole, 300 mM NaCl, supplemented with 10 mM β-mercaptoethanol).

The elution buffer was as described in 3.1.1.1 (0.1 M Tris-HCl, pH 7.4, 10 % (v/v) glycerol, 300 mM imidazole), as was the equilibration buffer (50 mM Tris-HCl, pH 8.0, 300 mM NaCl, 10 mM imidazole).

3.2.1.6 DNase in the larger culture extraction buffer

When larger bacterial cultures were grown in order to scale up the PEPC protein for extraction and purification, DNase was included in the extraction buffer to digest the large amounts of DNA present in the lysate. 1 µg DNase per mL of resuspended cells was added to the extraction buffer.

3.2.2 Protein expression

3.2.2.1 Test for recombinant PEPC expression in E.coli

The process to create the transformed BL21 (DE3) cells used for the establishment and optimisation of PEPC expression and purification using *E. coli* as an expression system is described in Chapter 4. LB media (100 mL) containing 100 µg/ml of ampicillin was inoculated

with 100 µl of the glycerol stock of transformed BL21 cells. One culture was made for each of the seven plasmids to be tested for PEPC expression. As the control, 50 mL of LB containing no antibiotic was inoculated with 50 µl of untransformed BL21 (DE3) cells (Agilent). The cultures were then grown at 37 °C and shaken at 200 rpm until an OD_{600} within the range of 0.40-0.60 was reached.

Once an OD_{600} within this range was reached, 15 mL of each culture was separated to represent the non-induced culture corresponding to each plasmid. For the control, 25 mL of the culture was separated to be the non-induced control. Protein expression was induced by the addition of IPTG (final concentration 0.5 mM), no IPTG was added to the non-induced cultures or the non-induced control. All cultures were incubated overnight at 25 °C and 200 rpm.

After overnight incubation, cells (15 mL per culture) were then harvested by centrifugation at 5,000 x *g* for 7 minutes at 4 °C. Cell pellets were resuspended in 4 mL extraction buffer (0.1 M Tris-HCl, pH 7.4, 10 % (v/v) glycerol, supplemented with 1 mM PMSF and 10 mM β-mercaptoethanol). Cell lysis was achieved by three sequential passes through a French pressure cell (Aminco) precooled to 4 °C at 1000 psi. 150 µl of the lysate for each culture was retained for SDS-PAGE gel analysis (3.1.2 SDS-PAGE gel analysis).

1 mL of the lysis solution for each culture was centrifuged for 5 minutes at 21,000 x *g* and 4 °C. After centrifugation the supernatant was removed and retained for purification, and 150 µl of the supernatant for each culture was retained for SDS-PAGE gel analysis (3.1.3 SDS-PAGE gel analysis).

3.2.2.2 Expression and extraction of recombinant PEPC protein for use in purification optimisation

The process to create the transformed BL21 (DE3) cells used for the establishment and optimisation of PEPC expression and purification using *E. coli* as an expression system is described in Chapter 4. These cells were used in the optimisation of the PEPC purification process. Three single colonies from the various BL21 transformation plates were used to

inoculate 5 mL starter cultures of LB media containing 100 µg/mL of ampicillin. These starter cultures were grown overnight at 37 °C and 160 rpm. After overnight incubation, the 5 mL starter cultures were used to inoculate LB media containing 100 µg/mL of ampicillin. The volumes of the LB media for inoculation ranged from 50 mL to 1 L depending on the quantity of protein required. The cultures were then grown at 37 °C and 160 rpm until an OD_{600} of within the range of 0.45-0.65 was reached. Protein expression was induced by the addition of IPTG (final concentration 0.5 mM) and the cultures were incubated overnight at room temperature and 160 rpm. Cells were then harvested by centrifugation at 6,000 x *g* for 10 minutes using a Hitachi R9A rotor. The supernatant was discarded. The cells were snap frozen in liquid nitrogen and stored at -20 °C until purification.

For protein purification, cell pellets were resuspended in 15 mL extraction buffer per 200 mL cell culture. The composition of the extraction buffer differed through the optimisation process (see 3.1.1). Cell lysis was achieved by three sequential passes through a French pressure cell (Aminco) pre-cooled to 4 °C at 1000 psi. 150 µl of the lysate for each culture was retained for SDS-PAGE gel analysis, added to 50 µl of 4X SDS reducing buffer, snap frozen in liquid nitrogen and stored at -20 °C until SDS-PAGE analysis (3.1.3 SDS-PAGE gel analysis). The lysis solution for each culture was centrifuged for 5 minutes at 15,000 rpm and 4 °C. After centrifugation the supernatant was removed and retained for purification. 150 µl of the supernatant for each culture was retained for SDS-PAGE gel analysis, added to 50 µl of 4X SDS reducing buffer, snap frozen in liquid nitrogen and stored at -20 °C until SDS-PAGE analysis (3.1.3 SDS-PAGE gel analysis).

3.2.3 SDS-PAGE and Western blot analysis.

SDS-PAGE analysis was carried out as described in the General Methods section of this thesis (2.6 SDS-PAGE gel analysis). Western blotting was carried out as described in the General Methods section 2.7 of this thesis using an anti-PEPC primary antibody and a HRP-conjugated anti-rabbit secondary antibody.

3.2.4 Ubiquitin protease expression and purification

Ubiquitin protease was expressed in and extracted from *E. coli* as described in 3.1.2.2 using ubiquitin protease extraction buffer (50 mM Tris-HCl, pH 8.0, 300 mM NaCl, 20 mM imidazole) supplemented with 1 mM PMSF (Baker et al., 2005). Lysates containing the ubiquitin protease were loaded onto chromatography columns with a 4 ml Ni-NTA agarose (Qiagen) solid phase, which had been pre-equilibrated with 10 x bed volumes of ubiquitin protease extraction buffer. The columns were washed with 20 x bed volumes of ubiquitin protease extraction buffer. Proteins were eluted from the column with elution buffer (50 mM Tris-HCl, pH 8.0, 300 mM NaCl, 200 mM imidazole), and collected as four fractions using 0.4 x bed volumes for fraction one and 1 x bed volume for the remaining three fractions. A dye-bind assay was used to determine that the eluted protein was contained in fractions two and three. The purified ubiquitin protease samples were placed into dialysis tubing (16 mm diameter, 25 mm flat width, Sigma-Aldrich) and into 1.8 L dialysis buffer (50 mM EPPS, pH 8.0, 20 % (v/v) glycerol). The dialysis reaction was incubated at 4 °C overnight. After dialysis the ubiquitin protease was quantified as described in General Methods section 2.11. Purified ubiquitin protease was stored in 20 % (v/v) glycerol at -80 °C after snap freezing in liquid nitrogen.

3.2.5 Protein purification using Ni-NTA agarose columns

The following purification was carried out at 4 °C. Soluble protein samples were loaded onto chromatography columns with a 4 ml Ni-NTA agarose (Qiagen) solid phase, which had been pre-equilibrated with 10 x bed volumes of extraction buffer. The composition of the extraction buffer differed through the optimisation process (see 3.1.1). 150 µl of the column eluant for each culture was retained for SDS-PAGE gel analysis, added to 50 µl of 4X SDS reducing buffer (components in General Methods section 2.6), snap frozen in liquid nitrogen and stored

at -20 °C until SDS-PAGE analysis (3.1.3 SDS-PAGE gel analysis). The columns were then washed with 20 x bed volumes of wash buffer. Proteins were eluted from the column with elution buffer (0.1 M Tris-HCl, pH 7.4, 10 % (v/v) glycerol, 300 mM imidazole), and collected as four fractions. For fraction one (FR1), 0.4 bed volumes of elution buffer were layered onto the Ni-NTA resin, the eluent was collected (FR1). 150 µl of FR1 for each culture was retained for SDS-PAGE gel analysis, added to 50 µl of 4X SDS reducing buffer, snap frozen in liquid nitrogen and stored at -20 °C until SDS-PAGE analysis (3.1.3 SDS-PAGE gel analysis). The column was capped and left for 5 minutes before proceeding with the elution. For each of fractions two, three and four (FR2, FR3, FR4), one bed volume of elution buffer was layered onto the Ni-NTA resin, and the resulting eluent was collected. 150 µl of FR2, FR3 and FR4 for each culture was retained for SDS-PAGE gel analysis, added to 50 µl of 4X SDS reducing buffer, snap frozen in liquid nitrogen and stored at -20 °C until SDS-PAGE analysis (3.1.3 SDS-PAGE gel analysis). A protein dye-bind assay was conducted by removing 5 µl samples of the four fractions (FR1, FR2, FR3 and FR4). The 5 µl fraction sample was combined with 145 µl of H_2O and finally 150 µl of Pierce™ Coomassie Plus (Bradford) Assay Reagent (Thermo Scientific). The fractions that contained protein (FR2 and FR3) were combined into one sample ready for cleavage of the polyhistidine-ubiquitin tag.

Purified His-tagged PEPC proteins were then digested with ubiquitin protease. For each mL of eluent (combined FR2 and FR3), 3 µl of 1.5 M mercaptoethanol and 40 µg of purified 6xHis-ubiquitin protease was added (3.1.4). The samples were incubated at 30°C for 60 minutes. After digestion, the purified protein samples were placed into dialysis tubing (16 mm diameter, 25 mm flat width, Sigma-Aldrich) and into 1.8 L dialysis buffer (50 mM EPPS, pH 8.0, 20 % (v/v) glycerol). The dialysis reaction was incubated at 4 °C overnight, with gentle stirring with a magnetic stir bar.

After dialysis the purified proteins were layered onto a pre-equilibrated Ni-NTA column (see above) and the cleaved purified PEPC protein was collected in the eluant. 0.4 bed volumes of

elution buffer were layered onto the Ni-NTA resin, the eluent was collected and retained with the eluent from the previous step, as it also contained the purified, de-tagged PEPC protein. 150 µl of the collected PEPC protein for each culture was retained for SDS-PAGE gel analysis, added to 50 µl of 4X SDS reducing buffer, snap frozen in liquid nitrogen and stored at -20 °C until SDS-PAGE analysis (3.1.3 SDS-PAGE gel analysis). The column was capped and left for 5 minutes before proceeding with the elution. Two bed volumes of elution buffer were layered onto the Ni-NTA resin, and the resulting eluent was collected (PEPC-FR1). A further two bed volumes of elution buffer were layered onto the Ni-NTA resin, and the resulting eluent was collected (PEPC-FR2). 150 µl of both PEPC-FR1 and PEPC-FR2 for each culture was retained for SDS-PAGE gel analysis, added to 50 µl of 4X SDS reducing buffer, snap frozen in liquid nitrogen and stored at -20 °C until SDS-PAGE analysis (3.1.3 SDS-PAGE gel analysis). A protein dye-bind assay was conducted by removing 5 µl samples of the three samples (PEPC, PEPC-FR1, PEPC-FR2). The 5 µl sample was combined with 145 µl of H_2O and finally 150 µl of Pierce™ Coomassie Plus (Bradford) Assay Reagent (Thermo Scientific). The purified PEPC protein was supplemented with 20 % (v/v) glycerol, snap frozen in liquid nitrogen and stored at -80 °C.

Protein samples were concentrated to 100 µl by centrifugation at 4 °C and 4,500 x *g* using a Thermo Scientific TX-150 Swinging Bucket rotor and Amicon Ultra-4 Centrifugal filters (100 kDa cut-off) in preparation for size-exclusion chromatography.

3.2.6 Gel filtration

3.2.6.1 Superdex 200 increase 10/300 GL

For purification of small volumes of protein, a Superdex 200 increase 10/300 GL column (GE Healthcare Life Sciences) was equilibrated with 20 mM HEPES, pH 7.5, 150 mM NaCl. Protein samples were separated at 0.6 ml/min with a Delta column pressure of 2.8 MPa, and 0.5 ml fractions were collected.

3.2.6.2 Highload 16/600 Superdex 200 Prep Grade

For purification of larger volumes of protein, a HiLoad 16/600 Superdex 200 Prep Grade (Amersham Biosciences) gel filtration column was equilibrated with 20 mM HEPES, pH 7.5, 150 mM NaCl. Protein samples were separated at 1 ml/min with a Delta column pressure of 0.3 MPa, and 1 ml fractions were collected.

3.2.7 Protein quantification

3.2.7.1 Bradford Assay

Proteins were quantified using a Bradford assay as described in General Methods section 2.11. In order to assess the accuracy of the Bradford method of correctly quantifying just the purified recombinant PEPC protein, 1 µg of each protein sample (*Panicum coloratum*, *S. viridis*, *Urochloa panicoides*, *Rhodothermus obamensis*, *P. coloratum* PEPC backbone + *S. viridis* PEPC insert, *U. panicoides* PEPC backbone + *P. coloratum* PEPC insert, and *S. viridis* PEPC backbone + *U. panicoides* PEPC insert) was loaded onto a SDS-PAGE gel. SDS-PAGE analysis was carried out as described in 3.1.3 SDS-PAGE gel analysis to assess the accuracy of the Bradford assay in quantifying the purified PEPC proteins.

3.2.7.2 SYPRO Ruby quantification with BSA protein standard

Protein samples, along with 100, 200, 400, 600, and 800 ng of BSA for a protein standard, were loaded onto a NuPAGE 4-12 % Bis-Tris Gel (Invitrogen) with Precision Plus Protein All Blue Standards (BioRad) and separated by SDS-PAGE. Gels were run in MES running buffer (50 mM MES, 50 mM Tris base, 3.5 mM SDS, 1 mM EDTA) at 4 °C and 200 V.

Gels were fixed in a solution containing 50 % (v/v) methanol and 7 % (v/v) acetic acid for 30 minutes with agitation on an orbital shaker (50 rpm). The wash step was repeated with fresh fixing solution. The gels were then stained overnight in SYPRO Ruby Protein Gel Stain (Invitrogen) with agitation on an orbital shaker (50 rpm). The staining step was completed keeping both gels and the SYPRO Ruby staining solution in darkness. After overnight staining, the gels were washed in a solution containing 10 % (v/v) methanol and 7 % (v/v) acetic acid for 30 minutes with agitation on an orbital shaker (50 rpm), keeping the gels in the dark. Before imaging, the gels were rinsed 3 times for 5 minutes in ultrapure water with agitation on an orbital shaker (50 rpm), keeping the gels in the dark. Gels were visualised on a ChemiDoc (Bio-Rad), using the inbuilt settings for SYPRO Ruby. Protein bands were quantified using the Quantity One software package (Bio-Rad) via the standard curve generated from 200, 400, 600, and 800 ng BSA samples. If a protein sample was outside of the 200 – 800 ng range of the BSA protein sample, the sample concentration was adjusted accordingly and another SYPRO ruby gel was run.

3.2.8 PEPC activity assays

In order to determined which gel filtration fractions contained active purified PEPC protein, PEPC activity assays were carried out as described in General Methods section 2.8.

3.3 Results

3.3.1 Test for recombinant PEPC expression in *E.coli*

Recombinant PEPC proteins were expressed in *E. coli*. (25 °C and 200 rpm) following induction by IPTG (0.5 mM final concentration). SDS-PAGE analysis of lysate and soluble protein samples showed protein bands corresponding to recombinant PEPC proteins in in both the induced lysate and induced soluble protein samples of *Panicum coloratum*, *S. viridis*, *Urochloa panicoides*, and *R. obamensis* (Figure 3.2). Protein bands corresponding to recombinant PEPC protein chimeras were also present in both the induced lysate and induced soluble protein samples *P. coloratum* PEPC backbone + *S. viridis* PEPC insert, *U. panicoides* PEPC backbone + *P. coloratum* PEPC insert, and *S. viridis* PEPC backbone + *U. panicoides* PEPC insert (Figure 3.2). PEPC protein was lost, however, between the lysate and the soluble protein steps as evidenced by the reduction in the size of the band corresponding to the PEPC protein (Figure 3.2). Protein samples from both induced and non-induced non-transformed *E. coli* cultures were collected for use as a negative control, although expression of PEPC was not seen in either induced or non-induced samples (Figure 3.2). Therefore, recombinant PEPC proteins were successfully expressed in *E. coli*.

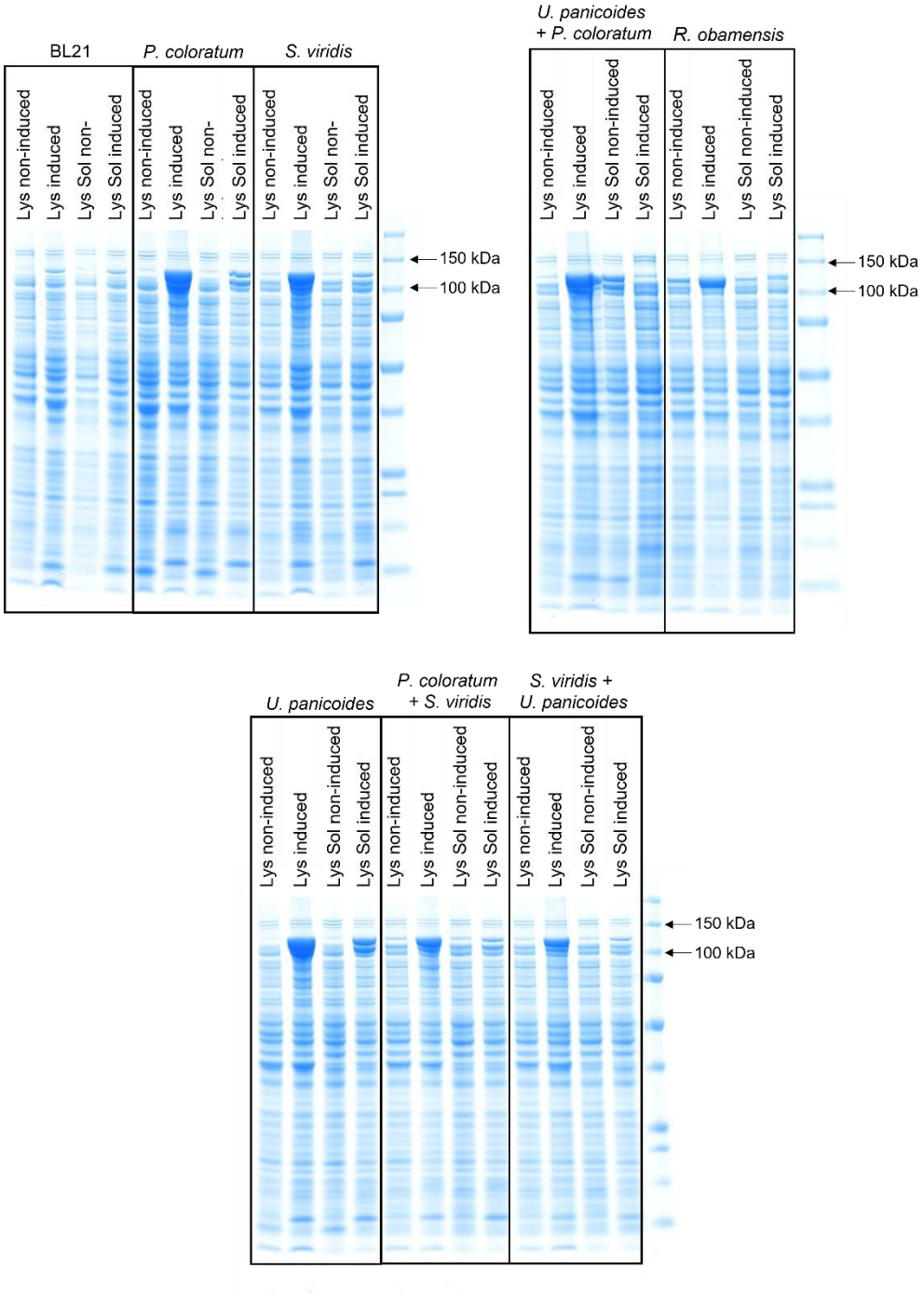

Figure 3.2. SDS-PAGE of lysate and soluble protein samples. Recombinant PEPC proteins from *Panicum coloratum*, *S. viridis*, *Urochloa panicoides*, and *R. obamensis* were successfully expressed in *E. coli*. Recombinant PEPC protein chimeras *P. coloratum* PEPC backbone + *S. viridis* PEPC insert (*P. coloratum* + *S. viridis*), *U. panicoides* PEPC backbone + *P. coloratum* PEPC insert (*U. panicoides* + *P. coloratum*), and *S. viridis* PEPC backbone + *U. panicoides* PEPC insert (*S. viridis* + *U. panicoides*) were also successfully expressed. After expression, cells were lysed and samples taken for SDS-PAGE (Lys). After centrifugation, the supernatant was removed, and samples taken for SDS-PAGE (Sol). PEPC expression was seen in induced samples, with protein being lost between the lysate and the soluble protein steps. Protein samples from both induced and non-induced *E. coli cultures* were collected (BL21), with no samples showing PEPC expression. The band corresponding to the ubiquitin tagged-PEPC peptide is between the 100 kDa and 150 kDa markers on the Precision Plus Protein All Blue Standards (BioRad) ladder.

3.3.2 Digestion of PEPC protein with ubiquitin protease

Recombinant PEPC proteins were expressed in *E. coli.* (25 °C and 200 rpm) following induction by IPTG (0.5 mM final concentration). SDS-PAGE analysis of fraction protein samples showed protein bands corresponding to recombinant PEPC proteins in fractions two and three of the elution after Ni-NTA purification of *Panicum coloratum*, *S. viridis*, and *R. obamensis* (Figure 3.3). Protein bands corresponding to recombinant PEPC protein chimeras were also present in fractions two and three of the elution after Ni-NTA purification of *P. coloratum* PEPC backbone + *S. viridis* PEPC insert, *U. panicoides* PEPC backbone + *P. coloratum* PEPC insert, and *S. viridis* PEPC backbone + *U. panicoides* PEPC insert (Figure 3.3). As expected, dye-bind assays showed that considerable protein was only present in fractions two and three and not fractions one and four (Figure 3.3). After digestion by ubiquitin protease to remove the poly-histidine tag, the purified PEPC protein was collected in the non-bind fraction that eluted off the Ni-NTA column (Figure 3.3). This can be seen as there is a considerable band corresponding to the PEPC protein in the PEPC protein (non-bind) lane of the SDS-PAGE gels between the 100 kDa and the 150 kDa markers of the Precision Plus Protein All Blue Standards (BioRad) (Figure 3.3). Some PEPC protein can still be seen in fraction 2 after digestion with ubiquitin protease (Figure 3.3). This protein would represent PEPC protein where the poly-histidine tag was not properly digested by ubiquitin protease.

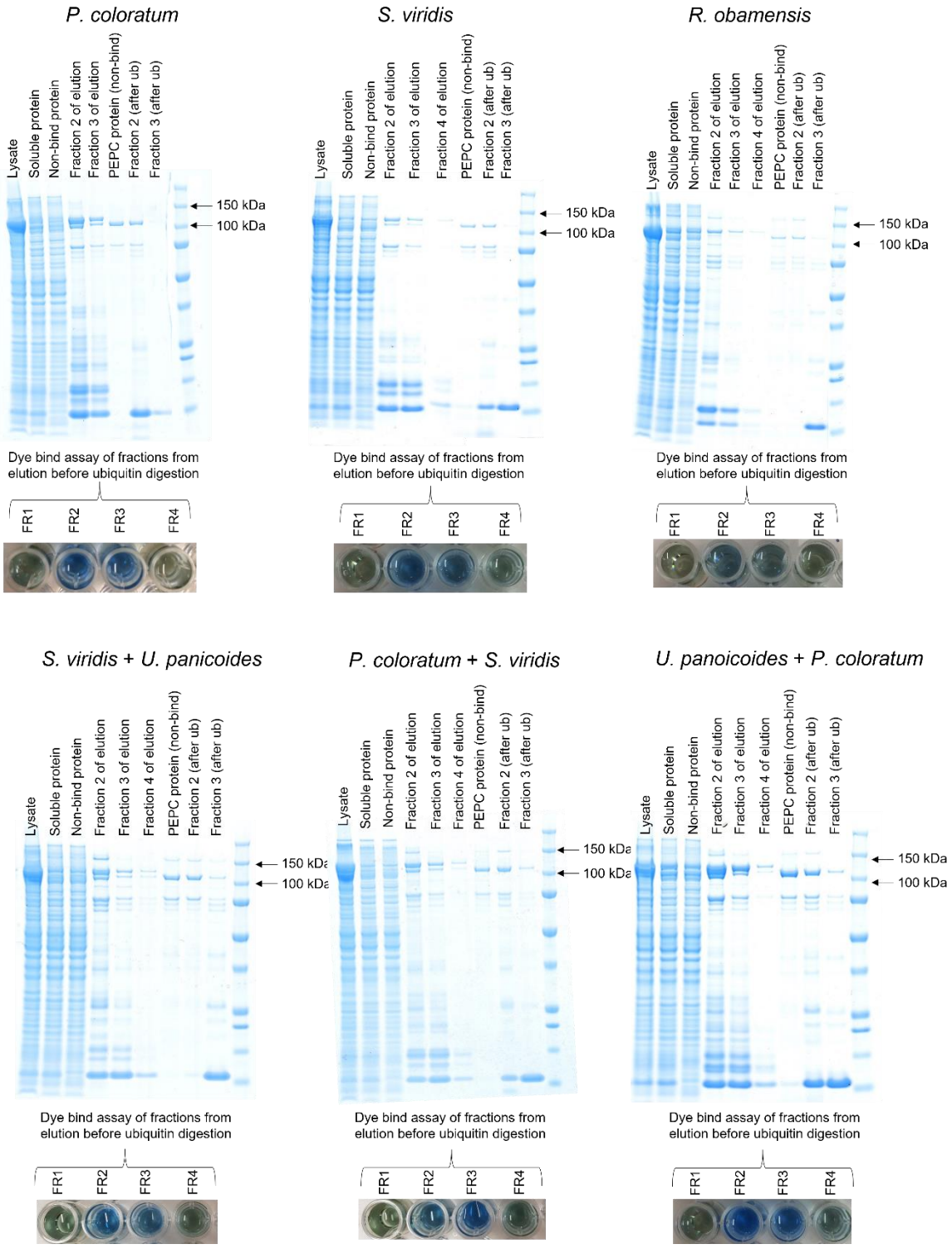

Figure 3.3. SDS-PAGE gels of lysate, soluble protein, non-bind protein, fractions 2, 3 and 4 of elution after Ni-NTA purification, PEPC protein after ubiquitin digestion, and fractions 2 and 3 after ubiquitin digestion. Dye bind assays are also shown for fraction 1, 2, 3, and 4 of elution after Ni-NTA purification. SDS-PAGE gels and dye bind assays are shown for recombinant PEPC proteins from *Panicum coloratum*, *S. viridis*, *R. obamensis* and recombinant PEPC protein chimeras *P. coloratum* PEPC backbone + *S. viridis* PEPC insert, *U. panicoides* PEPC backbone + *P. coloratum* PEPC insert, and *S. viridis* PEPC backbone + *U. panicoides* PEPC insert. The band corresponding to PEPC is between the 100 kDa and 150 kDa markers on the Precision Plus Protein All Blue Standards (BioRad) ladder.

3.3.3 Optimisation of buffers

3.3.3.1 Optimisation of imidazole concentration in wash buffer

In order to try and reduce the protein contaminants that were eluting with the purified recombinant PEPC proteins in fractions 2 and 3 of the Ni-NTA purification process, different concentrations of imidazole were tested in the wash buffer. Increasing the concentration of imidazole in the wash buffer can reduce the amount of non-specific protein binding to the Ni^{2+} matrix (Bornhorst and Falke, 2000). Four concentrations of imidazole were tested in the wash buffer (10, 20, 30, and 40 mM), and the amount of non-specifically bound protein contaminants that eluted with the recombinant PEPC protein was assessed. Protein contaminants were present with the recombinant PEPC protein at all imidazole concentrations tested (Figure 3.4). Protein contaminant levels appeared to be relatively similar between the 10 mM imidazole and the 20 mM imidazole tests (Figure 3.4). A slight reduction in protein contaminants was seen in the 40 mM imidazole test, but this also seemed to come with a reduction in the recovered recombinant PEPC protein (Figure 3.4). It was decided to continue the purification with the wash buffer containing 10 mM imidazole.

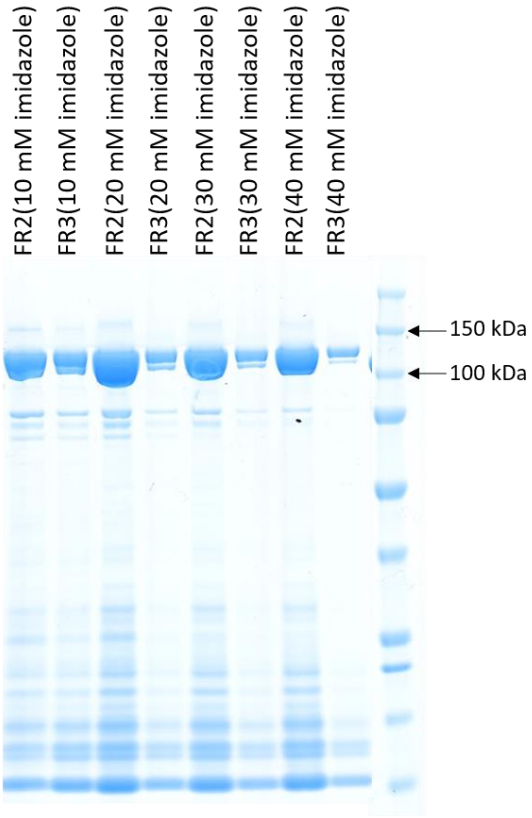

Figure 3.4. *U. panicoides* PEPC protein expressed in *E. coli* was used to test the ability of different concentrations of imidazole (10 mM, 20 mM, 30 mM, 40 mM) in the wash buffer to remove other protein contaminants. Fractions 2 and 3 (FR2, FR3), which contain the purified recombinant PEPC protein, are shown for each test concentration of imidazole. The band corresponding to the recombinant PEPC is between the 100 kDa and 150 kDa markers on the Precision Plus Protein All Blue Standards (BioRad) ladder.

3.3.3.2 Addition of $MgCl_2$ and glucose-6-phosphate to the extraction and wash buffers

In order to try and reduce the protein contaminants that were eluting with the purified recombinant PEPC proteins, $MgCl_2$ and G6P were added to the extraction and wash buffers. Three different additions to the extraction and wash buffers were trialled, 10 mM $MgCl_2$, 5 mM G6P, and 10 mM $MgCl_2$ with 5 mM G6P (Figure 3.5). After the final purification step, the amount of non-specifically bound protein contaminants that was present with the purified recombinant PEPC protein was assessed. Protein contaminants were present with the recombinant PEPC protein in all of the three extraction and wash buffers tested (Figure 3.5). The addition of 10 mM $MgCl_2$ to the extraction and wash buffer resulted in the largest purified

PEPC band, (Figure 3.5). The addition of 10 mM $MgCl_2$ with 5 mM G6P to the extraction and wash buffer appeared to result in the least amount of protein contaminants present with the purified recombinant PEPC, although much less PEPC was present than when just 10 mM $MgCl_2$ was included (Figure 3.5). Given the results of the test and the cost of G6P, it was decided to continue the purification with the extraction and wash buffer containing 10 mM $MgCl_2$.

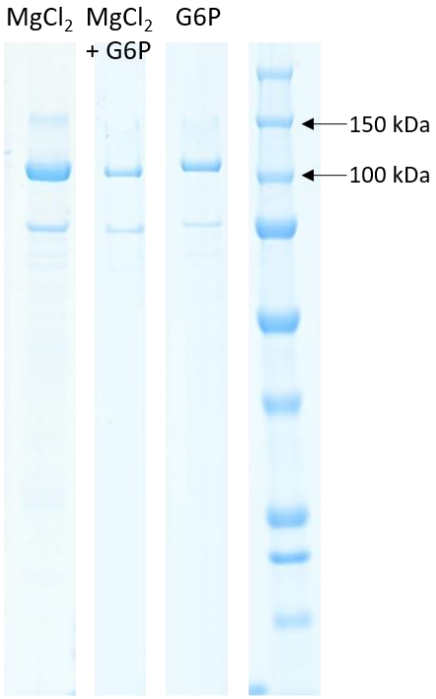

Figure 3.5. *S. viridis* PEPC protein expressed in *E. coli* was used to test the addition of 10 mM $MgCl_2$, 5 mM glucose-6-phosphate (G6P), and 10 mM $MgCl_2$ with 5 mM G6P in the extraction and wash buffers. The band corresponding to the purified PEPC with the ubiquitin tag removed is between the 100 kDa and 150 kDa markers on the Precision Plus Protein All Blue Standards (BioRad) ladder.

3.3.3.3 Addition of 300 mM NaCl to the extraction and wash buffers

In order to try and reduce the protein contaminants that were eluting with the purified recombinant PEPC proteins, 300 mM of NaCl was added to the extraction and wash buffers. Including NaCl in the extraction and wash buffers can reduce the amount of non-specific protein binding to the Ni^{2+} matrix (Bornhorst and Falke, 2000). After the final purification step,

the amount of non-specifically bound protein contaminants that were present with the purified recombinant PEPC protein was assessed. Protein contaminants were present with the recombinant PEPC protein in the extraction and wash buffers with and without 300 mM NaCl (Figure 3.6). The extraction and wash buffer containing 300 mM NaCl seemed to result in there being less contaminating protein present with the purified recombinant PEPC than when there was no NaCl present (Figure 3.6). Given the results of the test it was decided to continue the purification with the extraction and wash buffer containing 300 mM NaCl.

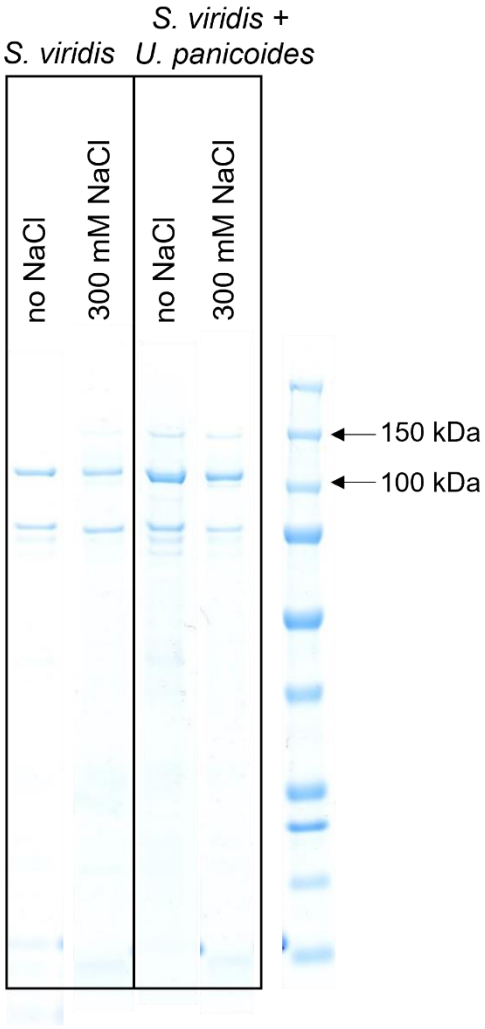

Figure 3.6. *S. viridis* and *S. viridis* PEPC backbone + *U. panicoides* PEPC insert (*S. viridis* + *U. panicoides*) PEPC proteins expressed in *E. coli* was used to test the addition of 300 mM NaCl in the extraction and wash buffers. The band corresponding to the purified PEPC with the ubiquitin tag removed is between the 100 kDa and 150 kDa markers on the Precision Plus Protein All Blue Standards (BioRad) ladder.

3.3.4 Western blot of PEPC protein samples

In order to confirm that the band between the 100 kDa and the 150 kDa band on the Precision Plus Protein All Blue Standards (BioRad) was PEPC, Western blotting was carried out on all protein samples. The purified recombinant PEPC protein samples from *R. obamensis*, *P. coloratum*, *S. viridis*, *U. panicoides*, and purified recombinant PEPC protein chimeras *P. coloratum* PEPC backbone + *S. viridis* PEPC insert, *U. panicoides* PEPC backbone + *P. coloratum* PEPC insert, and *S. viridis* PEPC backbone + *U. panicoides* PEPC insert all showed a signal between the 100 kDa and the 150 kDa band when using the anti-PEPC primary antibody (Figure 3.7). After protein samples were concentrated by centrifugation using Amicon

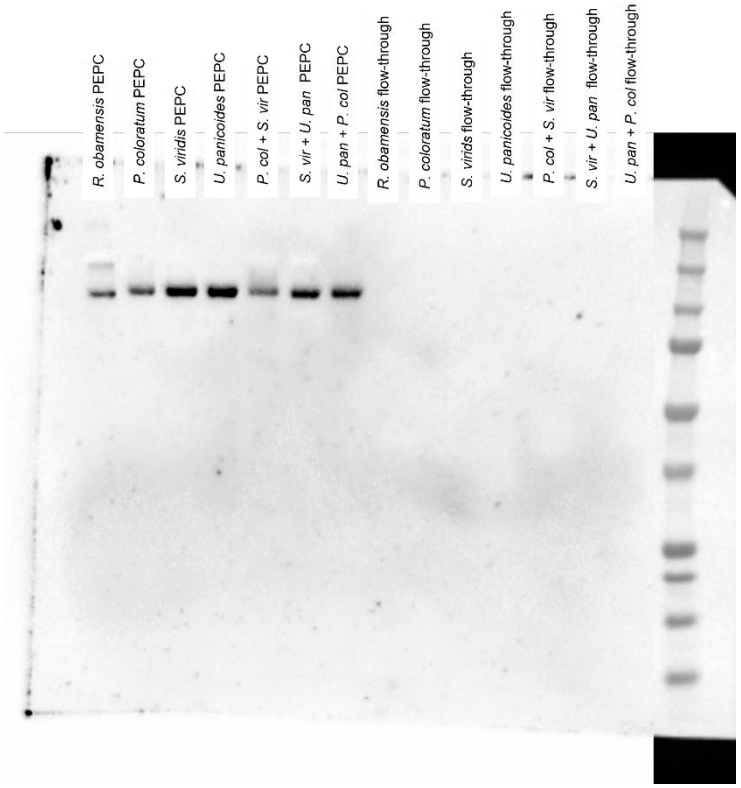

Figure 3.7. Western blot of recombinant PEPC proteins samples and their corresponding flow throughs after centrifugation with Amicon Ultra-4 centrifugal filters (100 kDa cut-off). Recombinant PEPC protein samples from *Panicum coloratum*, *S. viridis*, *Urochloa panicoides*, and *R. obamensis* and recombinant PEPC protein chimeras samples from *P. coloratum* PEPC backbone + *S. viridis* PEPC insert (Pcol+Svir), *U. panicoides* PEPC backbone + *P. coloratum* PEPC insert (Upan+Pcol), and *S. viridis* PEPC backbone + *U. panicoides* PEPC insert (Svir+Upan) all showed signals between the 100 kDa and 150 kDa markers on the Precision Plus Protein All Blue Standards (BioRad) ladder when the membrane was treated with an anti-PEPC primary antibody. After protein samples were concentrated by centrifugation using Amicon Ultra-4 Centrifugal filters (100 kDa cut-off), the flow-throughs (with no PEPC protein) were used as negative controls. No PEPC signal was seen for any of these flow-through samples.

Ultra-4 Centrifugal filters (100 kDa cut-off), the flow-throughs, which would not contain the PEPC protein, were used as negative controls. As expected, no PEPC signal was seen for any of these flow-through samples (Figure 3.7).

3.3.5 Gel filtration – Superdex 200 increase 10/300

A gel filtration step was added in after the purification of the PEPC protein by Ni-NTA IMAC in order to remove any inactivated PEPC protein aggregates and to reduce any other protein contaminants in the purified PEPC samples. Gel filtration was carried out using a Superdex 200 increase 10/300 column. In all recombinant PEPC protein samples (*Panicum coloratum*, *S. viridis*, *Urochloa panicoides*, *P. coloratum* PEPC backbone + *S. viridis* PEPC insert, *U. panicoides* PEPC backbone + *P. coloratum* PEPC insert, and *S. viridis* PEPC backbone + *U. panicoides* PEPC insert), two peaks were present (Figure 3.8, Figure 3.9). The first peak had no PEPC activity, although the SDS-PAGE analysis showed bands corresponding to PEPC protein in the fractions making up the first peak (Figure 3.8, Figure 3.9, 3.10). The SDS-PAGE analysis of the fractions making up the first peak also showed a lot of contaminating protein (Figure 3.10). This inactive PEPC and contaminating protein could be removed by gel filtration by not collecting the fractions associated with the first peak. The second peak had PEPC activity, and the SDS-PAGE analysis showed bands corresponding to PEPC protein in the fractions making up this second peak (Figure 3.8, Figure 3.9, 3.10). Some contaminating protein bands are still present in the fractions corresponding to the active PEPC protein (Figure 3.10). The second peak corresponded to proteins with an Mr consistent with the dimer form of the PEPC protein, estimated using the chromatogram provided in the manufacturer's column literature (Cytiva, 2020). Therefore, the active PEPC protein dimers are contained within the second peak, and the fractions corresponding to the second peak were collected for further studies.

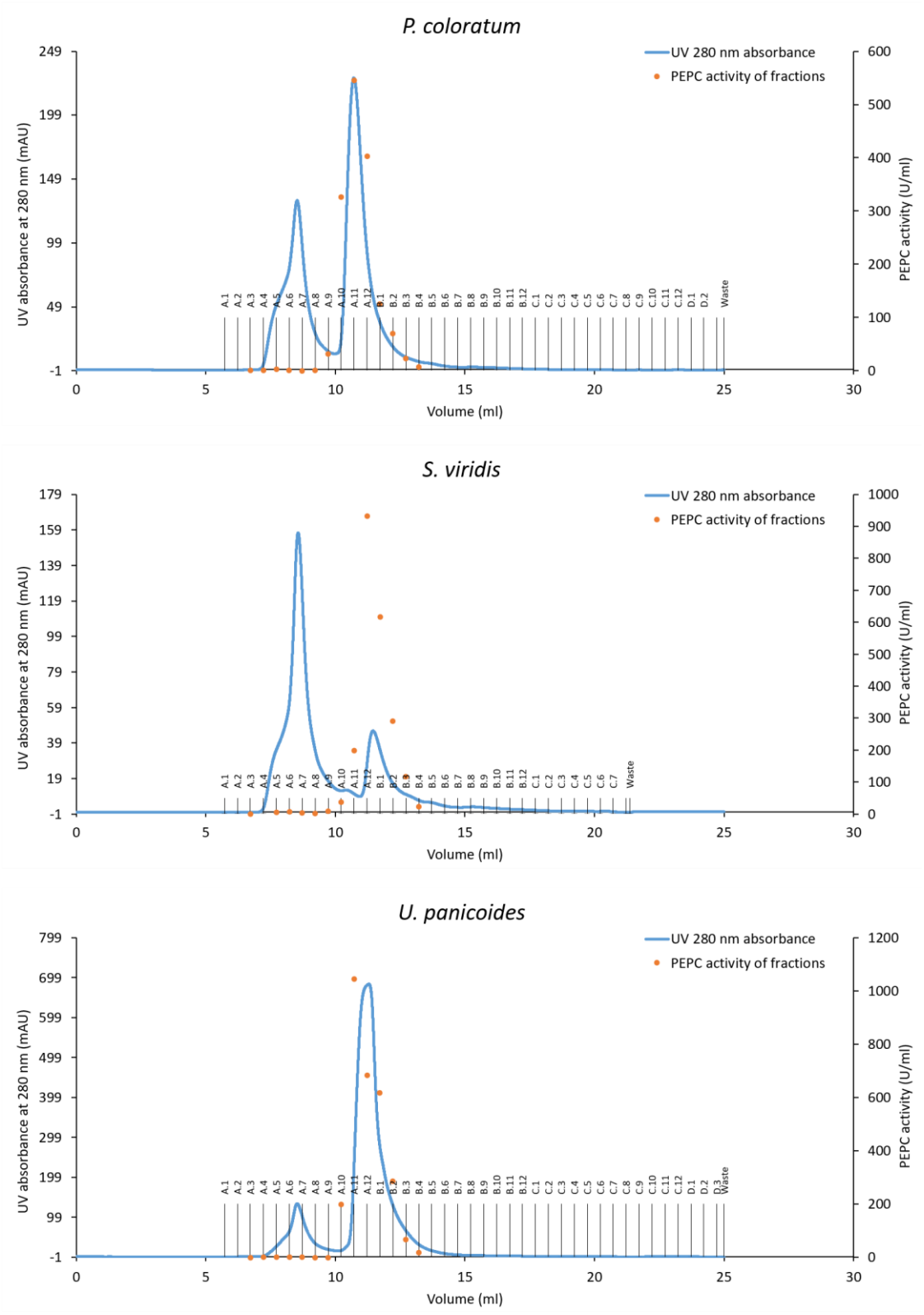

Figure 3.8. Results of gel filtration using a Superdex 200 increase 10/300 column and PEPC activity assay of gel filtration fractions for recombinant PEPC proteins from *Panicum coloratum*, *S. viridis*, *Urochloa panicoides*. The blue line shows the UV absorbance at 280 nm (mAU) of successive volumes eluting from the column. Faction numbers are indicated with lines (A.1-Waste). PEPC activity assays were conducted on the fractions, and PEPC activity (U/mL) are indicated with orange dots. In all cases, PEPC activity corresponded to the second peak.

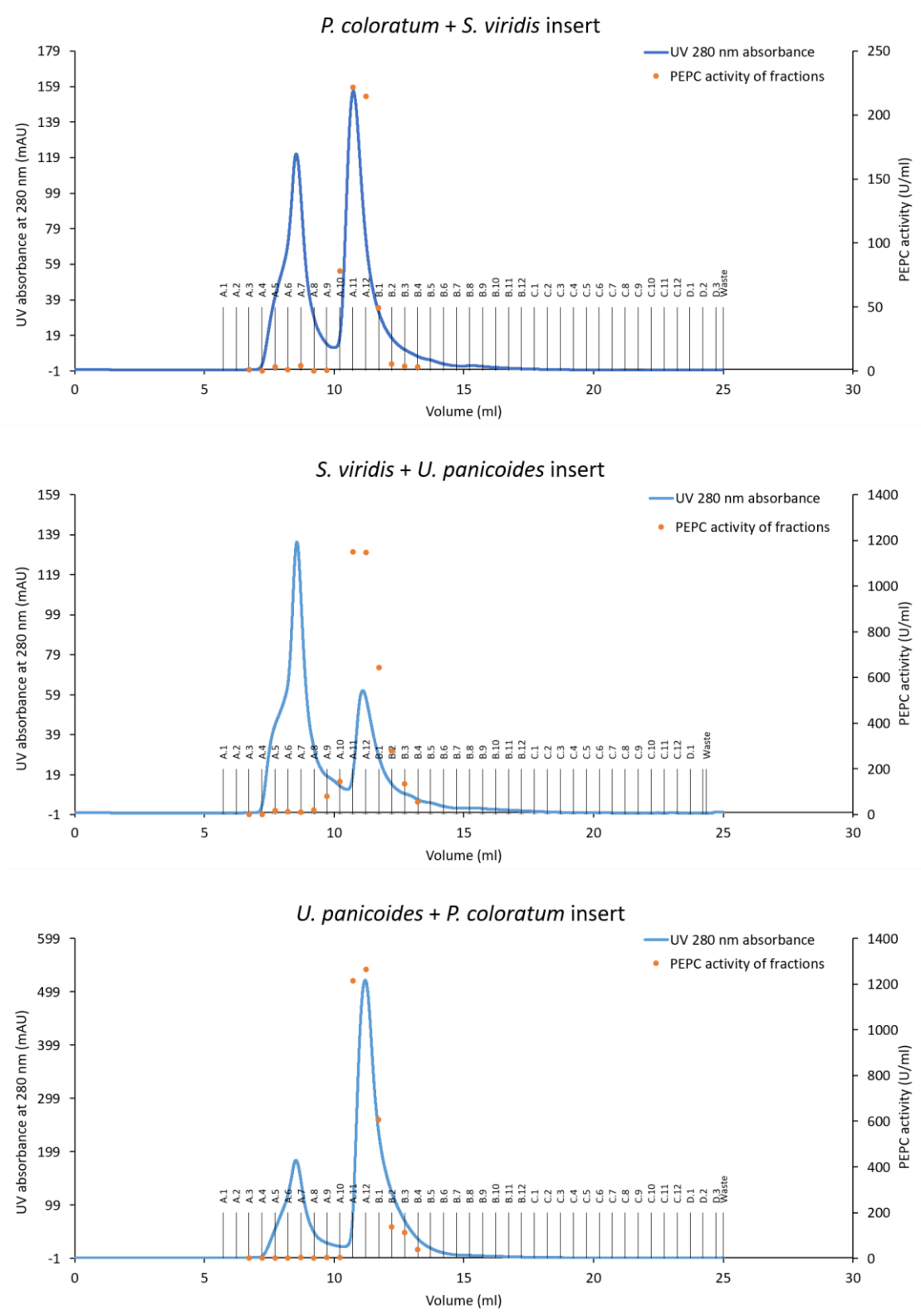

Figure 3.9. Results of gel filtration using a Superdex 200 increase 10/300 column and PEPC activity assay of gel filtration fractions for recombinant PEPC proteins from *P. coloratum* PEPC backbone + *S. viridis* PEPC insert, *U. panicoides* PEPC backbone + *P. coloratum* PEPC insert, and *S. viridis* PEPC backbone + *U. panicoides* PEPC insert. The blue line shows the UV absorbance at 280 nm (mAU) of successive volumes eluting from the column. Faction numbers are indicated with lines (A.1-Waste). PEPC activity assays were conducted on the fractions, and PEPC activity (U/mL) are indicated with orange dots. In all cases, PEPC activity corresponded to the second peak.

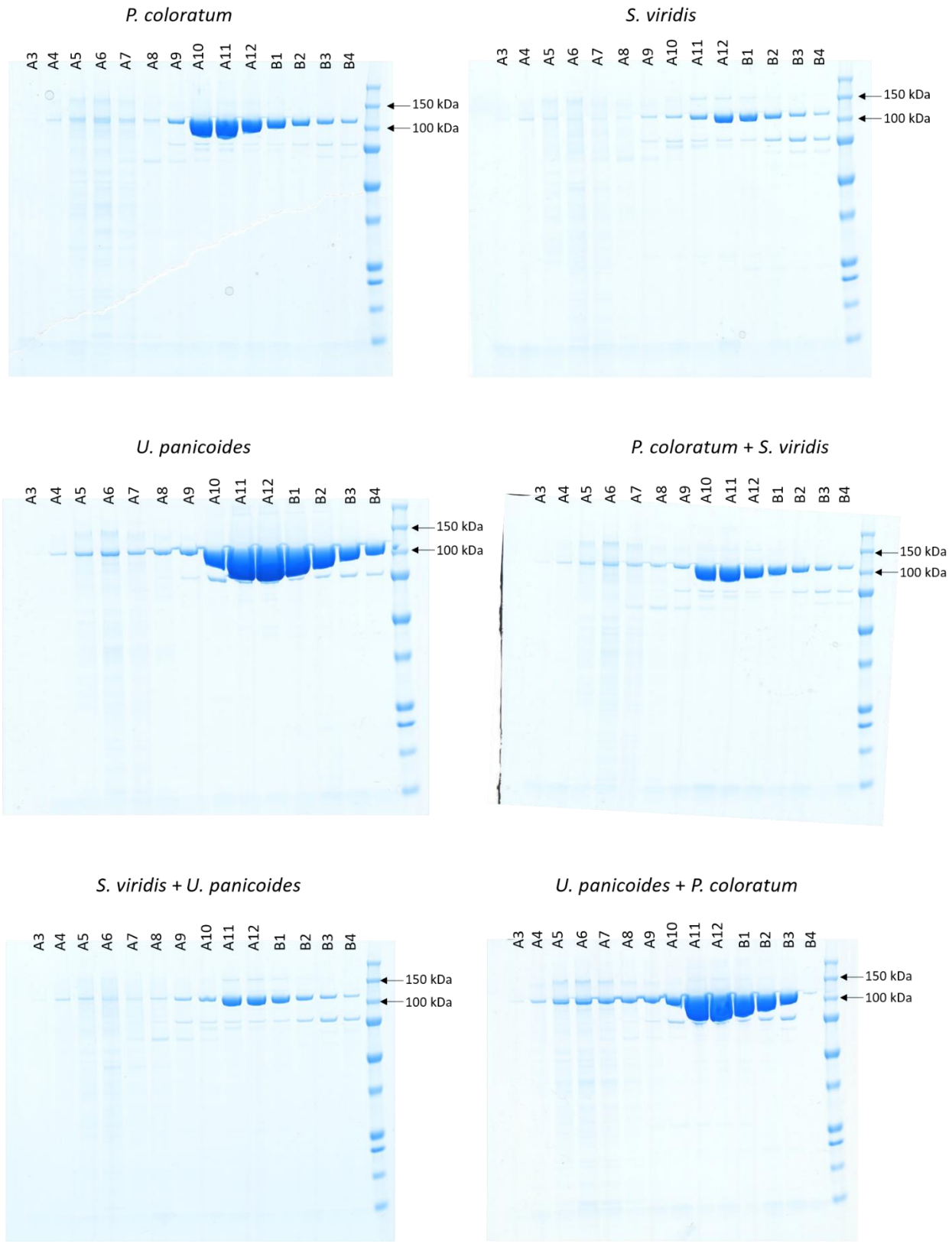

Figure 3.10. SDS-PAGE of gel fractions from gel filtration of purified PEPC proteins from *P. coloratum*, *S. viridis*, *U. panicoides*, *P. coloratum* PEPC backbone + *S. viridis* PEPC insert, *U. panicoides* PEPC backbone + *P. coloratum* PEPC insert, and *S. viridis* PEPC backbone + *U. panicoides* PEPC insert. The band corresponding to the purified PEPC with the ubiquitin tag removed is between the 100 kDa and 150 kDa markers on the Precision Plus Protein All Blue Standards (BioRad) ladder.

3.3.6 Quantification methods

3.3.6.1 Bradford assay for purified PEPC protein quantification

The results of the SDS-PAGE analysis of 1 µg of each protein sample based on the Bradford assay are shown in Figure 3.11. The size of the band corresponding to the purified PEPC protein in not the same in each of the samples, even though the same amount of protein per sample was loaded. Therefore, the contaminating proteins interfere with the quantification of PEPC protein when the Bradford assay is used as the quantification method. This is logical as the Bradford assay is an assay of total protein in a sample. Thus, the Bradford assay is not suitable for quantifying the amount of PEPC protein in a purified recombinant PEPC sample.

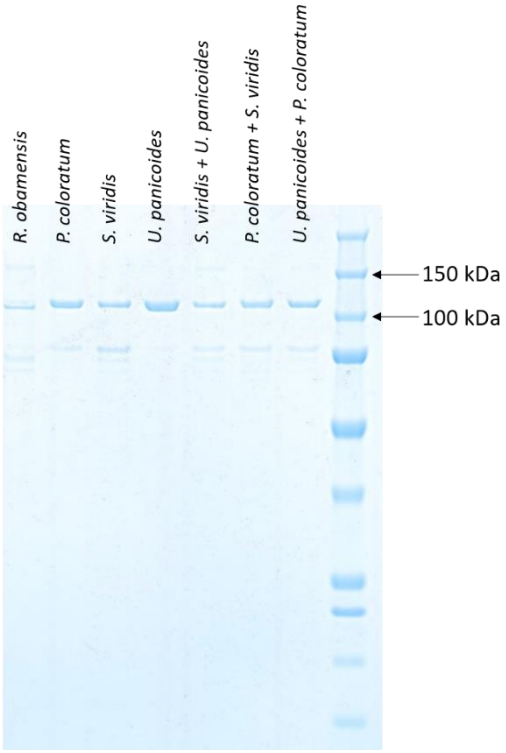

Figure 3.11. SDS-PAGE of 1 µg (based on Bradford assay) of purified PEPC proteins from *P. coloratum, S. viridis, U. panicoides, R. obamensis, P. coloratum* PEPC backbone + *S. viridis* PEPC insert, *U. panicoides* PEPC backbone + *P. coloratum* PEPC insert, and *S. viridis* PEPC backbone + *U. panicoides* PEPC insert. The band corresponding to the purified PEPC with the ubiquitin tag removed is between the 100 kDa and 150 kDa markers on the Precision Plus Protein All Blue Standards (BioRad) ladder. This band is not of equal size for each protein sample.

3.3.6.2 SYPRO Ruby assay for purified PEPC protein quantification

SYPRO Ruby was used to quantify PEPC proteins as it was possible to quantify only the bands corresponding to the PEPC proteins (Figure 3.12). Any contaminating bands present were deselected using the Quantity One software package (Bio-Rad) to make sure that they were not included in the PEPC quantification calculation.

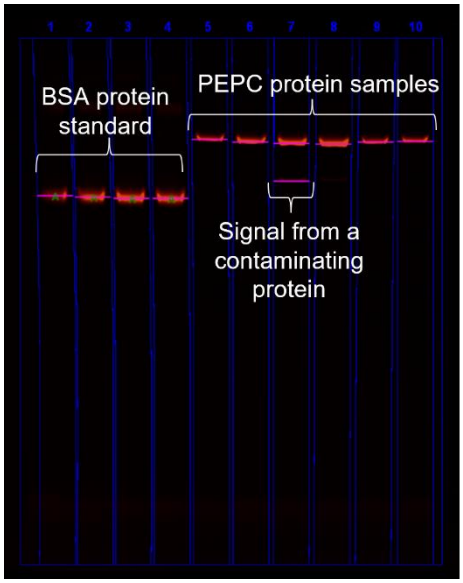

Figure 3.12. SYPRO Ruby gel showing selection of bands for quantification using the Quantity One software package (Bio Rad). The BSA protein standard (200, 400, 600, and 800 ng) can be seen on the left, with the leftmost band corresponding to the 200 ng band of BSA protein and the rightmost band corresponding to the 800 ng band of BSA protein. Signal from a contaminating protein is indicated on the gel, and this signal can be deselected so as to not influence the quantification of the PEPC protein.

3.3.7 Scaling up the production

In order to scale up the production of PEPC protein expression and purification, DNase was included in the extraction buffer to digest the large amounts of DNA present in the lysate. 1 µg DNase per mL of resuspended cells was added to the extraction buffer. A HiLoad 16/600 Superdex 200 Prep Grade gel filtration column was also used when purifying larger samples of protein as the Superdex 200 increase 10/300 GL was not able to cope with larger protein samples.

3.3.8 Final method based on the optimisation of the purification protocol

Extraction buffer (PEPC) and IMAC Wash Buffer

The extraction buffer is comprised of 0.1 M Tris-HCl, pH 7.4, 10 % (v/v) glycerol, 10 mM imidazole, 300 mM NaCl, 10 mM $MgCl_2$, supplemented with 10 mM β-mercaptoethanol, 1 mM PMSF and 1 µg DNase per mL of resuspended cells just before cell lysis.

The IMAC wash buffer is comprised of 0.1 M Tris-HCl, pH 7.4, 10 % (v/v) glycerol, 10 mM imidazole, 300 mM NaCl, 10 mM $MgCl_2$, supplemented with 10 mM β-mercaptoethanol just before use.

Elution Buffer

The extraction buffer is comprised of 0.1 M Tris-HCl, pH 7.4, 10 % (v/v) glycerol, and 300 mM Imidazole.

Dialysis Buffer

The dialysis buffer contains 0.5 M EPPS-OH, pH 8.0, 20 % (v/v) glycerol.

Pre-extraction preparation

1. IMAC columns were prepared by adding two bed volumes of the Ni-NTA agarose (Qiagen) resin slurry into a plastic column. For equilibration, ten bed volumes of wash buffer onto the Ni-NTA resin.
2. Abbreviations used in the following method and descriptions of what each protein sample contains are as follows:

Abbreviation	Protein sample
LYS	lysate
SOL	soluble protein
NB	non-bind protein
FR1	No Ni-NTA purified ^{H6}Ub-PEPC protein
FR2	Ni-NTA purified ^{H6}Ub-PEPC protein
FR3	Ni-NTA purified ^{H6}Ub-PEPC protein
FR4	No/little Ni-NTA purified ^{H6}Ub- PEPC protein
PEPC	Ni-NTA pure PEPC protein
PEPC-FR1	Protein left bound to the column (including ubiquitin protease and any undigested PEPC protein)

PEPC-FR2	Protein left bound to the column (including ubiquitin protease and any undigested PEPC protein)

Polyhistidine-ubiquitin-PEPC fusion protein extraction

3. *E. coli* cell pellets were resuspended in 15 mL extraction buffer per 200 mL cell culture and 1 mM PMSF and 1 µg DNase per mL of resuspended cells was added to the solution. Cell lysis was achieved by three sequential passes through a French pressure cell (Aminco) precooled to 4 °C at 1000 psi. 75 µl of lysate was added to 25 µl of 4X SDS reducing buffer (LYS), samples were snap frozen in liquid nitrogen and stored at -20 °C until SDS-PAGE analysis.
4. The lysed cells were centrifuged for 5 minutes at 15,000 rpm and 4 °C
5. The supernatant, containing soluble protein, was removed from the pellet and 75 µl of the supernatant was added to 25 µl of 4X SDS reducing buffer (SOL), samples were snap frozen in liquid nitrogen and stored at -20 °C until SDS-PAGE analysis.
6. From this point forward, the following steps were carried out at 4 °C.
7. The soluble protein was layered onto the equilibrated Ni-NTA resin and 75 µl of the column eluent was added to 25 µl of 4X SDS reducing buffer (NB), samples were snap frozen in liquid nitrogen and stored at -20 °C until SDS-PAGE analysis. The remaining column eluent was discarded.
8. Next, twenty bed volumes of wash buffer was run through the Ni-NTA resin, the column eluent was discarded.

Eluting the polyhistidine-ubiquitin-PEPC fusion protein

9. 0.4 bed volumes of elution buffer were layered onto the Ni-NTA resin, the eluent was collected (FR1). From the collected fraction 1, 75 µl was added to 25 µl of 4X SDS reducing buffer, samples were snap frozen in liquid nitrogen and stored at -20 °C until

SDS-PAGE analysis. The column was capped and left for 5 minutes before proceeding with the elution.

10. One bed volume of elution buffer was layered onto the Ni-NTA resin, and the resulting eluent was collected (FR2). From the collected fraction 2, 75 µl was added to 25 µl of 4X SDS reducing buffer, samples were snap frozen in liquid nitrogen and stored at -20 °C until SDS-PAGE analysis.
11. One bed volume of elution buffer was layered onto the Ni-NTA resin, and the resulting eluent was collected (FR3). From the collected fraction 3, 75 µl was added to 25 µl of 4X SDS reducing buffer, samples were snap frozen in liquid nitrogen and stored at -20 °C until SDS-PAGE analysis.
12. One bed volume of elution buffer was layered onto the Ni-NTA resin, and the resulting eluent was collected (FR4). From the collected fraction 4, 75 µl was added to 25 µl of 4X SDS reducing buffer, samples were snap frozen in liquid nitrogen and stored at -20 °C until SDS-PAGE analysis.
13. A protein dye-bind assay was conducted by removing 5 µl samples of the four fractions (FR1, FR2, FR3 and FR4). The 5 µl fraction sample was combined with 145 µl of H_2O and finally 150 µl of Pierce™ Coomassie Plus (Bradford) Assay Reagent (Thermo Scientific)
14. The fractions that contained protein (FR2 and FR3) were combined into one sample ready for cleavage of the polyhistidine-ubiquitin tag.

Cleaving the polyhistidine-ubiquitin tag

15. For each mL of eluent (combined FR2 and FR3), 3 µl of 1.5 M mercaptoethanol and 40 µg of purified 6xHis-ubiquitin protease was added (3.1.4).
16. The samples were incubated at 30°C for 60 minutes.

Dialysis

17. After digestion, the purified protein samples were placed into dialysis tubing (16 mm diameter, 25 mm flat width, Sigma-Aldrich) using dialysis clips to stop the sample escaping. The dialysis tubes with purified protein samples were placed into 1.8 L dialysis buffer (50 mM EPPS, pH 8.0, 20 % (v/v) glycerol).. The dialysis reaction was incubated at 4 °C overnight, with gentle stirring with a magnetic stir bar.
18. Dialysed protein samples were collected from dialysis tubing ready for removal of the cleaved polyhistidine-ubiquitin tag.

Collecting the pure PEPC protein

19. IMAC columns were prepared by adding two bed volumes of the Ni-NTA agarose (Qiagen) resin slurry into a plastic column. For equilibration, ten bed volumes of wash buffer onto the Ni-NTA resin.
20. The dialysed protein sample was layered onto the onto the equilibrated Ni-NTA resin, the eluent was collected and retained as it contained the purified, de-tagged PEPC protein (PEPC).
21. 0.4 bed volumes of elution buffer were layered onto the Ni-NTA resin, the eluent was collected and retained with the eluent from the previous step, as it contained the purified, de-tagged PEPC protein (PEPC). From the collected PEPC sample, 75 µl was added to 25 µl of 4X SDS reducing buffer, samples were snap frozen in liquid nitrogen and stored at -20 °C until SDS-PAGE analysis. The column was capped and left for 5 minutes before proceeding with the elution.
22. Two bed volumes of elution buffer were layered onto the Ni-NTA resin, and the resulting eluent was collected (PEPC-FR1). From the collected fraction, 75 µl was added to 25 µl of 4X SDS reducing buffer, samples were snap frozen in liquid nitrogen and stored at -20 °C until SDS-PAGE analysis.

23. A further two bed volumes of elution buffer were layered onto the Ni-NTA resin, and the resulting eluent was collected (PEPC-FR2). From the collected fraction, 75 µl was added to 25 µl of 4X SDS reducing buffer, samples were snap frozen in liquid nitrogen and stored at -20 °C until SDS-PAGE analysis.
24. A protein dye-bind assay was conducted by removing 5 µl samples of the three samples (PEPC, PEPC-FR1, PEPC-FR3). The 5 µl sample was combined with 145 µl of H_2O and finally 150 µl of Pierce™ Coomassie Plus (Bradford) Assay Reagent (Thermo Scientific).
25. The purified PEPC protein was supplemented with 20 % (v/v) glycerol, snap frozen in liquid nitrogen and stored at -80 °C.

Protein concentration

26. Protein samples were concentrated to 100 µl by centrifugation at 4 °C and 4,500 x *g* using a Thermo Scientific TX-150 Swinging Bucket rotor and Amicon Ultra-4 Centrifugal filters (100 kDa cut-off) in preparation for size-exclusion chromatography.

Gel filtration

27. As described in section 3.2.4 Gel filtration, using either a Superdex 200 increase 10/300 GL column (GE Healthcare Life Sciences) as described in 3.2.6.1 or a Highload 16/600 Superdex 200 Prep Grade (Amersham Biosciences) as described in 3.2.6.2 depending on protein sample size.

Protein Quantification

28. Protein concentrations were quantified using the SYPRO Ruby method as described in section 3.2.7.2 SYPRO Ruby quantification with BSA protein standard.

3.4 Discussion

A method for the expression, purification and quantification of PEPC protein using *E. coli* as an expression system has been successfully established and optimised. This method will be used in Chapter 4 to investigate differences in kinetic properties between enzymes expressed in and purified from *E. coli*.

3.4.1 PEPC protein purified as a dimer

The PEPC protein from many plant species have been purified in the more active tetrameric form, although it has also been shown to purify as a mixture of dimers and tetramers (Ting and Osmond, 1973c; Miziorko et al., 1974; Nott and Osmond, 1982; Huber et al., 1986; Iglesias et al., 1986; Stiborová and Leblová, 1986; Walker et al., 1986; Podesta and Andreo, 1989; Willeford et al., 1990; Arrio-Dupont et al., 1992; Svensson et al., 1997). The PEPC enzyme has an inherent tendency to dissociate into dimers, as it only has salt bridges between the Arg 438 of one subunit and Glu433 of another subunit holding the tetramer together (Kai et al., 1999). Given that 150 mM NaCl was included in the gel filtration buffer, it is not surprising that the PEPC protein eluted from the gel filtration columns as a dimer. NaCl has been shown to cause the PEPC tetramer to dissociate into dimers (Wagner et al., 1987; McNaughton et al., 1989; Podesta and Andreo, 1989). The fact that the *Paniceae* PEPCs were purified as a dimer is not concerning as a number of studies have found that whether the PEPC enzyme is a dimer or a tetramer depends on the conditions of the solution containing the PEPC. However, this may also suggest a further element of regulation of activity of PEPC isoforms from *Paniceae* C_4 grasses. When the dimeric PEPC is placed into a PEPC assay buffer which includes 5 mM $MgCl_2$, 1 mM $KHCO_3$, and 5 mM G6P, the dimeric PEPC protein will be induced to form tetramers. Mg^{2+}, G6P and HCO_3^- have all been shown to induce PEPC dimer to form PEPC tetramers (Wu and Wedding, 1985; Willeford et al., 1990; Wu et al., 1990; Meyer et al., 1991; Wedding et al., 1994). Therefore, it is likely that once the PEPC enzyme is in the PEPC activity buffer the enzyme will be in tetrameric form, even before PEP is added to initiate the reaction.

PEP, has also been shown to induce tetramer formation and stabilise the tetrameric form of the PEPC enzyme (Wu and Wedding, 1985, 1987; Willeford et al., 1990; Wu et al., 1990; Meyer et al., 1991; Willeford and Wedding, 1992; Wedding et al., 1994). Therefore, future experiments will be required to determine the significance of the recombinant PEPCs being purified in the dimer form. This will be important to unravel the mechanism for tetramer formation and how factors such as protein concentration, substrate, activator and inhibitor molecules influence PEPC quaternary structure both individually and in combination.

3.4.2 PEPC-negative strain of *E. coli*

A PEPC-negative strain of *E. coli* (PCR1) has been used for a handful of studies investigating PEPC kinetic and regulatory properties in the genus *Flaveria* and *Alternanthera* (Svensson et al., 1997; Westhoff et al., 1997; Bläsing et al., 2002; Gowik et al., 2006; DiMario and Cousins, 2019). Utilising this PCR1 strain for expressing and purifying recombinant PEPC would be highly beneficial as there would be no chance that untagged monomers of endogenous bacterial PEPC could combine with monomers of tagged recombinant PEPC protein to form heterologous dimers. Determining whether or not it is possible to obtain the PCR1 strain for any future PEPC kinetic studies should be investigated.

3.5 Conclusions

As a result of the work completed in this chapter, a method for the expression, purification and quantification of PEPC protein using *E. coli* as an expression system has been successfully established and optimised. This method can be used by the lab to investigate the different properties of PEPC proteins.

Chapter 4: PEPC Michaelis Menten kinetics in different C_4 photosynthetic subtypes

4.1 Introduction

4.1.1 C_4 photosynthetic subtypes

C_4 plants can be classified into three subcategories based on the most prevalent decarboxylating enzyme present in the bundle sheath cells: NADP-malic enzyme-type, NAD-malic enzyme-type or PEP carboxykinase-type (Kanai and Edwards, 1999). These subtypes are not mutually exclusive, however, as decarboxylation by the most abundant decarboxylating enzyme does not prevent low level activity of another (Furbank, 2011). Examples of this can be seen in the NADP-ME species sorghum, *Zea mays,* and *Panicum antidotale*, and the NAD-ME species *Bienertia sinuspersici*, *Cleome angustifolia*, and *Panicum coloratum*, all of which have PEPCK activity (Sharwood et al., 2016). Regardless of subtype, C_4 photosynthesis in all C_4 plants first involves the hydration of atmospheric CO_2 by CA, forming bicarbonate (HCO_3^-) (Figure 4.1; Tashian, 1989). This is followed by the carboxylation of PEP to form OAA, in a reaction catalysed by PEPC, in the mesophyll cytosol (Figure 4.1; Hatch et al., 1971; Kanai and Edwards, 1999). Given that each C_4 subtype has a different mesophyll environment, the PEPC enzyme could have continued to evolve to adapt for each the specific mesophyll conditions present in each subtype.

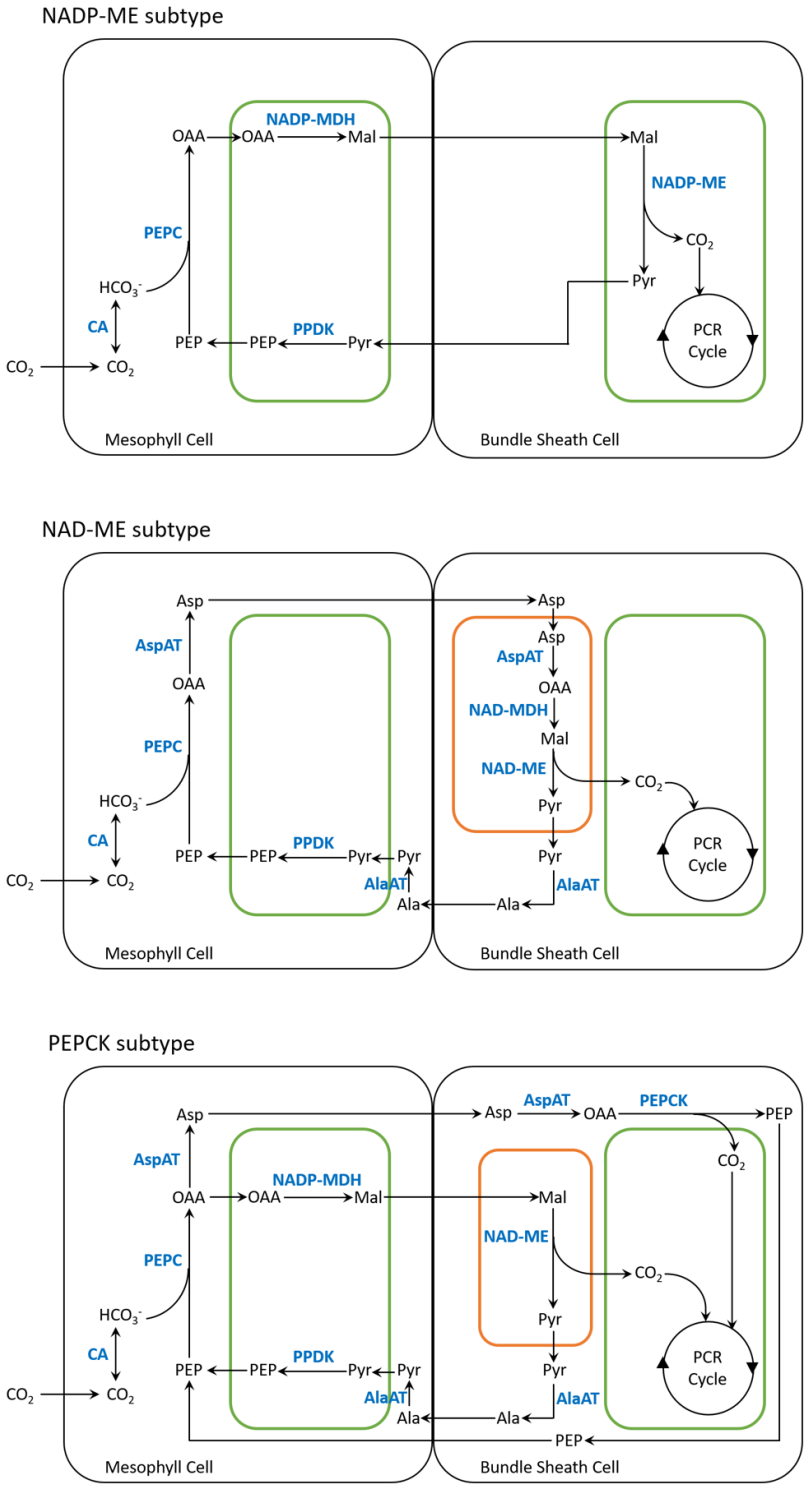

Figure 4.1. Schematics of NADP-ME, NAD-ME and PEPCK C_4 photosynthetic subtypes. Green boxes represent chloroplasts and orange boxes represent mitochondria. Metabolites are abbreviated as follows phosphoenolpyruvate (PEP), oxaloacetate (OAA), malate (Mal) aspartate (Asp), pyruvate (Pyr), and alanine (Ala). Enzymes involved in C_4 photosynthesis reactions are indicated in blue and are abbreviated as follow: carbonic anhydrase (CA), phosphoenolpyruvate carboxylase (PEPC), NADP-malate dehydrogenase (NADP-MDH), NADP-malic enzyme (NADP-ME), pyruvate phosphate dikinase (PPDK), aspartate aminotransferase (AspAT), alanine aminotransferase (AlaAT) and phosphoenolpyruvate carboxykinase (PEPCK). Figure adapted from Ludwig (2016).

4.1.1.1 NADP-ME Subtype

The OAA produced by the PEPC-catalysed carboxylation of PEP is transported into the mesophyll chloroplast where it is reduced to malate in a reaction catalysed by NADP-malate dehydrogenase (NADP-MDH) (Figure 4.1; Hatch and Slack, 1966; Kanai and Edwards, 1999). The malate diffuses into the bundle sheath cell and is transferred into the bundle sheath cell chloroplast where it is decarboxylated by NADP-ME, producing pyruvate and CO_2 (Figure 4.1; Hatch et al., 1971; Hatch et al., 1975; Kanai and Edwards, 1999). The CO_2 is fixed by Rubisco, entering the photosynthetic carbon reduction (PCR) cycle. The pyruvate diffuses into the mesophyll cell and is transported into the mesophyll chloroplast where it is phosphorylated to form PEP in a reaction catalysed by pyruvate phosphate dikinase (PPDK) (Figure 4.1; Kanai and Edwards, 1999). This regenerated PEP is transferred into the mesophyll cytosol, where it can then be carboxylated by PEPC to form OAA and the C_4 cycle can continue (Figure 4.1; Kanai and Edwards, 1999). The NADP-ME subtype is the most prevalent of the C_4 photosynthetic subtypes and includes the agriculturally important crop grasses *Zea mays* (maize), sorghum, sugar cane, and two millet species *Pennisetum glaucum* and *Setaria italica* (Sage et al., 1999; Ludwig, 2016).

4.1.1.2 NAD-ME Subtype

The OAA produced by the PEPC-catalysed carboxylation of PEP is transaminated to aspartate in a reaction catalysed by aspartate aminotransferase (AspAT) in the mesophyll cytosol (Figure 4.1; Kanai and Edwards, 1999). The resulting aspartate diffuses into the bundle sheath cell and enters the BSC mitochondrion where it is first converted back to OAA by AspAT (Figure 4.1; Hatch et al., 1975; Kanai and Edwards, 1999). The OAA is then reduced to malate in a reaction catalysed by NADP-MDH and the malate is then decarboxylated by NAD-ME producing pyruvate and CO_2 (Figure 4.1; Hatch et al., 1975; Kanai and Edwards, 1999). The CO_2 released by the decarboxylation of malate diffuses out of the bundle sheath cell mitochondrion and into the bundle sheath cell chloroplast, where Rubisco is located (Figure 4.1; Kanai and Edwards,

1999). The CO_2 is fixed by Rubisco, entering the PCR cycle (Figure 4.1; Ludwig, 2016). The pyruvate diffuses out of the mitochondrion into the bundle sheath cytosol where it is transaminated by alanine aminotransferase (AlaAT) forming alanine (Figure 4.1; Kanai and Edwards, 1999; Ludwig, 2016). The resulting alanine diffuses into the mesophyll cell cytosol where it is converted back into pyruvate by AlaAT (Figure 4.1; Kanai and Edwards, 1999; Ludwig, 2016). The pyruvate is transferred into the mesophyll chloroplast where it is phosphorylated by PPDK to form PEP (Figure 4.1; Kanai and Edwards, 1999). This regenerated PEP is transferred into the mesophyll cytosol, where it can then be carboxylated by PEPC to form OAA and the C_4 cycle can continue (Figure 4.1; Kanai and Edwards, 1999). The NAD-ME includes the agriculturally important crop grass *Panicum miliaceum*, one of the millet species (Sage et al., 1999).

4.1.1.3 PEPCK subtype

In the phosphoenolpyruvate carboxykinase (PEPCK subtype), the OAA produced by PEPC is converted to both malate and aspartate. The OAA produced by the PEPC-catalysed carboxylation of PEP is either transaminated to aspartate by AspAT in the mesophyll cytosol, or is transported into the mesophyll chloroplast where it is reduced to malate by NADP-MDH (Figure 4.1; Kanai and Edwards, 1999; Ludwig, 2016). The aspartate resulting from the former reaction diffuses into the bundle sheath cell, but instead of entering the mitochondrion it is deaminated back to OAA by AspAT in the bundle sheath cell cytosol (Figure 4.1; Kanai and Edwards, 1999; Ludwig, 2016). The OAA is then decarboxylated in a reaction catalysed by PEPCK, producing CO_2 and PEP (Figure 4.1; Hatch et al., 1975). The CO_2 released by the decarboxylation reaction diffuses into the bundle sheath cell chloroplast where it is fixed Rubisco, entering the PCR (Figure 4,1; Ludwig, 2016). The PEP diffuses into the mesophyll cell cytosol, where it can then be carboxylated by PEPC to form OAA and the C_4 cycle can continue (Figure 4.1; Wang et al., 2014). The malate formed in the mesophyll chloroplasts is transported out of the organelle, diffuses into the bundle sheath cell and is then transported into

the mitochondrion (Figure 4,1; Ludwig, 2016). Here the malate is decarboxylated by NAD-ME forming pyruvate and CO_2 (Figure 4,1; Kanai and Edwards, 1999). The CO_2 diffuses out of the bundle sheath cell mitochondrion and into the bundle sheath cell chloroplast, where it is fixed by Rubisco, entering the PCR cycle (Figure 4,1; Kanai and Edwards, 1999; Ludwig, 2016). Similarly to the NAD-ME pathway, the pyruvate is transaminated by AlaAT to forming alanine (Figure 4,1; Kanai and Edwards, 1999; Ludwig, 2016). The resulting alanine diffuses into the mesophyll cell cytosol where it is converted back into pyruvate by AlaAT (Figure 4,1; Kanai and Edwards, 1999; Ludwig, 2016). The pyruvate is transferred into the mesophyll chloroplast where it is converted to PEP by PPDK (Figure 4,1; Kanai and Edwards, 1999). This regenerated PEP is transferred into the mesophyll cytosol, where it can then be carboxylated by PEPC to form OAA and the C_4 cycle can continue (Figure 4,1; Kanai and Edwards, 1999).

4.1.2 Mesophyll environment in C_4 subtypes

High concentrations of malate in the mesophyll cells compared with the bundle sheath cells create concentration gradients sufficient to drive rapid diffusion of malate into the bundle sheath cells (Stitt and Heldt, 1985), driving the photosynthetic carbon flux. With estimated mesophyll malate concentrations of 11.18 mM in the presence of light and CO_2, and C_4 plants having recorded *in vitro* K_i malate (pH 7.0 – 8.0; 25 - 30 °C) between approximately 0.24 mM and 5 mM, cytosolic malate in the mesophyll should affect PEPC activity (Table 4.1, Table 4.3; Raghavendra and Das, 1975; McNaughton et al., 1989; Parvathi et al., 2000; Engelmann et al., 2003; Arrivault et al., 2017). Therefore, investigation of the inhibition of PEPCs enzymes by malate and aspartate will be investigated in this chapter of the thesis.

Table 4.1 Concentration of metabolites in the mesophyll and bundle sheath cells of *Zea mays* leaves. Data taken from Arrivault et al. (2017). Metabolites were quantified with LC-MS/MS and GC-MS spiked with authentic standards. Metabolites quantified were malate, aspartate, pyruvate, alanine, phosphenolpyruvate (PEP), phosphoglycerates (PGAs), and dihydroxyacetone phosphate (DHAP).

Compound	mM		
	Bundle Sheath Cells (BSCs)	Mesophyll Cells (MCs)	Concentration gradient (MCs to BSCs)
Malate (L)	5.20	11.18	5.99
Aspartate	0.21	1.17	0.96
Pyruvate	0.26	1.53	1.27
Alanine	11.33	10.65	-0.68
PEP	0.79	0.38	-0.40
PGAs	4.73	1.87	-2.87
DHAP	1.29	2.73	1.43

4.1.3 Deletion in PEPC sequence specific to PEPCK-subtype species

When conducting a review of C_4 PEPC sequences at the start of this thesis project, a PEPCK-specific deletion was discovered toward the C-terminal end of the primary sequence of the PEPC enzyme. This deletion was not observed in the sequence of the PEPC enzyme from NADP-ME and NAD-ME species. In the PEPCK species, six amino acids were missing from the primary sequence of PEPCK PEPC enzymes when compared to the PEPC sequences of NADP-ME and NADP-ME species (Figure 4.2). This PEPCK subtype specific region is

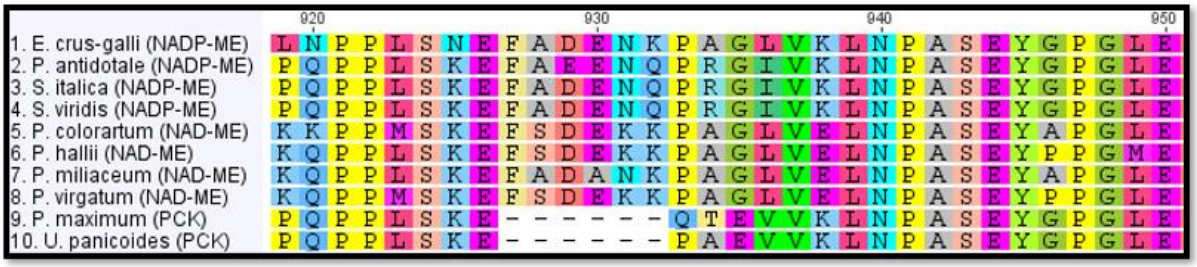

Figure 4.2. Section of the alignment of PEPC amino acid sequences from NADP-ME, NAD-ME and PEPCK subtypes showing six missing amino acids in the PEPCK PEPC sequences. The alignment includes the PEPC sequences of NADP-ME species Echinochloa crus-galli, Panicum antidotale, Setaria italica, and Setaria viridis, NAD-ME species Panicum coloratum, Panicum hallii, Panicum miliaceum, and Panicum virgatum and PEPCK species Panicum maximum (now Megathyrsus maximus) and Urochloa panicoides.

located amongst the malate and aspartate binding residues of the PEPC primary sequence (Figure 4.3). Therefore, the effect of this PEPCK-specific region on inhibition of the PEPC enzyme by malate and aspartate will be investigated in this chapter.

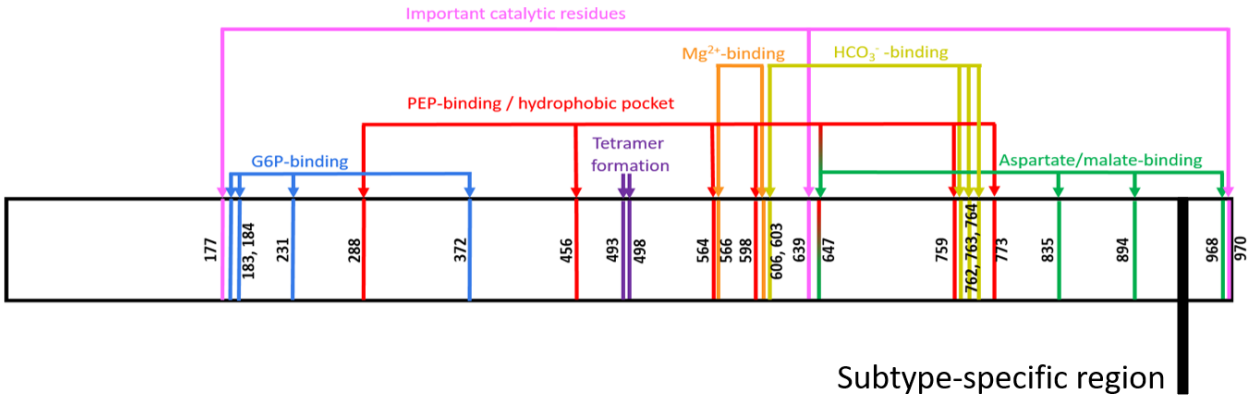

Figure 4.3. Location of the PEPCK-specific deletion with respect to the important residues for a functional phosphoenolpyruvate carboxylase. The subtype-specific region (indicated by a thick black line) is amongst the residues necessary for aspartate/ malate inhibitor interactions (shown in green). All numbering shown in the figure corresponds to the C_4 *Zea mays* PEPC monomer.

The location of this PEPCK-specific deletion in the tertiary sequence was investigated using I-TASSER (Yang et al., 2015; Yang and Zhang, 2015), according to General Methods section 2.12. The PEPC sequences from *Urochloa panicoides*, a PEPCK species and *Setaria viridis*, a NADP-ME species were submitted to I-TASSER and tertiary structures were obtained (Figure 4.4). When present in the PEPCs of NADP-ME and NAD-ME species, these six amino acid residues lie near the G6P-binding residues in the tertiary sequence (Figure 4.5). Although close to the malate/aspartate residues in the primary sequence, the six amino acids are not close to the malate/aspartate residues in the tertiary sequence (Figure 4.5). Therefore, the effect of this

PEPCK-specific region on activation of the PEPC enzyme by G6P will also be investigated in this chapter.

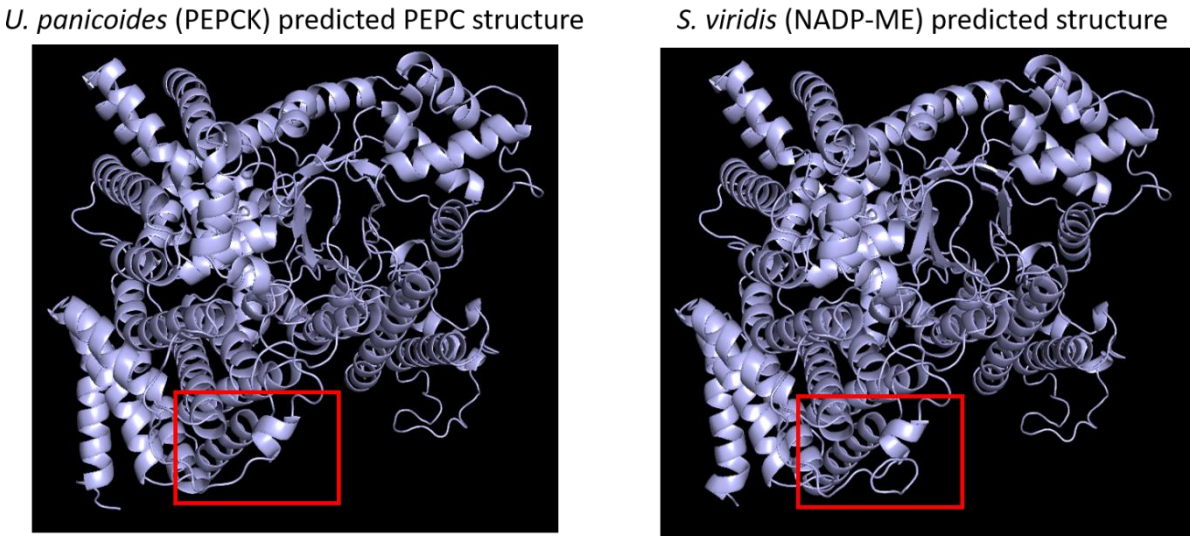

Figure 4.4. Location of the PEPCK-specific six amino acid deletion in the tertiary sequence of the PEPC enzyme. The tertiary structures of *U. panicoides*, a PEPCK species, and *S. viridis*, a NADP-ME species, are shown. The location of the PEPCK-specific six amino acid deletion is indicated by a red box on the *U. panicoides* PEPC structure. A corresponding red box on the *S. viridis* PEPC structure shows the location of the six amino acids present in the NADP-ME sequence. Structures were obtained from I-TASSER (Yang et al., 2015; Yang and Zhang, 2015).

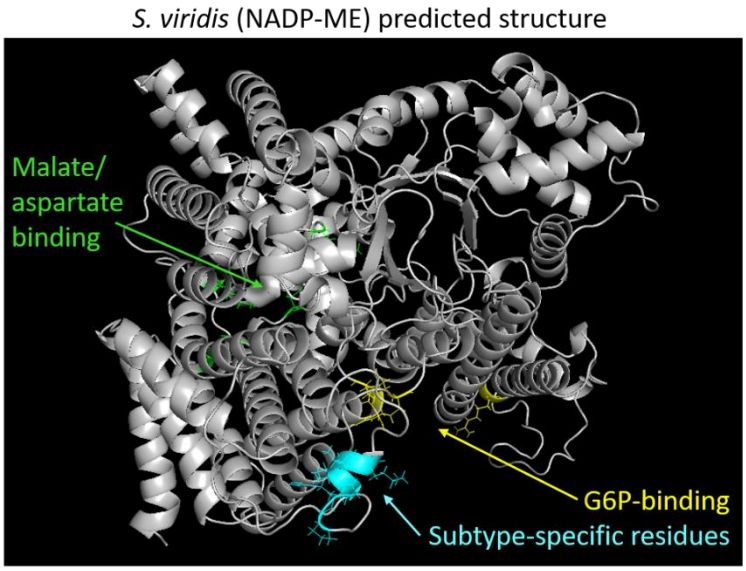

Figure 4.5. The six amino acids of the subtype-specific sequence lie near the G6P-binding residues in the PEPC tertiary sequence. The *S. viridis* PEPC structure shows the location of the six amino acids present in the NADP-ME sequence in blue and G6P-binding residues in yellow. The malate/aspartate-binding residues are indicated in green.

4.1.4 Experimental Objectives

The experimental objective of this chapter is to investigate the effects of the PEPCK-specific region on PEPC enzyme kinetics. This will be achieved by using the method established in Chapter 3 to express and purify PEPC proteins using *E. coli* as an expression system and pHUE as the expression vector. PEPC constructs designed to investigate the effects of the PEPCK deletion on PEPC kinetic properties can be seen in Figure 4.6.

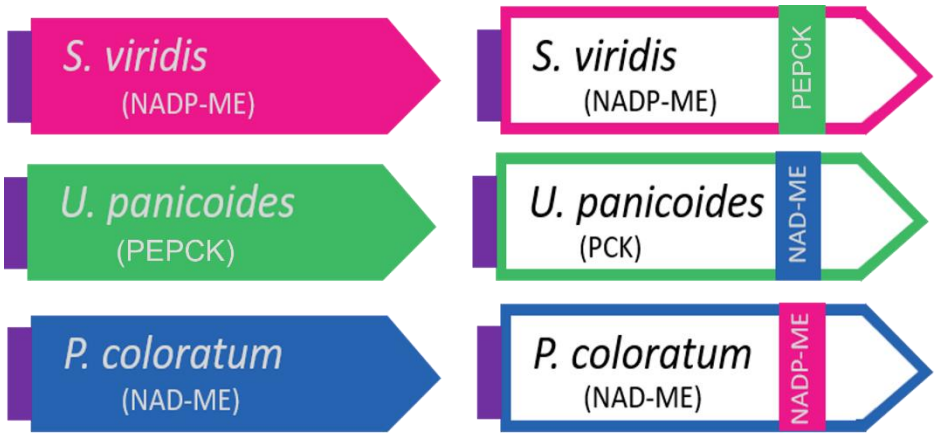

Figure 4.6. Constructs designed for *E. coli* expression to investigate the effects of the PEPCK-specific deletion on PEPC kinetic properties. *S. viridis* was chosen as the NADP-ME representative, *P. coloratum* was chosen as the NAD-ME representative, and *U. panicoides* as the PEPCK species. Three protein chimeras were also designed *P. coloratum* PEPC backbone + *S. viridis* PEPC insert of the region of interest, *U. panicoides* PEPC backbone + *P. coloratum* PEPC insert of the region of interest, and *S. viridis* PEPC backbone + *U. panicoides* PEPC insert of the region of interest.

4.2 Methods

4.2.1 Meta-analysis of PEPC kinetic and inhibition data

A meta-analysis of PEPC kinetic properties from a variety of different plant, bacterial and archaeal species was conducted. Available information regarding K_mPEP, $K_m Mg^{2+}$, $K_m HCO_3^-$, V_{max}, k_{cat}, and pH and temperature optimums were analysed. A meta-analysis of PEPC inhibition kinetic properties from a variety of different plant, bacterial and archaeal species was also conducted. Information regarding K_i of inhibitors malate and aspartate, I_{50} of inhibitors malate and aspartate were analysed.

4.2.2 Preparation of PEPC genes for synthesis

The sequences of *Rhodothermus obamensis* (X99379.1), *Setaria viridis* (Sevir.4G143500.1, Phytozome), *Panicum coloratum* (sequence provided by Alex Watson-Lazowski) and *Urochloa panicoides* (sequence provided by Alex Watson-Lazowski) were optimised for expression in *Escherichia coli* using Geneious. A SacII restriction site was added at the 5' end of the PEPC sequence and a HindIII restriction site was added at the 3' end of the PEPC sequence for insertion into the pET-28a (+) ubiquitin vector pHUE (Catanzariti et al., 2004). All SacII and HindIII sites within the PEPC sequences were removed by changing the nucleotide sequence whilst keeping the protein sequence unaltered. The *S. viridis*, *P. coloratum* and *U. panicoides* nucleotide sequences were altered to introduce a BamHI restriction site 3' to the area of interest and a BmtI restriction site 5' to the area of interest without altering the protein sequence. The 5' end of the *S. viridis*, *P. coloratum* and *U. panicoides* nucleotide sequences had a 12 bp linker sequence added followed by the nucleotide sequence for the region to be exchanged. The exchange regions had a 3' BamHI restriction site and a 5' BmtI restriction site. The *P. coloratum* sequence had a 5' linker sequence followed by the nucleotide sequence for the *S. viridis* exchange region. The *S. viridis* sequence had a 5' linker sequence followed by the nucleotide sequence for the *U. panicoides* exchange region. The *U. panicoides*

sequence had a 5' linker sequence followed by the nucleotide sequence for the *P. coloratum* exchange region. The sequences were synthesised by GenScript and provided in pUC57 vector with ampicillin resistance.

4.2.3 Creation of thermally competent *E. coli* TOP10 competent cells

Thermally competent *E. coli* TOP10 cells were created using the method outlined in General Methods section 2.2.

4.2.4 Heat shock transformation of *E. coli* TOP10, *E. coli* XL-1 Blue, and *E. coli* BL21 (DE3) competent cells

Heat shock transformation of *E. coli* TOP10, *E. coli* XL-1 Blue, and *E. coli* BL21 (DE3) competent cells was carried out using the method described in General Methods section 2.3.

4.2.5 Plasmid isolation

Plasmids were isolated as described in General Methods section 2.4.

4.2.6 Restriction enzyme cloning of PEPC gene into pHUE

SacII and HindIII double digests, and SacII, HindIII and ScaI triple digests were conducted on the pHUE vector and the four pUC57-PEPC plasmids, respectively. The 30 µl reaction volumes for the four PEPC sequence plasmids contained 1X CutSmart Buffer (NEB), 10 U SacII (NEB), 10 U HindIII (NEB), 10 U ScaI (NEB) and 6 µl of pUC57-PEPC plasmid preparation. The 30 µl reaction volume for the pHUE plasmid contained 1X CutSmart Buffer (NEB), 10 U SacII (NEB), 10 U HindIII (NEB), and 10 µl of pHUE plasmid preparation. The digestion reactions

were incubated overnight at 37 °C. 20 U of alkaline phosphatase (Promega) was added to the pHUE plasmid digests, and the reactions were incubated at 37 °C for a further 1.5 hours. Digest products were supplemented with 4X gel loading dye (NEB) and were run at 80 V on a 1 % agarose/ 1X TAE (40 mM Tris Base, 20 mM acetic acid, 1 mM EDTA) gel with 1X SYBR™ Safe DNA Gel Stain (Thermofisher) for visualisation and were visualised using a blue light transilluminator. The gel bands corresponding to the 5,900-base pair pHUE vector backbone, and the 2824 – 2908 base pair PEPC sequences were excised and DNA extracted using the Wizard® SV Gel and PCR Clean-Up System (Promega). Manufacturer's specifications were followed when using the Wizard® SV Gel and PCR Clean-Up System (Promega), except for the elution step where 40 µl of nuclease free water heated to 65 °C was used, centrifugation was conducted for 2 minutes instead of 1, and the modified elution step was repeated. Samples were vacuum concentrated for 40 minutes.

Ligation reactions were conducted with 1X T_4 DNA ligase buffer (NEB), 400 U T_4 DNA ligase (NEB), 2 µl linearised and de-phosphorylated pHUE vector, and 6 µl of linearised PEPC sequence, in a final volume of 10 µl. A reaction with 6 µl of ddH_2O instead of a linearised PEPC sequence was included as a control. The ligation reactions were incubated overnight at 15 °C. The entire 10 µl of the reaction mixture was used to transform 200 µl *E. coli* XL-1 Blue competent cells as described in the General Methods section 2.3.

Cells were plated on LB-agar plates, containing 100 µg/mL ampicillin. The plates were incubated overnight at 37 °C. Colonies were used to inoculate LB media containing 100 µg/mL ampicillin, and incubated overnight at 37 °C and 220 rpm. Plasmids were isolated as described in 4.1.4. SacII and HindIII restriction enzyme double digests were conducted to confirm successful cloning. The 20 µl reactions contained 1X CutSmart Buffer (NEB), 10 U SacII (NEB), 10 U HindIII (NEB) and 2 µl of plasmid. The digests were incubated at 37 °C for one hour before being supplemented with 4X gel loading dye (NEB) and run at 80 V on a 1 %

agarose/ 1X TAE gel with 1X SYBR™ Safe DNA Gel Stain (Thermofisher) for visualisation and visualised using a blue light transilluminator.

4.2.7 Restriction enzyme cloning region swapping to create protein chimeras

SacII, HindIII and AloI triple digests were conducted on the pUC57-PEPC vectors of *P. coloratum* and *U. panicoides*. the 30 µl reaction volumes contained 1X CutSmart Buffer (NEB), 1X Buffer R (Fermentas), 10 U SacII (NEB), 10 U HindIII (NEB), 1 U AloI (Fermentas) and 6 µl of the pUC57-PEPC plasmid preparation. A SacII, HindIII and NaeI triple digest was conducted on the pUC57-PEPC vector of *S. viridis.* The 30 µl reaction volume contained 1X CutSmart Buffer (NEB), 10 U SacII (NEB), 10 U HindIII (NEB), 5 U NaeI (NEB) and 6 µl of the pUC57-PEPC plasmid preparation. The reactions were incubated overnight at 37 °C. Digest products were supplemented with 4 X gel loading dye (NEB) and run at 80 V on a 1 % agarose/ 1X TAE gel with 1X SYBR™ Safe DNA Gel Stain (Thermofisher) for visualisation and were visualised using a blue light transilluminator. The gel bands corresponding to the 2801 - 2820 nucleotide pUC57+exchange segment backbone were excised and DNA extracted using the Wizard SV Gel and PCR Clean-Up System (Promega). Samples were vacuum concentrated for 60 minutes.

20 µl reaction contained 1 X NEBuffer 2 (NEB), 40 µM dNTPs, 5 U Klenow fragment (NEB) and 2.5 µl of linearised pUC57 + exchange segment. The reaction was incubated at room temperature for 10 minutes before being heated at 75 °C for 10 min to terminate the reaction. Ligation reactions were conducted with 1 X T_4 DNA ligase buffer (NEB), 600 U T_4 DNA ligase (NEB), and 20 µl Klenow reaction in a final volume of 25 µl. The ligation reactions were incubated overnight at 15 °C. The entire 25 µl of the reaction mixture was used to transform 200 µl *E. coli* XL-1 Blue competent cells, using the heat shock method as described in 4.1.3. Cells were plated on LB-agar plates, containing 100 µg/mL ampicillin. The plates were incubated overnight at 37 °C. Single colonies were used to inoculate LB media containing 100 µg/mL ampicillin, and incubated overnight at 37 °C and 220 rpm. Plasmids were extracted

using the Isolate II Plasmid Mini Kit (Bioline), as per the manufacturer's specifications. BmtI and BamHI double digests were conducted to confirm successful cloning. The 20 µl reactions contained 1X CutSmart Buffer (NEB), 10 U BmtI (NEB), 10 U BamHI (NEB) and 2 µl of plasmid. The digests were incubated at 37 °C for one hour before being supplemented with 4X gel loading dye (NEB) and run at 80 V on a 1-% agarose/ 1X TAE gel with 1X SYBR™ Safe DNA Gel Stain (Thermofisher) for visualisation and were visualised using a blue light transilluminator.

BmtI and BamHI double digests were conducted on the pHUE-PEPC backbones and the pUC57-exchange segment plasmids, for *P. coloratum*, *S. viridis* and *U. panicoides*. The 30 µl reaction volumes for the three pUC57-exchange segment plasmids contained 1X CutSmart Buffer (NEB), 10 U BmtI (NEB), 10 U BamHI (NEB) and 6 µl of the pUC57-exchange segment plasmid preparation. The 30 µl reaction volume for the three pHUE-PEPC backbones contained 1X CutSmart Buffer (NEB), 10 U BmtI (NEB), 10 U BamHI (NEB), and 10 µl of the pHUE-PEPC backbone preparation. The reactions were incubated overnight at 37 °C. 20 U alkaline phosphatase (Promega) was added to the pHUE-PEPC backbone digestions, and the reactions were incubated for a further 1.5 hours at 37 °C. Digest reactions were supplemented with 4X gel loading dye (NEB) and run at 80 V on a 1 % agarose/ 1X TAE gel with 1X SYBR™ Safe DNA Gel Stain (Thermofisher) for visualisation and were visualised using a blue light transilluminator. The gel bands corresponding to the 8,715 nucleotide pHUE-PEPC backbones, and the 79 - 97 nucleotide PEPC exchange segment inserts were excised and DNA extracted using the Wizard SV Gel and PCR Clean-Up System (Promega). Samples were vacuum concentrated for 40 minutes. Ligation reactions were conducted with 1X T_4 DNA ligase buffer (NEB), 400 U T_4 DNA ligase (NEB), 2 µl linearised and de-phosphorylated pHUE-PEPC backbone, and 6 µl of linearised PEPC exchange segment insert, in a final volume of 10 µl. Reactions with 6 µl of ddH_2O in place of the linearised PEPC exchange segment insert were included as a control with each of the pHUE-PEPC backbones. The combinations of pHUE-PEPC backbone and PEPC exchange segment insert were as follows: *P. coloratum* pHUE-

PEPC backbone with the *S. viridis* PEPC exchange segment insert, *U. panicoides* pHUE-PEPC backbone with the *P. coloratum* PEPC exchange segment insert, and *S. viridis* pHUE-PEPC backbone with the *U. panicoides* PEPC exchange segment insert. The ligation reactions were incubated overnight at 15 °C. The entire 10 µl of the reaction mixture was used to transform 200 µl *E. coli* XL-1 Blue competent cells as described in 4.1.3. Cells were plated on LB-agar plates, containing 100 µg/mL ampicillin. The plates were incubated overnight at 37 °C. Colonies were used to inoculate LB media containing 100 µg/mL ampicillin, and incubated overnight at 37 °C and 220 rpm. Plasmids were extracted using the Isolate II Plasmid Mini Kit (Bioline), as per the manufacturer's specifications.

Samples were sent to The Biomolecular Resource Facility (BRF) at The John Curtin School of Medical Research for Sanger sequencing to confirm successful region swapping was confirmed using a primer with the sequence 5' - CGTACATCACCACCCTGAACG -3'.

4.2.8 Protein expression

Transformations of *E. coli* BL21(DE3) cells (Agilent) with plasmids *P. coloratum* PEPC-pHUE plasmid, *S. viridis* PEPC-pHUE plasmid, *U. panicoides* PEPC-pHUE plasmid, *P. coloratum* PEPC backbone + *S. viridis* PEPC insert-pHUE plasmid, *U. panicoides* PEPC backbone + *P. coloratum* PEPC insert-pHUE plasmid, and *S. viridis* PEPC backbone + *U. panicoides* PEPC insert-pHUE plasmid were conducted according to the 4.1.4. Glycerol stocks were made of the *E. coli* BL21(DE3) cells containing each of the plasmids above. Protein expression was carried out according to the method described in the General Methods section 2.5. Cells were then harvested by centrifugation at 6,000 x *g* for 10 minutes using a Hitachi R9A rotor. The supernatant was discarded, and the cells were snap frozen in liquid nitrogen and stored at -20 °C until purification.

4.2.9 Protein purification using Ni-NTA agarose columns

Proteins were purified using Ni-NTA agarose columns using the optimised method described in Chapter 3 of this thesis (3.2.6).

4.2.10 SDS-PAGE gel analysis

SDS-PAGE analysis was carried out as described in the General Methods section 2.6.

4.2.11 Gel filtration

Proteins for k_{cat}, V_{max}, K_mPEP, and $K_m HCO_3^-$ analyses were purified using a HiLoad 16/600 Superdex 200 Prep Grade (Amersham Biosciences) gel filtration column as described Chapter 3 of this thesis (3.1.6.2). Proteins for I_{50} malate and aspartate determination were purified using a Superdex 200 increase 10/300 GL column (GE Healthcare Life Sciences) as descried in Chapter 3 of this thesis (3.1.6.1).

4.2.12 Protein quantification

Proteins were quantified using SYPRO Ruby as described in the optimised method outlined in Chapter 3 of this thesis (3.2.6).

4.2.13 K_mPEP, k_{cat}, and V_{max} determination in the presence and absence of glucose-6-phosphate

PEPC activity was assayed as described in the General Methods section 2.8, with G6P (5 mM) either present or absent in the buffer. was included n Instead of initiating the reaction with 5

mM of PEP, the PEP concentration was varied. For each PEPC enzyme, sixteen activity assays were conducted with PEP final concentrations of 20 mM, 17.5 mM, 15 mM, 12.5 mM, 10 mM, 7.5 mM, 5 mM, 2.5 mM, 2 mM, 1.5 mM, 1 mM, 0.75 mM, 0.5 mM, 0.25 mM, 0.125 mM, 0.0625 mM. This range of PEP concentrations was used given the results of the meta-analysis of K_mPEP of C_4 PEPC enzymes in section 4.3.1 and Appendix 1. For each enzyme, three different enzyme preparations were used and each kinetic measurement was repeated three times. Analysis of PEPC kinetics data was performed as described in the General Methods section 2.8. In order to determine the kinetic parameters of K_mPEP and V_{max}, non-linear regression analysis was conducted using the Origin software package (Version 2020, OriginLab Corporation). To calculate k_{cat}, the V_{max} values (µmol min^{-1} mg^{-1}) calculated in origin were used. The molecular weight for each protein was calculated using sequence information and the ExPASy (the Expert Protein Analysis System) tool at https://web.expasy.org/compute_pi/ (Swiss Institute of Bioinformatics; Gasteiger et al., 2005).

4.2.14 $K_m HCO_3^-$ determination

To determined $K_m HCO_3^-$, HCO_3^--dependent PEPC activity assays were conducted at 25 °C in a 600 µl cuvette linked to mass-spectrometer using the MIMS PEPC assay protocol as described by DiMario and Cousins (2019). CO_2 calibrations were conducted as described by (DiMario and Cousins, 2019) prior to each HCO_3^- curve. The assay buffer (100 mM HEPES-KOH, pH 7.6, 10 mM $MgCl_2$) was bubbled with N_2 gas for at least one hour before the assays were performed to remove CO_2. After the assay buffer was placed in the cuvette, 1 mM DTT, 50 µg ml^{-1} carbonic anhydrase, 5 mM G6P, 5 mM PEP and one of seven different concentrations of $NaHCO_3$ (1000, 750, 500, 350, 200, 100, and 50 µM) were added. Reactions were initiated by the addition of the PEPC protein. In order to determine the kinetic parameter of $K_m HCO_3^-$, the HCO_3^- response curve data was fitted to the Hill equation:

$$V = \frac{V\text{max} \times [HCO_3^-]^h}{(K_m HCO_3^-)^h + [HCO_3^-]^h}$$

using Excel's Solver function.

4.2.15 IC_{50} malate and aspartate determination in the presence and absence of glucose-6-phosphate

PEPC activity was assayed as described in the General Methods section 2.8, with G6P (5 mM) either present or absent in the buffer. For each PEPC enzyme, fifteen activity assays were conducted with 6.5 mM, 5 mM, 4.5 mM, 4 mM, 3 mM, 2.5 mM, 2 mM, 1.5 mM, 1.25 mM, 1 mM, 0.75 mM, 0.5 mM, 0.25 mM, 0.125 mM, 0.0625 mM malate included in the assay mixture. For each enzyme, one enzyme preparation was used and each kinetic measurement was repeated two or three times. Analysis of PEPC kinetics data was performed as described in the General Methods section 2.8. In order to determine the kinetic parameter of IC_{50} malate, non-linear regression analysis was conducted using the Origin software package (Version 2020, OriginLab Corporation).

4.2.16 Statistical analyses

Statistical analyses were carried out as described in the General Methods section 2.9.

4.3 Results

4.3.1 Meta-analysis of PEPC kinetic and inhibition data

4.3.1.1 Michaelis Menten kinetics for PEPC

The results of an extensive literature review of PEPC kinetic properties from a variety of different plant, bacterial and archaeal species are displayed in Appendix 1. Available information regarding K_mPEP, $K_m Mg^{2+}$, $K_m HCO_3^-$, V_{max}, k_{cat}, and pH and temperature optimums is collated (Appendix 1).

G6P has been shown to reduce the K_mPEP across C_3, C_3-C_4 intermediate, C_4-like and C_4 species (Ting and Osmond, 1973a; Ting and Osmond, 1973c; Huber and Edwards, 1975; Uedan and Sugiyama, 1976; Nakamoto et al., 1983; Bauwe and Chollet, 1986; Bandarian et al., 1992; Law and Plaxton, 1995; Svensson et al., 1997; Westhoff et al., 1997; Bläsing et al., 2000; Frank et al., 2001; Bläsing et al., 2002; Engelmann et al., 2003; Takahashi-Terada et al., 2005; Gowik et al., 2006; Endo et al., 2008). One exception has been reported, the K_mPEP for PEPC from the C_3-C_4 intermediate species increased slightly in the presence of G6P from 0.006 mM to 0.008 mM. Other metabolites, such as Acetyl-CoA, glutamine, and fructose-1,6-bisphosphate, have been shown to reduce the K_mPEP of bacterial species (Wohl and Markus, 1972; Izui et al., 1981; Terada and Izui, 1991; Rivoal et al., 1996; Rivoal et al., 1998).

The PEPC from bacterial, C_3, C_3-C_4 intermediate, C_4-like, and C_4 species, have shown changes in K_mPEP with changing pH both in the presence and absence of G6P (Uedan and Sugiyama, 1976; Holaday and Black, 1981; Nakamoto et al., 1983; Law and Plaxton, 1995; Gao and Woo, 1996; Rivoal et al., 1996; Dong et al., 1998; Rivoal et al., 1998; Frank et al., 2001; Bläsing et al., 2002; Chen et al., 2002; Engelmann et al., 2003). The PEPC from CAM species *Bryophyllum fedtschenkoi* has shown changes in K_mPEP with changing temperatures, with K_mPEP values of 1.7 mM at 11 °C , 0.7 mM at 25 °C, and 2.4 mM at 40 °C (Jones et al., 1978).

C_3 species have PEPCs with reported K_mPEP in the range of 0.008 - 0.08 mM (pH 7.0 - 8.0; 25 – 30 °C) in the presence of G6P and 0.013 – 0.4 mM (pH 7.0 – 8.3; 25 – 30 °C) in the absence of G6P (Maruyama et al., 1966; Ting and Osmond, 1973b; Ting and Osmond, 1973c; Miziorko et al., 1974; Holaday and Black, 1981; Nakamoto et al., 1983; Bauwe and Chollet, 1986; Law and Plaxton, 1995; Svensson et al., 1997; Westhoff et al., 1997; Bläsing et al., 2000; Bläsing et al., 2002; Engelmann et al., 2003; Gowik et al., 2006; Jacobs et al., 2008). C_4 species, on the other hand, have PEPCs with reported K_mPEP in the range of 0.02 – 0.6 mM (pH 7.0 – 8.0; 22 – 37 °C) in the presence of G6P and 0.09 – 7.9 mM (pH 7.0 – 9.0; 22 – 37 °C) in the absence of G6P (Ting and Osmond, 1973a, 1973b; Ting and Osmond, 1973c; Huber and Edwards, 1975; Raghavendra and Das, 1975; Uedan and Sugiyama, 1976; Raghavendra and Vallejos, 1980; Bauwe and Chollet, 1986; Iglesias et al., 1986; Samaras et al., 1988; Bandarian et al., 1992; Janc et al., 1992; Gao and Woo, 1996; Svensson et al., 1997; Westhoff et al., 1997; Dong et al., 1998; Bläsing et al., 2000; Hamel and Simon, 2000; Frank et al., 2001; Bläsing et al., 2002; Engelmann et al., 2003; Pierre et al., 2004; Takahashi-Terada et al., 2005; Gowik et al., 2006; Lara et al., 2006; Endo et al., 2008; Jacobs et al., 2008).

The $K_m HCO_3^-$ values for PEPCs are not as well studied as the K_mPEP values. C_3 species have PEPCs with reported $K_m HCO_3^-$ in the range of 0.018 – 0.8 mM (pH 7.5 – 8.0; 25 – 30 °C) in the absence of G6P (Maruyama et al., 1966; Ting and Osmond, 1973c; Miziorko et al., 1974; Holaday and Black, 1981; Law and Plaxton, 1995). One $K_m HCO_3^-$ in the presence of G6P has been reported to be 0.064 mM (pH 7.6; 30 °C) for the C_3 species *Flaveria pringleii* (DiMario and Cousins, 2019). C_4 species have PEPCs with reported $K_m HCO_3^-$ in the range of 0.0266 – 0.8 mM (pH 7.6 – 8.0; 27 – 30 °C) in the presence of G6P and 0.011 – 2 mM (pH 7.3 – 9.0; 25 – 30 °C) in the absence of G6P (Coombs et al., 1973; Ting and Osmond, 1973c; Bauwe, 1986; Iglesias et al., 1986; Janc et al., 1992; Gao and Woo, 1996; Dong et al., 1998; Parvathi et al., 2000; Boyd et al., 2015; DiMario and Cousins, 2019).

The presence of G6P has been shown to increase or have no effect on the V_{max} and k_{cat} values of PEPCs from C_3, C_3-C_4 intermediate, C_4-like and C_4 species (Uedan and Sugiyama, 1976; Nakamoto et al., 1983; Law and Plaxton, 1995; Bläsing et al., 2000; Frank et al., 2001; Bläsing et al., 2002; Engelmann et al., 2003; Takahashi-Terada et al., 2005; Gowik et al., 2006). Two exceptions have been reported, *Zea mays* PEPC V_{max} decreased slightly from 16.4 µM PEP min^{-1} mg^{-1} to 15.1 µM PEP min^{-1} mg^{-1} (pH 7.0; 25 °C) in the presence of G6P, although other studies on *Zea mays* PEPC have not found the same trend (Uedan and Sugiyama, 1976; Frank et al., 2001; Takahashi-Terada et al., 2005). The other exception was the PEPC of *Alternanthera sessilis*, where the reported k_{cat} value decreased slightly from 22 s^{-1} to 20 s^{-1} (25 °C) in the presence of G6P, although this decrease was not seen in the V_{max} value in the presence of G6P (Gowik et al., 2006).

Investigating the natural variation in the V_{max} values of PEPCs from archaeal, bacterial, and plant species could highlight PEPCs with fast catalytic activity that could possibly outperform the PEPCs in C_4 crop species. Given that the V_{max} values are measured in numerous different units, only those that could be accurately converted to the form µmol min^{-1} mg^{-1} were considered in this summary, although Vmax values with other units can be found in Appendix 1.

V_{max} values for two archaeal species have been reported in the absence of G6P. *Clostridium perfringens* has a V_{max} value of 40 µmol min^{-1} mg^{-1} (37 °C) and *Sulfolobus solfataricus* has a V_{max} value of 2.1 µmol min^{-1} mg^{-1} (pH 8.0; 80 °C) (Ettema et al., 2004; Dharmarajan et al., 2011). The V_{max} values for bacterial species have been reported within the range of 0.32 – 60 µmol min^{-1} mg^{-1} (pH 7.5 – 9.5; 22 – 30 °C) (Hoban and Lyric, 1975; Owttrim and Colman, 1986; Terada and Izui, 1991; Charles and Sykora, 1992; Rivoal et al., 1996; Chen et al., 2002; Park et al., 2015; Del Prete et al., 2016). One bacterial species, *Rhodothermus obamensis*,

outperformed the rest with a particularly high V_{max} value of 100 µmol min^{-1} mg^{-1} (pH 8.0) (Takai et al., 1997).

C_3 species have PEPCs with reported k_{cat} values in the range of 20 – 60 s^{-1} (pH 7.6 – 8.0; 25 °C) in the presence of G6P and 22 – 51 s^{-1} (pH 7.6 – 8.0; 25 °C) in the absence of G6P (Bläsing et al., 2000; Bläsing et al., 2002; Gowik et al., 2006). C_3 species have PEPCs with reported V_{max} values in the range of 5.1– 32 µmol min^{-1} mg^{-1} (pH 7.0 – 8.0; 25 – 30 °C) in the presence of G6P and 0.09 - 31 µmol min^{-1} mg^{-1} (pH 7.0 – 8.0; 25 – 30 °C) in the absence of G6P (Law and Plaxton, 1995; Svensson et al., 1997; Bläsing et al., 2000; Bläsing et al., 2002; Engelmann et al., 2003; Gowik et al., 2006; Lara et al., 2006; DiMario and Cousins, 2019)

One C_3-C_4 intermediate species, *Alternanthera tenella*, has a PEPCs with reported k_{cat} values of 33 s^{-1} (25 °C) in the presence of G6P and 33 s^{-1} (25 °C) in the absence of G6P (Gowik et al., 2006). C_3-C_4 intermediate species and C_4-like species have PEPCs with reported V_{max} values in the range of 18 – 27 s^{-1} (pH 7.6 – 8.0; 25 °C) in the presence of G6P and 17.64 – 26 s^{-1} (pH 7.6 – 8.0; 25 °C) in the absence of G6P (Engelmann et al., 2003; Gowik et al., 2006). The single-cell C_4 species *Bienertia sinuspersici* and *Suaeda aralocaspica* have V_{max} values in the absence of G6P of 1.96 µmol min^{-1} mg^{-1} and 1.67 µmol min^{-1} mg^{-1} respectively (Lara et al., 2006).

C_4 species have PEPCs with reported k_{cat} values in the range of 38 – 55 s^{-1} (pH 7.6 – 8.0; 25 °C) in the presence of G6P and 38 – 49 s^{-1} (pH 7.6 – 8.0; 25 °C) in the absence of G6P (Bläsing et al., 2000; Bläsing et al., 2002; Gowik et al., 2006). C_4 species have PEPCs with reported V_{max} values in the range of 8.1 – 31.9 µmol min^{-1} mg^{-1} (pH 7.3 – 8.0; 25 – 30 °C) in the presence of G6P and 0.64 –29 µmol min^{-1} mg^{-1} (pH 7.0 – 9.0; 25 – 30 °C) in the absence of G6P (Iglesias et al., 1986; Gao and Woo, 1996; Svensson et al., 1997; Dong et al., 1998; Bläsing et al., 2000;

Parvathi et al., 2000; Bläsing et al., 2002; Engelmann et al., 2003; Takahashi-Terada et al., 2005; Gowik et al., 2006; Lara et al., 2006; Endo et al., 2008; DiMario and Cousins, 2019). Although no C_3, C_3-C_4 intermediate, C_4-like species has a PEPC whose V_{max} value obviously exceeds the V_{max} values of PEPCs from C_4 species, the bacterial species, *Rhodothermus obamensis*, with the V_{max} value of 100 µmol min^{-1} mg^{-1} (pH 8.0) far exceeds the V_{max} values of PEPCs from C_4 species (Takai et al., 1997). The *Rhodothermus obamensis* PEPC was chosen to assess its performance at 25 °C to see if it is a good candidate for introduction into C_4 plants.

4.3.1.2 Inhibition of the PEPC enzyme

An extensive literature review was conducted into PEPC inhibition kinetic properties from a variety of different plant, bacterial and archaeal species. The results regarding K_i of inhibitors malate and aspartate, IC_{50} of inhibitors malate and aspartate are displayed in Appendix 2 and interesting points are summarised below.

Across CAM, C_3, and C_4 species, changes in pH have been shown to drastically change the sensitivity of the PEPC enzyme to its inhibitors malate and aspartate (Jones et al., 1978; Jones et al., 1981; Nott and Osmond, 1982; Iglesias et al., 1986; Law and Plaxton, 1995; Frank et al., 2001).

G6P has been shown to alleviate the inhibitory effects of aspartate on PEPC in a bacterial species and alleviate the inhibitory effects of malate on PEPC in C_3, C_3-C_4 intermediate and C_4 species (Dong et al., 1998; Chen et al., 2002; Engelmann et al., 2003; Pierre et al., 2004; Takahashi-Terada et al., 2005; Jacobs et al., 2008). Two notable exceptions exist in *Flaveria brownii*, a C_4-like species, and *Flaveria trinervia*, a C_4 NADP-ME species, where the presence of G6P resulted in a decrease in the K_i-malate and therefore an increase in sensitivity of the

PEPC enzyme to malate (Engelmann et al., 2003; Jacobs et al., 2008). This increase in sensitivity of the PEPC enzyme to malate in the presence of G6P does not appear to be subtype specific as is not observed in *Digitaria sanguinalis* and *Zea mays*, other NADP-ME species (Dong et al., 1998; Pierre et al., 2004; Takahashi-Terada et al., 2005).

C_3 species have PEPCs with reported IC_{50} malate in the absence of G6P in the range of 0.015 – 8.0 mM (pH 7.0-8.0; 25 - 30 °C) and one reported IC_{50} malate of 5.5 mM the presence of G6P (pH 7.6; 25 °C) (Law and Plaxton, 1995; Svensson et al., 1997; Westhoff et al., 1997; Bläsing et al., 2002; Lara et al., 2006; Jacobs et al., 2008; Paulus et al., 2013; Paulus et al., 2013). An IC_{50} aspartate of 0.054 mM in the absence of G6P was reported for the PEPC of *Musa cavendishii* (pH 7.0; 30 °C) (Law and Plaxton, 1995). The *Musa cavendishii* PEPC lost all sensitivity to aspartate in the absence of G6P when the pH was 8.0 (Law and Plaxton, 1995). The PEPC from the C_3 species *Flaveria pringleii* has a reported K_i malate of 1.4 mM in the presence of G6P (pH 7.6; 25 °C) and 0.2 mM in the absence of G6P (pH 7.6; 25 °C) (Engelmann et al., 2003).

C_4 species have PEPC enzymes with reported IC_{50} malate in the presence of G6P in the range of 4 – 22 mM (pH 7.3-7.6; 25 - 30 °C) and IC_{50} malate in the absence of G6P in the range of 0.82 – 10 mM (pH 7.0-8.0; 25 - 30 °C) (Iglesias et al., 1986; Svensson et al., 1997; Westhoff et al., 1997; Dong et al., 1998; Bläsing et al., 2002; Pierre et al., 2004; Takahashi-Terada et al., 2005; Lara et al., 2006; Endo et al., 2008; Jacobs et al., 2008; Paulus et al., 2013; Paulus et al., 2013) K_i malate in the presence of G6P have been reported in the range of 0.8 – 0.95 mM for C_4 PEPC enzymes (pH 7.0-7.6; 25 °C). (McNaughton et al., 1989; Engelmann et al., 2003). In the absence of G6P, C_4 PEPCs have K_i malate reported in the range of 0.24 –5 mM (pH 7.3-8.0; 25 - 30 °C) (Raghavendra and Das, 1975; Parvathi et al., 2000; Engelmann et al., 2003). Inhibition of C_4 PEPC enzymes has been demonstrated with IC_{50} aspartate in the absence of

G6P falling between 0.74 mM to greater than 20 mM (pH 7.0-8.0; 30 °C) (Iglesias et al., 1986; Endo et al., 2008).

4.3.2 K_mPEP of PEPC and PEPC chimeras in the presence and absence of glucose-6-phosphate

The *R. obamensis* PEPC enzyme was not active at 25 °C and only started to show some activity when assay temperatures were over 40°C (data not shown) so no further analysis was performed on this enzyme.

Table 4.2 K_mPEP of *Setaria viridis*, *Urochloa panicoides*, and *Panicum coloratum* PEPC enzymes, and PEPC chimeras in the presence and absence of glucose-6-phosphate (G6P). Each value is the average of 3 biological replicates, with the standard error between these replicates indicated. Values were determined using a NADH-linked spectrophotometric assay at 25 °C with 1 μg PEPC protein, initiated with the addition of phosphoenolpyruvate (0 – 20 mM final concentration). Two-way ANOVA was conducted for statistical analyses with posthoc Tukey honestly significant difference (HSD) tests performed to determine statistically significant differences ($P < 0.05$). Different letters indicate statistically significant differences at $P<0.05$.

	K_m PEP (mM)	
	with 5 mM G6P	no G6P
S. viridis (NADP-ME)	0.31 ± 0.02 [c]	0.66 ± 0.01 [c]
S. viridis + PEPCK sequence	0.29 ± 0.01 [c]	0.55 ± 0.02 [c]
U. panicoides (PEPCK)	0.18 ± 0.00 [c]	0.42 ± 0.01 [c]
U. panicoides + NAD-ME sequence	0.20 ± 0.01 [c]	0.30 ± 0.02 [c]
P. coloratum (NAD-ME)	2.92 ± 0.13 [b]	7.32 ± 0.60 [a]
P. coloratum + NADP-ME sequence	2.76 ± 0.43 [b]	6.84 ± 0.18 [a]

All enzymes had a lower K_mPEP when in the presence of 5 mM G6P compared to without G6P (Figure 4.7; Table 4.2). This difference, however, was only statistically significant for the *P. coloratum* PEPC enzyme and the *P. coloratum* PEPC with the sequence from a NADP-ME species enzyme (Table 4.2). This lowering of K_mPEP when in the presence of G6P has been reported for a number of plant PEPC enzymes, regardless of photosynthetic type or C_4 photosynthetic subtype (Appendix 1; Ting and Osmond, 1973a; Ting and Osmond, 1973c;

Huber and Edwards, 1975; Uedan and Sugiyama, 1976; Nakamoto et al., 1983; Bauwe and Chollet, 1986; Bandarian et al., 1992; Law and Plaxton, 1995; Svensson et al., 1997; Westhoff et al., 1997; Bläsing et al., 2000; Frank et al., 2001; Bläsing et al., 2002; Engelmann et al., 2003; Takahashi-Terada et al., 2005; Gowik et al., 2006; Endo et al., 2008). K_mPEP values are very well documented for NADP-ME PEPC enzymes, with less reported values for PEPC enzymes from NAD-ME species and only two reported K_mPEP values for PEPCK species (Appendix 1, Figure 4.7). The K_mPEP values determined for the *S. viridis* enzyme in the presence and absence of G6P, 0.31 mM ± 0.02 and 0.66 mM ± 0.01, respectively, fall within

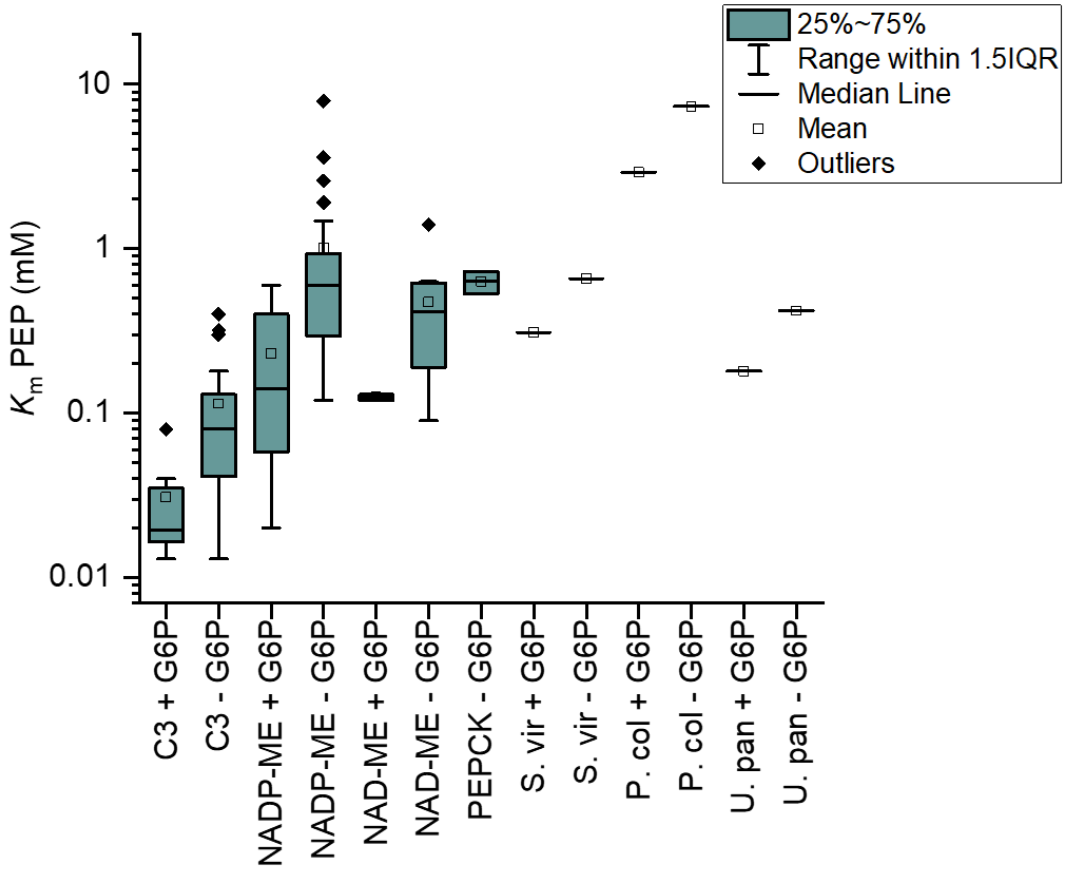

Figure 4.7. K_mPEP (mM) ranges in the presence and absence of glucose-6-phosphate (G6P) for C_3, and NADP-ME, NAD-ME and PEPCK species compared to the K_mPEP values determined for *Setaria viridis* (S. vir), *Urochloa panicoides* (U. pan), and *Panicum coloratum* (P. col) PEPC enzymes. K_mPEP values determined in the presence of G6P are indicated by + G6P, K_mPEP values determined in the absence of G6P are indicated by - G6P. 12 reported values make up the C_3 + G6P boxplot, 29 for the C_3 - G6P, 17 for NADP-ME + G6P, 32 for NADP-ME - G6P, 2 for NAD-ME + G6P, 10 for NAD-ME – G6P, and 2 for PEPCK – G6P.

the ranges reported for K_mPEP values in the presence and absence of G6P for NADP-ME species (Table 4.2, Figure 4.7).

The K_mPEP of *U. panicoides* was determined to be 0.18 mM ± 0.00 in the presence of 5 mM G6P and 0.42 mM ± 0.01 in the absence of G6P (Table 4.2). Whilst no data for K_mPEP in the presence of G6P for a PEPCK species was found in the literature, two reported K_mPEP values in the absence of G6P have been reported. The K_mPEP determined for *U. panicoides* in the absence of G6P is lower than the K_mPEP values reported for both the PEPCK species *Panicum maximum* and *Chloris gayana* (Figure 4.7; Ting and Osmond, 1973c). This indicates that the PEPC enzyme of *Urochloa panicoides* has a greater affinity for PEP in the absence of G6P than any other measured PEPCK species. The K_mPEP determined for *U. panicoides* in the presence of G6P is the first reported K_mPEP value for a PEPCK species.

The K_mPEP of *P. coloratum* was determined to be 2.92 mM ± 0.10 in the presence of 5 mM G6P and 7.32 mM ± 0.49 in the absence of G6P (Table 4.2). The K_mPEP of the *P. coloratum* (NAD-ME) enzyme in the presence of 5 mM G6P is considerable larger considerably larger than the two reported K_mPEP values in the presence of G6P of NAD-ME species (Figure 4.10; Ting and Osmond, 1973a; Ting and Osmond, 1973c). The larger the K_mPEP of the PEPC enzyme, the less affinity it has for PEP. Even the activated K_mPEP of *P. coloratum* is far greater than the K_mPEP values reported for unactivated PEPC enzymes from NAD-ME species (Figure 4.10). The K_mPEP value of the *P. coloratum* enzyme in the absence of G6P is also significantly larger than any reported K_mPEP values for NAD-ME species in the absence of G6P (Figure 4.10; Ting and Osmond, 1973a, 1973b; Ting and Osmond, 1973c; Raghavendra and Vallejos, 1980; Iglesias et al., 1986; Lara et al., 2006).

Two-way ANOVA showed that the K_mPEP of both *S. viridis* and *U. panicoides* were statistically different from the K_mPEP of *P. coloratum* PEPC both in the presence and absence of G6P.

The K_mPEP of the *S. viridis* PEPC with the sequence from a PEPCK species was determined to be 0.29 mM ± 0.01 in the presence of 5 mM G6P and 0.55 mM ± 0.02 in the absence of G6P (Table 4.2). Two-way ANOVA showed no statistical significance between the K_mPEP of *S. viridis* PEPC with the sequence from a PEPCK species in the presence and absence of G6P. The K_mPEP of *U. panicoides* PEPC with the sequence from a NAD-ME species was determined to be 0.20 mM ± 0.01 in the presence of 5 mM G6P and 0.30 mM ± 0.02 in the absence of G6P (Table 4.2). Two-way ANOVA showed that the difference between K_mPEP *of U. panicoides* PEPC with the sequence from a NAD-ME species in the presence and absence of G6P had no statistical significance. The K_mPEP of *P. coloratum* PEPC with the sequence from a NADP-ME species was determined to be 2.76 mM ± 0.43 in the presence of 5 mM G6P and 6.84 mM ± 0.18 in the absence of G6P (Table 4.2). Two-way ANOVA confirmed that there was a statistically significant difference between K_mPEP in the presence and absence of G6P for the *P. coloratum* PEPC with the sequence from a NADP-ME species enzyme.

Two-way ANOVA confirmed that there was no statistically significant difference between K_mPEP of PEPC for any of the species when compared to their respective enzyme chimeras, either in the presence or absence of G6P.

4.3.3 $K_m HCO_3^-$ of PEPC and PEPC chimeras in the presence glucose-6-phosphate.

The results described for Table 4.3 relate to experiments conducted by Dr Robert Di Mario in collaboration with Asaph Cousins' lab at Washington State University. The $K_m HCO_3^-$ of the *S. viridis* PEPC enzyme was determined to be 23.26 µM ± 0.74 in the presence of 5 mM G6P (Figure 4.8; Table 4.3). The $K_m HCO_3^-$ of the *U. panicoides* was determined to be 26.18 µM ± 1.04 in the presence of 5 mM G6P (Table 4.3). The $K_m HCO_3^-$ of the *P. coloratum* enzyme was determined to be 41.27 µM ± 1.38 in the presence of 5 mM G6P (Figure 4.8; Table 4.3). One-way ANOVA showed that the K_mPEP of both *S. viridis* and *U. panicoides* were statistically different from the K_mPEP of *P. coloratum* PEPC.

Table 4.3 $K_m HCO_3^-$ of *Setaria viridis*, *Urochloa panicoides*, and *Panicum coloratum* PEPC enzymes, and PEPC chimeras in the presence of glucose-6-phosphate (G6P). Each value is the average of 3 biological replicates, with the standard error between these replicates indicated. Values were determined using MIMS assay at 25 °C, initiated by the addition of PEPC protein. One-way ANOVA was conducted for statistical analyses with posthoc Tukey honestly significant difference (HSD) tests performed to determine statistically significant differences ($P < 0.05$). Different letters indicate statistically significant differences at $P<0.05$. The data in this table was obtained by Robert Di Mario from Asaph Cousins' lab.

	K_m HCO_3^- (µM)
S. viridis (NADP-ME)	23.26 ± 1.42 [a]
S. viridis + PEPCK sequence	20.75 ± 0.24 [a]
U. panicoides (PEPCK)	26.18 ± 1.04 [a]
U. panicoides + NAD-ME sequence	22.32 ± 1.22 [a]
P. coloratum (NAD-ME)	41.27 ± 1.38 [b]
P. coloratum + NADP-ME sequence	36.35 ± 2.01 [b]

The $K_m HCO_3^-$ of the *S. viridis* PEPC with the sequence from a PEPCK species was determined to be 20.75 µM ± 0.24 in the presence of 5 mM G6P (Figure 4.8; Table 4.3). The $K_m HCO_3^-$ of the *U. panicoides* PEPC with the sequence from a NAD-ME species was determined to be 22.32 µM ± 1.22 in the presence of 5 mM (Figure 4.8; Table 4.3). The $K_m HCO_3^-$ of the *P.*

coloratum PEPC with the sequence from a NADP-ME species was determined to be 36.35 µM ± 2.01 in the presence of 5 mM G6P (Figure 4.8; Table 4.3).

One-way ANOVA confirmed that there was no statistically significant differences between $K_mHCO_3^-$ of PEPC for any of the species when compared to their respective enzyme chimeras, in the presence of 5 mM G6P. The $K_mHCO_3^-$ for the *P. coloratum* PEPC and the *P. coloratum* PEPC with the sequence from a NADP-ME species were both statistically different to the PEPCs from the other species.

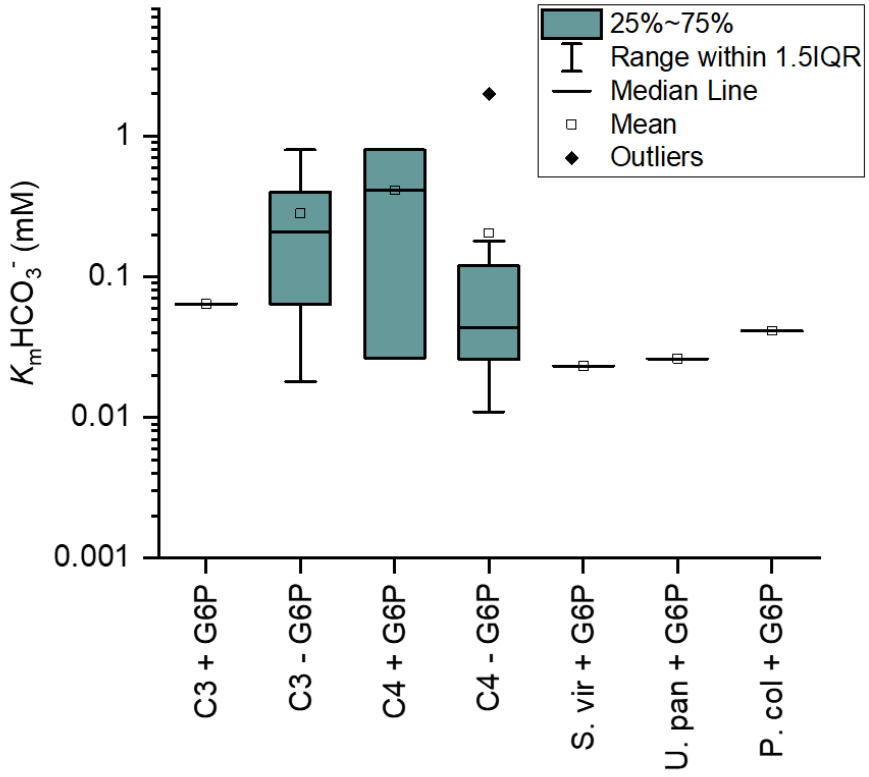

Figure 4.8. $K_mHCO_3^-$ (µM) ranges in the presence and absence of glucose-6-phosphate (G6P) for C_3 and C_4 species compared to the $K_mHCO_3^-$ values determined for *Setaria viridis* (S. vir), *Urochloa panicoides* (U. pan), and *Panicum coloratum* (P. col) PEPC enzymes in the presence of G6P. $K_mHCO_3^-$ values determined in the presence of G6P are indicated by + G6P, $K_mHCO_3^-$ values determined in the absence of G6P are indicated by - G6P. 1 reported value makes up the

C_3 + G6P boxplot, 6 for the C_3 - G6P, 2 for C_4 + G6P (all NADP-ME species) and 14 for C_4 – G6P (8 NADP-ME species, 5 NAD-ME species and 1 PEPCK species).

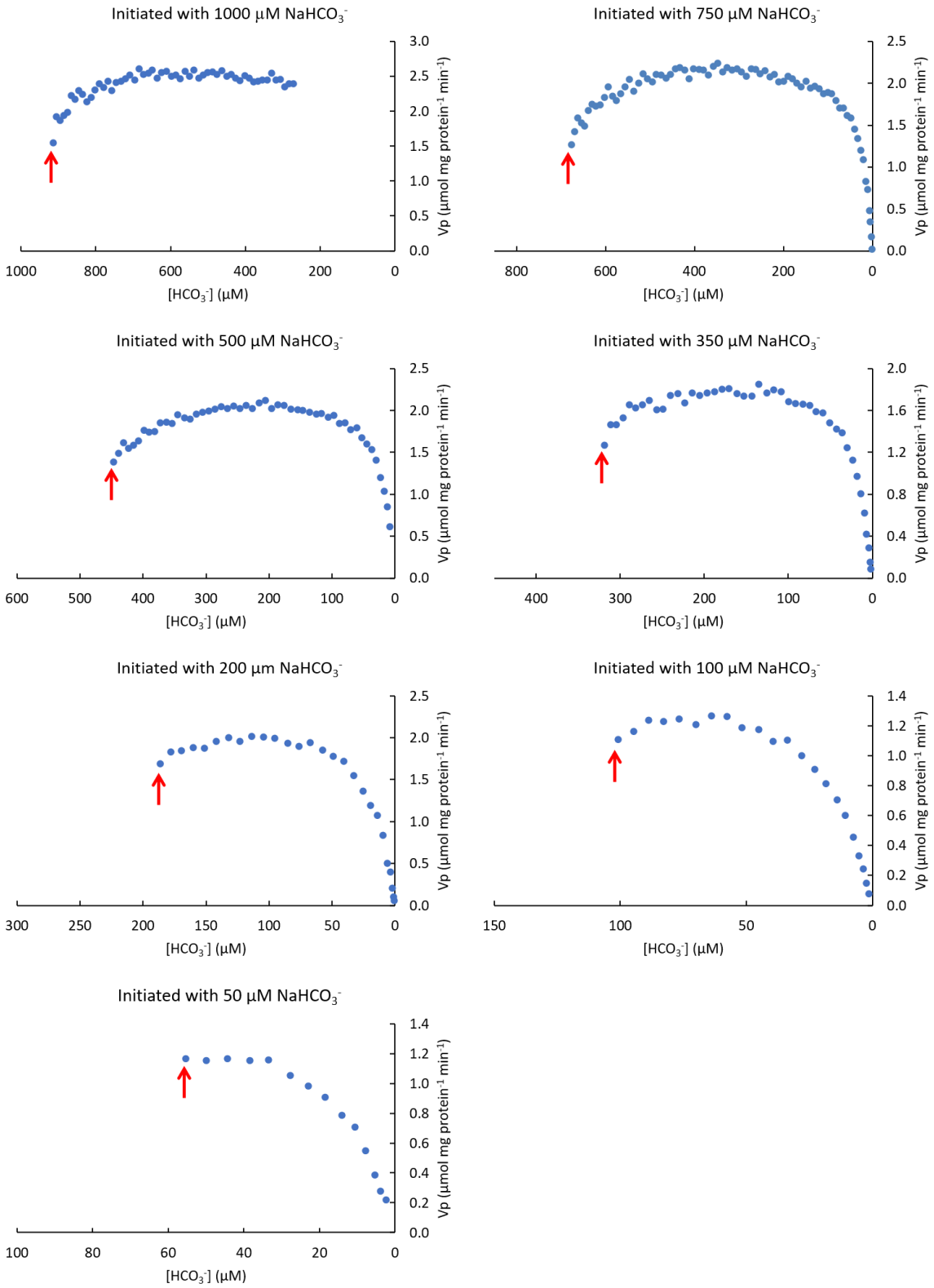

Figure 4.9. *Setaria viridis* PEPC activity as determined by membrane inlet mass spectrometry. Assays contained one of seven different concentrations of $NaHCO_3$ (1000, 750, 500, 350, 200, 100, and 50 µM), and were initiated by the addition of PEPC protein. Initiation of the assay is indicated by the red arrows. HCO_3^- was consumed as the reaction progressed, therefore, movement from left to right across the $[HCO_3^-]$ axes of the graphs indicate progression of the PEPC activity assay. Figures show a lag after initiation with the PEPC protein before the *S. viridis* PEPC enzyme activity reaches maximal rate.

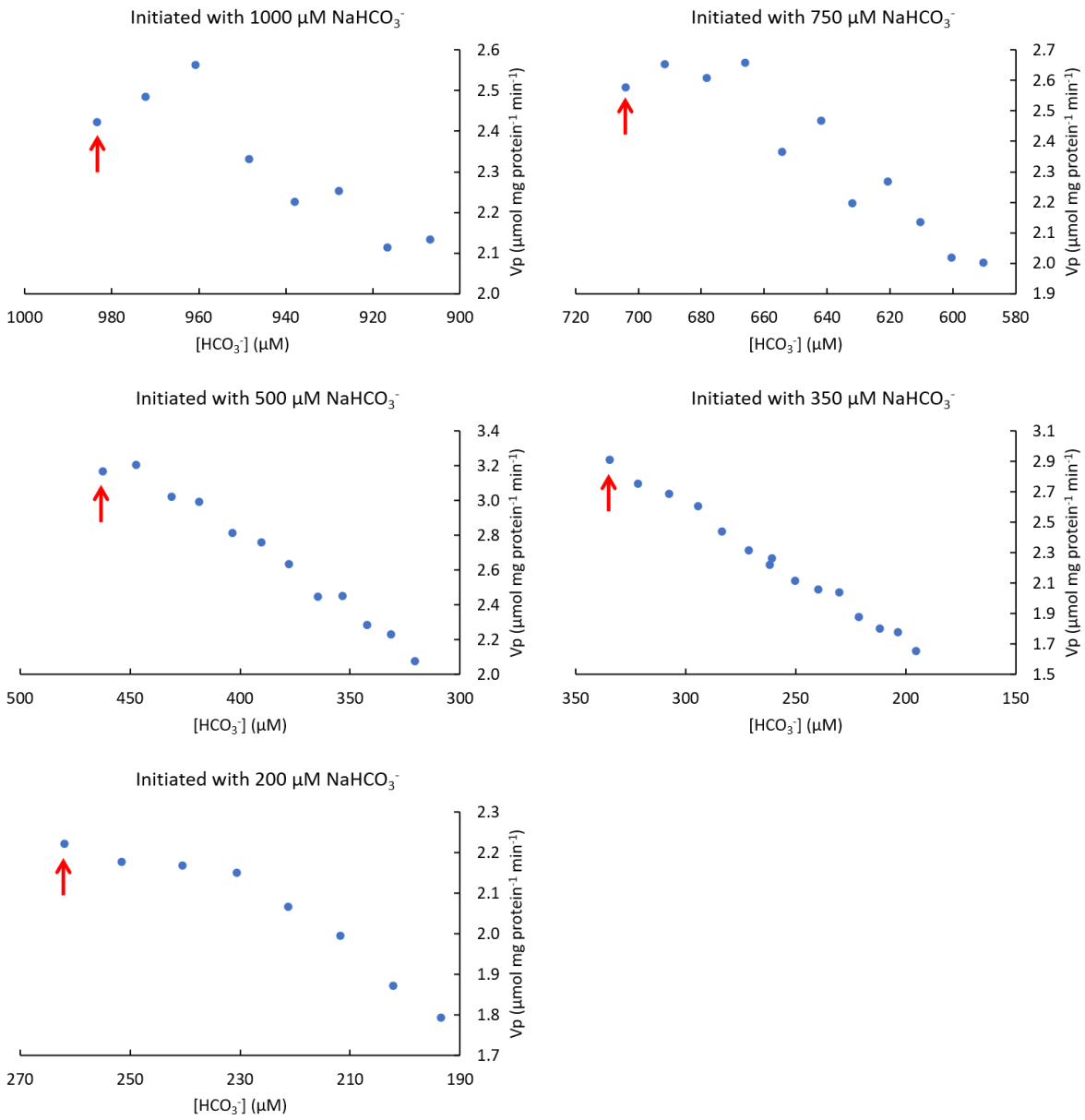

Figure 4.10. *Panicum coloratum* PEPC activity as determined by membrane inlet mass spectrometry. Assays contained one of seven different concentrations of $NaHCO_3$ (1000, 750, 500, 350, 200, 100, and 50 µM), and were initiated by the addition of PEPC protein. Initiation of the assay is indicated by the red arrows. HCO_3^- was consumed as the reaction progressed, therefore, movement from left to right across the $[HCO_3^-]$ axes of the graphs indicate progression of the PEPC activity assay. Figures show rapid reduction in PEPC enzyme activity after initiation with PEPC protein.

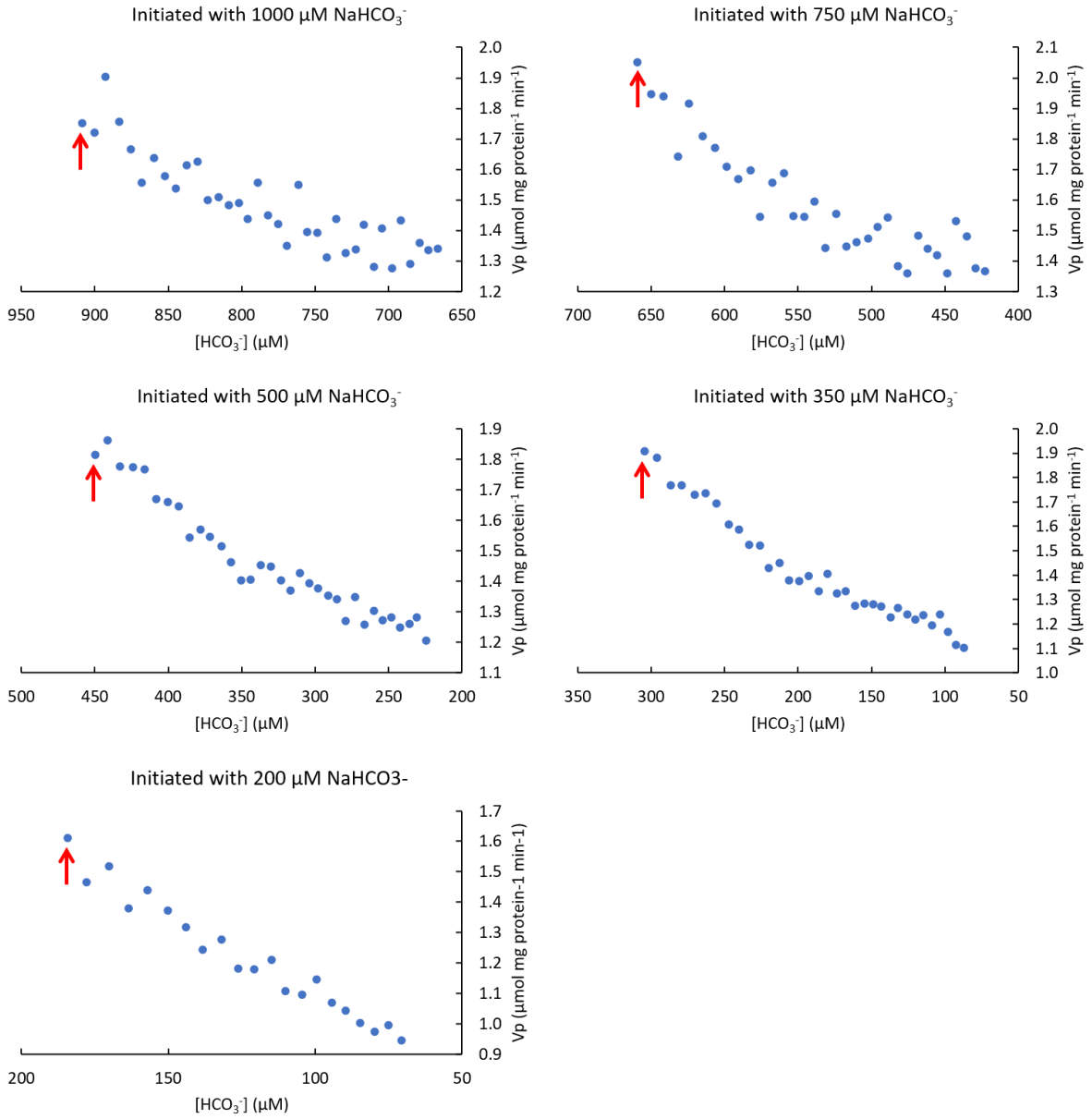

Figure 4.11. *Urochloa panicoides* PEPC activity as determined by membrane inlet mass spectrometry. Assays contained one of seven different concentrations of $NaHCO_3$, five of which are shown here (1000, 750, 500, 350, and 200 µM), and were initiated by the addition of the PEPC protein. Initiation of the assay is indicated by the red arrows. HCO_3^- was consumed as the reaction progressed, therefore, movement from left to right across the [HCO_3^-] axes of the graphs indicate progression of the PEPC activity assay. Figures show rapid reduction in PEPC enzyme activity after initiation with the PEPC protein.

4.3.4 V_{max} and k_{cat} of PEPC and PEPC chimeras in the presence and absence of glucose-6-phosphate

The V_{max} of *S. viridis* PEPC was determined to be 30.72 µmol min^{-1} mg^{-1} ± 0.74 in the presence of 5 mM G6P and 29.60 µmol min^{-1} mg^{-1} ± 1.78 in the absence of G6P (Table 4.4). Two-way ANOVA showed no statistical significance between the V_{max} of *S. viridis* PEPC in the presence and absence of G6P. The V_{max} of *U. panicoides* was determined to be 47.29 µmol min^{-1} mg^{-1} ± 1.98 in the presence of 5 mM G6P and 34.75 µmol min^{-1} mg^{-1} ± 3.41 in the absence of G6P (Figure 4.12, Table 4.4). Two-way ANOVA showed that the difference between *U. panicoides* PEPC V_{max} in the presence and absence of G6P had no statistical significance. The V_{max} of *P. coloratum* was determined to be 22.98 µmol min^{-1} mg^{-1} ± 3.24 in the presence of 5 mM G6P and 20.00 µmol min^{-1} mg^{-1} ± 2.93 in the absence of G6P (Figure 4.12, Table 4.4). Two-way ANOVA confirmed that there was no statistically significant difference between V_{max} in the presence and absence of G6P for the *P. coloratum* PEPC enzyme.

Table 4.4 V_{max} of *Setaria viridis*, *Urochloa panicoides*, and *Panicum coloratum* PEPC enzymes, and PEPC chimeras in the presence and absence of glucose-6-phosphate (G6P). Each value is the average of 3 biological replicates, with the standard error between these replicates indicated. Values were determined using a NADH-linked spectrophotometric assay at 25 °C with 1 µg PEPC protein, initiated with the addition of phosphoenolpyruvate (0 – 20 mM final concentration). Two-way ANOVA was conducted for statistical analyses with posthoc Tukey honestly significant difference (HSD) tests performed to determine statistically significant differences ($P < 0.05$). Different letters indicate statistically significant differences at $P<0.05$

	V_{max} (µmol min^{-1} mg^{-1})	
	with 5 mM G6P	no G6P
S. viridis (NADP-ME)	30.72 ± 0.74 ^{a,b,c}	29.60 ± 1.78 ^{a,b}
S. viridis + PEPCK sequence	28.94 ± 1.67 ^{a,b}	29.88 ± 1.22 ^{a,b}
U. panicoides (PEPCK)	47.29 ± 1.98 ^{b,c,d}	34.75 ± 3.41 ^{a,b,c}
U. panicoides + NAD-ME sequence	67.48 ± 9.57 ^{d}	52.12 ± 8.89 ^{c,d}
P. coloratum (NAD-ME)	22.98 ± 3.24 ^{a}	20.00 ± 2.93 ^{a}
P. coloratum + NADP-ME sequence	15.21 ± 1.15 ^{a}	14.46 ± 0.83 ^{a}

The V_{max} of *S. viridis* PEPC with the sequence from a PEPCK species was determined to be 28.94 µmol min^{-1} mg^{-1} ± 1.67 in the presence of 5 mM G6P and 29.88 µmol min^{-1} mg^{-1} ± 1.22 in the absence of G6P (Figure 4.12, Table 4.4). Two-way ANOVA showed no statistical significance between the V_{max} of *S. viridis* PEPC with the sequence from a PEPCK species in the presence and absence of G6P. The V_{max} of *U. panicoides* PEPC with the sequence from a NAD-ME species was determined to be 67.48 µmol min^{-1} mg^{-1} ± 9.57 in the presence of 5 mM G6P and 52.12 µmol min^{-1} mg^{-1} ± 8.89 in the absence of G6P (Figure 4.12, Table 4.4). Two-way ANOVA showed that the difference between *U. panicoides* PEPC with the sequence from

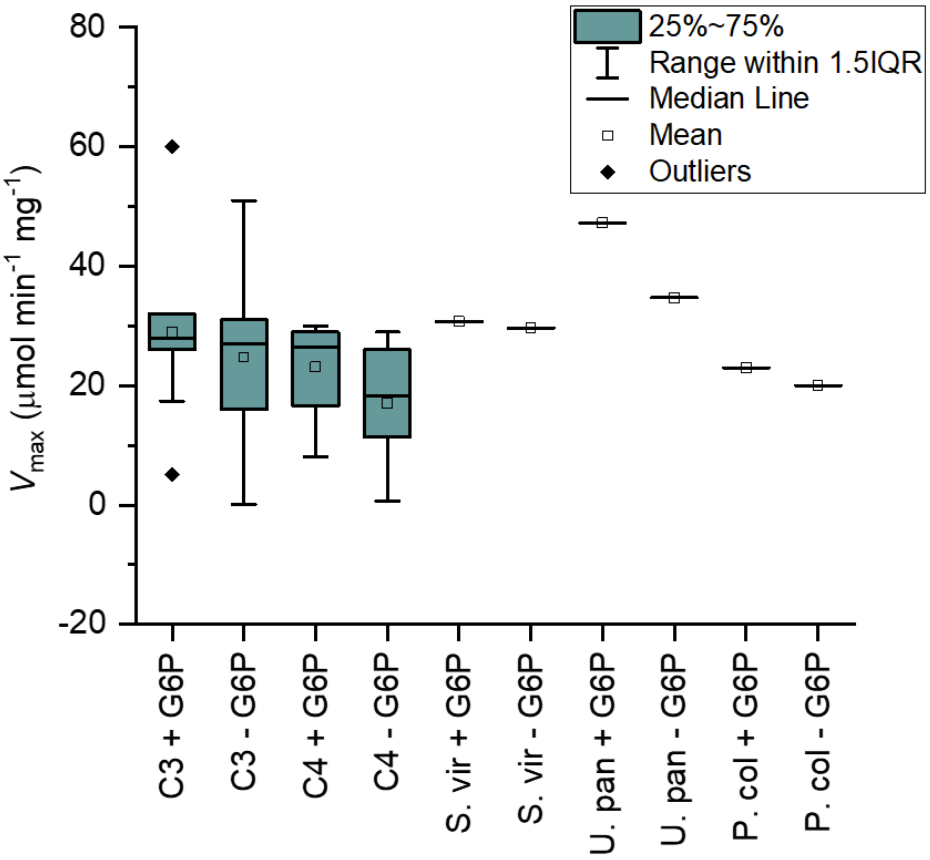

Figure 4.12. V_{max} (µmol min^{-1} mg^{-1}) ranges in the presence and absence of glucose-6-phosphate (G6P) for C_3 and C_4 species compared to the V_{max} values determined for *Setaria viridis* (S. vir), *Urochloa panicoides* (U. pan), and *Panicum coloratum* (P. col) PEPC enzymes in the presence of G6P. V_{max} values determined in the presence of G6P are indicated by + G6P, V_{max} values determined in the absence of G6P are indicated by - G6P. Nine reported values makes up the C_3 + G6P boxplot, 11 for the C_3 - G6P, 11 for C_4 + G6P (all NADP-ME species) and 19 for C_4 – G6P (3 NAD-ME species, 16 NADP-ME species).

a NAD-ME species V_{max} in the presence and absence of G6P had no statistical significance. The V_{max} of *P. coloratum* PEPC with the sequence from a NADP-ME species was determined to be 15.21 µmol min^{-1} mg^{-1} ± 1.15 in the presence of 5 mM G6P and 14.46 µmol min^{-1} mg^{-1} ± 0.83 in t he absence of G6P (Figure 4.12, Table 4.4). Two-way ANOVA confirmed that there was no statistically significant difference between V_{max} in the presence and absence of G6P for the *P. coloratum* PEPC with the sequence from a NADP-ME species enzyme.

Two-way ANOVA confirmed that there was no statistically significant difference between V_{max} of PEPC for any of the species when compared to their respective enzyme chimeras, either in the presence or absence of G6P.

The k_{cat} of *S. viridis* PEPC was determined to be 56.31 s^{-1} ± 1.35 in the presence of 5 mM G6P and 54.26 s^{-1} ± 3.26 in the absence of G6P (Table 4.5). Two-way ANOVA showed no statistical significance between the k_{cat} of *S. viridis* PEPC in the presence and absence of G6P. The k_{cat} of *U. panicoides* was determined to be 85.62 s^{-1} ± 3.56 in the presence of 5 mM G6P and 62.92 s^{-1} ± 6.18 in the absence of G6P (Figure 4.13, Table 4.5). Two-way ANOVA showed that the difference between *U. panicoides* PEPC k_{cat} in the presence and absence of G6P had no statistical significance. The k_{cat} of *P. coloratum* was determined to be 41.79 s^{-1} ± 5.89 in the presence of 5 mM G6P and 36.37 s^{-1} ± 5.32 in the absence of G6P (Figure 4.13, Table 4.5). Two-way ANOVA confirmed that there was no statistically significant difference between k_{cat} in the presence and absence of G6P for the *P. coloratum* PEPC enzyme.

The k_{cat} of *S. viridis* PEPC with the sequence from a PEPCK species was determined to be 52.70 s^{-1} ± 3.04 in the presence of 5 mM G6P and 54.39 s^{-1} ± 2.22 in the absence of G6P (Figure 4.13, Table 4.5). Two-way ANOVA showed no statistical significance between the k_{cat} of *S. viridis* PEPC with the sequence from a PEPCK species in the presence and absence of G6P. The k_{cat} of *U. panicoides* PEPC with the sequence from a NAD-ME species was determined to be 123.07 s^{-1} ± 17.46 in the presence of 5 mM G6P and 95.05 s^{-1} ± 16.21 in the absence of G6P (Table 4.5). Two-way ANOVA showed that the difference between *U. panicoides* PEPC with the sequence from a NAD-ME species k_{cat} in the presence and absence of G6P had no statistical significance. The k_{cat} of *P. coloratum* PEPC with the sequence from a NADP-ME species was

Table 4.5 k_{cat} of *Setaria viridis*, *Urochloa panicoides*, and *Panicum coloratum* PEPC enzymes, and PEPC chimeras in the presence and absence of glucose-6-phosphate (G6P). Each value is the average of 3 biological replicates, with the standard error between these replicates indicated. Values were determined using a NADH-linked spectrophotometric assay at 25 °C with 1 µg PEPC protein, initiated with the addition of phosphoenolpyruvate (0 – 20 mM final concentration). Two-way ANOVA was conducted for statistical analyses with posthoc Tukey honestly significant difference (HSD) tests performed to determine statistically significant differences ($P < 0.05$). Different letters indicate statistically significant differences at $P<0.05$

	K_{cat} (s^{-1})	
	with 5 mM G6P	no G6P
S. viridis (NADP-ME)	56.31 ± 1.35 ^{a,b,c}	54.26 ± 3.26 ^{a,b}
S. viridis + PEPCK sequence	52.70 ± 3.04 ^{a,b}	54.39 ± 2.22 ^{a,b}
U. panicoides (PEPCK)	85.62 ± 3.56 ^{b,c,d}	62.92 ± 6.18 ^{a,b,c}
U. panicoides + NAD-ME sequence	123.07 ± 17.46 ^{d}	95.05 ± 16.21 ^{c,d}
P. coloratum (NAD-ME)	41.79 ± 5.89 ^{a}	36.37 ± 5.32 ^{a}
P. coloratum + NADP-ME sequence	27.67± 2.09 ^{a}	26.28 ± 1.50 ^{a}

determined to be 27.67 s^{-1} ± 2.09 in the presence of 5 mM G6P and 26.28 s^{-1} ± 1.50 in the absence of G6P (Table 4.5). Two-way ANOVA confirmed that there was no statistically significant difference between k_{cat} in the presence and absence of G6P for the *P. coloratum* PEPC with the sequence from a NADP-ME species enzyme.

Two-way ANOVA confirmed that there was no statistically significant difference between k_{cat} of PEPC for any of the species when compared to their respective enzyme chimeras, either in the presence or absence of G6P.

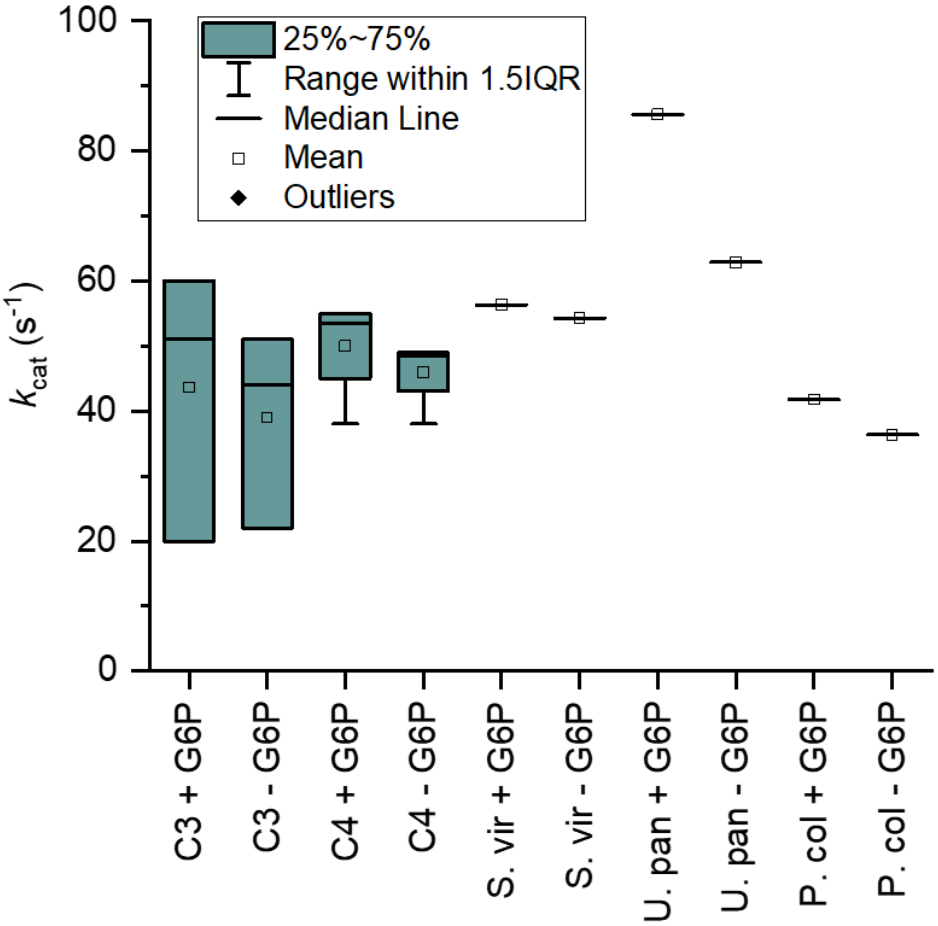

Figure 4.13. k_{cat} (s^{-1}) ranges in the presence and absence of glucose-6-phosphate (G6P) for C_3 and C_4 species compared to the k_{cat} values determined for *Setaria viridis* (S. vir), *Urochloa panicoides* (U. pan), and *Panicum coloratum* (P. col) PEPC enzymes in the presence of G6P. k_{cat} values determined in the presence of G6P are indicated by + G6P, k_{cat} values determined in the absence of G6P are indicated by - G6P. Three reported values makes up the C_3 + G6P boxplot, 3 for the C_3 - G6P, 4 for C_4 + G6P (all NADP-ME species) and 4 for C_4 – G6P (all NADP-ME species).

4.3.5 I_{50} malate and I_{50} aspartate

Table 4.6 I_{50} malate of *Setaria viridis*, *Urochloa panicoides*, and *Panicum coloratum* PEPC enzymes, and PEPC chimeras in the presence and absence of glucose-6-phosphate (G6P). Each value is the average of two or three technical replicates, with the standard error between these replicates indicated. Values were determined using a NADH-linked spectrophotometric assay at 25 °C with 1 μg PEPC protein, initiated with the addition of phosphoenolpyruvate (5 mM final concentration). Malate concentrations of mM, 5 mM, 4.5 mM, 4 mM, 3 mM, 2.5 mM, 2 mM, 1.5 mM, 1.25 mM, 1 mM, 0.75 mM, 0.5 mM, 0.25 mM, 0.125 mM, 0.0625 mM were used in assays to determine I_{50} malate.

	I_{50} malate (mM)	
	with 5 mM G6P	no G6P
S. viridis (NADP-ME)	5.00 ± 0.11	4.63 ± 0.09
S. viridis + PEPCK sequence	No inhibition	5.25 ± 0.19
U. panicoides (PEPCK)	No inhibition	6.11 ± 0.05
U. panicoides + NAD-ME sequence	5.13 ± 0.69	4.51 ± 0.12
P. coloratum (NAD-ME)	1.34 ± 0.04	1.33 ± 0.04
P. coloratum + NADP-ME sequence	1.20 ± 0.01	1.02 ± 0.01

The I_{50} malate of *S. viridis* PEPC enzyme was determined to be 5.00 mM ± 0.11 in the presence of 5 mM G6P and 4.63 mM ± 0.09 in the absence of G6P (Figure 4.14, Table 4.6). The I_{50} malate of the *U. panicoides* PEPC enzyme was not inhibited across the malate range tested in the presence of 5 mM G6P and its I_{50} value in the absence of G6P was determined to be 6.11 mM ± 0.05 (Table 4.6). The I_{50} malate of the *P. coloratum* PEPC enzyme was determined to be 1.20 mM ± 0.01 in the presence of 5 mM G6P and 1.02 mM ± 0.01 in the absence of G6P (Figure 4.14, Table 4.6).

The *S. viridis* PEPC enzyme with the sequence from a PEPCK species was not inhibited in the presence of 5 mM G6P and the I_{50} malate in the absence of G6P was 5.25 ± 0.19 (Figure 4.14, Table 4.6). The I_{50} malate of the *U. panicoides* PEPC with the sequence from a NAD-ME species was determined to be 5.13 mM ± 0.69 in the presence of 5 mM G6P and 4.51 ± 0.12 in the absence of G6P (Figure 4.14, Table 4.6). The I_{50} malate of the *P. coloratum* PEPC with the

sequence from a NADP-ME species was determined to be 1.20 mM ± 0.01 in the presence of 5 mM G6P and 1.02 ± 0.01 in the absence of G6P (Figure 4.14, Table 4.6).

None of the PEPC enzymes of any of the species tested nor the enzyme chimeras showed any inhibition by aspartate in the 0 – 6 mM range tested.

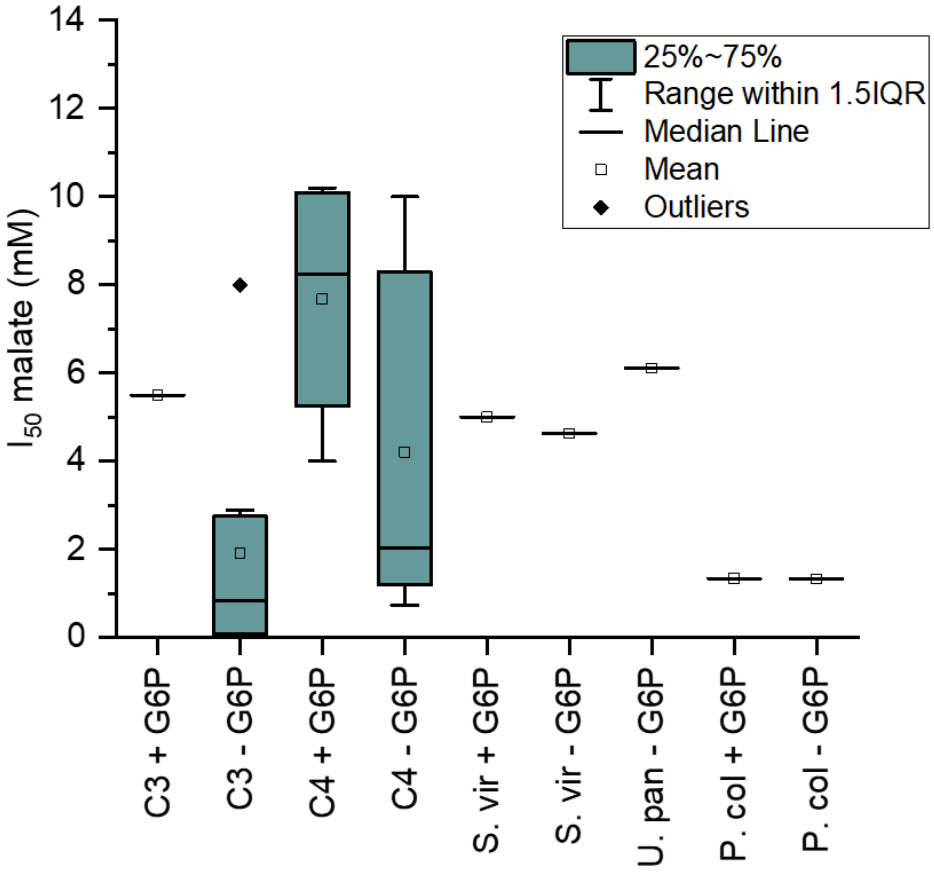

Figure 4.14. I_{50} (mM) ranges in the presence and absence of glucose-6-phosphate (G6P) for C_3 and C_4 species compared to the I_{50} values determined for *Setaria viridis* (S. vir), *Urochloa panicoides* (U. pan), and *Panicum coloratum* (P. col) PEPC enzymes in the presence of G6P. I_{50} values determined in the presence of G6P are indicated by + G6P, I_{50} values determined in the absence of G6P are indicated by - G6P. One reported value makes up the C_3 + G6P boxplot, 8 for the C_3 - G6P, 4 for C_4 + G6P (all NADP-ME species) and 16 for C_4 – G6P (3 NAD-ME species, 13 NADP-ME species). The *Urochloa panicoides* (U. pan) enzyme was not inhibited in the 0 – 6.5 mM range tested, so has been omitted from the boxplot.

4.4 Discussion

The aim of this chapter was to investigate the effects of the PEPCK-specific six amino acid deletion on PEPC enzyme kinetics. This was investigated by determining carboxylation and inhibition kinetics data for one NADP-ME species, one NAD-ME species and one PEPCK species and three enzyme chimeras with shuffled PEPCK-specific regions. The results and possible effect of this region on K_mPEP, $K_m HCO_3^-$, $k_{cat,}$ V_{max}, and inhibition by malate and aspartate are discussed here.

4.4.1 K_mPEP

4.4.1.1 Is P. coloratum PEPC an efficient enzyme?

The K_mPEP data obtained for *P. coloratum* indicates that it has an unusually low affinity for the substrate PEP. When comparing the value of K_mPEP in the absence of G6P of *P. coloratum* (7.32 mM ± 0.49) across all plant species regardless of photosynthetic type, only a handful of species come anywhere close to the high K_mPEP value of *P. coloratum*. *Bryophyllum fedtschenkoi* (CAM species) and *Setaria verticillata* (NADP-ME) have reported K_mPEP values of 2.4 mM and 1.9 mM, respectively, and *Zea mays* (NADP-ME) has a particularly wide range of reported K_mPEP values in the absence of G6P of between 0.1 – 7.9 mM, respectively (Appendix 1; Ting and Osmond, 1973b; Ting and Osmond, 1973c; Uedan and Sugiyama, 1976; Mukerji, 1977; Jones et al., 1978; Samaras et al., 1988; Bandarian et al., 1992; Janc et al., 1992; Dong et al., 1998; Frank et al., 2001; Takahashi-Terada et al., 2005; Endo et al., 2008). The *P. coloratum* PEPC appears to have a such a poor affinity for its substrate PEP, which raises questions as to the overall performance of this PEPC enzyme in photosynthesis. A study measuring PEPC activity of leaf extracts from a variety of C_4 grasses found that *P. coloratum* had the second lowest PEPC activity across the species investigated, seemingly supporting the

finding that the *P. coloratum* PEPC enzyme may not be an efficient PEPC (Figure 4.16; Pinto et al., 2014).

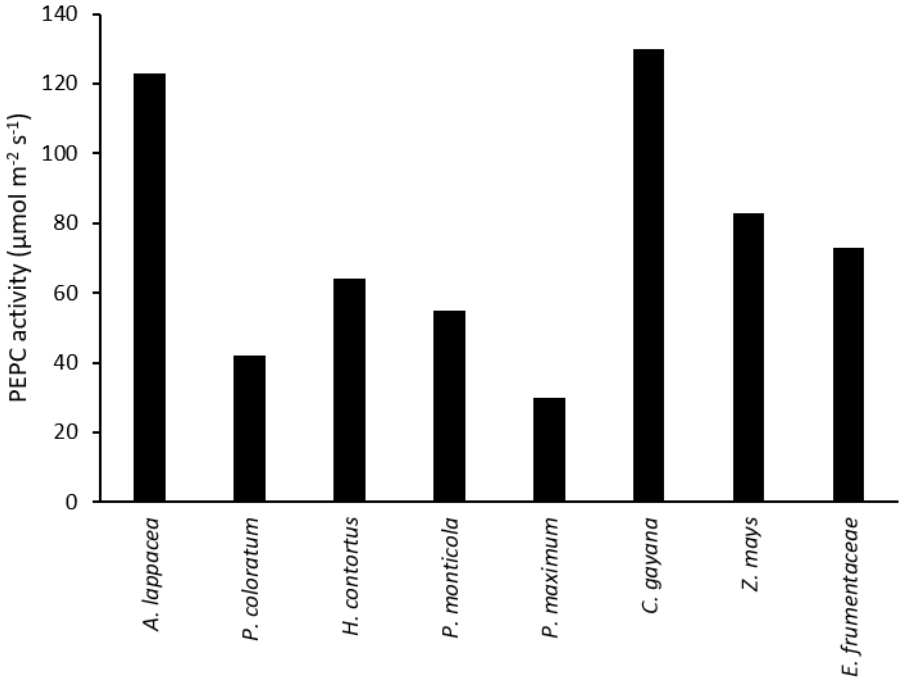

Figure 4.16. PEPC activity (µmol m^{-2} s^{-1}) from a number of C_4 grass species. Data taken from Pinto et al. (2014). PEPC activity was determined using leaf extracts and a NADH-coupled spectrophotometric assay.

4.4.1.2 Effect of PEPCK deletion on K_mPEP?

Although there was no statistically significant difference between K_mPEP of PEPC for any of the species when compared to their respective enzyme chimeras, either in the presence or absence of G6P, further testing needs to be performed (more replicates and repeated experimentation) before a conclusion can be reached about the effect that the sequence under examination has on K_mPEP of the PEPC enzymes (Table 4.2).

4.4.2. *K*mHCO_3^-

It has been hypothesised that during the evolution from C_3 to C_4 photosynthesis, C_4 PEPCs were under selective pressure to have a greater affinity for bicarbonate, and thus smaller $K_m HCO_3^-$ value than those of the C_3 enzymes (Jacobs et al., 2008; DiMario and Cousins, 2019). Comparisons of the $K_m HCO_3^-$ values determined for the *S. viridis*, *U. panicoides*, and *P. coloratum* PEPC enzymes to reported $K_m HCO_3^-$ values for C_3 PEPC enzymes, appear, for the most part, to support this hypothesis (Figure 4.8, Appendix 1, Table 4.3). The *S. viridis*, *U. panicoides*, and *P. coloratum* PEPC enzymes all have $K_m HCO_3^-$ values in the presence of G6P smaller than the only reported C_3 $K_m HCO_3^-$ value (0.064 mM) for the activated enzyme of *Flaveria pringlei* (Figure 4.8, Appendix 1, Table 4.3; DiMario and Cousins, 2019). The activated PEPC enzymes from *S. viridis*, *U. panicoides*, and *P. coloratum* also have $K_m HCO_3^-$ values lower than all but one of the reported $K_m HCO_3^-$ values for the unactivated PEPC enzymes for C_3 species, with the PEPC from *Atriplex hastata* being the notable exception (Figure 4.8, Appendix 1, Table 4.3; Maruyama et al., 1966; Ting and Osmond, 1973c; Miziorko et al., 1974; Holaday and Black, 1981; Law and Plaxton, 1995). The only reported $K_m HCO_3^-$ value in the presence of G6P falls within the range of activated C_4 PEPC enzymes, but given that there were only two reported values for $K_m HCO_3^-$ in the presence of G6P, it is difficult to make any kind of comment on the validity of the hypothesis (Coombs et al., 1973; DiMario and Cousins, 2019). There is a large overlap between the unactivated $K_m HCO_3^-$ values of C_3 and C_4 species, although overall the range of unactivated $K_m HCO_3^-$ values are greater for C_3 PEPCS than C_4 PEPCs (Figure 4.8, Appendix 1; Maruyama et al., 1966; Coombs et al., 1973; Ting and Osmond, 1973c; Miziorko et al., 1974; Holaday and Black, 1981; Bauwe, 1986; Iglesias et al., 1986; Janc et al., 1992; Law and Plaxton, 1995; Gao and Woo, 1996; Dong et al., 1998; Parvathi et al., 2000; Boyd et al., 2015; DiMario and Cousins, 2019). This appears to provide some support for the hypothesis, however, it is clear that to properly investigate the

hypothesis that C_4 PEPCs were under selective pressure to have a greater affinity for bicarbonate, $K_mHCO_3^-$ values from more PEPC enzymes from both C_3 and C_4 species need to be determined.

The PEPCs of *S. viridis*, *U. panicoides*, and *P. coloratum* PEPC also have lower $K_mHCO_3^-$ values than two C_3-C_4 intermediate species, *Coleataenia prionitis* with a $K_mHCO_3^-$ of 300 µM (30°C), and *Panicum milioides* with a $K_mHCO_3^-$ of 400 – 800 µM (30°C) (Holaday and Black, 1981). Again, however, both values were determined in the absence of G6P. Therefore, the hypothesis that C_4 PEPCs were under selective pressure to have a greater affinity for bicarbonate requires more targeted research. There is one C_3 species which appears to undermine this hypothesis. *Atriplex hastata* has a $K_mHCO_3^-$ of 18 µM (pH 7.8; 30°C) in the absence of G6P (Ting and Osmond, 1973c). It would appear that, in this case, the unactivated PEPC enzyme of *A. hastata* has a higher affinity for bicarbonate than the activated C_4 PEPC enzymes of *S. viridis*, *U. panicoides*, and *P. coloratum*. In fact, when considering the $K_mHCO_3^-$ values of C_4 species (Appendix 1) only the PEPC from *Amaranthus hypochondriacus* has a lower $K_mHCO_3^-$ value (11 µM), and thus a higher affinity for bicarbonate that the unactivated PEPC enzyme of *A. hastata*. (Coombs et al., 1973; Ting and Osmond, 1973c; Mukerji, 1977; O'Leary, 1982; Bauwe, 1986; Iglesias et al., 1986; Janc et al., 1992; Gao and Woo, 1996; Dong et al., 1998; Parvathi et al., 2000; Boyd et al., 2015; DiMario and Cousins, 2019).

From the data obtained for this thesis, the $K_mHCO_3^-$ of the *S. viridis* PEPC enzyme assayed in the presence of G6P (23.26 µM ± 0.74), was lower than Boyd et al. (2015) reported $K_mHCO_3^-$ of *S. viridis* PEPC enzyme assayed in the absence of G6P (60.2 µM). This suggests an activation of the *S. viridis* enzyme by G6P resulting in a lowering of the $K_mHCO_3^-$. This

lowering of the $K_mHCO_3^-$ in the presence of G6P is also seen in the NADP-ME species *Pennisetum purpureum* (Appendix 1; Coombs et al., 1973). *Pennisetum purpureum* is the only species in the literature with reported $K_mHCO_3^-$ values both in the presence and absence of G6P.

4.4.2.1 Could OAA or pyruvate interfere the $K_mHCO_3^-$ MIMS assays?

The *Setaria viridis* PEPC showed a lag in activity after initiation of the assay with the PEPC protein before the *S. viridis* PEPC enzyme reached a maximal rate (Figure 4.9). This indicates that the enzyme took time to be activated by one of the assay buffer components. Samaras et al. (1988) hypothesised that PEP could be the *in vivo* activator of *Setaria verticillata* PEPC. In this case, any one of $MgCl_2$, G6P, PEP or $NaHCO_3$ could be responsible for the activation observed.

The PEPC enzymes from *Panicum coloratum* and *Urochloa panicoides* showed rapid reduction in activity after the initiation of the assay (Figure 4.10, Figure 4.11). This indicates the presence of a potent inhibitor in the reaction. This same rapid inhibition was not observed in the spectrophotometric PEPC enzymes assays. Therefore, something present in the MIMS PEPC assay, but absent in the NADH-coupled spectrophotometric assay, must have caused this inhibition. The NADH-coupled spectrophotometric assay consists of two reactions (Figure 4.17). Firstly, PEPC catalyses the carboxylation of PEP by bicarbonate to form OAA (Figure 4.17). Secondly, malate dehydrogenase (MDH) catalyses the reduction of OAA formed in the first reaction to malate (Figure 4.17). In the MIMS reaction, however, only the PEPC-catalysed

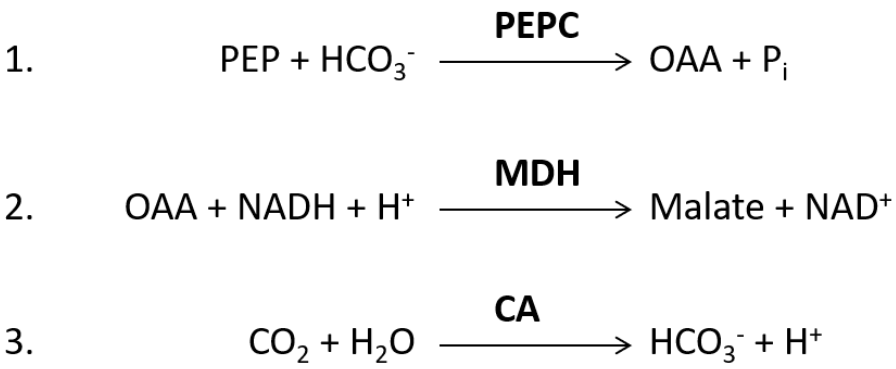

Figure 4.17. Reactions of the NADH-coupled spectrophotometric assay and the MIMS PEPC assay. In reaction 1, PEPC catalyses the carboxylation of phospho*enol*pyruvate (PEP) by bicarbonate (HCO_3^-) to form oxaloacetate (OAA) and inorganic phosphate (Pi). In reaction 2, malate dehydrogenase (MDH) catalyses the reduction of OAA formed in reaction 1 to malate. This reaction requires energy in the form of NADH. In reaction 3, carbonic anhydrase catalyses the hydration of CO_2 to form bicarbonate. Reactions 1 and 2 are occur in the spectrophotometric assay measuring PEPC activity and reactions 1 and 3 occur in the MIMS PEPC activity assay.

carboxylation of PEP by bicarbonate to form OAA occurs. This OAA remains in the reaction solution and is not converted to malate. Therefore, it seems likely that it is the OAA remaining in the reaction solution in the MIMS assay that is responsible for the rapid inhibition of both the *Panicum coloratum* and *Urochloa panicoides* PEPC enzymes. The hydration of CO_2 to form bicarbonate also occurs in the MIMS reaction, but given that HCO_3^- is a substrate of PEPC and no substrate inhibition of PEPC enzymes has been reported, it is not likely to be the cause of PEPC inhibition (Figure 4.17).

OAA inhibition of the PEPC enzyme has been reported in a number of plant species including *Setaria italica*, *Pennisetum purpureum* and *Amaranthus viridis* (Coombs et al., 1973; Raghavendra and Das, 1975; Iglesias et al., 1986), as well as in the bacterial species *C. peniocystis* (Owttrim and Colman, 1986). The study by (Raghavendra and Das, 1975) reported a K_i for OAA of 1 mM (Appendix 1), with OAA being an even more potent inhibitor of the *Setaria italica* PEPC enzyme than malate (Ki malate: 5 mM). This was also seen in *Amaranthus viridis*, with I_{50} OAA of 1.0 mM (pH 7.0; 30 °C) and 0.5 mM (pH 8.0; 30 °C) compared to I_{50} malate of 2.5 mM (pH 7.0; 30 °C) and 10 mM (pH 8.0; 30 °C) (Iglesias et al., 1986). OAA was

also reported to be a more effective inhibitor of the C_4 *Pennisetum purpureum* PEPC enzyme than malate (Coombs et al., 1973). Therefore, it is probable that OAA is a potent inhibitor of the *Panicum coloratum* and *Urochloa panicoides* PEPC enzymes. An investigation into the inhibitory effects of OAA on the PEPC enzymes investigated warrants further investigation.

Pyruvate inhibition has been observed in numerous plant species including *Amaranthus viridis* (C_4), *Atriplex spongiosa* (C_4), *Atriplex hastata* (C_3), *Gossypium hirsutum* (C_3) (Mukerji and Ting, 1971; Ting and Osmond, 1973c; Iglesias et al., 1986). Although OAA does convert to pyruvate in solution, its half-life to convert to pyruvate at 25 °C in biological aqueous solution is 14 hours (Yu and Sivitz, 2020). Therefore, it is highly unlikely that the rapid reduction in activity observed is a result of inhibition by pyruvate.

Although there was no statistically significant difference between $K_mHCO_3^-$ of PEPC for any of the species when compared to their respective enzyme chimeras in the presence of 5 mM G6P, further testing needs to be performed (more replicates and repeated experimentation) before a conclusion can be reached about the effect that the sequence under examination has on $K_mHCO_3^-$ of the PEPC enzymes.

4.4.4 k_{cat} and V_{max}

P. coloratum, *S. viridis*, and *U. panicoides* PEPC enzymes had lower k_{cat} values in the absence of G6P than in the presence of G6P, although none of these differences were statistically significant (Table 4.5). k_{cat} values reported for *Flaveria pringleii* (C_3 species) and *Flaveria trinervia* (NADP-ME species) also show slightly lower k_{cat} values for their PEPC enzyme in

the absence of G6P (Appendix 1; Bläsing et al., 2000; Bläsing et al., 2002). On the other hand, reported k_{cat} values for *Alternanthera pungens* (NADP-ME species) and *Alternanthera tenella* (C_3-C_4 intermediate species) were identical in the presence and absence of G6P (Appendix 1; Gowik et al., 2006). Given the relatively few species investigated, it is difficult to make a generalisation on the impact of G6P on the k_{cat} values of PEPC enzymes. The k_{cat} values of PEPC enzymes from a greater number of species needs further investigation.

The k_{cat} values for C_4 PEPC enzymes have only been reported for NADP-ME species, so the the k_{cat} values obtained for both *U. paniocides* (PEPCK) and *P. coloratum* (NAD-ME) are a first in the literature. The k_{cat} values determined for the *S. viridis* enzyme in the presence and absence of G6P fall just above the ranges reported for k_{cat} values in the presence and absence of G6P for C_4 species (Figure 4.14, Appendix 1, Table 4.5). The k_{cat} values determined for the *P. coloratum* enzyme in the presence of G6P falls within the C_4 range, and the value determined in the absence of G6P falls just below the C_4 range (Figure 4.14, Appendix 1, Table 4.5). The k_{cat} values determined for the *U. panicoides* enzyme in the presence and absence of G6P fall considerably above the ranges reported for k_{cat} values in the presence and absence of G6P for C_4 species (Figure 4.14, Appendix 1, Table 4.5). *Urochloa panicoides*, therefore, appears to have a superior k_{cat} value.

Although there was no statistically significant difference between k_{cat} PEPC for any of the species when compared to their respective enzyme chimeras in the presence and absence of G6P, further testing needs to be performed (more replicates and repeated experimentation) before a conclusion can be reached about the effect that the sequence under examination has on k_{cat} of the PEPC enzymes.

Only NADP-ME and NAD-ME species have recorded V_{max} values in the form µmol min^{-1} mg^{-1} recorded in the absence of G6P, and only NADP-ME species have recorded V_{max} values in the form µmol min^{-1} mg^{-1} recorded in the presence of G6P (Appendix 1; Iglesias et al., 1986; Gao and Woo, 1996; Svensson et al., 1997; Dong et al., 1998; Bläsing et al., 2000; Parvathi et al., 2000; Bläsing et al., 2002; Engelmann et al., 2003; Takahashi-Terada et al., 2005; Gowik et al., 2006; Lara et al., 2006; Endo et al., 2008; DiMario and Cousins, 2019). Given that no V_{max} values in the form µmol min^{-1} mg^{-1} have been reported for PEPCK species, the V_{max} values obtained for the *U. panicoides* PEPC enzyme are a first in this regard. The V_{max} values of *P. coloratum* PEPC fall within the range of V_{max} values for C_4 PEPC, whilst the V_{max} values of *S. viridis* PEPC fall just above C_4 range (Figure 4.12, Appendix 1, Table 4.4). The V_{max} of *U. panicoides* fall well above the C_4 range. Given that only NAD-ME and NADP-ME species had V_{max} values reported in µmol min^{-1} mg^{-1}, it might seem that PEPCK species as a group might have superior V_{max} values. This isn't the case, however, as is elucidated when examining V_{max} values reported µmoles per minute per mg of chlorophyll. The V_{max} values reported for PEPCK species examined were no greater than those of the NAD-ME and NADP-ME species (Ting and Osmond, 1973b; Ting and Osmond, 1973c). Thus, it seems that *U.* panicoides has superior catalytic properties that aren't characteristic of the PEPCK subtype as a whole. Thus, the *Urochloa panicoides* enzyme would be an interesting enzyme for further study and an exciting candidate to transform into a NADP-ME model species, such as *Setaria viridis* to examine its impact on photosynthesis.

Given that there was no statistically significant difference between V_{max} of PEPC for any of the species when compared to their respective enzyme chimeras in the presence of 5 mM G6P, further testing needs to be performed (more replicates and repeated experimentation) before a conclusion can be reached about the effect that the sequence under examination has on V_{max} of the PEPC enzymes.

4.4.5 Inhibition by malate

P. coloratum, *S. viridis*, and *U. panicoides* PEPC enzymes had lower I_{50} values in the absence of G6P than in the presence of G6P (Table 4.6, Figure 4.14). Although the difference between the I_{50} values of the *Panicum coloratum* enzyme in the presence of absence of G6P was very small (Table 4.6, Figure 4.14). G6P has been shown to alleviate the inhibitory effects of malate on PEPC in C_3, C_3-C_4 intermediate and C_4 species (Dong et al., 1998; Chen et al., 2002; Engelmann et al., 2003; Pierre et al., 2004; Takahashi-Terada et al., 2005; Jacobs et al., 2008). Two notable exceptions exist in *Flaveria brownii*, a C_4-like species, and *Flaveria trinervia*, a C_4 NADP-ME species, where the presence of G6P resulted in a decrease in the K_i-malate and therefore an increase in sensitivity of the PEPC enzyme to malate (Engelmann et al., 2003; Jacobs et al., 2008).

When the *S. viridis* PEPC enzyme is given the six-base deletion from the *U. panicoides* PEPCK sequence, the PEPC enzyme goes from having an I_{50} malate of 5.00 mM to being uninhibited by malate (Table 4.6). Alternatively, when the PEPCK deletion in the *U. panicoides* enzyme is replaced by the six amino acids from the NAD-ME *P. coloratum* PEPC enzyme, the *U. panicoides* enzyme goes from being uninhibited by malate, to having an I_{50} malate of 5.13 mM (Table 4.6). This indicates that this PEPCK-specific six-base deletion might affect the extent to which PEPC enzymes are inhibited by malate. In order to investigate this further, more species need to be investigated and reciprocal region swaps between protein pairs need to be conducted. Danila et al. (2018) conducted an investigation into C_4 subtype-specific density of plasmodesmata using 13 C_4 species in the PACMAD clade covering 4 independent origins of C_4 photosynthesis. These grass species examined included 4 NAD-ME species (*Leptochloa fusca, Astrebla lappacea, Panicum coloratum*, and *Panicum miliaceum*), 6 NADP-ME species (*Paspalum dilatatum, Sorghum bicolor, Zea mays, Setaria viridis Cenchrus ciliaris*, and *Panicum antidotale*), and 3 PEPCK species (*Chloris gayana*, *Panicum maximum*, and *Urochloa panicoides*). To properly investigate whether this PEPCK-specific six-base deletion

might affect the extent to which PEPC enzymes are inhibited by malate taking PEPCs from a sample of representative species such as this and performing region swaps would be highly recommended.

Given that C_4 species have a I_{50} malate in the range of 0.82 – 10.0 mM, further studies are needed covering this range. Also, given that only 2 or three technical replicates were used to generate the current initial data, kinetic analysis on three biological replicates across a malate range of 0 – 15 mM is recommended.

4.5 Conclusions

In conclusion, K_mPEP, $K_m HCO_3^-$, k_{cat} and V_{max} values were obtained for the *S. viridis*, *P. coloratum*, and *U. panicoides* PEPC enzymes. The k_{cat} values obtained for both *U. paniocides* (PEPCK) and *P. coloratum* (NAD-ME) are a first in the literature as no k_{cat} values have been published for PEPCK or NAD-ME species. No V_{max} values in the form μmol min^{-1} mg^{-1} have been reported for PEPCK species, so V_{max} value obtained for the *U. panicoides* PEPC enzyme is a first in this regard. K_mPEP, $K_m HCO_3^-$, k_{cat} and V_{max} values were also obtained for the three PEPC enzyme chimeras. None of the PEPC enzymes or PEPC enzyme chimeras were inhibited by aspartate over the 0 – 6 mM range tested. I_{50} malate values were calculated for the *S. viridis*, *P. coloratum*, and *U. panicoides* PEPC enzymes and the enzyme chimeras. From the data obtained, it appears that the PEPCK-specific six amino acid deletion affects the extent to which PEPC enzymes are inhibited by malate. In order to further investigate this, more species need to be investigated and reciprocal region swaps between protein pairs need to be conducted. The kinetic analysis needs to be conducted on three biological replicates across a malate range of 0 – 15 mM.

Chapter 5: PEPC overexpression in *Setaria viridis* and the reduction in malate sensitivity of the PEPC enzyme in *Setaria viridis*

5.1 Introduction

5.1.1 What PEPC overexpression in C_4 plants could tell us about limiting steps of C_4 photosynthesis

Modelling of the C_4 biochemical pathway has shown that differences in maximal PEPC activity (V_{pmax}) will impact the initial slope of the CO_2 response curve (CO_2 assimilation rate (A) v CO_2 partial pressure in the intercellular airspace (Ci)), with a proportional relationship between V_{pmax} and the initial slope (Figure 5.1; von Caemmerer, 2000). When modelled, the saturated rate of the CO_2 response curve is proportional to the maximal Rubisco activity (V_{cmax}). This may not be the case *in vivo*, however, where PEP regeneration capacity may be limiting, and leakiness and bundle-sheath CO_2 partial pressures may not continue to increase with increasing CO_2 concentrations (von Caemmerer, 2000). Rubisco activity is just one of a number of factors

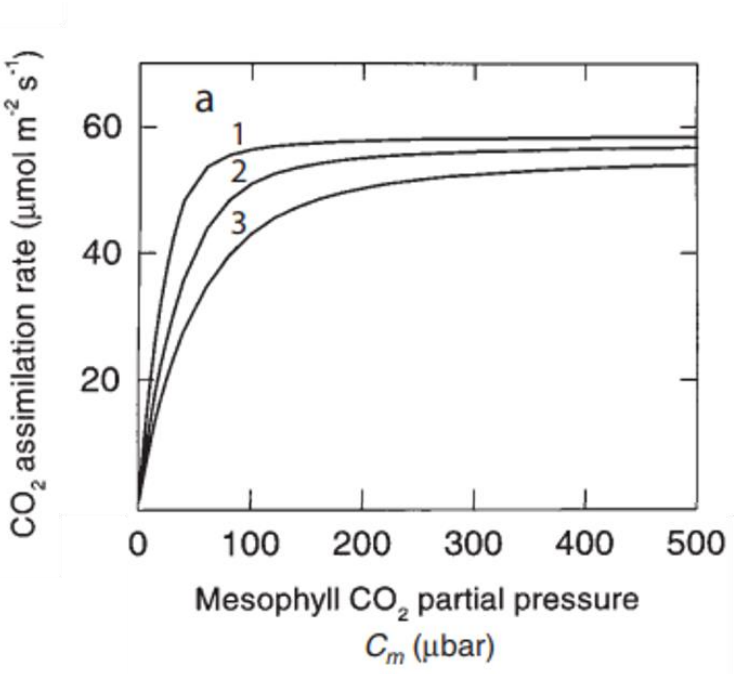

Figure 5.1. CO_2 response curve with various maximum PEPC activities (V_{pmax}). In this model there is no limitation by PEP regeneration. The initial slope of the curve is affected by the V_{pmax}. (1 = V_{pmax} of 180 µmol m^{-2} s^{-1}; 2 = V_{pmax} of 120 µmol m^{-2} s^{-1}; 3 = V_{pmax} of 80 µmol m^{-2} s^{-1}). Figure from von Caemmerer (2000).

thought to influence the saturated rate of the CO_2 response curve, with substrate regeneration of the C_3 and C_4 cycles and chloroplast electron transport also influencing the saturated rate (von Caemmerer and Furbank, 2016). Modelling has elucidated that when PEPC expression is very low in a CO_2 saturated environment, a corresponding reduction in the saturated rate of CO_2 assimilation would be observed, as Rubisco would no longer be saturated with CO_2 in the bundle sheath cells (von Caemmerer, 2000). It has been hypothesised that PEPC 'is unlikely to be a key limiting step at ambient CO_2' (von Caemmerer and Furbank, 2016). Investigating PEPC overexpression in C_4 plants will determine whether or not PEPC is limiting CO_2 assimilation rate. The results from such an investigation would help to inform future C_4 modelling and provide valuable *in vivo* information.

5.1.2 PEPC overexpression in C_3 plants

There has been much effort aimed at overexpressing PEPC in C_3 plants in order to improve C_3 plant productivity through the introduction of a single-cell C_4 pathway, such as that seen in aquatic species *Hydrilla verticillata* and *Orcuttia viscida*, or terrestrial species *Suaeda aralocaspica* and *Bienertia sinuspersici* into the mesophyll of C_3 plants (Taniguchi et al., 2008; von Caemmerer et al., 2014; Kandoi et al., 2016). To work towards this goal, PEPC has often been expressed in tandem with other C_4 photosynthetic genes, such as PPDK, NADP-ME, PEPCK, NADP-malate dehydrogenase (MDH) (Häusler et al., 2001; Taniguchi et al., 2008; Zhang et al., 2014). Recently, introducing a two-cell C_4 pathway into rice (C_3) has become the focus of the international C_4 rice project, in order to improve yield (Ermakova et al., 2020). Overexpression of PEPC in C_3 plants has also helped to characterise its role in various physiological pathways (Jeanneau et al., 2002). Following is a summary of the findings of PEPC overexpression in C_3 plants.

C_4 PEPCs have been overexpressed in a variety of C_3 plants in multiple attempts to improve C_3 plant productivity. The overexpression of *Zea mays* (C_4) PEPC in *Nicotiana tabacum* (C_3) resulted in higher PEPC activity of transgenics compared to the wild type, as well as higher levels of malate. The CO_2 compensation point and photosynthetic rate of these transgenics was

not significantly affected (Hudspeth et al., 1992). Another study investigating the overexpression of *Zea mays* (C_4) PEPC in *Nicotiana tabacum* under the control of a constitutive promoter (CaMV 35S) found that the increased PEPC activity in the transgenic plants resulted in decreased growth rate compared to wild-type plants, decreased chlorophyll content per leaf area compared to wild-type, and 'the quantum yield of photosynthesis in the transgenic plants was not affected by changes in leaf temperature' (Kogami et al., 1994).

Overexpression of *Zea mays* (C_4) PEPC in rice (C_3) resulted in enhanced drought tolerance of transgenic plants compared to wild type, caused by an increase in intercellular CO_2 concentration which, protected peptides, photosynthetic complexes and thylakoid membranes against oxidative damage (Shen et al., 2015). Another study of *Zea mays* (C_4) PEPC overexpression in rice (C_3) with increased PEPC activity reported no change to photosynthetic rates of transformants compared to wild-type, but a reduction in the inhibition of photosynthesis by O_2 (Ku et al., 1999). Further study of these transformants revealed enhanced respiration in the transgenic plants compared to wild-type (Agarie et al., 2001), and higher aluminium tolerance when compared to wild-type (Begum et al., 2009). Furthermore, Ku et al. (1999) showed that PEPC transgenics showed greater dry weight accumulation in the panicle, sheath, stem and leaves when compared to wild-type. These plants also had significantly higher levels of soluble sugar and protein found in the grain, but a decrease in starch (Xia and Cao, 2013). Another study of *Zea mays* (C_4) PEPC overexpression in rice (C_3) found a slight reduction in photosynthetic rates of the transgenic rice plants compared to the wild-type (Taniguchi et al., 2008).

An overexpression of PEPC from maize (C_4) in wheat (C_3), led to an increase in PEPC activity resulting in higher maximum net photosynthetic rates, as well as an increase in overall diurnal photosynthesis when compared to the control (Zhang et al., 2014). Overexpression of maize PEPC in wheat has also been reported to cause enhanced drought tolerance, conferred by an increase in soluble sugar and protein, proline, and enhanced water use efficiency, as well as increase grain yield under drought stress (Qin et al., 2016).

Overexpression of *Zea mays* (C_4) PEPC in *Arabidopsis thaliana* (C_3) under control of a constitutive promoter, and the resulting increase in PEPC enzymatic activity, led to an increase in protein content. This is hypothesised to have been caused by the anaplerotic function of PEPC, providing an increase in 4-carbon carboxylic acids. The transgenic plants were reported to have enhanced electron transport rate, higher chlorophyll content, reduced non-photochemical quenching, and enhanced salt stress tolerance. Also reported were increases in CO_2 assimilation rate, dry weight and starch content of the transgenic PEPC overexpressors compared to the wild-type (Kandoi et al., 2016). An attempt to overexpress Sorghum (C_4) PEPC in *Arabidopsis thaliana* under control of a constitutive promoter, actually caused a decrease in both PEPC content and activity in the leaves, when compared to the wild-type. This caused malate, glutamine, and fumarate expression to be significantly reduced with no change in sucrose and glucose content. The reduction of PEPC content and activity had no effect on growth under normal conditions but did cause diminished growth under salt stress (Lebouteiller et al., 2007).

As can be seen from the multitude of studies regarding C_4 PEPC overexpression in C_3 species, an increase in PEPC activity can have a wide variety of effects in C_3 transgenics. Some results appear to be contradictory, with an increase in PEPC activity having no effect on photosynthetic rates in rice, but an increase in photosynthetic rates in wheat and *Arabidopsis thaliana*.

Bacterial PEPCs have also been the focus of overexpression studies in C_3 plants. Studies investigating the overexpression of a bacterial PEPC (*Corynebacterium glutamicum*) in the C_3 species *Solanum tuberosum* and corresponding increased PEPC activity has reported to be linked to a decrease in growth rate, increased malate, starch, and sucrose levels, accelerated stomatal opening, a lower CO_2 compensation point (Γ^*), and enhanced respiration in the light and dark when compared to wild-type plants. No difference in steady state CO_2 assimilation or CO_2 incorporation into leaf discs was observed between wild-type and transformants (Gehlen

et al., 1996; Häusler et al., 1999). Overexpression of PEPC genes from *Corynebacterium glutamicum* or *Solanum tuberosum* in *Nicotiana tabacum* or *Solanum tuberosum* resulted in an induction of a NADP-ME, as well as an increase in the activity of a variety of other enzymes, although this was less pronounced in the tobacco transformants. The Γ* varied amongst the different transformants (Häusler et al., 2001).

Synechococcus vulcanus, a cyanobacterial species, has a PEPC with almost no sensitivity to feedback inhibition. This PEPC was overexpressed in *Arabidopsis thaliana* (C_3) under a constitutive promoter and resulted in poor growth and no true leaf development, accompanied by a significant decrease in levels of phenylalanine (Phe) and tyrosine (Tyr), and increases in asparagine, glutamine and arginine (Chen et al., 2004). *Solanum tuberosum* (C_3) PEPC was modified at either the N-terminal phosphorylation site or a portion of the PEPC was replaced with a homologous PEPC sequence from *Flaveria trinervia* (C_4), both modified PEPCs had decreased sensitivity to feedback inhibition by malate and lower K_m PEP. Overexpression of these modified PEPCs in *Solanum tuberosum* resulted in inhibition of plant growth and diminished tuber yield, stemming from a decrease in soluble sugars and starch in favour of malate and amino acid production (Rademacher et al., 2002).

Overexpression of *Jatropha curcas* C_3-type PEPC in *Nicotiana tabacum* (C_3), resulting in increased PEPC enzymatic activity, led to an alteration in fatty acid composition and total fatty acid content in transgenic *Nicotiana tabacum* compared to wild-type (Fan et al., 2013).
An investigation into the overexpression of PEPC from *Solanum tuberosum* (C_3) in *Arabidopsis thaliana* (C_3), both under constitutive and dark-induced control, showed increases in stomatal conductance, CO_2 assimilation rates, dark respiration, and transpiration, compared to wild-type plants (Kebeish et al., 2012).

Given that PEPC overexpression in C_3 plants has resulted in highly variable results, the overexpression of PEPC in plants is an interesting area of research. As C_3 photosynthesis does not involve PEPC, introducing the C_4 photosynthetic isoform of PEPC into C_3 species could be

expected to result in variable results, and could be influenced by the identity of the C_4 PEPC, the promoter utilised for C_4 PEPC expression, the C_3 recipient species, and any other genes introduced in tandem with the C_4 PEPC. It is clear that there is still much to discover in this area. The lack of published PEPC overexpression studies in C_4 plants makes this a promising avenue for research to investigate the influence of increased PEPC expression on C_4 photosynthesis.

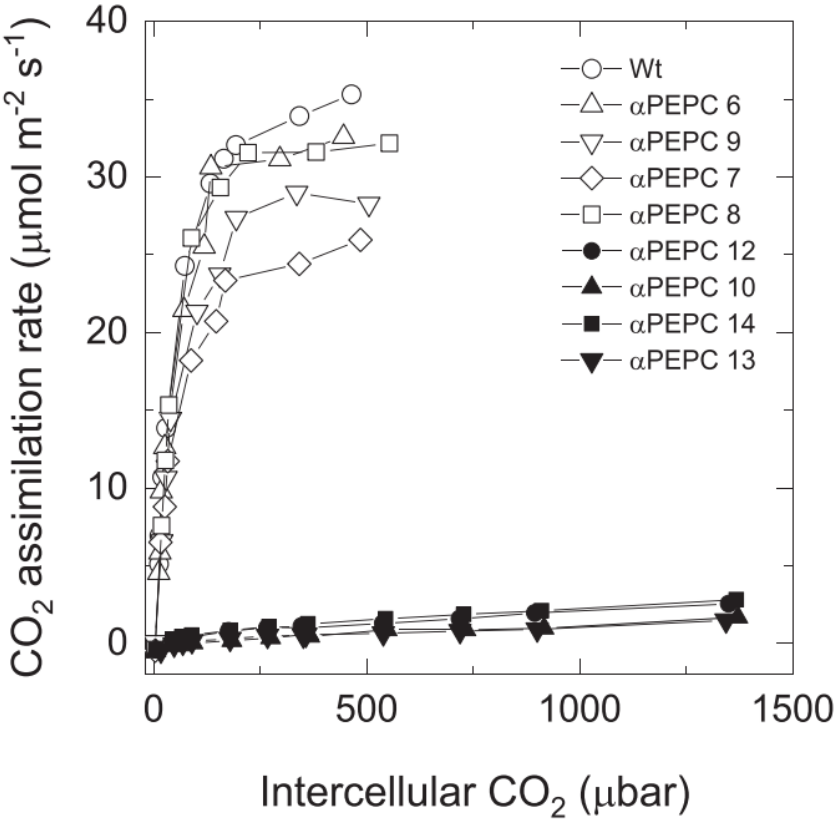

Figure 5.2. CO_2 response curve (CO_2 assimilation rate (µmol m^{-2} s^{-1}) v intercellular CO_2 concentration (µbar)) of the leaves of wild-type and individual T_0 *Setaria viridis* plants. White symbols represent plants with wild-type levels of PEPC activity and black symbols indicate plants with significantly reduced PEPC activity. Measurements were made at 1500 µmol quanta m^{-2} s^{-1}, 21 % oxygen and a leaf temperature of 25 °C. Image from Alonso-Cantabrana et al. (2018).

5.1.3 Reduction of PEPC expression

The results of unpublished data regarding the overexpression of cDNA for a sorghum C_4 PEPC in maize was presented in the review paper of Jeanneau et al. (2002). Photosynthetic PEPC levels were increased 2.2-fold causing pleiotropic physiological effects, including improved water use efficiency under drought conditions. Although PEPC overexpression in C_4 plants has not been published, PEPC reduction in C_4 plants is more widely published. RNA interference was used to create *S. viridis* mutants with very low C_4 PEPC activities (Alonso-Cantabrana et al., 2018). These transgenics had very low CO_2 assimilation rates (Figure 5.2), increased plasmodesmata density, due to increase in pit fields, at the mesophyll-bundle sheath cell interface. Measurements of these transgenics allowed the bundle sheath conductance to CO_2 diffusion (g_{bs}) to be calculated (Alonso-Cantabrana et al., 2018).

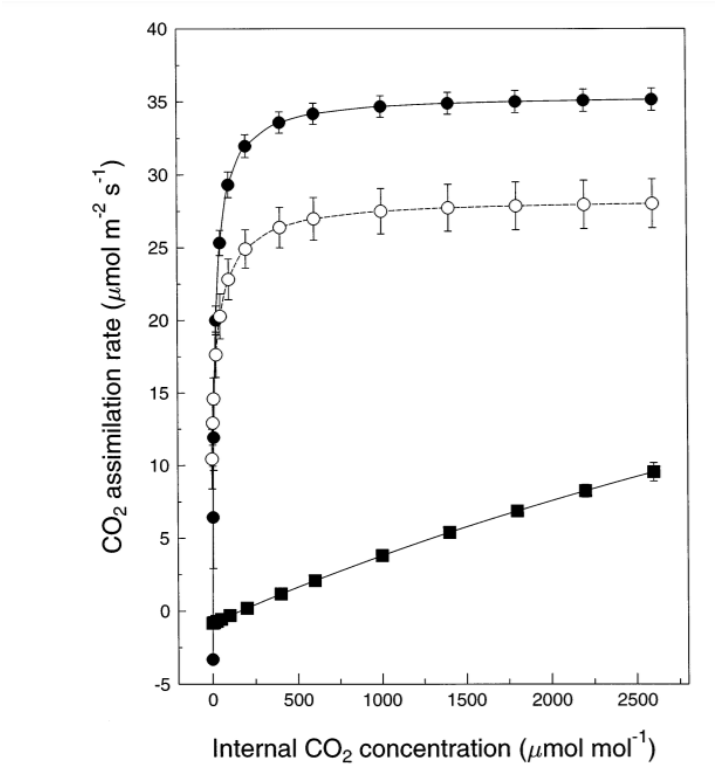

Figure 5.3. CO_2 response curve (CO_2 assimilation rate (µmol m^{-2} s^{-1}) v internal CO_2 concentration (µmol mol^{-1})) of wild-type (●), heterozygous (○) and homozygous (■) PEPC mutant plants. Measurements were made at a photosynthetic proton flux density of 2000 µmol m^{-2} s^{-1}. Image from Dever et al. (1997).

A study using 3,3-dichloro-2-(dihydroxyphosphinoylmethyl)-propenoate (DCDP) to inhibit PEPC activity in excised leaves of seven C_4 species found that PEPC inhibition in C_4 plants strongly eliminated CO_2 assimilation (Jenkins, 1989).

Mutants of the C_4 NAD-ME plant, *Amaranthus edulis*, with reduced PEPC activity were created using sodium azide (Dever et al., 1995). A reduction in the maximum CO_2 assimilation rate was observed for those mutants when compared to the wild-type, with mutants having a lower carboxylation efficiency (Figure 5.3; Dever et al., 1997). Further studies on these *Amaranthus edulis* PEPC mutants, examining both heterozygous and homozygous individuals, showed a reduction of CO_2 assimilation in air compared to wild-type plants (Cousins et al., 2007). Similar stomatal conductance between the wild-type and heterozygote mutant was observed, however, the homozygous mutant displayed differences in steady-state stomatal conductance and stomatal opening, leading to the conclusion that C_4 PEPC isoform has a role in stomatal opening (Cousins et al., 2007). Another study involving heterozygous mutant *Amaranthus edulis* plants with reduced PEPC activity showed a decrease in the initial slope of CO_2 response curves (CO_2 assimilation rate versus intercellular CO_2 concentration) when compared to wild-type plants (Figure 5.4; Bailey et al., 2000). Mutant plants also had reduced photosynthetic rates at high light intensities (Bailey et al., 2000).

As can be seen from these studies, a reduction in maximal PEPC activity does indeed appear to reduce the initial slope of the CO_2 response curve (CO_2 assimilation rate (A) v CO_2 partial pressure in the intercellular airspace (Ci)), as predicted by biochemical modelling of the C_4 pathway. Combining PEPC overexpression data with the available PEPC reduction data would provide valuable insights into the effects of PEPC activity in C_4 photosynthesis.

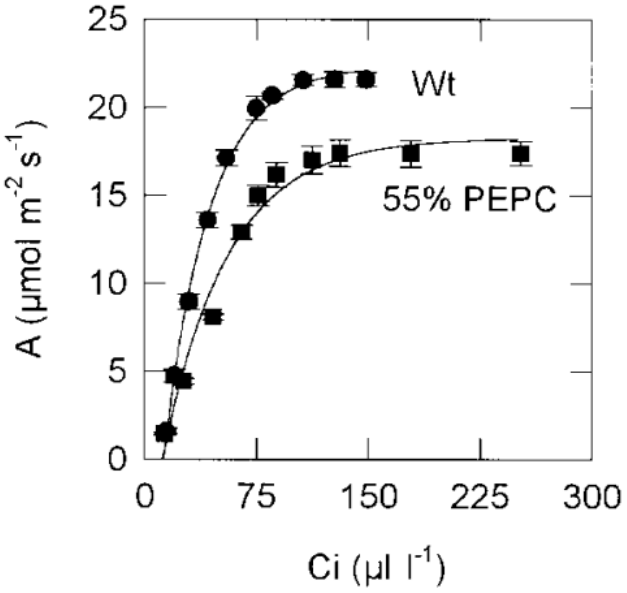

Figure 5.4. CO_2 response curve (CO_2 assimilation rate (µmol m^{-2} s^{-1}) v intercellular CO_2 concentration (µl l^{-1})) of wild-type and heterozygous PEPC mutant plants. Measurements were made at a proton flux density of 1200 µmol m^{-2} s^{-1}. Image from Bailey et al. (2000).

5.1.4 *Setaria viridis* – a model C_4 species

C_4 photosynthesis has arisen independently 22 to 24 times within the grasses (Poaceae), with independent lineages in the subfamilies Panicoideae, Chloridoideae, Aristidoideae and Micrairoideae (Grass Phylogeny Working, 2012; Sage, 2016). With the major C_4 grass crops belonging to the Panicoideae (Figure 5.5), including sugarcane (*Saccharum officinarum* (NADP-ME)), sorghum (*Sorghum bicolor* (NADP-ME)), maize (*Zea mays* (NADP-ME)), millets (proso millet (*Panicum miliaceum* (NAD-ME)), pearl millet (*Pennisetum glaucum* (NADP-ME)), foxtail millet (*Setaria italica* (NADP-ME))), and switchgrass (*Panicum virgatum* (NAD-ME)), it is important to have a closely related C_4 model from within the same subfamily (Sage et al., 1999; Brutnell et al., 2010).

Setaria viridis (NADP-ME) is closely related to the major C_4 crops, also belonging to the Panicoideae clade (Figure 5.5), and has become a model for C_4 crop. Its relatively small diploid genome (approximately 515 Mb), short stature, rapid 6-to-9-week generation time, self-pollination and high-volume seed production make *S. viridis* ideal as a model (Defelice, 2002;

Brutnell et al., 2010; Li and Brutnell, 2011; Van Eck, 2018). The genome sequence for *S. viridis* available (Bennetzen et al., 2012), and this coupled with the *Agrobacterium*-mediated transformation that has been developed, through both seed-derived callus and floral dip methods, has facilitated genetic engineering studies in this model C_4 grass (Martins et al., 2015; Martins et al., 2015; Van Eck and Swartwood, 2015; Van Eck, 2018; Nguyen et al., 2020).

As *Setaria viridis* has become a model C_4 species with many features making it ideal for study, it was chosen as the species in which to investigate the role of PEPC activity in C_4 photosynthesis.

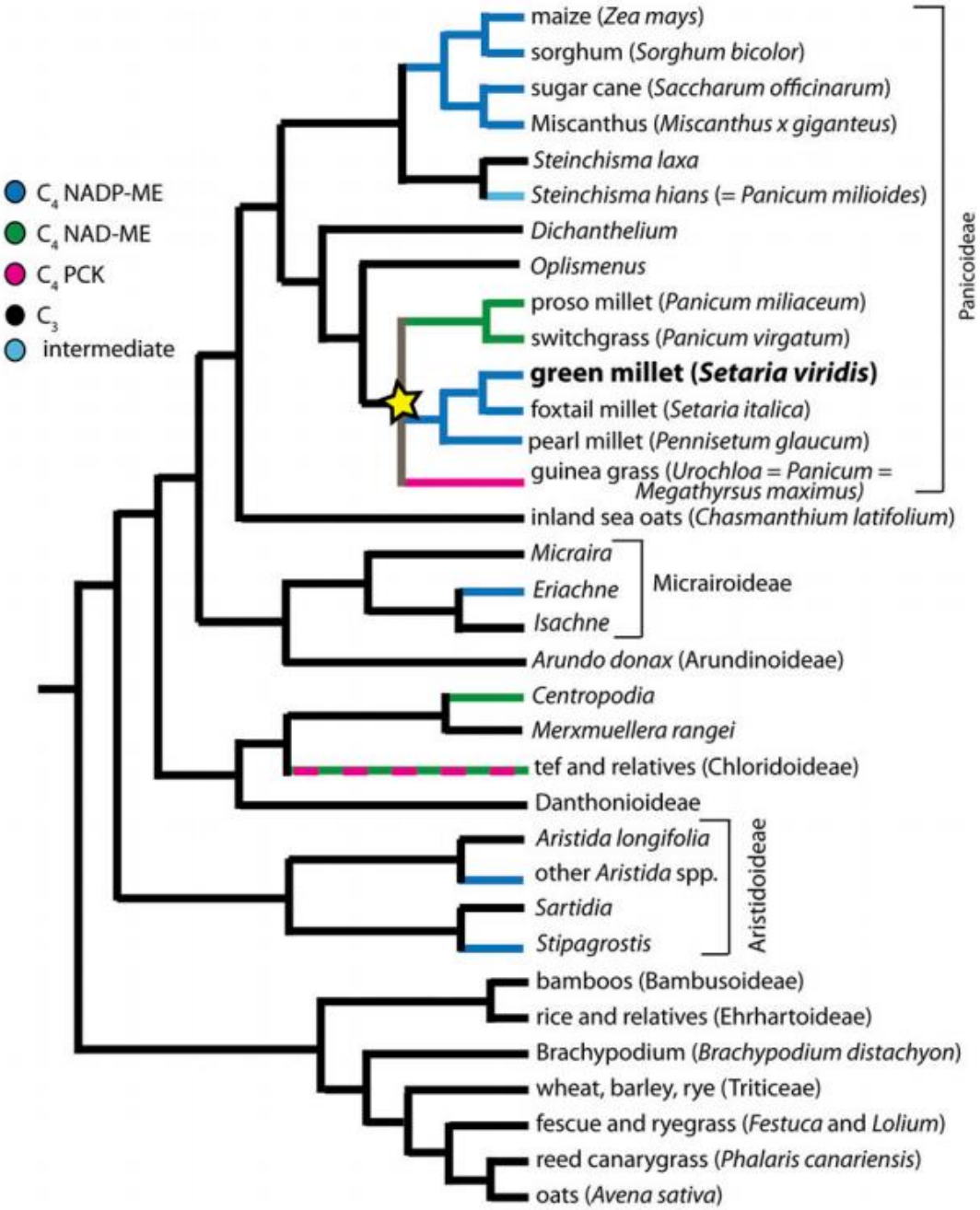

Figure 5.5. Phylogenetic relationships of the grass family. Setaria viridis is indicated in bold. C_4 NADP-ME species are indicated with a dark blue bar, C_4 NAD-ME species are indicated with a green bar, C_4 PEPCK species indicated with a pink bar. C_3 species are indicated with a black bar, and light blue bars indicate C_3-C_4 intermediate species. Image from Brutnell et al. (2010).

5.1.5 Inhibition of the PEPC enzyme by malate

As discussed in Chapter 4 of this thesis, high concentrations of malate in the mesophyll cells compared to the bundle sheath cells create concentration gradients sufficient to drive rapid diffusion of malate into the bundle sheath cells (Stitt and Heldt, 1985), driving the photosynthetic carbon flux. With estimated mesophyll malate concentrations of 11.18 mM in the presence of light and CO_2, and C_4 plants having recorded *in vitro* K_i malate (pH 7.0 – 8.0; 25 - 30 °C) between approximately 0.24 mM and 5 mM, cytosolic malate in the mesophyll should affect PEPC activity (Table 4.1, Table 4.3; Raghavendra and Das, 1975; McNaughton et al., 1989; Parvathi et al., 2000; Engelmann et al., 2003; Arrivault et al., 2017). Therefore, investigation of the inhibition of PEPCs enzymes by malate and aspartate will be investigated in this chapter of the thesis.

Site-directed mutagenesis studies by (Endo et al., 2008), investigated the effects of mutating two malate-binding residues in the *Zea mays* PEPC enzyme. These malate binding residues, K835 and R894 were both mutated to glycine residues. This drastically increased the I_{50} malate of the *Zea mays* PEPC enzyme from 1.6 mM in the wild-type enzyme to >20 mM in both the K835G and the R894G mutant enzymes (Table 5.1; Endo et al., 2008). Whilst the malate sensitivity of the *Zea mays* PEPC enzyme was significantly reduced in the mutant enzymes,

Table 5.1 IC_{50} of wild-type (WT) *Zea mays* PEPC enzyme and two mutant PEPC enzymes K835G and R894G, mutated at malate-binding residues. Data taken from Endo et al. (2008). PEPC activity was measured by NADH-coupled spectrophotometric assay.

Enzyme	I_{50} malate (mM)
WT	1.6
K835G	>20
R894G	>20

catalytic activity remained unchanged (Endo et al., 2008). To address if malate inhibition of PEPC has any *in vivo* effects on photosynthesis, a PEPC enzyme will be modified at these malate-binding residues and expressed in the C_4 plant *Setaria viridis*.

5.1.6 Experimental objectives

One of the experimental objectives of this chapter is to investigate the effects of overexpression of the PEPC protein on photosynthesis using *Setaria viridis* as a model C_4 species. Combining any PEPC overexpression data obtained with previously reported PEPC reduction data would provide valuable insights into the effects of PEPC activity in C_4 photosynthesis. The second experimental objective of this chapter is to investigate if malate inhibition of PEPC has any *in vivo* effects on photosynthesis. This will be accomplished by modifying a PEPC enzyme to abolish malate sensitivity and expressing the mutant enzyme in *Setaria viridis*.

5.2 Methods

5.2.1 Design and assembly of the PEPC overexpression Golden Gate plasmid

5.2.1.1 N-terminal tags and PEPC protein function

Previous studies have shown that an N-terminal tag of up to 159 amino acids does not affect PEPC kinetic properties (Takahashi-Terada et al., 2005; Endo et al., 2008). Therefore, an AcV5 tag will be used on the N-terminus of the PEPC protein to distinguish the endogenous PEPC from the transgenic PEPC.

5.2.1.2 PEPC overexpression plasmid design

A PEPC overexpression plasmid was designed with a *Zea mays* PEPC promoter for mesophyll-specific expression of the PEPC enzyme, and a nosT terminator (Figure 5.6). These were Golden Gate modules available in the Furbank and von Caemmerer labs. A N-terminal AcV5 tag was included in order to distinguish between the native *S. viridis* PEPC enzyme and the ectopic PEPC enzyme (Figure 5.6). The AcV5 tag was chosen as it had been successfully used to tag proteins that were subsequently expressed in the A10 ecotype of *S. viridis* in the von Caemmerer lab.

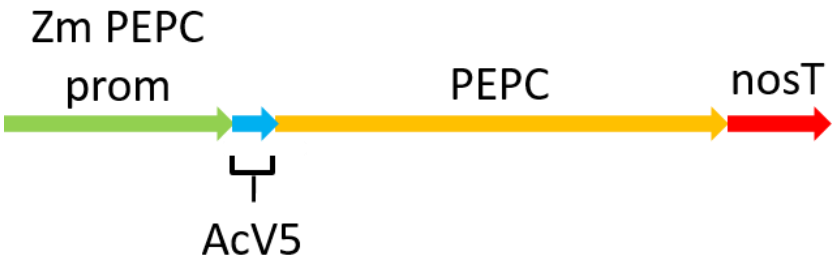

Figure 5.6. Planned PEPC overexpression construct. The plasmid has a *Zea mays* PEPC promoter for mesophyll-specific expression of the PEPC enzyme, and a nosT terminator. A N-terminal AcV5 tag was included in order to distinguish between the native *S. viridis* PEPC enzyme and the heterologous PEPC enzyme.

5.2.1.3 Preparation of PEPC gene for synthesis

PEPCs from *Setaria viridis* were identified on Phytozome (https://phytozome-next.jgi.doe.gov/) using the BLAST function (Phytozome accessions: Sevir.4G143500.1, Sevir.1G020600.1, Sevir.2G179400.1, Sevir.5G328100.2, Sevir.5G328100.1, Sevir.5G145500.1, and Sevir.5G072900.1). Nucleotide and protein alignments were made of these sequences on Geneious. All protein sequences were scrutinised to ensure that all essential residues for PEPC function were present. The C_4 sequence was identified by the presence of a serine residue at position 780 (*Zea mays* numbering).

An alignment of C_4 NADP-ME grass PEPC sequences was made, both at the nucleotide and the protein level. The C_4 NADP-ME grass PEPC sequences used were *Setaria viridis* (Sevir.4G143500.1, Phytozome), *Setaria* italica (Seita.4G175200.1, Phytozome), *Sorghum bicolor* (Sobic.010G160700.1, Phytozome), *Saccharum officinarum* (CAC08829.1, NCBI), *Saccharum spontaneum* (CAC85930.1, NCBI) and *Zea mays* (GRMZM2G083841_T01, Phytozome). From a percent identity matrix, the *Sorghum bicolor* sequence (Accession number: Sobic010G160700.1 (Phytozome)) was chosen for PEPC overexpression in *Setaria viridis* as it had the lowest percent identity to the *Setaria viridis* C_4 PEPC protein sequence. A codon usage table for *Setaria viridis* was created using the nuclear-encoded, highly expressed Rubisco activase (Phytozome accession: Sevir.3G024200.1) using the Countcodon program available at https://www.kazusa.or.jp/codon/countcodon.html (Nakamura et al., 2000).

A nucleotide alignment was made of the PEPCs from *Setaria viridis* (Phytozome accessions: Sevir.4G143500.1, Sevir.1G020600.1, Sevir.2G179400.1, Sevir.5G328100.2, Sevir.5G328100.1, Sevir.5G145500.1, and Sevir.5G072900.1) and the *Sorghum bicolor* C_4 PEPC sequence (Accession number: Sobic010G160700.1 (Phytozome). The *Sorghum bicolor* sequence was codon modified to reduce the nucleotide similarity to all of the *S. viridis* PEPC sequences and keeping, where possible, the same overall usage as the codon usage table indicated (Figure 5.8).

5.2.1.4 Golden Gate linker sequences

The L0 Golden Gate linker sequences specific to an N-terminal tag were added to the 5´ (5´-CACTCTGTGAAGACAAAATG´3) and 3´ (5´-GGAGGTTGGTCTTCGAAGTG´3) ends of the AcV5 sequence. The L0 Golden Gate linker sequences specific to an gene for expression were added to the 5´ (5´-CACTCTGTGAAGACAAAGTG´3) and 3´(5´-GCTTTGGTCTTCACGAAGTG´3) ends of the codon modified *S. bicolor* sequence.

5.2.1.5 Gene synthesis

Genes were sent for synthesis according to General Methods section 2.1.

5.2.1.6 Golden Gate cloning reactions to construct the PEPC overexpression plasmid

The following is the general reaction used in the golden gate cloning process. Each 15 mL Golden Date reaction contained 1X T4 buffer (NEB), 1 µl of BpiI (Thermofisher; Level 0 and Level 2) or 10 U BsaI (NEB; Level 2), 400 U T4 DNA ligase (NEB) 3 µg BSA, 100 ng each of the plasmid backbone, promoter, coding sequence (CDS), terminator, and any tags. The Golden Gate cloning reaction was carried out with thermocycler conditions of: 25 cycles of [37°C for 3 min and 16 °C for 4 min]; 1 cycle of [50 °C for 5 min]; 1 cycle of [80 °C for 5 min].

For the level 0 reaction of the N-terminal AcV5 tag the reaction included 100 ng of EC41258 (L0 plasmid acceptor; spectinomycin resistance), 100 ng of AcV5 tag and 1 µl BpiI (Thermofisher).

For the level 0 reaction of the codon modified *S. bicolor* PEPC sequence the reaction included 100 ng of EC41264 (L0 plasmid acceptor; spectinomycin resistance), 100 ng of *S. bicolor* PEPC and 1 µl BpiI (Thermofisher).

For the level 1 reaction to create the PEPC overexpression level 1 vector the reaction included EC17017 (*Zea mays* PEPC promoter), EC17018 (*Zea mays* PEPC promoter 5´ UTR), EC34016 (AcV5 tag), EC34017 (*Sorghum bicolor* PEPC), EC41421 (tnos terminator), EC47742 (L1 acceptor plasmid; ampicillin resistance) and 10 U BsaI (NEB).

For the level 2 reaction to create the PEPC overexpression level 2 vector the reaction included PEPC overexpression L1 vector, EC17100 (Hygromycin resistance L1 vector), ELE2 EC41744

(End linker for after a position 2 in a multigene construct), pISCL4723 (L2 acceptor plasmid; kanamycin resistance) and 1 µl BpiI (Thermofisher).

5.2.1.7 Heat shock transformation of E. coli TOP10 competent cells with the Golden Gate reaction products

After the reaction, 1 µl of the reaction mix was used to transform 50 µL *E. coli* TOP10 competent cells, using the heat shock as described in the General Methods section 2.3 of this thesis with the following exceptions. Cells were plated on LB-agar plates, containing 100 µg/mL of the appropriate antibiotic, along with 1 mg isopropyl thiogalactopyranoside (IPTG) and 2.04 mg 5-bromo-4-chloro-3-indolyl-β-D-galactopyranoside (X-Gal) for blue-white selection. White colonies were used to inoculate LB media containing 100 µg/mL spectinomycin, and incubated overnight at 37 °C and 220 rpm.

5.2.1.8 Colony PCRs

Colony PCRs were carried out on white colonies from the transformation plates to confirm the presence of the transformed plasmid. Reactions contained 1 X Promega mastermix (Promega), 1 µM forward primer, and 1µM reverse primer. Primer combinations to confirm the presence of the Level 1 PEPC overexpression and the Level 2 PEPC overexpression vectors can be found in Table 5.2. The reaction mixtures were inoculated with cells from a colony. The colony PCR reactions were carried out with thermocycler conditions of: 1 cycle of [95 °C for 3 min], 30 cycles of [95 °C for 20 sec, 56°C for 20 sec, 72 °C for 1 min], and one cycle of [72 °C for 5 min].

Table 5.2 Primers used in colony PCR reactions to confirm the presence of the transformed PEPC overexpression plasmid.

PEPC Overexpression Level 1 Vector				
RL8	CCTTCATAGTCGGCGGAGAC	RL7	GAGCCAAGCCAAAAAGGAGC	608
PEPC Overexpression Level 2 Vector				
Forward Primer		Reverse Primer		Product size (base pairs)
Name	Sequence	Name	Sequence	
RL8	CCTTCATAGTCGGCGGAGAC	Seq pOsActin 1-RP	TGGAGACTATTGTCCAGTTGGC	2000

From each colony PCR reaction, 10 µl was analysed by gel electrophoresis according to the protocol in the General Methods section 2.13. Overnight cultures were made using colonies with confirmed presence of the transformed plasmid by inoculating 5 ml of LB supplemented with the appropriate antibiotic. These cultures were incubated overnight at 37 °C and 220 rpm.

5.2.1.9 Plasmid isolation

Plasmids were extracted using the Isolate II Plasmid Mini Kit (Bioline) as described in the General Methods section 2.4.

5.2.1.10 Confirmation of correctly assembled PEPC overexpression Level 2 vector by sequencing

Samples were sent to The Biomolecular Resource Facility (BRF) at The John Curtin School of Medical Research for Sanger sequencing to confirm that the PEPC overexpression Level 2 vector was correctly assembled. Sequencing primers used in the Sanger sequencing reactions can be found in Table 5.3.

Table 5.3 Sequencing primers used to confirm that the PEPC overexpression Level 2 vector was correctly assembled.

Primer Name	Primer sequence (5´ to -3´)
seq-pOsActin1-RP	TGGAGACTATTGTCCAGTTGGC
seq-pActin1-RP2	TGGTGGTGGTAGGGTTGG
seq-pActin1-RP3	TGAATGACCCTCCCGCAAGAA
seq-HYG1	TATTCCTTTGCCCTCGGAC
seq-HYG2	ACGCCATGTAGTGTATTGAC
seq-HYG3	CGGTGAGTTCAGGCTTTTTC
RL5	AACGTATTCGCGATCCCTCC
RL8rev	GTCTCCGCCGACTATGAAGG
RL12	GCGATGTGTTGTTGGCACTT
RL22	CCCAAGACGAGATGAGATATGG
RL23	CGCACTGCATTGATCATACTCC
RL24	GATCGCTCTTGGATCTACTCAG
RL25	GGAATTCGACAAACACTTCCTG
RL26	GAAAGTTGATGGAGGAAATGGC
seq-ZmPEPC-FP	ACTGCACCCTCAACCACATC

5.2.2 Design and assembly of the plasmid to carry both a *S. viridis* C_4-PEPC RNAi silencing construct and a heterologous PEPC expression construct containing modified PEPC with abolished malate sensitivity

5.2.2.1 Plasmid design

An RNAi PEPC plasmid designed consisting of two main parts a *S. viridis* C_4-PEPC RNAi silencing construct and a heterologous PEPC expression construct containing modified PEPC with abolished malate sensitivity. The RNAi section consists of two 109 base pair sequences, identical to a section of the C_4-specific *S. viridis* PEPC sequence, in opposite orientations. These 109 base pair sequences are separated by a linker sequence to create a hairpin. Driving expression of this *S. viridis* C_4-PEPC RNAi silencing construct was a *Panicum miliaceum* PEPC promoter for mesophyll-specific expression of the C_4-PEPC RNAi hairpin, and a nosT terminator (Figure 5.7). This was to reduce the expression of endogenous *S. viridis* PEPC

enzyme. The second part of the plasmid was designed to introduce a PEPC with abolished malate sensitivity. This consisted of a *Zea mays* PEPC promoter for mesophyll-specific expression of the PEPC enzyme, and a nosT terminator (Figure 5.6). A N-terminal AcV5 tag was included in order to distinguish between native *S. viridis* PEPC enzymes and the ectopic PEPC enzyme (Figure 5.7).

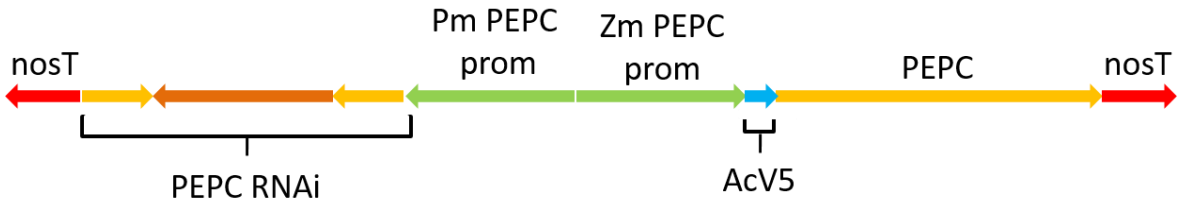

Figure 5.7. Planned *S. viridis* C_4-PEPC RNAi silencing and heterologous malate-binding PEPC mutant expression plasmid. The former construct comprises of two 109 base pair sequences, identical to a section of the C_4-specific *S. viridis* PEPC sequence, in opposite orientations separated by a linker sequence. Expression of this PEPC RNAi sequence is driven by a *Panicum miliaceum* (Pm) promoter and terminated by a nosT terminator sequence. The second part of the plasmid contains a *Zea mays* (Zm) PEPC promoter for mesophyll-specific expression of the PEPC enzyme, and a nosT terminator. A N-terminal AcV5 tag was included in order to distinguish between the native *S. viridis* PEPC enzyme and the heterologous PEPC enzyme.

5.2.2.2 Preparation of modules for synthesis

The seven *S. viridis* PEPC sequences were scrutinised to find an approximately 100 base pair long sequence from the C_4 PEPC gene that had the greatest dissimilarity to the non-C_4 PEPC sequences. A 109 base pair sequence specific to the C_4 PEPC from *S. viridis* was chosen (Figure 5.8). An intronic sequence was chosen and the 109 base pair RNAi sequence at its reverse complement were added to the 5´ and 3´ ends. The intron was then divided in half creating two sequences, one with a 5´ RNAi sequence and half the intronic sequence, and one with the intronic sequence and a 3´ reverse complement RNAi sequence.

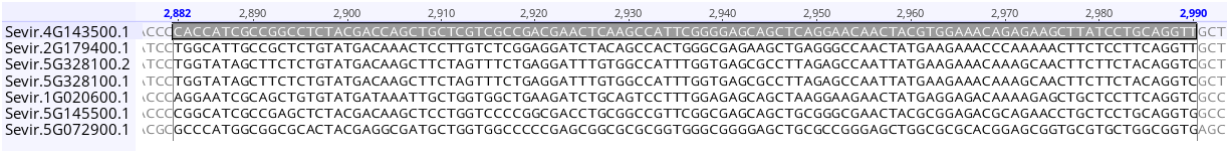

Figure 5.8. Alignment of the seven *S. viridis* PEPC sequences (Sevir.4G143500.1 (C_4), Sevir.1G020600.1, Sevir.2G179400.1, Sevir.5G328100.2, Sevir.5G328100.1, Sevir.5G145500.1, and Sevir.5G072900.1) showing the 109 base pair sequence chosen for RNAi. The sequence highlighted on the Sevir.4G143500.1 (C_4) sequence is the sequence that was used for the RNAi sequence.

5.2.2.3 Golden Gate linker sequences

The L0 Golden Gate linker sequences specific to an open reading frame with a C-terminal tag were added to the 5´ (5´-CACTCTGTGAAGACAAAATG´3) and 3´ (5´-GGGGTGTGGTCTTCGAAGTG´3) ends of the RNAi and 5´ intron sequence. The L0 Golden Gate linker sequences specific to a C-terminal tag were added to the 5´ (5´-CACTCTGTGAAGACTCGGTG´3) and 3´(5´-GCTTAGGTCTTCGAAGTG´3) ends of the RNAi and 3´ intron sequence.

5.2.2.4 Gene synthesis

Genes were sent for synthesis according to General Methods section 2.1.

5.2.2.5 Site-directed mutagenesis of the codon modified S. bicolor PEPC sequence

The codon modified *S. bicolor* enzyme described above (5.2.1.1) was the PEPC sequence used to undergo site-directed mutagenesis. Site-directed mutagenesis was carried out using the QuikChange II Site-Directed Mutagenesis Kit (Agilent Technologies) according to the manufacturer's specifications. Mutagenic primers were designed according to the guidelines specified in the QuikChange II Site-Directed Mutagenesis Kit (Agilent Technologies) protocol (Table 5.4). To create the K835G single mutation in the PEPC *S. bicolor* sequence, a mutagenesis reaction was conducted on the *S. bicolor* PEPC sequence using primers RL13 and RL14 (Table 5.4). To create the K835G/R894G double mutation, a mutagenesis reaction was conducted on the K835G PEPC mutant using primers RL15 and RL16 (Table 5.4).

Table 5.4 Primers used to create the K835G PEPC malate-binding mutant and the K835G/R894G PEPC malate-binding double mutant.Primers RL13 and RL14 were used to create the K835G point mutation and primers RL15 and RL16 were used to create the R894G point mutation.

Primer Name	Primer sequence (5´ to -3´)
RL13	AATGTAGTTATATAAGGATTTCCGAGTCTAAGGCCTTGTTTGAGG
RL14	CCTCAAACAAGGCCTTAGACTCGGAAATCCTTATATAACTACATT
RL15	CCCAGGATCGCCTCCAGCGAACACCATTTCCAATAAATCG
RL16	CGATTTATTGGAAATGGTGTTCGCTGGAGGCGATCCTGGG

Samples were sent to The Biomolecular Resource Facility (BRF) at The John Curtin School of Medical Research for Sanger sequencing to confirm the presence of either the K835G (RL55, 5´-ATGGCCCTTCTTTCGCGTTA-3´) or the R894G mutation (RL26; 5´-GAAAGTTGATGGAGGAAATGGC-3´).

5.2.2.6 Golden Gate cloning reactions to construct RNAi+K835G and RNAI+K835G/R894G plasmids

Golden Gate cloning reactions were carried out as specified in 5.2.1.4.

For the level 0 reaction of the 5´ RNAi + half intron sequence the reaction included 100 ng of EC15456 (L0 plasmid acceptor; spectinomycin resistance), 100 ng of 5´ RNAi + half intron and 1 µl BpiI (Thermofisher).
For the level 0 reaction of the 3´ RNAi + half intron sequence the reaction included 100 ng of EC15458 (L0 plasmid acceptor; spectinomycin resistance), 100 ng of 3´ RNAi + half intron and 1 µl BpiI (Thermofisher).

For the level 1 reaction to create the RNAi PEPC level 1 vector the reaction included EC17063 (*Panicum miliaceum* PEPC promoter), EC34018 (5´ RNAi + half intron sequence), EC34019 (3´ RNAi + half intron sequence), EC41421 (tnos terminator), EC47742 (L1 acceptor plasmid; ampicillin resistance) and 10 U BsaI (NEB).

For the level 1 reaction to create the K835G PEPC level 1 vector the reaction included EC17017 (*Zea mays* PEPC promoter), EC17018 (*Zea mays* PEPC promoter 5´ UTR), EC34016 (AcV5 tag), EC34028 (K835G *Sorghum bicolor* PEPC), EC41421 (tnos terminator), EC47742 (L1 acceptor plasmid; ampicillin resistance) and 10 U BsaI (NEB).

For the level 1 reaction to create the K835G/R894G PEPC level 1 vector the reaction included EC17017 (*Zea mays* PEPC promoter), EC17018 (*Zea mays* PEPC promoter 5´ UTR), EC34016 (AcV5 tag), EC34029 (K835G/R894G *Sorghum bicolor* PEPC), EC41421 (tnos terminator), EC47742 (L1 acceptor plasmid; ampicillin resistance) and 10 U BsaI (NEB).

For the level 2 reaction to create the PEPC overexpression level 2 vector the reaction included RNAi Level 1 vector, either the K835G PEPC level 1 vector or the K835G/R894G PEPC level

1, EC17100 (Hygromycin resistance L1 vector), ELE3 EC41766 (End linker for after a position 2 in a multigene construct), pISCL4723 (L2 acceptor plasmid; kanamycin resistance) and 1 µl BpiI (Thermofisher).

Heat shock transformation of E. coli TOP10 competent cells with the Golden Gate reaction products was performed as described in 5.2.1.5 of this Chapter's Methods section.

5.2.2.7 Restriction enzyme digestion and Colony PCR

For the K835G PEPC level 1 vector and the K835G/R894G PEPC level 1 vector, colony PCRs were carried out on white colonies from the transformation plates to confirm the presence of the transformed plasmid. Colony PCRs were carried out as described in Methods section 5.2.1.6 of this chapter using the primers in Table 5.5

Table 5.5 Primers used in colony PCR reactions to confirm the presence of the transformed the K835G PEPC level 1 and the K835G/R894G PEPC level 1 plasmids.

Forward Primer		**Reverse Primer**		**Product size (base pairs)**
Name	Sequence (5´ to -3´)	Name	Sequence (5´ to -3´)	
seq-ZmPEPC-FP	ACTGCACCCTCAACCACATC	RL18	AGCCTCATGAGAATTTTATCAAAGT	969

For the RNAi Level 1 vector, colony PCRs could not be carried out because of the hairpin that would be formed under PCR conditions. Therefore, colonies from the transformation plate were used to inoculate aliquots of LB media containing 100 µg/ml of ampicillin and the culture was incubated at 37 °C and 220 rpm overnight. Plasmids were extracted using the Isolate II Plasmid Mini Kit (Bioline) as described in the General Methods section 2.4. DraIII and ScaI double digests were carried out on the plasmid preparations. The 20 µl reaction volumes for the four PEPC sequence plasmids contained 1X CutSmart Buffer (NEB), 10 U ScaI (NEB), 10 U DraIII (NEB), 10 U ScaI (NEB) and 2 µl of Level 1 RNAi plasmid preparation. The reaction

mixtures were incubated for 2 hours at 37 °C. From each restriction enzyme reaction, 12 µl was analysed by gel electrophoresis according to the protocol in the General Methods section 2.13 to confirm the presence of bands 4588 bp, 1324 bp, and 3001 bp in size.

5.2.2.8 Confirmation of correctly assembled S. viridis C_4-PEPC RNAi silencing and K835G PEPC, and S. viridis C_4-PEPC RNAi silencing and K835G/R894G PEPC Level 2 vectors

Samples were sent to The Biomolecular Resource Facility (BRF) at The John Curtin School of Medical Research for Sanger sequencing to confirm that the *S. viridis* C_4-PEPC RNAi silencing and K835G PEPC, and *S. viridis* C_4-PEPC RNAi silencing and K835G/R894G PEPC Level 2 vectors were correctly assembled. Sequencing primers used in the Sanger sequencing reactions can be found in Table 5.6.

Table 5.6 Sequencing primers used to confirm that the *S. viridis* C_4-PEPC RNAi silencing and K835G PEPC, and *S. viridis* C_4-PEPC RNAi silencing and K835G/R894G PEPC Level 2 vectors were correctly assembled.

Primer Name	Primer sequence (5´ to -3´)
seq-pOsActin1-RP	TGGAGACTATTGTCCAGTTGGC
seq-pActin1-RP2	TGGTGGTGGTAGGGTTGG
seq-pActin1-RP3	TGAATGACCCTCCCGCAAGAA
seq-HYG1	TATTCCTTTGCCCTCGGAC
seq-HYG2	ACGCCATGTAGTGTATTGAC
seq-HYG3	CGGTGAGTTCAGGCTTTTTC
RL5	AACGTATTCGCGATCCCTCC
RL8rev	GTCTCCGCCGACTATGAAGG
RL22	CCCAAGACGAGATGAGATATGG
RL24	GATCGCTCTTGGATCTACTCAG
RL25	GGAATTCGACAAACACTTCCTG
RL26	GAAAGTTGATGGAGGAAATGGC
seq-PmPEPC-FP	ACACCACTCGCTCAAGTTCAA
seq-PmPEPC-FP1	ATCCCCCTCTAATCTTGTGCT
seq-PmPEPC-FP2	TGTCTACGGCCTGATCCAGA
seq-PmPEPC-FP3	TCTCAAGGCTAACAATAATCCCG
HA63	ATTGCAGTACGGCGAGTCAA
RL55	ATGGCCCTTCTTTCGCGTTA
scr-pL2B-FP2	CGAGTGGTGATTTTGTGCCG
scr-pLOV-SC-FP	CGAGTCAGTGAGCGAGGAAG

5.2.3 Preparation and transformation of chemically competent *Agrobacterium tumefaciens* cells

5.2.3.1 Preparation of chemically competent Agrobacterium tumefaciens cells

Chemically competent cells *Agrobacterium tumefaciens* strain AGL1 were prepared according to the protocol by Weigel and Glazebrook (2006). Agrobacterium AGL1 cells were streaked for single colonies on a LB-agar (1.5%) plate containing 50 mg/L of rifampicin. Plates were then incubated at 28 °C for 48 hours. A single colony was used to inoculate 3 ml of LB media containing 25 mg/L of rifampicin, the culture was incubated at 28 °C and 150 rpm overnight.

A 1 ml aliquot of the overnight culture was used to inoculate 200 ml of LB media containing 25 mg/L of rifampicin. The culture was incubated at 28 °C and 150 rpm until an OD_{600} of between 0.5 and 0.8 was reached. Cells were collected by centrifugation at 5000 rpm for 10 minutes at room temperature. The cell pellet was washed with sterile TE buffer (10 mM Tris-Cl, pH 7.5 1 mM EDTA), resuspended in LB media, aliquoted and snap frozen in liquid nitrogen.

5.2.3.2 Transformation of Agrobacterium tumefaciens

Chemically competent *Agrobacterium tumefaciens* (AGL1) cells were transformed with the PEPC overexpression plasmid, the *S. viridis* C_4-PEPC RNAi silencing and K835G PEPC plasmid, or the *S. viridis* C_4-PEPC RNAi silencing and K835G/R894G PEPC plasmid according to the freeze-thaw protocol by (Weigel and Glazebrook, 2006). Chemically competent *Agrobacterium tumefaciens* (AGL1) cells were thawed on ice. After thawing 10 µl of purified plasmid DNA was added to the cells and the mixture was incubated on ice for a further 5 minutes. The mixture was then transferred to liquid nitrogen and incubated for 5 minutes. The cells were then quickly transferred to a 37 °C water bath and incubated for 5 minutes. After incubation, 1 ml of LB was added to the mixture and the tube was placed on a rocking table for between 2 to 4 hours at room temperature. The cells were collected by brief centrifugation and plated onto LB-agar plates contaning 10 µg/ml of rifampicin and and 50 µg/ml of kanamycin. The plates were incubted for two days at 28 °C. One colony was taken from each plate and streaked for single colonies on a new LB-agar plates contaning 10 µg/ml of rifampicin and and 50 µg/ml of kanamycin. The plate was incubated for two days at 28 °C. Small liquid cultures of the restreaked colonies were grown and colony PCR was performed to verify the presence of plasmid DNA.

In order to assess whether the PEPC overexpression plasmid was successfully transformed 1 µl of resuspended *Agrobacterium* cells were included in a PCR reaction mixture containing 0.4 X Taq polymerase mastermix (New England Bioloabs), 1 µM RL8 and 1 µM Seq pOsActin1-RP (Table 5.2). In order to assess whether the *S. viridis* C_4-PEPC RNAi silencing and K835G

PEPC plasmid, or the *S. viridis* C_4-PEPC RNAi silencing and K835G/R894G PEPC plasmid were successfully transformed 1 µl of resuspended *Agrobacterium* cells were included in a PCR reaction mixture containing 0.4 X Taq polymerase mastermix (New England Bioloabs), 1 µM seq-ZmPEPC-FP and 1 µM RL18 (Table 5.5). The thermocylcer settings for the PCR reaction were: 95 °C for 3 mins, 30 cycles of [95 °C for 20 seconds, 58 °C for 20 seconds and 72 °C for 2.5 seconds], and finally 72 °C for 5 minutes. The PCR reactions were supplemented with 4X gel loading dye (NEB) and run at 80 V on a 1 % agarose/ 1X TAE gel with 1X SYBR™ Safe DNA Gel Stain (Thermofisher) for visualisation and visualised using a ChemiDoc (BioRad). Glycerol stocks were made of the appropriate clones and stored at – 20 °C.

5.2.4 Initiation of *Setaria viridis* callus and callus subculture

S. viridis callus initiation and subculture was conducted according to the protocol by Van Eck et al. (2017). *S. viridis* callus was initiated by mechanically removing the seed coats from *S. viridis* seeds. Seeds were sterilised by a 3-minute incubation in a solution containing 10 % sodium hypochlorite with 0.1 % TWEEN 20. Seeds were rinsed three times in sterile water. Seeds were left to dry before being placed on callus induction medium (CIM) plates (4.3 g/L MS salts, 10 ml/L 100X MS vitamins stock, 40 g/L maltose, 35 mg/L $ZnSO_4.7H_2O$, 0.6 mg/L $CuSO_4.5H_20$, pH 5.8, 4 g/L Gelzan (Caisson Labs), 0.5 mg/L kinetin and 2 mg/L 2,4-D). The cultures were incubated at 24 °C in the dark. After 4-5 weeks the callus was subcultured onto fresh CIM plates. Any gelatinous callus or seedling structures were removed at this time and callus was placed back at 24 °C in the dark. After a further 2-3 weeks callus was subcultured. This involved removing any gelatinous callus and dissecting the remaining callus into 2 – 3 mm pieces. The divided callus was placed onto fresh CIM plates and was placed back at 24 °C in the dark for 1-2 weeks at which time *Agrobacterium tumefaciens*-mediated transformation of the callus was performed.

5.2.5 *Agrobacterium tumefaciens*-mediated transformation of *Setaria viridis* callus.

Stable *Agrobacterium tumefaciens*-mediated transformation of the *Setaria viridis* callus was carried out as described by Van Eck et al. (2017). *Agrobacterium tumefaciens* AGL1 which contained the PEPC overexpression plasmid, the *S. viridis* C_4-PEPC RNAi silencing and K835G PEPC plasmid, or the *S. viridis* C_4-PEPC RNAi silencing and K835G/R894G PEPC plasmid was streaked onto LB-agar plates contaning 10 μg/ml of rifampicin and and 50 μg/ml of kanamycin for selection. Plates were incubated at 28 °C for 48 hours. Four single colonies were then selected and used to inoculate 50 mL of LB media supplemented with 10 μg/ml of rifampicin and and 50 μg/ml of kanamycin. The LB media was incubated for at least 18 hours at 28 °C and 125 rpm until an OD_{600} of 0.6 was reached. The culture was centrifuged to collect the cells. The supernatant was then discarded and the cells were resuspended in 50 mL CIM (4.3 g/L MS salts, 10 ml/L 100X MS vitamins stock, 40 g/L maltose, 35 mg/L $ZnSO_4.7H_2O$, 0.6 mg/L $CuSO_4.5H_20$, pH 5.8) and supplemented with 0.2 mM acetosyringone and 0.1% (v/v) synperonic. Calli were incubated in excess *Agrobacterium* suspension for 5 minutes with gentle rocking. The *Agrobacterium* suspension was removed from the calli.

5.2.6 Callus after transformation

S. viridis callus subculture after transformation was conducted according to the protocol by Van Eck et al. (2017). After the *Agrobacterium tumefaciens*-mediated transformation of the *Setaria viridis* callus was performed, calli were placed onto CIM plates topped with sterile filter paper. The plates were sealed with parafilm and incubated at 22 °C in the dark. After three days, the callus was transferred to selective CIM plates (4.3 g/L MS salts, 10 ml/L 100X MS vitamins stock, 40 g/L maltose, 35 mg/L $ZnSO_4.7H_2O$, 0.6 mg/L $CuSO_4.5H_20$, pH 5.8, 4 g/L Gelzan (Caisson Labs), 0.5 mg/L kinetin and 2 mg/L 2,4-D, 150 mg/L timentin, 40 mg/L hygromycin). Plates were then incubated at 24 °C in the dark for 16 days. Callus was then transferred to selective plant regeneration media (PRM) (4.3 g/L MS salts, 10 ml/L 100X MS vitamins stock, 20 g/L sucrose, pH 5.8, 7 g/L Phytoblend (Caisson Labs), 2 mg/L kinetin 150 mg/L timentin, 15 mg/L hygromycin), and incubated at 24 °C under the light conditions of 16-

hour photoperiod with a light intensity of 60 µmol m^{-2} s^{-1}. The callus was transferred to fresh PRM selective every 2-3 weeks. Once shoots had developed and were approximately 8 mm tall, they were transferred to selective rooting media (RM) (2.15 g/L MS salts, 10 ml/L 100X MS vitamins stock, 30 g/L sucrose, pH 5.7, 7 g/L Phytoblend (Caisson Labs), 150 mg/L timentin, 20 mg/L hygromycin) in Magenta GA7 vessels. Once the shoots had well-developed secondary roots systems and the shoots were approximately 4 cm, they were transferred to 1.7 L pots filled with Seed Raising and Superior Germinating Mix (Debco) supplemented with Osmocote slow-release fertiliser (Scotts). The seedlings were grown in conditions mentioned in 5.2.7 Growth of *Setaria viridis* plants.

5.2.7 Growth of *Setaria viridis* plants

T_1, T_2, and wild-type seeds were germinated on rooting media (as described in 5.2.6) to encourage germination. Wild-type plants were grown from seed that had not been through the tissue culture process. After germination, germinated seeds were transferred to 1.7 L pots filled with Seed Raising and Superior Germinating Mix (Debco) supplemented with Osmocote slow-release fertiliser (Scotts). Pots were watered daily. For all experiments, more plants were grown than necessary and the largest, healthiest plants were chosen for experimentation.

T_0, T_1, T_2, and wild-type plants were grown in controlled environment growth chambers with the following conditions: 16-hour photoperiod with a light intensity of 500 µmol m^{-2} s^{-1}, a daytime temperature of 28 °C, and a 20 °C night temperature. Daytime relative humidity was 55% with a 70 % relative humidity at night.

5.2.8 Digital PCR

In order to determine the hygromycin copy number of the transformant seedlings, leaf samples were sent to IDna Genetics Ltd. (Centrum, Norwich Research Park, Colney lane, Norwich, NR4 7U, Norfolk, UK) for droplet digital PCR analysis.

5.2.9 Extraction of PEPC and Rubisco from leaf discs

Extractions were performed at room temperature with either a mortar and pestle (T_1 and T_2 leaf samples) or a glass homogeniser (T_0 leaf samples). T_1 and T_2 leaf samples were taken from 14-day old (± 2 days) plants between 8:30 am and 2:30 pm. Leaf discs were punched from approximately half-way along the length of the uppermost, fully expanded leaf using a 6.55 mm diameter leaf punch. Samples were either frozen in liquid nitrogen for later analysis or immediately extracted. Samples extracted by glass homogeniser were extracted in 500 µl extraction buffer (50 mM HEPES, pH 7.8, 1 mM EDTA, 10 mM DTT and 1% (w/v) PVPP) with 25 µl of protein inhibitor cocktail (Sigma). Samples extracted by mortar and pestle were extracted in 990 µl extraction buffer (50 mM HEPES, pH 7.8, 1 mM EDTA, 10 mM DTT and 1% (w/v) PVPP) with 25 µl of protein inhibitor cocktail (sigma) and were ground in a mortar and pestle with acid-washed sand. The extracts were pipetted into 1.5 ml microcentrifuge tubes, heated at 65 °C for 10 minutes and centrifuged at 21 000 x *g* for 1 minute.

5.2.10 SDS-PAGE and Western Blots

SDS-PAGE analysis was carried out as described in the General Methods section 2.6 of this thesis. Western blotting was carried out as described in the General Methods section 2.7 of this thesis using either an anti-PEPC antibody (AS09 458, Agrisera) or an anti-AcV5 tag antibody (ab49581, abcam) as the primary antibody. A HRP-conjugated anti-mouse or a HRP-conjugated anti-rabbit secondary antibody was used for the anti-AcV5 tag antibody and the anti-PEPC antibody, respectively.

5.2.11 PEPC and Rubisco spectrophotometric activity assays of leaf extracts and data analysis

PEPC activity was assayed and data analysed as described in the General Methods section 2.8 with 20 µl of leaf extract used per assay.

Rubisco activity was assayed at 25 °C following the NADH-coupled spectrophotometric assay with the rate of NADH oxidation monitored at 340 nm using a Cary 60 UV-Vis spectrophotometer (Agilent)(Kubien et al., 2011). The assay buffer contained 100 mM EPPS-NaOH, pH 8, 20 mM $MgCl_2$, 1mM EDTA, 20 mM $NaHCO_3$, 0.2 mM NADH, 1 mM ATP, 5 mM phosphocreatine and 0.01% (v/v) coupling enzyme mix and 0.4 mM RuBP. The reaction was initiated with the addition of the RuBP. Leaf extract (40 µl) was activated for 10 – 15 minutes in assay buffer before initiating the reaction (Sharwood et al., 2016).

A slope running average was determined using three absorbance data points and the corresponding time points. Using the highest running average points spanning a time of at least 60 seconds, the slope of the change in absorbance vs the change in time was calculated. The Rubisco activity rate was determined using the following equation:

Rubisco activity (µmol CO_2 m^{-2} sec^{-1}) = [($|\Delta OD_{340}|$ × total assay volume × total extract volume)/(4 ×6.22 × 10^{-3} ×volume of leaf extract used ×leaf area)]

Where 6.22 × 10^{-3} is the extinction coefficient of NADH (6.22 × 10^{-3} mM^{-1} cm^{-1}) and absolute value of the change in absorbance at 340 nm per second ($|\Delta OD_{340}|$). Given for every one molecule of RuBP that is carboxylated by Rubisco, four molecules of NADH oxidised there is a 4 in the equation.

5.2.12 Total soluble protein determination of leaf extracts

Total soluble protein determination of leaf extracts was carried out using the Bradford method as described in the General Methods section 2.11 of this thesis.

5.2.13 Fresh weight and dry weight

For the T_2 generation, fresh weight and dry weight was calculated for 17-day old plants, five plants per line of 15-1 (15 = T_0 line, 1 = T_1 plant), 15-2 (15 = T_0 line, 2 = T_1 plant), 15-26 (15 = T_0 line, 26 = T_1 plant) and wild-type. Plants were harvested at soil level and weighed

immediately to determine fresh weight. Plants were then dried at 60 °C for seven days and weighed again to determine dry weight. A fresh weight to dry weight ratio was calculated.

5.2.14 Gas Exchange measurements of *S. viridis* plants

Gas exchange measurements of *S. viridis* plants was performed as described in the General Methods section 2.10 of this thesis.

5.2.15 Analysis of Gas exchange data and fitting C_4 photosynthesis model

The net CO_2 assimilation rate measurements made over a range of intercellular CO_2 partial pressure (C_i) using a LI-COR 6400XT portable gas exchange system (LI-COR Biosciences) (5.2.14), were used to fit the enzyme limited rate equations given by von Caemmerer (2000) in excel. Fitting the C_4 photosynthesis model allowed modelled values for V_{pmax} and V_{cmax} to be obtained for the plants measured by gas exchange analysis.

5.2.16 Statistical tests

Carried out as specified in the General Methods section 2.9.

5.3 Results

5.3.1 Identifying the PEPCs of *Setaria viridis*

Setaria viridis PEPC nucleotide and corresponding protein sequences were identified using Phytozome. These PEPC sequences, Sevir.4G143500.1, Sevir.1G020600.1, Sevir.2G179400.1, Sevir.5G328100.2, Sevir.5G328100.1, Sevir.5G145500.1, and Sevir.5G072900.1 were found to have all of the essential residues for PEPC function (Table 5.7). All protein sequences had residues required for G6P-binding (R183, R184, R231, R372), Mg^{2+}-binding (E566, D603) and HCO_3^--binding (K606, K762, R763, R/K764) (Table 5.7). All

Table 5.7 *Setaria viridis* PEPCs (Sevir.4G143500.1, Sevir.1G020600.1, Sevir.2G179400.1, Sevir.5G328100.2, Sevir.5G328100.1, Sevir.5G145500.1, and Sevir.5G072900.1) identified from Phytozome using the BLAST function . Table shows the presence (indicated by "Y") of all essential residues (*Zea mays* numbering) for PEPC function in each *S. viridis* PEPC protein sequence. The presence of either an alanine (A) or a serine (S) at position 780 (*Zea mays* numbering) for each protein sequence is indicated.

	4G143500.1 (C_4 isoform)	1G020600.1	2G179400.1	5G328100.2	5G328100.1	5G145500.1	5G072900.1
H177	Y	Y	Y	Y	Y	Y	Y
R183	Y	Y	Y	Y	Y	Y	Y
R184	Y	Y	Y	Y	Y	Y	Y
R231	Y	Y	Y	Y	Y	Y	Y
W288	Y	Y	Y	Y	Y	Y	Y
R372	Y	Y	Y	Y	Y	Y	Y
R456	Y	Y	Y	Y	Y	Y	Y
E493	Y	Y	Y	Y	Y	Y	Y
R498	Y	Y	Y	Y	Y	Y	Y
L564	Y	Y	Y	Y	Y	Y	Y
E566	Y	Y	Y	Y	Y	Y	Y
M598	Y	Y	Y	Y	Y	Y	Y
D603	Y	Y	Y	Y	Y	Y	Y
K606	Y	Y	Y	Y	Y	Y	Y
H639	Y	Y	Y	Y	Y	Y	Y
R647	Y	Y	Y	Y	Y	Y	Y
R759	Y	Y	Y	Y	Y	Y	Y
K762	Y	Y	Y	Y	Y	Y	Y
R763	Y	Y	Y	Y	Y	Y	Y
R/K764	Y	Y	Y	Y	Y	Y	Y
R773	Y	Y	Y	Y	Y	Y	Y
780 (A=C_3, S = C_4)	S	A	A	A	A	A	A
K835	Y	Y	Y	Y	Y	Y	Y
R894	Y	Y	Y	Y	Y	Y	Y
N968	Y	Y	Y	Y	Y	Y	Y
G970	Y	Y	Y	Y	Y	Y	Y
TOTAL AMINO ACIDS	965	966	968	967	967	1016	1036

protein sequences had residues necessary for PEP-binding or creating the hydrophobic pocket (W288, R456, L564, M598, R647 and R773) and all had the important catalytic residues (H177, G970) (Table 5.7). All protein sequences had the two residues involved in tetramer formation (E493, R498) as well as all residues necessary for aspartate/malate allosteric inhibitor interactions (R647, K835, R894, N968) (Table 5.7). Given that all PEPCs identified had all residues necessary for proper PEPC function, all were considered when designing the nucleotide sequence for the PEPC for overexpression. Sevir.4G143500.1 was determined to be the C_4 PEPC isoform as it was the only protein sequence with a serine present at position 780 (*Zea mays* numbering) (Table 5.7). Sevir.1G020600.1, Sevir.2G179400.1, Sevir.5G328100.2,

Sevir.5G328100.1, Sevir.5G145500.1, and Sevir.5G072900.1 all had the non-C_4 alanine at this position (Table 5.7).

5.3.2 Codon modifying *S. bicolor* C_4 PEPC for expression in *S. viridis*

From the protein alignment of the C_4 NADP-ME grass PEPC sequences *Setaria viridis* (Sevir.4G143500.1, Phytozome), *Setaria italica* (Seita.4G175200.1, Phytozome), *Sorghum bicolor* (Sobic.010G160700.1, Phytozome), *Saccharum officinarum* (CAC08829.1, NCBI), *Saccharum spontaneum* (CAC85930.1, NCBI) and *Zea mays* (GRMZM2G083841_T01, Phytozome), the *Sorghum bicolor* sequence (Accession number: Sobic010G160700.1 (Phytozome)) was identified as having the lowest percent identity to the *Setaria viridis* PEPC protein sequence (Table 5.8).

Table 5.8 Percent identity of the C_4 NADP-ME PEPC protein sequences from *Setaria italica* (Seita.4G175200.1, Phytozome), *Sorghum bicolor* (Sobic.010G160700.1, Phytozome), *Saccharum officinarum* (CAC08829.1, NCBI), *Saccharum spontaneum* (CAC85930.1, NCBI) and *Zea mays* (GRMZM2G083841_T01, Phytozome), compared to the *Setaria viridis* (Sevir.4G143500.1, Phytozome) PEPC sequence

	Percent identity to the *S. viridis* 4G143500.1 PEPC protein sequence
S. italica 4G175200.1	99.69%
S. officinarum CAC08829.1	82.05%
S. spontaneum CAC85930.1	82.16%
S. bicolor 010G160700.1	81.20%
Z. mays GRMZM2G083841_T01	84.18%

An alignment of the seven *Setaria viridis* PEPCs (Sevir.4G143500.1, Sevir.1G020600.1, Sevir.2G179400.1, Sevir.5G328100.2, Sevir.5G328100.1, Sevir.5G145500.1, and Sevir.5G072900.1), the original *S. bicolor* PEPC sequence was used as a guide for the selection of the codon for each amino acid in codon modified PEPC of *S. bicolor*. Where possible, a codon that was not used in one of the seven *S. viridis* PEPC sequences was selected (Appendix 3). The codon usage table for *Setaria viridis* Rubisco activase (Phytozome accession: Sevir.3G024200.1) was generated (Figure 5.9) and, where possible, the rough ratio of codons used in the *S. bicolor* codon modified PEPC was kept the same as in *Setaria viridis* Rubisco activase. The codon usage of the codon modified *S. bicolor* PEPC was generated (Figure 5.10).

Rubisco activase (Sevir.3G024200.1)

fields: [triplet] [frequency: **per thousand**] ([number])

UUU	21.0(9)	UCU	7.0(3)	UAU	11.7(5)	UGU	0.0(0)
UUC	18.7(8)	UCC	25.7(11)	UAC	18.7(8)	UGC	7.0(3)
UUA	4.7(2)	UCA	9.3(4)	UAA	0.0(0)	UGA	0.0(0)
UUG	18.7(8)	UCG	18.7(8)	UAG	2.3(1)	UGG	11.7(5)
CUU	14.0(6)	CCU	11.7(5)	CAU	11.7(5)	CGU	9.3(4)
CUC	21.0(9)	CCC	16.4(7)	CAC	9.3(4)	CGC	9.3(4)
CUA	14.0(6)	CCA	4.7(2)	CAA	28.0(12)	CGA	4.7(2)
CUG	11.7(5)	CCG	7.0(3)	CAG	16.4(7)	CGG	16.4(7)
AUU	32.7(14)	ACU	16.4(7)	AAU	18.7(8)	AGU	4.7(2)
AUC	18.7(8)	ACC	9.3(4)	AAC	28.0(12)	AGC	2.3(1)
AUA	23.4(10)	ACA	23.4(10)	AAA	21.0(9)	AGA	25.7(11)
AUG	25.7(11)	ACG	2.3(1)	AAG	37.4(16)	AGG	9.3(4)
GUU	18.7(8)	GCU	14.0(6)	GAU	39.7(17)	GGU	14.0(6)
GUC	11.7(5)	GCC	18.7(8)	GAC	25.7(11)	GGC	21.0(9)
GUA	11.7(5)	GCA	18.7(8)	GAA	32.7(14)	GGA	21.0(9)
GUG	7.0(3)	GCG	9.3(4)	GAG	30.4(13)	GGG	25.7(11)

Figure 5.9. Codon usage table for *Setaria viridis* Rubisco activase (Phytozome accession: Sevir.3G024200.1) using the Countcodon program. This program is available at https://www.kazusa.or.jp/codon/countcodon.html .

Codon modified *S. bicolor* PEPC

fields: [triplet] [frequency: **per thousand**] ([number])

UUU	28.1(27)	UCU	1.0(1)	UAU	23.9(23)	UGU	1.0(1)
UUC	9.4(9)	UCC	14.6(14)	UAC	5.2(5)	UGC	10.4(10)
UUA	9.4(9)	UCA	5.2(5)	UAA	0.0(0)	UGA	0.0(0)
UUG	56.1(54)	UCG	23.9(23)	UAG	1.0(1)	UGG	15.6(15)
CUU	9.4(9)	CCU	26.0(25)	CAU	15.6(15)	CGU	7.3(7)
CUC	26.0(25)	CCC	21.8(21)	CAC	4.2(4)	CGC	6.2(6)
CUA	10.4(10)	CCA	3.1(3)	CAA	35.3(34)	CGA	1.0(1)
CUG	2.1(2)	CCG	5.2(5)	CAG	3.1(3)	CGG	4.2(4)
AUU	24.9(24)	ACU	17.7(17)	AAU	21.8(21)	AGU	4.2(4)
AUC	6.2(6)	ACC	5.2(5)	AAC	6.2(6)	AGC	4.2(4)
AUA	19.8(19)	ACA	30.1(29)	AAA	45.7(44)	AGA	31.2(30)
AUG	24.9(24)	ACG	1.0(1)	AAG	15.6(15)	AGG	12.5(12)
GUU	31.2(30)	GCU	22.9(22)	GAU	43.7(42)	GGU	6.2(6)
GUC	13.5(13)	GCC	24.9(24)	GAC	11.4(11)	GGC	15.6(15)
GUA	16.6(16)	GCA	23.9(23)	GAA	61.3(59)	GGA	20.8(20)
GUG	2.1(2)	GCG	5.2(5)	GAG	22.9(22)	GGG	20.8(20)

Figure 5.10. Codon usage table for the codon modified *Sorghum bicolor* PEPC using the Countcodon program. This program is available at https://www.kazusa.or.jp/codon/countcodon.html (Nakamura et al., 2000).

5.3.2 *S. viridis* C_4-PEPC RNAi silencing and K835G PEPC, and *S. viridis* C_4-PEPC RNAi silencing and K835G/R894G PEPC T_0 plant screens

All T_0 transformants were the result of a unique transformation event as each plant originated form a separate transformed callus. In order to determine the number of copies of the hygromycin gene in the apparent transformants, leaf samples were sent for droplet digital PCR analysis (IDna Genetics Ltd.). Analysis of the 54 T_0 K835G transformants showed that 18 were single copy transformants, and 9 were null mutants, where no copies of the hygromycin gene from the *S. viridis* C_4-PEPC RNAi silencing and heterologous malate-binding PEPC mutant expression plasmid were detected (Table 5.9). Analysis of the 40 T_0 K835G + R894G transformants showed that 15 were single copy transformants, and 9 were null mutants, where no copies of the hygromycin gene from the *S. viridis* C_4-PEPC RNAi silencing and heterologous malate-binding PEPC mutant expression plasmid were detected (Table 5.10).

Table 5.9 Droplet digital PCR results for T_0 K835G plants identifying the number of copies of the hygromycin gene. Leaf samples from apparent T_0 transformants were sent to IDna Genetics Ltd. for analysis.

T_0 Line	Number of copies of the hygromycin gene
K835G 1	2
K835G 2	4
K835G 3	0
K835G 4	3 to 4
K835G 5	1
K835G 6	3
K835G 7	2
K835G 8	7
K835G 9	5
K835G 10	1
K835G 11	4
K835G 12	0
K835G 13	0
K835G 14	2
K835G 15	1
K835G 16	0
K835G 17	0
K835G 18	2
K835G 19	0
K835G 20	2

T_0 Line	Number of copies of the hygromycin gene
K835G 21	4
K835G 22	4
K835G 23	0
K835G 24	4
K835G 25	1
K835G 26	1
K835G 27	2
K835G 28	0
K835G 29	1
K835G 31	1
K835G 32	1
K835G 33	4
K835G 34	2
K835G 35	1
K835G 36	2
K835G 37	1
K835G 38	0
K835G 39	2
K835G 40	2
K835G 42	6

T_0 Line	Number of copies of the hygromycin gene
K835G 44	1
K835G 45	1
K835G 46	5
K835G 48	18
K835G 49	2
K835G 50	2
K835G 51	1
K835G 52	1
K835G 53	1
K835G 54	1
K835G 55	2
K835G 56	1
K835G 60	2
K835G 61	1

Table 5.10 Droplet digital PCR results for T_0 K835 + R894G plants identifying the number of copies of the hygromycin gene. Leaf samples from apparent T_0 transformants were sent to IDna Genetics Ltd. for analysis.

T_0 Line	Number of copies of the hygromycin gene	T_0 Line	Number of copies of the hygromycin gene
K835G+R894G 1	1	K835G+R894G 21	1
K835G+R894G 2	2	K835G+R894G 22	1
K835G+R894G 3	0	K835G+R894G 23	1
K835G+R894G 4	2	K835G+R894G 24	2
K835G+R894G 5	0	K835G+R894G 25	1 to 2
K835G+R894G 6	1	K835G+R894G 26	2
K835G+R894G 7	0	K835G+R894G 27	1
K835G+R894G 8	3 to 4	K835G+R894G 28	1
K835G+R894G 9	1	K835G+R894G 29	1
K835G+R894G 10	4	K835G+R894G 30	2
K835G+R894G 11	2	K835G+R894G 31	10
K835G+R894G 12	0	K835G+R894G 32	2
K835G+R894G 13	1	K835G+R894G 33	2
K835G+R894G 14	1	K835G+R894G 34	0
K835G+R894G 15	1	K835G+R894G 36	2
K835G+R894G 16	0	K835G+R894G 37	0
K835G+R894G 17	1	K835G+R894G 38	1
K835G+R894G 18	2	K835G+R894G 39	<1
K835G+R894G 19	0	K835G+R894G 40	1
K835G+R894G 20	2	K835G+R894G 41	0

Unfortunately, Western Blot analysis using an anti-ACV5 antibody of protein extracted from leaf samples from the transgenic plants and the wild-type MEO34V returned signals in both the wild-type and null mutants (results not shown). This was also seen in the PEPC overexpression experiments. Therefore, these plants could not be easily screened by Western blot analysis in the T_1 generation as planned, and the experiment was ended here.

5.3.3 PEPC overexpression T_0 plant screens

All T_0 transformants were the result of a unique transformation event as each plant originated form a separate transformed callus. In order to determine the number of copies of the hygromycin gene in the apparent transformants, leaf samples were sent for droplet digital PCR analysis (IDna Genetics Ltd.). Analysis of the of the 37 T_0 transformants showed that 14 were single copy transformants, and 8 were null mutants, where no copies of the hygromycin gene from the PEPC overexpression plasmid were detected (Table 5.11).

Table 5.11 Droplet digital PCR results for T_0 plants identifying the number of copies of the hygromycin gene. Leaf samples from apparent T_0 transformants were sent to IDna Genetics Ltd. for analysis.

T_0 Line	Number of copies of the hygromycin gene	T_0 Line	Number of copies of the hygromycin gene
PEPC OE 1	1	PEPC OE 19	2
PEPC OE 2	1	PEPC OE 20	0
PEPC OE 3	0	PEPC OE 21	1
PEPC OE 4	2	PEPC OE 22	2
PEPC OE 5	1	PEPC OE 23	1
PEPC OE 6	1	PEPC OE 24	6
PEPC OE 7	5 to 6	PEPC OE 25	2
PEPC OE 8	0	PEPC OE 26	1
PEPC OE 9	6	PEPC OE 27	1
PEPC OE 10	1	PEPC OE 28	3
PEPC OE 11	2	PEPC OE 29	0
PEPC OE 12	1	PEPC OE 30	1
PEPC OE 13	0	PEPC OE 31	0
PEPC OE 14	0	PEPC OE 32	3
PEPC OE 15	1	PEPC OE 33	3
PEPC OE 16	2	PEPC OE 34	2 to 3
PEPC OE 17	3	PEPC OE 35	1
PEPC OE 18	4	PEPC OE 36	1
		PEPC OE 37	0

Figure 5.11. Western Blot of 28 T_0 *Setaria viridis* plants using an anti-AcV5 tag antibody (Abcam). The signal corresponding to PEPC tagged with AcV5 is between the 100 kDa and 150 kDa markers on the Precision Plus Protein All Blue Standards (BioRad) ladder. Null mutants identified by digital PCR are indicated by asterisks (*) and were used as negative controls. Unfortunately, all of the apparent null mutants have a signal corresponding to the anti-AcV5. Numbers indicate the T_0 transgenic plant number. Loading was based on leaf area.

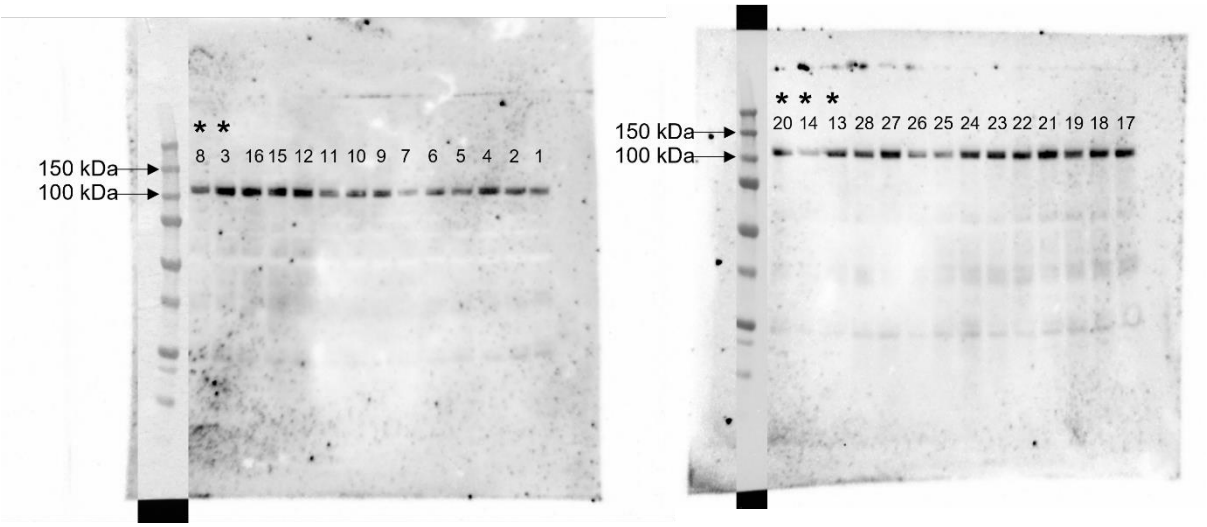

T_0 screens were conducted by Western blotting with an anti-AcV5 antibody (Abcam), to determine which transgenic plants has the greatest amount of ectopic PEPC expression (Figure 5.12). All T_0 transgenic plants had an AcV5 signal when samples were analysed by Western Blot (Figure 5.11), including T_0 plants 3, 8, 13, 14, and 20, identified as null mutants by digital PCR. In order to assess if the hygromycin gene was actually present in these T_0 plants, plants 3, 8, 13, 14, and 20 were analysed by PCR (Figure 5.12; PCR conducted by Dr. Xueqin Wang). PCR analysis determined that the hygromycin gene was present in all of T_0 plants 3, 8, 13, 14, and 20 and these plants were not null mutants as digital PCR analysis suggested (Figure 5.12). Excluding the falsely identified null mutants, lines with the strongest AcV5 signal and one copy of the hygromycin gene were selected for screening in the T_1 generation. Therefore, lines 2, 12, 15, 21, 23, and 27 were chosen for further analysis in the T_1 generation.

Western Blot analysis using an anti-ACV5 antibody of protein extracted from wild-type MEO34V returned a signal in the wild-type samples (results not shown). Therefore, the anti-AcV5 antibody cross-reacts with the *S. viridis* MEO34V wild-type.

Figure 5.12. Polymerase Chain Reaction (PCR) on A.10 ecotype of *Setaria viridis* (used as the wildtype negative control) and samples from the T_0 null mutant 3, 8, 13, 14, and 20 (identified by digital PCR). Primers were used to amplify a 419 base pair section of the hygromycin gene from the PEPC overexpression construct. The PCR was conducted by Dr. Xueqin Wang.

5.3.4 T_1 plant screens for increased PEPC activity

In order to screen large numbers of T_1 plants for increased PEPC activity, the method of screening by total PEPC activity was chosen. This was deemed the best way to determine if there was greater expression of active PEPC protein rather than just greater expression of inactive PEPC protein. Each batch of T_1 plants grown were screened for PEPC activity per leaf area. This was compared to the wild-type *S. viridis* plant with the greatest PEPC activity per leaf area (Figure 5.13). Although lines 2 and 12 appeared promising in the T_0 generation, the T_1 plants tested all had activities lower than the wild-type *S. viridis* plant with the greatest PEPC activity per leaf area (Figure 5.13). Lines 15, 21, 23 and 27 all had some individual plants with PEPC activities greater than the wild-type *S. viridis* plant with the greatest PEPC activity per leaf area (Figure 5.13). These lines, however, also had individual plants that were greatly outperformed in terms of PEPC activity than the wild-type *S. viridis* plant with the greatest PEPC activity per leaf area (Figure 5.13). This suggests incredible variation in PEPC activity between the progeny of a single T_0 individual. Plants with at least 10% greater PEPC activity than the highest performing wildtype were selected to continue into the T_2 generation (Table 5.12). T_0 lines 15, 21, 23, 27 had between four and nine T_1 individual plants that had 11-30% greater PEPC activity per leaf area than the best performing wild-type (Table 5.12).

Table 5.12 Percentage by which T_1 mutant plants outperformed the wild-type *S. viridis* plant with the greatest PEPC activity per leaf area with respect to PEPC activity. PEPC activity was measured in μmol HCO_3^- m^2- min^{-1}.

T_0 Line 15	
T_1 plant number	Percent PEPC activity greater than the wild-type S. viridis plant with the greatest PEPC activity per leaf area
1	33%
2	21%
5	12%
26	28%

T_0 Line 21	
T_1 plant number	Percent PEPC activity greater than the wild-type S. viridis plant with the greatest PEPC activity per leaf area
1	11%
10	20%
17	28%
18	23%
20	29%

T_0 Line 23	
T_1 plant number	Percent PEPC activity greater than the wild-type S. viridis plant with the greatest PEPC activity per leaf area
4	13%
8	14%
9	25%
11	11%
12	21%
15	30%
19	15%
27	11%
31	29%

T_0 Line 27	
T_1 plant number	Percent PEPC activity greater than the wild-type S. viridis plant with the greatest PEPC activity per leaf area
3	26%
7	21%
11	22%
15	25%
30	16%
31	21%

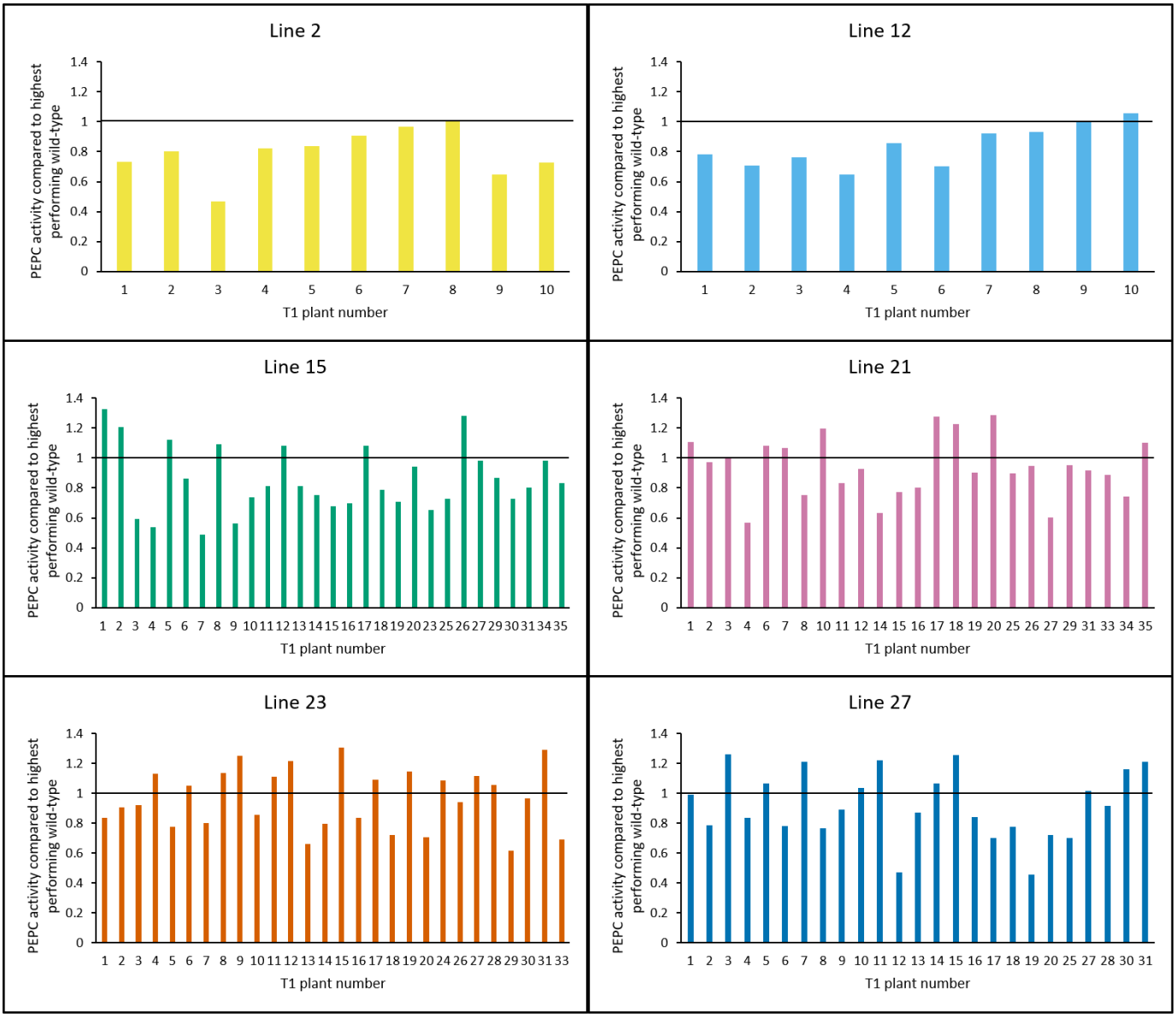

Figure 5.13. Ratio of T_1 mutant PEPC activity compared to wild-type PEPC activity. PEPC activity was measured in µmol HCO_3^- m^2- min^{-1}. The black line on each graph indicates the PEPC activity level of the wild-type with the greatest PEPC activity. Individuals that were identified as having greater than 1.1 times the PEPC activity of the best performing wild type were taken forward for experiments in the T_2 generation

5.3.5 T_2 plant analysis

To begin with, 5 biological replicates of progeny from each T_1 plant was decided as sufficient for the T_2 analyses. When it was apparent that there was no statistical difference between mutant lines and wild-type plants, this number was increased to 10 biological replicates to reduce variability in the data.

5.3.5.1 T_2 plant PEPC activity

PEPC activity was determined for PEPC plants from the original T_0 line 21 (Figure 5.14, Table 5.13). From the T_1 generation, individual plants 21-17, 21-18 and 21-20 had 28 %, 23 % and 29 % greater PEPC activity per leaf area, respectively, than the best performing wild-type (Table 5.12). Plants were grown from seeds of each of these T_1 individuals, and PEPC activity (µmol HCO_3 m^{-2} sec^{-1}) was determined for 4 wild-type plants and 5 or 6 plants in the 21-17 line, the 21-18 line, and the 21-20 line (Figure 5.14, Table 5.13). Statistical analysis by one way ANOVA showed no difference in PEPC activity between any of the groups. The gas exchange measurements made using a LI-COR 6400XT portable gas exchange system (LI-COR Biosciences), were used to fit the enzyme limited rate equations given by von Caemmerer

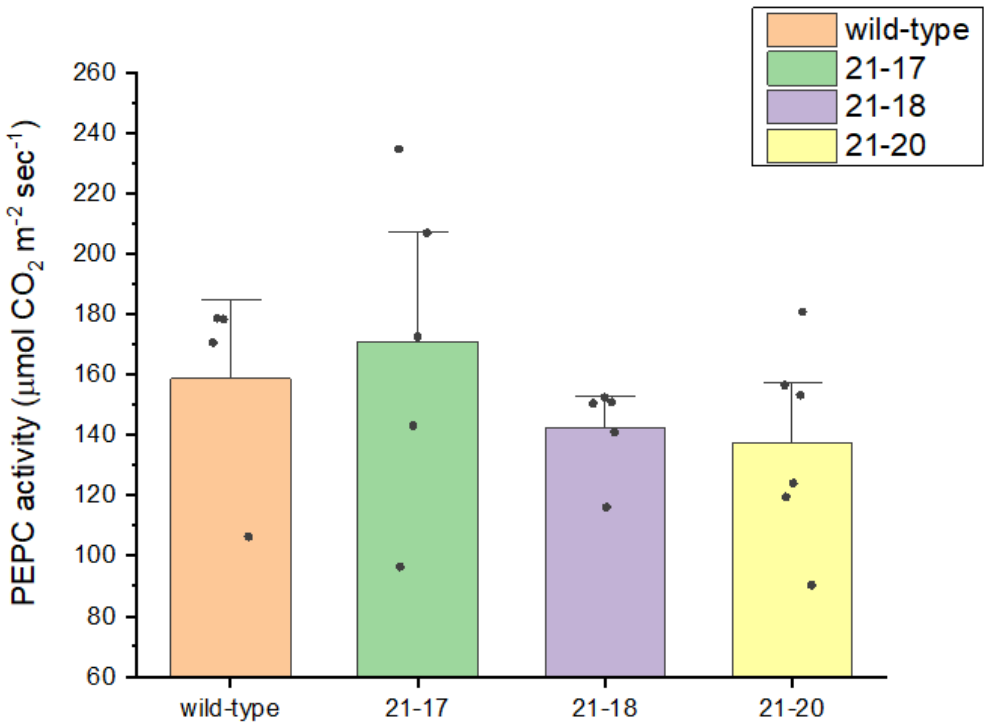

Figure 5.14. PEPC activity (µmol HCO_3 m^{-2} sec^{-1}) in wild-type, line 21-17, line 21-18, and line 21-20 plants. Dots indicate the PEPC activity for individual plants included in the bar graph. Error bars denote SE, n=5 or 6 for transgenic lines and n=4 for wild-type, plants were 13- and 14-day old plants. Statistical analysis by one way ANOVA showed no difference between any of the groups.

(2000). Fitting the C_4 photosynthesis model allowed modelled values for V_{pmax} to be obtained for the plants measured by gas exchange analysis (Table 5.13).

Table 5.13 PEPC activity (µmol HCO_3 m^{-2} sec^{-1}) and modelled V_{pmax} (µmol CO_2 m^{-2} sec^{-1}) in wild-type, line 21-17, line 21-18, and line 21-20 plants. Plants were 13- and 14-day old plants, n=5 or 6 for transgenic lines and n=4 for wild-type.

	PEPC activity (µmol CO_2 m^{-2} s^{-1})	Vpmax (µmol CO_2 m^{-2} s^{-1}) (Modelled)
wild-type	158.70 ± 15.13	159.52 ± 5.46
21-17	170.93 ± 21.63	217.60 ± 15.40
21-18	142.39 ± 6.10	161.64 ± 10.90
21-20	137.61 ± 12.04	149.65 ± 10.00

PEPC activity was also determined for PEPC plants from the original T_0 line 15 (Figure 5.15, Table 5.14). From the T_1 generation, individual plants 15-1, 15-2 and 15-3 had 33 %, 21 % and 28 % greater PEPC activity per leaf area, respectively, than the best performing wild-type (Table 5.12). Plants were grown from seeds of each of these T_1 individuals, and PEPC activity (µmol HCO_3 m^{-2} sec^{-1}) was determined for 4 wild-type plants and 5 or 6 plants in the 15-1 line, the 15-2 line, and the 15-26 line (Figure 5.15, Table 5.14). Statistical analysis by one way ANOVA showed no difference in PEPC activity between any of the groups. Similarly to line 21, the gas exchange measurements made were used to fit the enzyme limited rate equations given by von Caemmerer (2000). Fitting the C_4 photosynthesis model allowed modelled values for V_{pmax} to be obtained for the plants measured by gas exchange analysis (Table 5.14).

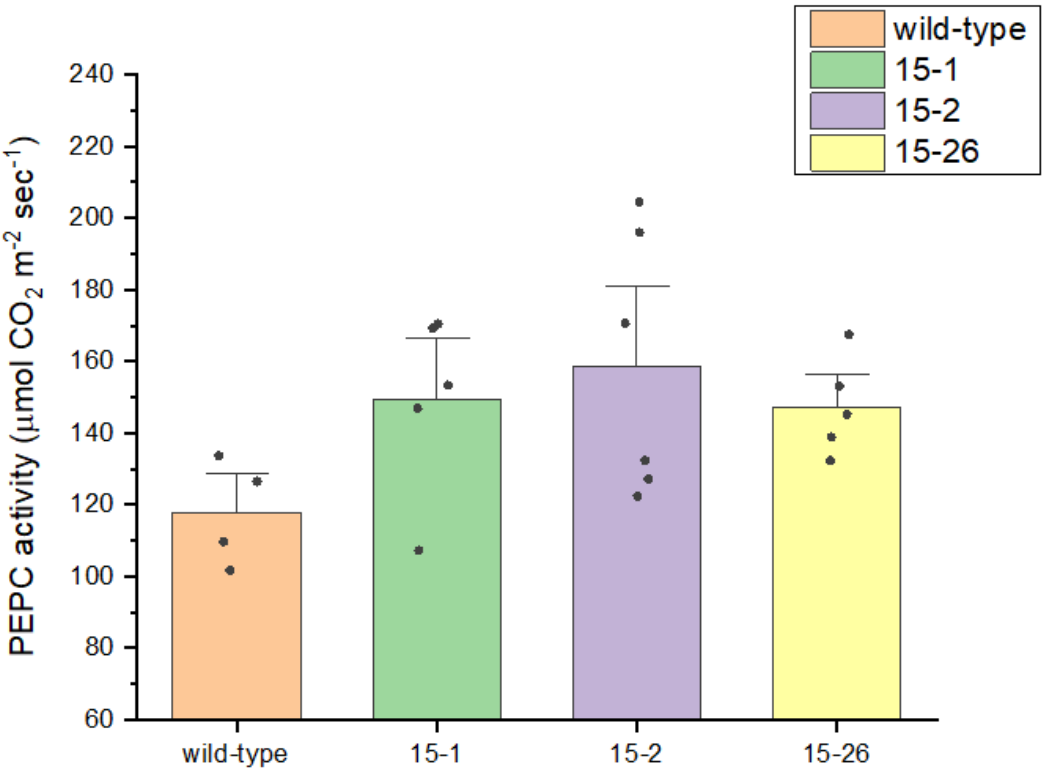

Figure 5.15. PEPC activity (µmol HCO_3 m^{-2} sec^{-1}) in wild-type, line 15-1, line 15-2, and line 15-26 plants. Dots indicate the PEPC activity for individual plants included in the bar graph. Error bars denote SE, n=5 for transgenic lines and n=4 for wild-type, plants were 13- and 14-day old plants. Statistical analysis by one way ANOVA showed no difference between any of the groups.

Table 5.14 PEPC activity (µmol HCO_3 m^{-2} sec^{-1}) and modelled V_{pmax} (µmol CO_2 m^{-2} sec^{-1}) in wild-type, line 15-1, line 15-2, and line 15-26 plants. Plants were 13- and 14-day old plants, n=5 or 6 for transgenic lines and n=4 for wild-type.

	PEPC activity (µmol CO_2 m^{-2} s^{-1})	Vpmax (µmol CO_2 m^{-2} s^{-1}) (Modelled)
wild-type	117.77 ± 6.38	131.07 ± 17.94
15-1	149.32 ± 10.27	168.28 ± 28.73
15-2	158.70 ± 13.57	180.79 ± 17.65
15-26	147.28 ± 5.44	155.79 ± 28.65

From Figure 5.15 it can be seen that lines 15-1, 15-2 and 15-26 look like they might have greater PEPC activity than the wild-type. As there was no statistical difference between mutant lines and wild-type plants, the number of biological replicates was increased to 10 in order to reduce variability in the data between mutant lines and the wild-type *S. viridis*. Therefore, the experiment was repeated for PEPC plants from the original T_0 line 15. Plants were grown from seeds of each of these T_1 individuals, and PEPC activity (µmol HCO_3 m^{-2} sec^{-1}) was determined for 10 wild-type plants and 10 plants in the 15-1 line, the 15-21 line, and the 15-26 line (Figure 5.16, Table 5.15). Statistical analysis by one way ANOVA showed that lines 15-1 and 15-2 are significantly different, and that lines 15-1 and 15-26 are significantly different. No difference between the wild-type and any of the mutants was observed. The gas exchange measurements

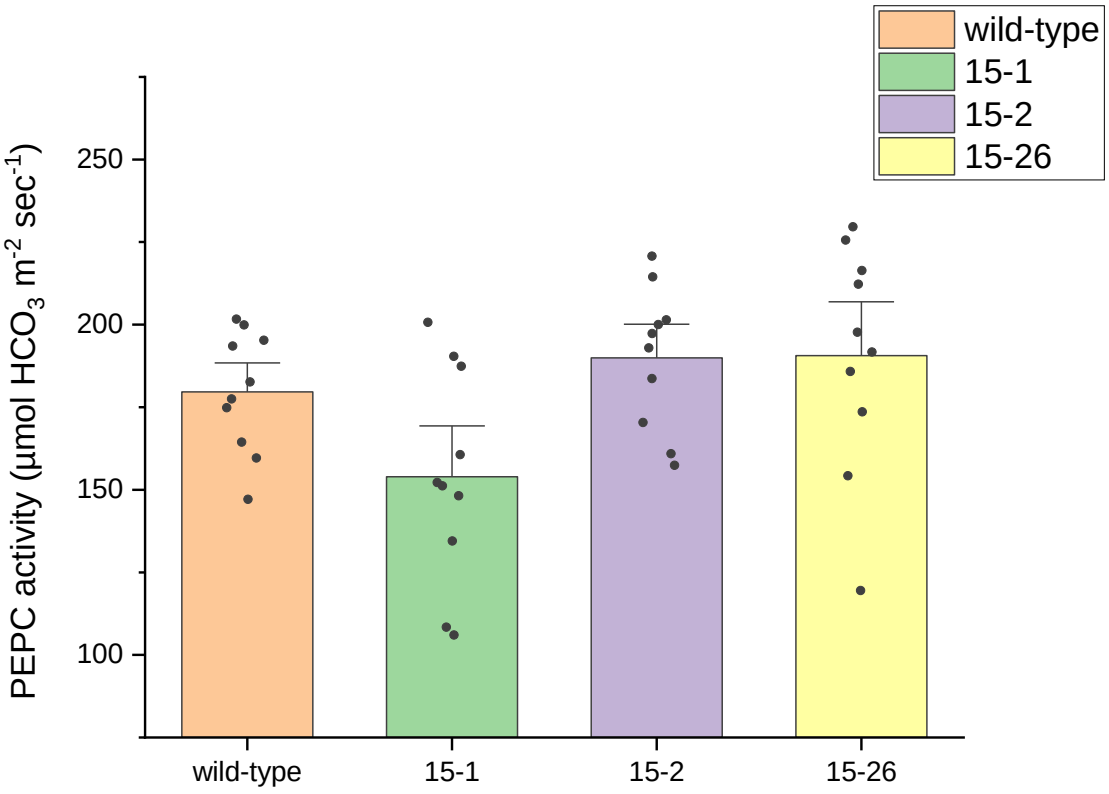

Figure 5.16. PEPC activity (µmol HCO_3 m^{-2} sec^{-1}) in wild-type, line 15-1, line 15-2, and line 15-26 plants. Dots indicate the PEPC activity for individual plants included in the bar graph. Error bars denote SE, n=10, plants were 15- and 16-day old plants. Statistical analysis by one way ANOVA showed that 15-1 and 15-2 are significantly different, and 15-1 and 15-26 are significantly different. No difference between the wild-type and any of the mutants was observed.

made using a LI-COR 6400XT portable gas exchange system (LI-COR Biosciences), were used to fit the enzyme limited rate equations given by von Caemmerer (2000). Fitting the C_4 photosynthesis model allowed modelled values for V_{pmax} to be obtained for the plants measured by gas exchange analysis (Table 5.15).

Table 5.15 PEPC activity (µmol HCO_3 m^{-2} sec^{-1}), modelled V_{pmax} (µmol CO_2 m^{-2} sec^{-1}), Rubisco activity (µmol CO_2 m^{-2} sec^{-1}), and modelled V_{cmax} (µmol CO_2 m^{-2} sec^{-1}) in wild-type, line 15-2, line 21-18, and line 21-20 plants. Plants were 15- and 16-day old plants. For activity measurements n=10 and for modelled values from gas exchange data n=5. ANOVA for the modelled values showed no significant difference between any of the groups. ANOVA for the PEPC activity data showed that 15-1 and 15-2 are significantly different; and 15-1 and 15-26 are significantly different.

	PEPC activity (µmol CO_2 m^{-2} s^{-1})	Vpmax (µmol CO_2 m^{-2} s^{-1}) (Modelled)	Rubisco activity (µmol CO_2 m^{-2} s^{-1})	Vcmax (µmol CO_2 m^{-2} s^{-1}) (Modelled)
wild-type	179.64 ± 5.53	167.36 ± 17.98	24.00 ± 2.35	32.46 ± 1.21
15-1	153.96 ± 9.74	150.69 ± 17.31	22.32 ± 1.77	32.32 ± 1.12
15-2	189.91 ± 6.46	128.71 ± 16.45	22.65 ± 1.99	34.82 ± 1.23
15-26	190.63 ± 10.31	149.64 ± 35.17	23.43 ±2.25	35.17 ± 1.56

5.3.5.2 T_2 plant Rubisco activity

Rubisco activity was calculated for the each of the plants in the experiments above, but given that PEPC activity was not significantly increased from the wild-type, only the results for the experiment on line 15 with the 10 biological replicates is shown in this thesis. Rubisco activity (µmol CO_2 m^{-2} sec^{-1}) was determined for 10 wild-type plants and 10 plants in the 15-1 line, the 15-21 line, and the 15-26 line (Figure 5.17, Table 5.15). Statistical analysis by one way

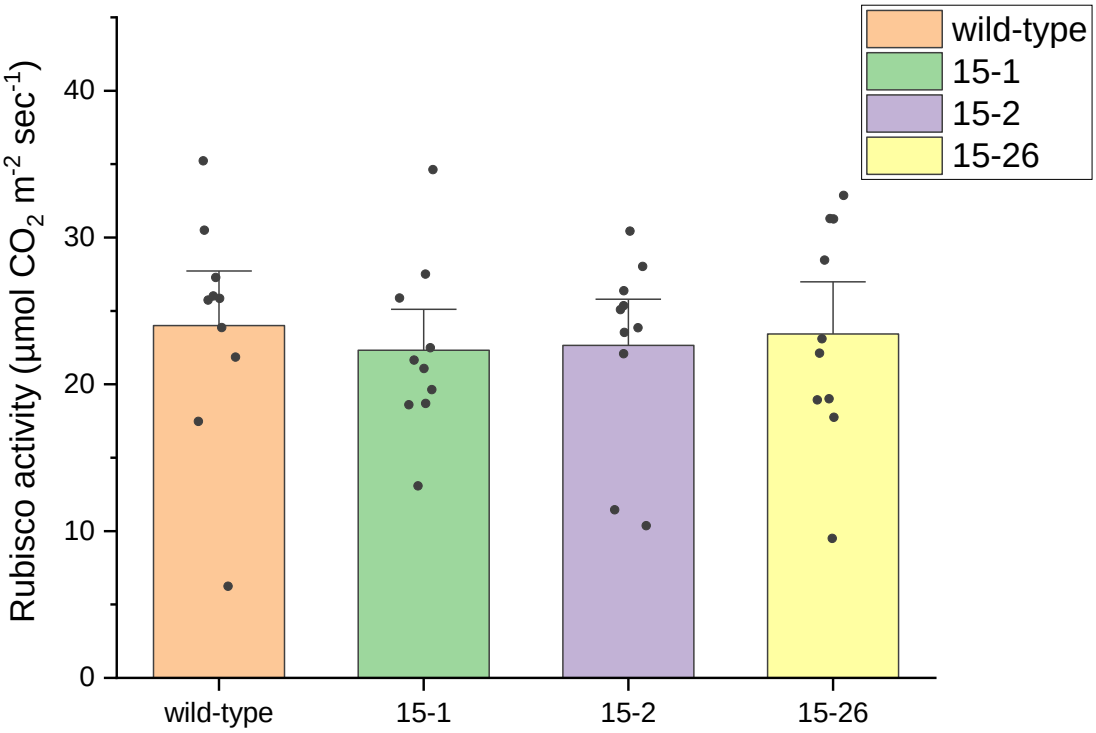

Figure 5.17. Rubisco activity (µmol CO_2 m^{-2} sec^{-1}) in wild-type, line 15-1, line 15-2, and line 15-26 plants. Dots indicate the PEPC activity for individual plants included in the bar graph. Error bars denote SE, n=10, plants were 15- and 16-day old plants. Statistical analysis by one way ANOVA showed no difference between any of the groups.

ANOVA showed no difference between any of the groups. The gas exchange measurements made using a LI-COR 6400XT portable gas exchange system (LI-COR Biosciences), were used to fit the enzyme limited rate equations given by von Caemmerer (2000). Fitting the C_4 photosynthesis model allowed modelled values for V_{cmax} to be obtained for the plants measured by gas exchange analysis (Table 5.15).

5.3.5.3 T_2 plant total protein

Again, total protein was calculated for the each of the plants in the experiments described in 5.3.4.1, but given that PEPC activity was not significantly increased from the wild-type, only the results for the experiment on line 15 with the 10 biological replicates is shown in this thesis.

Total protein (g m^{-2}) was determined for 10 wild-type plants and 10 plants in the 15-1 line, the 15-21 line, and the 15-26 line (Figure 5.18). Statistical analysis by one way ANOVA showed no difference between any of the groups.

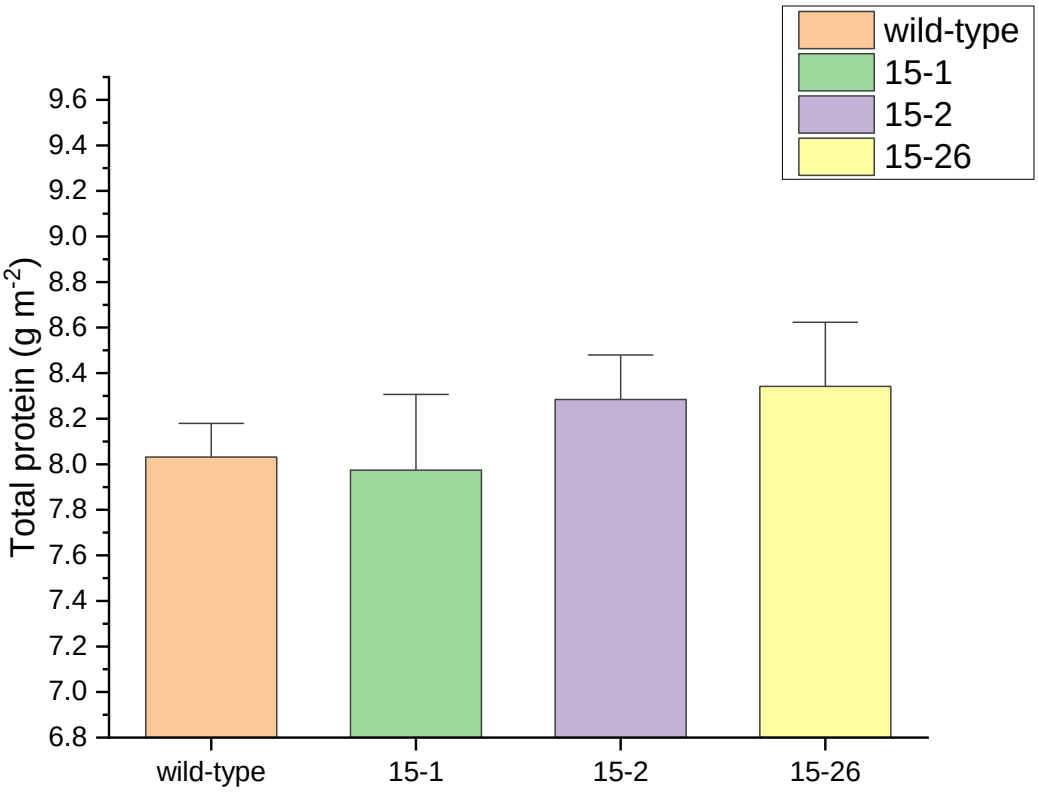

Figure 5.18. Total protein (g m^{-2}) in wild-type, line 15-1, line 15-2, and line 15-26 plants. Error bars denote SE, n=10, plants were 15- and 16-day old plants. Statistical analysis by one way ANOVA showed no difference between any of the groups.

5.3.5.4 T_2 plant ACi curve data

ACi curves (CO_2 assimilation rate (µmol m^{-2} s^{-1}) vs intercellular CO_2 (µbar)) were generated for plants from the original T_0 line 21 and wild-type plants (Figure 5.19). ACi curves were generated using gas exchange data collected for 4 wild-type plants and 5 or 6 plants in the 21-17 line, the 21-18 line, and the 21-20 line (Figure 5.19). ACi curves (CO_2 assimilation rate (µmol m^{-2} s^{-1}) vs intercellular CO_2 (µbar)) were also generated for plants from the original T_0 line 15 and wild-type plants (Figure 5.19). ACi curves were generated using gas exchange data

collected for 5 wild-type plants and 5 plants in the 15-1 line, the 15-2 line, and the 15-26 line (Figure 5.20).

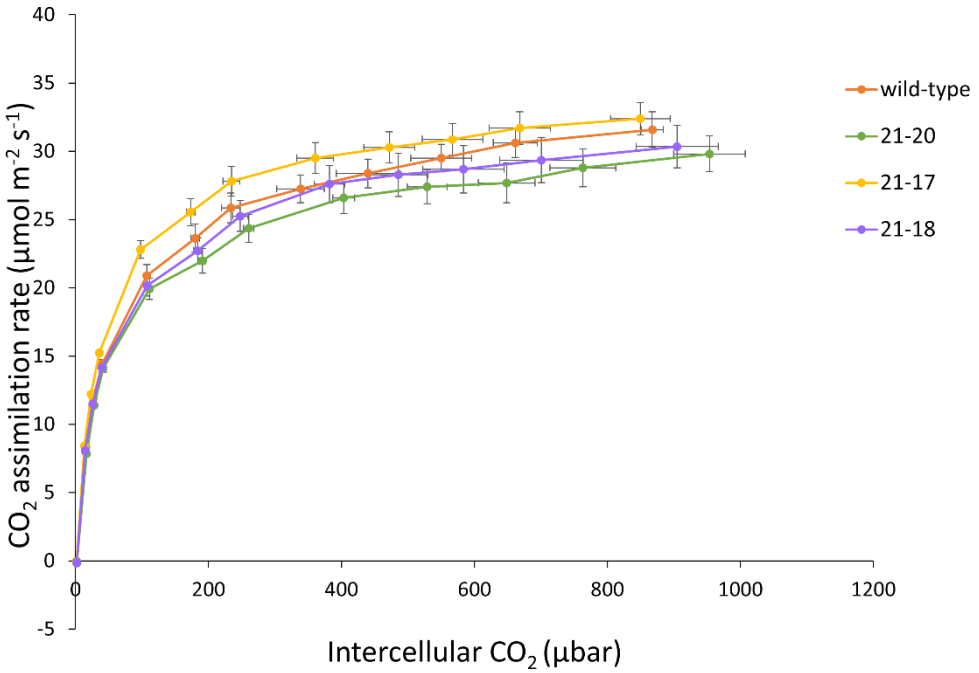

Figure 5.19. CO_2 response curves of leaves of wild-type and T_2 plants from the 21-17, 21-18, and 21-20 lines. Plants were measured with a leaf temperature of 25 °C and an irradiance of 1,800 µmol photons m^{-2} s^{-1}. Error bars denote SE, n=5 or 6 for transgenic plants lines and n =4 for wild-type.

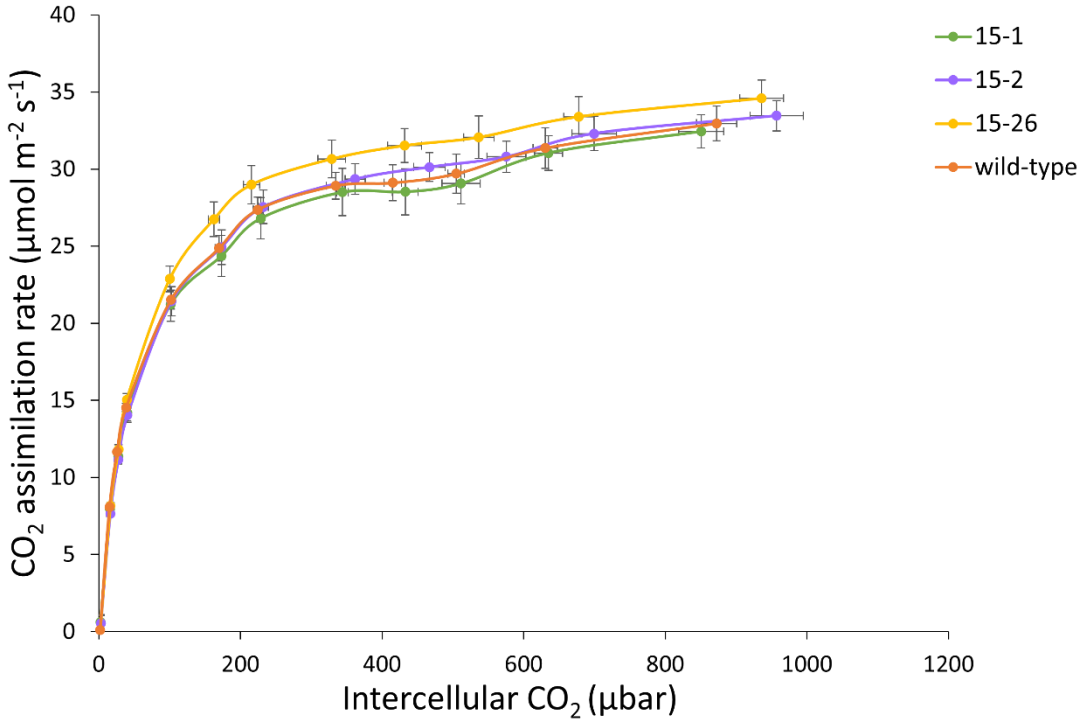

Figure 5.20. CO_2 response curves of leaves of wild-type and T_2 plants from the 15-1, 15-2, and 15-26 lines. Plants were measured with a leaf temperature of 25 °C and an irradiance of 1,800 µmol photons m^{-2} s^{-1}. Error bars denote SE, n=5.

5.3.5.5 T_2 fresh weight and dry weight

Fresh and dry weight (g) were calculated for five wild-type plants and five plants in the 15-1 line, the 15-21 line, and the 15-26 line (Figure 5.21, Figure 5.22). Statistical analysis by one way ANOVA showed no difference between any of the groups for both fresh and dry weight. The fresh weight and dry weight measurements were used to calculate the fresh weight/dry weight ratio for the wild-type plants and the 15-1 line, the 15-21 line, and the 15-26 line plants (Figure 5.23). Statistical analysis by one way ANOVA showed no statistical difference between any of the groups.

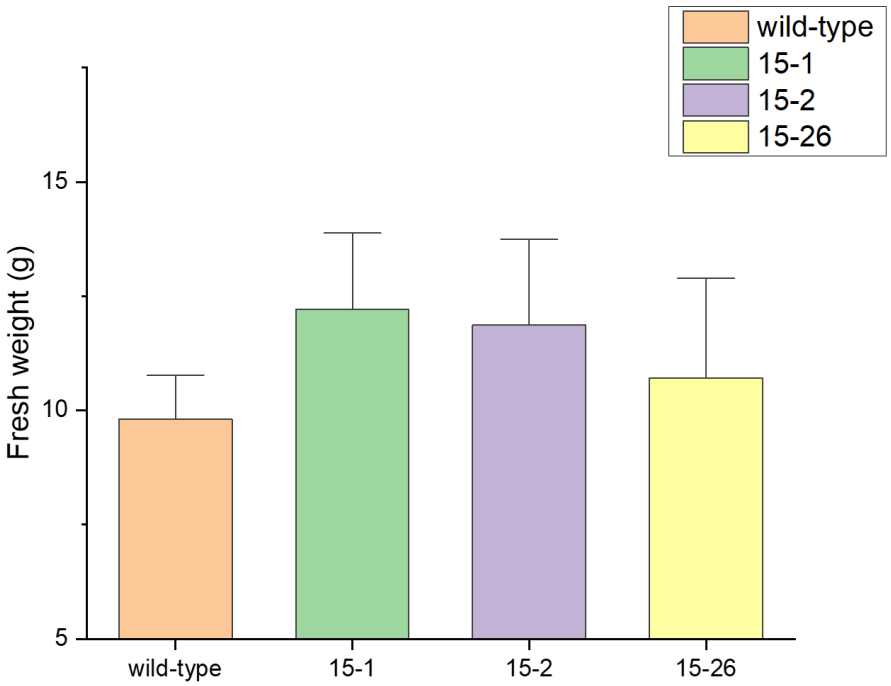

Figure 5.21. Fresh weight (g) in wild-type, line 15-1, line 15-2, and line 15-26 plants. Error bars denote SE, n=5, plants were 17-day old plants. ANOVA showed no difference between any of the groups.

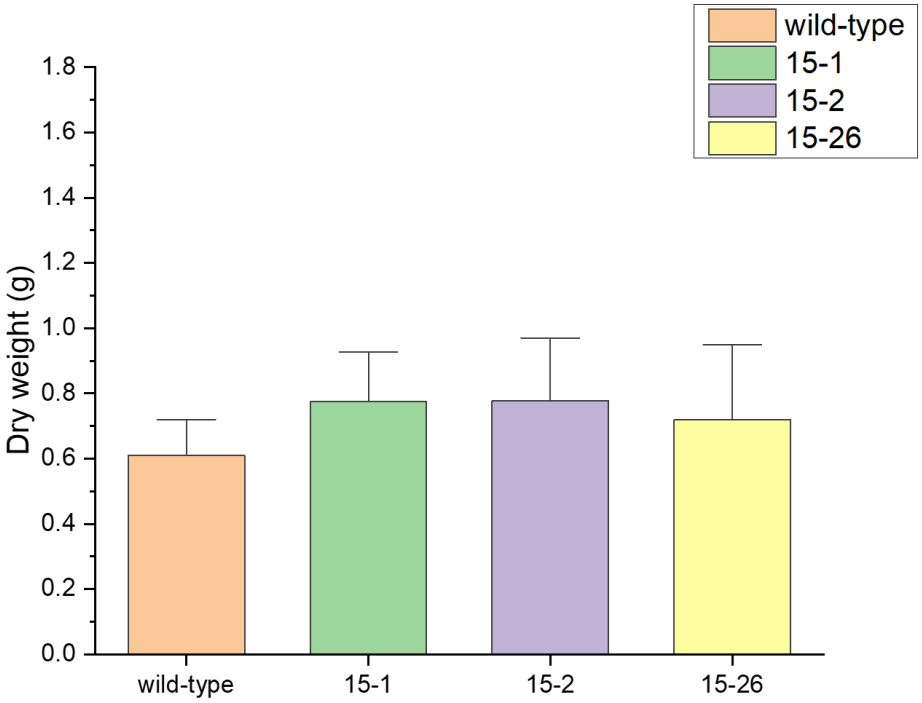

Figure 5.22. Dry weight (g) in wild-type, line 15-1, line 15-2, and line 15-26 plants. Error bars denote SE, n=5, plants were 17-day old plants. ANOVA showed no difference between any of the groups.

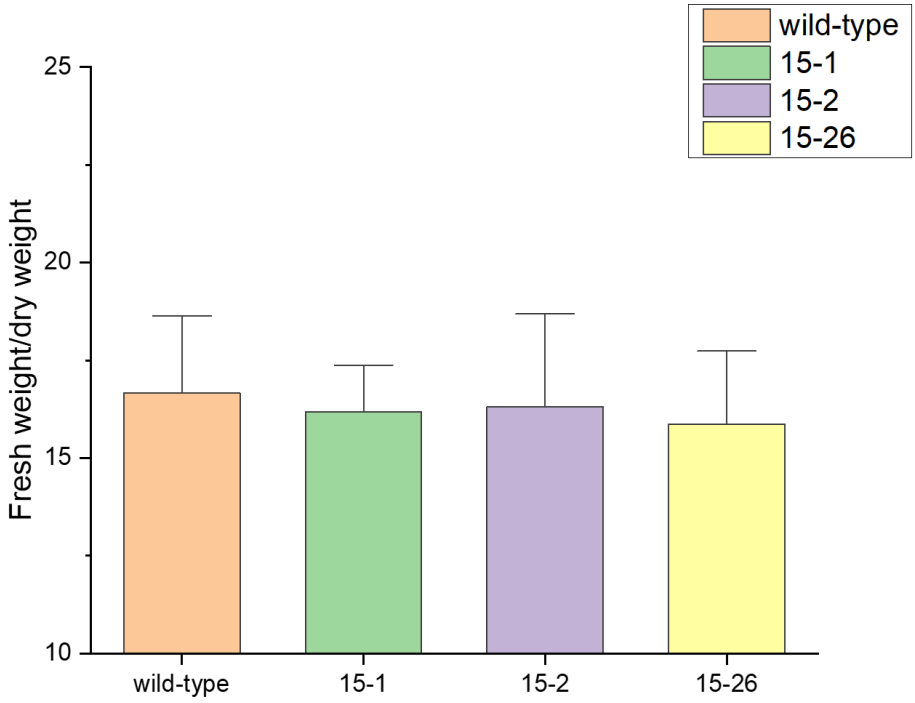

Figure 5.23. Fresh weight/dry weight in wild-type, line 15-1, line 15-2, and line 15-26 plants. Error bars denote SE, n=5, plants were 17-day old plants. ANOVA showed no difference between any of the groups.

5.3.5.6 T_0 Western blotting analysis with equal total protein loading

After the T_2 analysis was completed, it was decided to see if SDS and Western blot analysis by equal total protein loading rather than by equal leaf area would tell a different story with respect to PEPC protein quantities (Figure 5.24). Single protein bands were present for all samples at

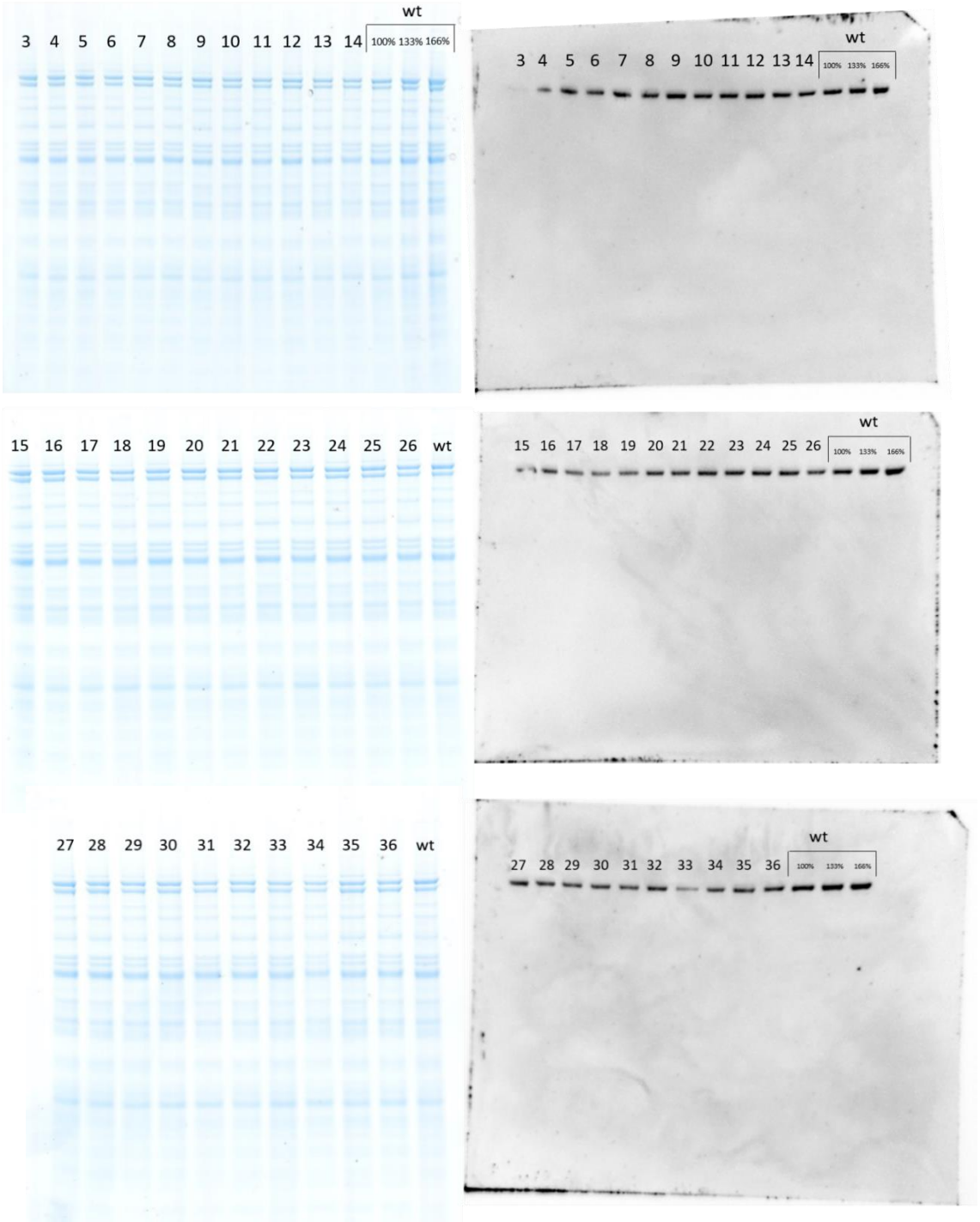

Figure 5.24. T_0 leaf protein samples loaded on a leaf protein basis. 3µg of protein was loaded for each leaf sample. Wild-type protein samples were loaded using 3, 4 and 5 µg of protein.

the expected molecular weight of PEPC monomer. The strong Western PEPC signals seen for lines 15, 12, 21, 23 and 27 compared to other transgenic lines when samples were loaded on a leaf area basis (Figure 5.11), did not appear to correlate to a strong Western PEPC signal when samples were loaded on a protein basis.

5.4 Discussion

The aims of this chapter were to investigate the effects of overexpression of the PEPC protein on photosynthesis using *Setaria viridis* as a model C_4 species and to investigate if malate inhibition of PEPC has any *in vivo* effects on photosynthesis. The attempts to create *S. viridis* plants overexpressing the PEPC enzyme and *S. viridis* plants expressing a PEPC with reduced malate sensitivity are discussed here.

5.4.1 MEO34V wild-type *S. viridis* plants and AcV5 signal

The cross reactivity of the anti-AcV5 antibody with MEO34V wild-type *S. viridis* plant samples requires thorough investigation. Western Blot analysis experiments using the anti-AcV5 antibody in this chapter resulted in consistent signals from protein extracted from the wild-type MEO34V leaf samples. AcV5 signal has also been seen consistently in the mesophyll cells of wild-type MEO34V plants (results from microscopy experiments conducted by other Furbank and von Caemmerer lab members). This is unusual given that the AcV5 tag was used successfully and no cross reactivity was seen in the A10 *S. viridis* ecotype. Two possibilities appear to exist here. Firstly, a transgene could be present in the MEO34V wild-type seed that was received by the von Caemmerer and Furbank labs and the seedstock is not from wild-type MEO34V *S. viridis* but from a transgenic MEO34V *S. viridis*. Secondly, the cross reactivity of the anti-AcV5 antibody with the MEO34V wild-type *S. viridis* is unique to this particular *S. viridis* ecotype. It is important to determine which of the two possibilities is actually happening as it will determine what steps need to be taken to resolve this issue. If, after investigation it is

proven that there is no evidence a transgene in the MEO34V wild-type, then the AcV5 tag should not be used with this ecotype of *Setaria viridis*.

5.4.2 Redesigning the PEPC overexpression experiment

From the experiments carried out in this chapter, it would seem that a number of issues need to be addressed in order to successfully obtain C_4 plants that successfully overexpress PEPC. As seen from the results, there were no significant differences between the PEPC activity (µmol HCO_3 m^{-2} sec^{-1}) of any of the transgenic lines and the wild-type *S. viridis* plants. When the natural variation in PEPC activity of the wild-type *S. viridis* plants is taken into consideration, this is hardly surprising. In just one experiment, the wild-type PEPC activity of ten *S. viridis*

plants ranged from a low of 147.12 µmol HCO_3 m^{-2} sec^{-1} to 201.65 µmol HCO_3 m^{-2} sec^{-1}. The lowest performing wild-type plant had only 73% of the PEPC activity of the highest performing wild-type plant (Figure 5.16). This natural genetic variation in PEPC activity was seen across many experiments when batches of wild-type *S. viridis* plants were assayed. Informal statistical analyses showed no statistically significant impact of time of day on PEPC activity. When examining the T_1 plants from a single transformation event, huge variation in PEPC activity is also seen within each line. For example, looking at the T_1 plants of line 15, the highest performer outperformed the wild-type in terms of PEPC activity by 33 %, whilst the lowest performing T_1 plant had just 54 % of the wild-type PEPC activity (Figure 5.13, Table 5.12). For line 21 the highest performer outperformed the wild-type in terms of PEPC activity by 29 %, whilst the lowest performing T_1 plant had just 57 % of the wild-type PEPC activity (Figure 5.13, Table 5.12). For line 23 the highest performer outperformed the wild-type in terms of PEPC activity by 30 %, whilst the lowest performing T_1 plant had just 62 % of the wild-type PEPC activity (Figure 5.13, Table 5.12). For line 27 the highest performer outperformed the wild-type in terms of PEPC activity by 26 %, whilst the lowest performing

T_1 plant had just 47 % of the wild-type PEPC activity (Figure 5.13, Table 5.12). Looking at the PEPC activities of T_2 plants all descendent from the single transformation event, the 30 plants covered a wide range of PEPC values from 106.03 µmol HCO_3 m^{-2} sec^{-1} right up to 229.61 µmol HCO_3 m^{-2} sec^{-1} (Figure 5.16). This is a huge range of PEPC activity values, best performing plant having more than double the PEPC activity of the lowest performing plant. Even looking at plants descendent from the same T_1 individual there is massive variation in PEPC activity. In T_2 plants descendent from T_1 individual 15-1 the lowest performing individual had PEPC activity of 106.03 µmol HCO_3 m^{-2} sec^{-1} and the best performing individual had PEPC activity of 200.71 µmol HCO_3 m^{-2} sec^{-1} (Figure 5.27). In T_2 plants descendent from T_1 individual 15-2 the lowest performing individual had PEPC activity of 157.39 µmol HCO_3 m^{-2} sec^{-1} and the best performing individual had PEPC activity of 220.72 µmol HCO_3 m^{-2} sec^{-1} (Figure 5.16). In T_2 plants descendent from T_1 individual 15-26 the lowest performing individual had PEPC activity of 119.48 µmol HCO_3 m^{-2} sec^{-1} and the best performing individual had PEPC activity of 229.61 µmol HCO_3 m^{-2} sec^{-1} (Figure 5.16). Therefore, with such great natural variation in PEPC activity levels in *S. viridis* and so much variation within transgenic lines, the question needs to be asked as to whether *S. viridis* is an appropriate model for PEPC overexpression studies.

In order to redesign this experiment, the natural variation in PEPC activity of wild-type C_4 grasses with established transformation protocols should be assessed. The plant with the smallest range of PEPC expression should be chosen for the model for future PEPC overexpression experiment. Both *Zea mays* and *Sorghum* C_4 grasses have established transformation protocols and have successfully been transformed (Gurel et al., 2008; Salesse-Smith et al., 2018). Therefore, these two grasses would be candidates for the model C_4 grass for future PEPC overexpression experiments.

5.4.3 Redesigning the S. viridis C4-PEPC RNAi silencing and K835G PEPC, and S. viridis C4-PEPC RNAi silencing and K835G/R894G PEPC experiments

The attempt to express the *S. viridis* C4-PEPC RNAi silencing and K835G PEPC, and *S. viridis* C4-PEPC RNAi silencing and K835G/R894G PEPC constructs to investigate the effects of a malate insensitive PEPC enzyme *in planta* in *Setaria viridis* was ultimately unsuccessful. The unforeseen cross reactivity of the anti-AcV5 antibody and the MEO34V *S. viridis* ecotype, meant that mutant plants could not be cheaply screened as planned. Given the recent success of the CRISPR/Cas9 technology in many plant species, however, revisiting this experiment using the CRISPR/Cas9 technology will allow for a more sophisticated approach. Since the start of these experiments in 2017, CRISPR/Cas9 technology has been used successfully in *Setaria viridis* (Weiss et al., 2020; Basso et al., 2021). Utilising CRISPR/Cas9 technology for this experiment would mean that expression of the native *S. viridis* C_4 PEPC enzyme would not need to be knocked out. Site-specific mutations of the sequence coding for the C_4 PEPC enzyme at malate-binding residues in the *S. viridis* genome would be possible using engineered guide RNAs. This would eliminate the complications associated with completely knocking out expression of the native *S. viridis* C_4 PEPC enzyme, attempting to reach equivalent levels of expression with a transgene and possible co-suppression of other *S. viridis* PEPCs. Therefore, revisiting this experiment using CRISPR/Cas9 technology provides an exciting opportunity to investigate the effects of malate regulation of the C_4 PEPC enzyme *in planta*.

5.5 Conclusions

The PEPC overexpression experiments and the *S. viridis* C4-PEPC RNAi silencing and K835G PEPC, and *S. viridis* C4-PEPC RNAi silencing and K835G/R894G PEPC experiments were ultimately unsuccessful due to range of unforeseen factors including cross reactivity of the AcV5 antibody in the MEO34V *S. viridis* ecotype. However, this research has provided valuable information on how to redesign these experiments for future studies.

General discussion and conclusions

Based on published literature and the research and observations presented in this thesis, Figure 6.1 is a current model of PEPC function. PEPC catalyses the irreversible β-carboxylation of PEP by HCO_3^-, to form OAA and inorganic phosphate (Pi), requiring either Mg^{2+} or Mn^{2+} as an obligatory cofactor. Formation of the more active PEPC tetramer from the less active dimeric form is promoted by the presence of PEP, G6P, Mg^{2+}, and HCO_3^-, all of which are either substrates, necessary cofactors or activators of the enzyme. PEPC is activated by phosphorylation, G6P, triose phosphates and glycine and inhibited by OAA, malate and aspartate. This General Discussion will focus on PEPC oligomerisation, metabolic regulation, and the influence of the amount of PEPC on photosynthesis.

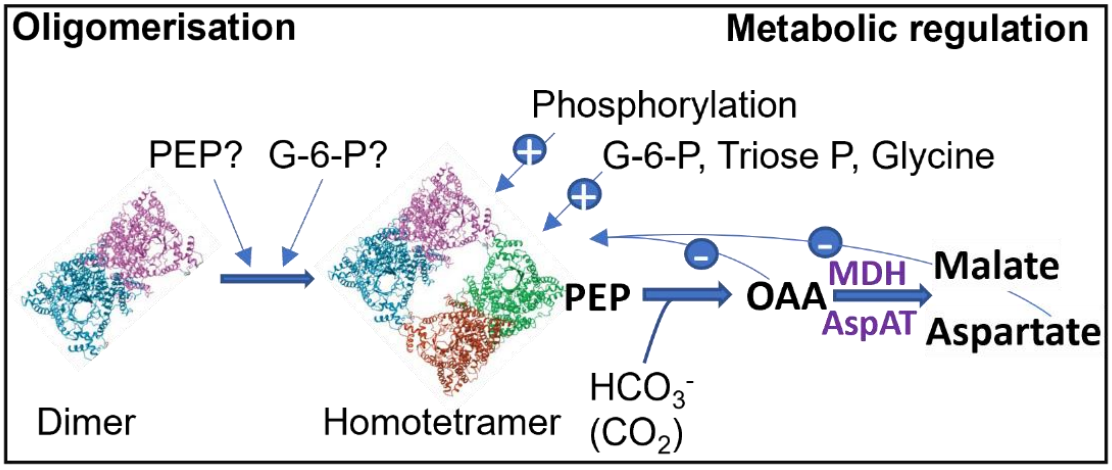

Figure 6.1. Current model of PEPC function based on published literature and the research and observations presented in this thesis. Abbreviations are as follows phosphoenolpyruvate (PEP), glucose-6-phosphate (G-6-P), triose phosphates (Triose P), oxaloacetate (OAA), malate dehydrogenase (MDH), aspartate aminotransferase (AspAT).

6.1 PEPC oligomerisation

From the results of Chapter 3, the PEPC enzymes from *U. panicoides*, *P. coloratum*, and *S. viridis* were purified as dimers after expression in *E. coli*. This was in direct contrast to many studies which report PEPC protein being purified in the more active tetrameric form, although some studies have reported a mixture of dimers and tetramers being purified (Ting and

Osmond, 1973c; Miziorko et al., 1974; Nott and Osmond, 1982; Huber et al., 1986; Iglesias et al., 1986; Stiborová and Leblová, 1986; Walker et al., 1986; Podesta and Andreo, 1989; Willeford et al., 1990; Arrio-Dupont et al., 1992; Svensson et al., 1997). The PEPC enzyme has an inherent tendency to dissociate into dimers, as it only has salt bridges between the Arg 438 of one subunit and Glu433 of another subunit holding the tetramer together (Kai et al., 1999). When looking at the structure of the PEPC enzyme tetramer, it does seem implausible that the two large PEPC dimers would be held tightly together by these salt bridges alone. Some studies have looked into the effects of the conditions of the solution containing PEPC on the oligomerisation status of the PEPC enzyme. Incubation of the PEPC enzyme with Mg^{2+}, PEP, G6P, and HCO_3^- has been shown to induce the formation of PEPC tetramers or to stabilise the tetrameric form (Wu and Wedding, 1985; Wu and Wedding, 1987; Willeford et al., 1990; Wu et al., 1990; Meyer et al., 1991; Willeford and Wedding, 1992; Wedding et al., 1994). Incubation of the PEPC enzyme with malate or NaCl has been shown to induce the formation of dimers (Wu and Wedding, 1985; Nimmo et al., 1986; Wagner et al., 1987; Wu and Wedding, 1987; McNaughton et al., 1989; Podesta and Andreo, 1989; Willeford et al., 1990; Wu et al., 1990; Meyer et al., 1991). Studies have also demonstrated a concentration-dependent oligomerisation of the PEPC enzyme, with dissociation of the PEPC tetramer into dimers at low concentrations, and formation of the tetramer at high concentrations of PEPC protein (Jones et al., 1978; Nott and Osmond, 1982; Nimmo et al., 1987; McNaughton et al., 1989; Willeford et al., 1990; Wu et al., 1990; Meyer et al., 1991; Willeford and Wedding, 1992).

While there have been a number of studies on PEPC oligomerisation, many of these were conducted using gel filtration. A synthesis of these studies using small angle X-ray scattering (SAXS) to investigate substrate-mediated oligomerisation and inhibitor-mediated oligomerisation would be a nice addition to the literature. SAXS is very effective at measuring the quaternary structure of proteins in a solution, and is especially effective when the crystal structure of the protein is known, as is the case with PEPC (Korasick and Tanner, 2018).

6.2 Metabolic regulation

In Chapter 4 of this thesis, it was found that there is an influence of biochemical subtype on inhibition of the PEPC enzyme by malate. A six-amino acid deletion specific to the PEPCK subtype reduces the sensitivity of the PEPC enzyme to inhibition by malate. Examining how this region interacts with malate would be a very interesting area for research. This could be investigated by crystallising PEPC enzymes and enzyme chimeras in the presence of malate and solving their structures. Two crystallography studies by crystallising the PEPC enzymes of the C_3 *F. pringlei* and the C_4 *F. trinervia* with aspartate elucidated how the inhibitor molecule interacted with the PEPC enzymes give the C_4 PEPC enzyme a greater tolerance to aspartate (Paulus et al., 2013; Paulus et al., 2013).

In Chapter 4, the k_{cat} values determined for the *U. panicoides* enzyme in the presence and absence of G6P were presented. When compared to the ranges reported for k_{cat} values in the presence and absence of G6P for C_4 and C_3 species, the C_4 PEPC enzyme from *U. panicoides* fell considerably above the range (Figure 4.14, Table 4.2, Table 4.7). *U. panicoides*, therefore, has a PEPC enzyme with a superior k_{cat} value. Given the superior catalytic properties of the *U. panicoides* enzyme, exciting opportunities exist to express this PEPC enzyme in other C_4 plants to improve photosynthesis. A recent study by members of the C_4 Rice Project introduced a five-gene construct containing 5 coding regions for the *Zea mays* C_4 photosynthetic genes of carbonic anhydrase, PEPC, NADP-malate dehydrogenase, PPDK, and NAD-ME into rice (*Oryza sativa*). This was done in an attempt to introduce the C_4 photosynthetic mechanism into rice in order to improve photosynthetic efficiency among other things. C_4 PEPC was successfully expressed resulting in an increase in CO_2 flux through PEPC, albeit at 2 % of the flux seen in *Zea mays* wild-type plants. With its superior k_{cat} values, the *U. panicoides* enzyme could be an exciting candidate for the PEPC enzyme to be introduced into rice as part of the C_4 Rice Project in order to try and increase the CO_2 flux through PEPC in the transformed rice

plant. CO_2 flux through PEPC in transformed rice plants could be increased to required levels with less PEPC protein than would be required for the same flux through *Zea mays* PEPC.

Chapter 4 of this thesis presented observations from MIMS experiments which suggest that OAA has potent inhibitory effects on the PEPC enzymes from both *U. panicoides* (PEPCK) and *Panicum coloratum* (NAD-ME). No such inhibitory effects were observed on the PEPC enzyme from *Setaria viridis*. As discussed previously, OAA inhibition of the PEPC enzyme has been reported in three plant species, *Setaria italica* (NADP-ME), *Pennisetum purpureum* (NADP-ME) and *Amaranthus viridis* (NAD-ME), but is not as well documented as the inhibitory effects of malate (Coombs et al., 1973; Raghavendra and Das, 1975; Iglesias et al., 1986). Given that OAA has been reported to be an even more potent inhibitor of the PEPC enzyme than malate, an investigation into the inhibitory effects of OAA on a wide sample of PEPC enzymes should be conducted (Coombs et al., 1973; Raghavendra and Das, 1975; Iglesias et al., 1986). In order to determine the I_{50} of OAA or the K_i of OAA, PEPC activity could be measured by MIMS as described in the Methods section of Chapter 4, and the assay could be initiated with PEP. The assay mixtures would contain different concentrations of OAA and the I_{50} of OAA or the K_i of OAA could be determined. Using an NADH-coupled spectrophotometric assay to determine PEPC activity would not be appropriate as the assay relies on the OAA produced by PEPC being converted to malate by MDH, with NADH being consumed in the process. Thus, any OAA added to the assay solution to test inhibitory effects would be immediately converted by the MDH. Therefore, measuring PEPC activity by MIMS is recommended. Given that regardless of biochemical subtype, all C_4 plants produce OAA from the carboxylation of PEP by PEPC, OAA would be present in the mesophyll environment. It would be interesting to investigate OAA as a possible feedback inhibitor of the C_4 photosynthetic cycle. An experiment by Leegood and Caemmerer (1988) measured OAA levels in *Amaranthus edulis*, and found increasing levels of OAA in the mesophyll cells with increasing irradiance. The PEPC amino acids involved in the inhibitory interactions with OAA are not documented, so this would be another area in which new research could be conducted.

Crystallography studies, similar to those conducted by Paulus et al. (2013), however, with PEPC being crystallised with OAA would elucidate the residues involved in OAA inhibition. After candidate residues have been identified, these residues could be mutated to abolish their chemical properties, and kinetic studies between mutant and wild-type PEPC enzymes could be conducted to confirm if the candidate residues are indeed involved in OAA inhibition of PEPC.

Investigating the effects of malate, aspartate, and OAA inhibition on the C_4 enzyme *in planta* would provide valuable insights into how the C_4 PEPC enzyme is regulated in its natural environment. In Chapter 5 of this thesis the attempt to investigate the effects of a malate insensitive PEPC enzyme *in planta* in *Setaria viridis* was ultimately unsuccessful. As discussed, given the recent success of the CRISPR/Cas9 technology in many plant species, revisiting this experiment using the CRISPR/Cas9 technology will allow for a more sophisticated and hopefully successful approach (Weiss et al., 2020; Basso et al., 2021). Utilising CRISPR/Cas9 technology for this experiment would mean that expression of the native C_4 PEPC enzyme in the C_4 model plant species chosen would not need to be knocked out. Site-specific mutations of the sequence coding for the C_4 PEPC enzyme at malate/aspartate-binding residues or at OAA-binding residues that are discovered in the future in the C_4 plant genome would be possible using engineered guide RNAs. Therefore, investigating the effects of malate, aspartate, and OAA inhibition on the C_4 enzyme *in planta* using CRISPR/Cas9 technology would provide an exciting opportunity to investigate the effects of inhibitor regulation of the C_4 PEPC enzyme *in planta*.

6.3 Influence of amount of PEPC on photosynthesis

As discussed in Chapter 5, C_4 PEPC protein expression has been successfully reduced in *S. viridis* using RNA interference (Alonso-Cantabrana et al., 2018). The reduction in C_4 PEPC activity seen in the transgenics resulted in very low CO_2 assimilation rates and increased

plasmodesmata density (Alonso-Cantabrana et al., 2018). *Amaranthus edulis* (NAD-ME) mutants with reduced PEPC activity, created using sodium azide, showed a reduction in the maximum CO_2 assimilation rate and reduced carboxylation efficiency (Dever et al., 1995; Dever et al., 1997; Cousins et al., 2007). Another study involving heterozygous mutant *Amaranthus edulis* plants with reduced PEPC activity showed a decrease in the initial slope of CO_2 response curves, with mutant plants exhibiting reduced photosynthetic rates at high light intensities (Bailey et al., 2000). A reduction in maximal PEPC activity does, therefore, appear to reduce the initial slope of the initial slope of the CO_2 response curve, as predicted by biochemical modelling of the C_4 pathway. Unfortunately, the attempts to obtain PEPC overexpression in *Setaria viridis* was unsuccessful and no PEPC overexpression data was obtained to combine with reduction data. The results from Chapter 5 of this thesis show that a lot of work still needs to be done to obtain C_4 plants overexpressing PEPC and provided insights into how to successfully obtain PEPC overexpressing plants in the future. The natural variation present in PEPC activity of the wild-type *S. viridis* plants would make it hard to get transgenic plants with increased PEPC activity that is statistically different to the wild-type. As discussed in Chapter 5, a huge variation in PEPC activity was seen within single lines of transgenic plants as well. Therefore, with such great natural variation in PEPC activity levels in *S. viridis* and so much variation within transgenic lines, the question needs to be asked as to whether *S. viridis* is an appropriate model for PEPC overexpression studies.

In order to redesign this experiment, the natural variation in PEPC activity of wild-type C_4 grasses with established transformation protocols should be assessed. The plant with the smallest range of PEPC expression should be chosen for the model for future PEPC overexpression experiment. Both *Zea mays* and *Sorghum* C_4 grasses have established transformation protocols and have successfully been transformed (Gurel et al., 2008; Salesse-Smith et al., 2018). Therefore, these two grasses would be candidates for the model C_4 grass for future PEPC overexpression experiments.

The results from Chapter 5 also showed that there is cross reactivity of the anti-AcV5 antibody with the samples from the MEO34V wild-type *S. viridis* plant. The two possibilities that exist are that a transgene is present in the MEO34V wild-type seed that was received by the von Caemmerer and Furbank labs and the seedstock is not from wild-type MEO34V *S. viridis* but from a transgenic MEO34V *S. viridis* or the cross reactivity of the anti-AcV5 antibody with the MEO34V wild-type *S. viridis* is unique to this particular *S. viridis* ecotype. It is important to determine which of the two possibilities is actually happening as it will determine what steps need to be taken to resolve this issue. If, after investigation it is proven that there is no evidence a transgene in the MEO34V wild-type, then the AcV5 tag should not be used with this ecotype of *Setaria viridis*. A FLAG-tag would be recommended for use instead of the AcV5 tag (Hopp et al., 1988).

6.4 Conclusions

The overall results of this thesis have shown that there is still more to learn about the regulatory properties of the C_4 PEPC enzyme. This thesis has also highlighted that there are C_4 PEPC enzymes with superior catalytic properties available for transformation into plants. Therefore, increasing photosynthesis through PEPC modification is a prime opportunity and will allow plants to function more efficiently in an increasingly hot, dry climate.

References

ABARES (2021) Australian crop report: June 2021 No.198. *In.* ABARES : Australian Bureau of Agricultural and Resource Economics and Sciences : Department of Agriculture, Water and the Environment

Agarie S, Sasaki H, Matsuoka M, Miyao Tokutomi M (2001) Overexpression of C_4 phosphoenolpyruvate carboxylase increased carbon isotope discrimination in transgenic rice plants. Plant Production Science **4:** 311-312

Agetsuma M, Furumoto T, Yanagisawa S, Izui K (2005) The ubiquitin-proteasome pathway is involved in rapid degradation of phosphoenolpyruvate carboxylase kinase for C_4 photosynthesis. Plant and Cell Physiology **46:** 389-398

Aigner H, Wilson RH, Bracher A, Calisse L, Bhat JY, Hartl FU, Hayer-Hartl M (2017) Plant Rubisco assembly in *E. coli* with five chloroplast chaperones including BSD2. Science **358:** 1272-1278

Akyildiz M, Gowik U, Engelmann S, Koczor M, Streubel M, Westhoff P (2007) Evolution and function of a cis-regulatory module for mesophyll-specific gene expression in the C_4 dicot *Flaveria trinervia*. The Plant Cell **19:** 3391-3402

Alonso-Cantabrana H, Cousins AB, Danila F, Ryan T, Sharwood RE, von Caemmerer S, Furbank RT (2018) Diffusion of CO_2 across the mesophyll-bundle sheath cell interface in a C_4 plant with genetically reduced PEP carboxylase activity. Plant Physiology **178:** 72-81

Andrews TJ (1996) The bait in the Rubisco mousetrap. Nature Structural Biology **3:** 3-7

Arrio-Dupont M, Bakrim N, Echevarria C, Gadal P, Le Maréchal P, Vidal J (1992) Compared properties of phosphoenolpyruvate carboxylase from dark- and light-adapted *Sorghum* leaves: use of a rapid purification technique by immunochromatography. Plant Science **81:** 37-46

Arrivault S, Obata T, Szecówka M, Mengin V, Guenther M, Hoehne M, Fernie AR, Stitt M (2017) Metabolite pools and carbon flow during C_4 photosynthesis in maize: $^{13}CO_2$ labeling kinetics and cell type fractionation. Journal of Experimental Botany **68:** 283-298

Ashton AR, Burnell JN, Furbank RT, Jenkins CLD, Hatch MD (1990) 3 - Enzymes of C_4 Photosynthesis. *In* PJ Lea, ed, Methods in Plant Biochemistry, Vol 3. Academic Press, pp 39-72

Bailey KJ, Battistelli A, Dever LV, Lea PJ, Leegood RC (2000) Control of C_4 photosynthesis: effects of reduced activities of phosphoenolpyruvate carboxylase on CO_2 assimilation in *Amaranthus edulis* L. Journal of experimental botany **51:** 339-346

Bainbridge G, Madgwick P, Parmar S, Mitchell R, Paul M, Pitts J, Keys AJ, Parry MAJ (1995) Engineering Rubisco to change its catalytic properties. Journal of Experimental Botany **46:** 1269-1276

Baker RT (1996) Protein expression using ubiquitin fusion and cleavage. Current Opinion in Biotechnology **7:** 541-546

Baker RT, Catanzariti AM, Karunasekara Y, Soboleva TA, Sharwood R, Whitney S, Board PG (2005) Using Deubiquitylating Enzymes as Research Tools. *In* Methods in Enzymology, Vol 398. Elsevier Science & Technology, United States, pp 540-554

Baker RT, Smith SA, Marano R, McKee J, Board PG (1994) Protein expression using cotranslational fusion and cleavage of ubiquitin. Mutagenesis of the glutathione-binding site of human Pi class glutathione S-transferase. The Journal of Biological Chemistry **269:** 25381-25386

Bandarian, Poehner WJ, Grover SD (1992) Metabolite activation of crassulacean acid metabolism and C_4 phosphoenolpyruvate carboxylase. Plant Physiology **100:** 1411-1416

Bandurski RS (1955) Further studies on the enzymatic synthesis of oxalacetate from phosphorylenolpyruvate and carbon dioxide. The Journal of Biological Chemistry **217:** 137

Bassham JA, Calvin M (1957) The path of carbon in photosynthesis. Prentice-Hall, Englewood Cliffs, New Jersey

Basso MF, Duarte KE, Santiago TR, Souza WRd, Garcia BdO, Bárbara Dias Brito da C, Kobayashi AK, Molinari HBC (2021) Efficient genome editing and gene knockout in *Setaria viridis* with CRISPR/Cas9 directed gene editing by the non-homologous end-joining pathway. Plant Biotechnology **38:** 227-238

Bauwe H (1986) An efficient method for the determination of K_m values for HCO_3^- of phosphoenolpyruvate carboxylase. Planta **169:** 356-360

Bauwe H, Chollet R (1986) Kinetic properties of phosphoenolpyruvate carboxylase from C_3, C_4 and C_3-C_4 intermediate species of *Flaveria* (Asteraceae). Plant Physiology **82:** 695-699

Bauwe H, Hagemann M, Fernie AR (2010) Photorespiration: players, partners and origin. Trends in Plant Science **15:** 330-336

Begum HH, Osaki M, Watanabe T, Shinano T (2009) Mechanisms of aluminum tolerance in phosphoenolpyruvate carboxylase transgenic rice. Journal of Plant Nutrition **32:** 84-96

Bennetzen JL, Schmutz J, Jenkins J, Barry K, Lindquist E, Hellsten U, Deshpande S, Wang X, Wu X, Mitros T, Triplett J, Yang X, Wang HAO, Ye C-Y, Mauro-Herrera M, Wang LIN, Li P, Sharma M, Sharma R, Ronald PC, Panaud O, Kellogg EA, Brutnell TP, Percifield R, Doust AN, Tuskan GA, Rokhsar D, Devos KM, Hawkins J, Pontaroli AC, Estep M, Feng L, Vaughn JN, Grimwood J, Oak Ridge National Lab ORTN (2012) Reference genome sequence of the model plant *Setaria*. Nature Biotechnology **30:** 555-561

Black CC, Mollenhauer HH (1971) Structure and distribution of chloroplasts and other organelles in leaves with various rates of photosynthesis. Plant Physiology **47:** 15-23

Bläsing OE, Ernst K, Streubel M, Westhoff P, Svensson P (2002) The non-photosynthetic phosphoenolpyruvate carboxylases of the C_4 dicot *Flaveria trinervia* — implications for the evolution of C_4 photosynthesis. Planta **215:** 448-456

Bläsing OE, Westhoff P, Svensson P (2000) Evolution of C_4 phosphoenolpyruvate carboxylase in *Flaveria*, a conserved serine residue in the carboxyl-terminal part of the enzyme is a major determinant for C_4-specific characteristics. The Journal of Biological Chemistry **275:** 27917

BOM, CSIRO (2022) State of the Climate. *In*,

Bornhorst JA, Falke JJ (2000) [16] Purification of proteins using polyhistidine affinity tags. *In* Methods in Enzymology, Vol 326. Elsevier Science & Technology, United States, pp 245-254

Bouvier JW, Emms DM, Rhodes T, Bolton JS, Brasnett A, Eddershaw A, Nielsen JR, Unitt A, Whitney SM, Kelly S (2021) Rubisco adaptation is more limited by phylogenetic constraint than by catalytic trade-off. Molecular Biology and Evolution **38:** 2880-2896

Bowes G, Ogren WL, Hageman RH (1971) Phosphoglycolate production catalyzed by ribulose diphosphate carboxylase. Biochemical and Biophysical Research Communications **45:** 716-722

Boyd RA, Gandin A, Cousins AB (2015) Temperature responses of C_4 photosynthesis: biochemical analysis of rubisco, phosphoenolpyruvate carboxylase, and carbonic anhydrase in *Setaria viridis*. Plant Physiology **169:** 1850

Bradford MM (1976) A rapid and sensitive method for the quantitation of microgram quantities of protein utilizing the principle of protein-dye binding. Analytical Biochemistry **72:** 248-254

Bräutigam A, Gowik U (2016) Photorespiration connects C_3 and C_4 photosynthesis. Journal of Experimental Botany **67:** 2953

Brutnell TP, Wang L, Swartwood K, Goldschmidt A, Jackson D, Zhu X-G, Kellogg E, Eck JV (2010) *Setaria viridis*: A model for C_4 photosynthesis. The Plant Cell **22:** 2537-2544

Cabido M, Pons E, Cantero JJ, Lewis JP, Anton A (2008) Photosynthetic pathway variation among C_4 grasses along a precipitation gradient in Argentina. Journal of Biogeography **35:** 131-140

Carmo-Silva E, Scales JC, Madgwick PJ, Parry MAJ (2015) Optimizing Rubisco and its regulation for greater resource use efficiency. Plant, Cell and Environment **38:** 1817-1832

Catanzariti AM, Soboleva TA, Jans DA, Board PG, Baker RT (2004) An efficient system for high-level expression and easy purification of authentic recombinant proteins. Protein Science **13:** 1331-1339

Cavalar M, Phlippen Y, Kreuzaler F, PeterhÄNsel C (2007) A drastic reduction in DOF1 transcript levels does not affect C_4-specific gene expression in maize. Journal of Plant Physiology **164:** 1665-1674

Charles AM, Sykora Y (1992) Purification and characterization of the phosphoenolpyruvate carboxylase from the facultative chemolithotroph *Thiobacillus novellus* (ATCC 8093). Antonie van Leeuwenhoek **62:** 155-165

Chen L-M, Li K-Z, Miwa T, Izui K (2004) Overexpression of a cyanobacterial phosphoenolpyruvate carboxylase with diminished sensitivity to feedback inhibition in *Arabidopsis* changes amino acid metabolism. Planta **219:** 440-449

Chen L-m, Omiya T, Hata S, Izui K (2002) Molecular characterization of a phosphoenolpyruvate carboxylase from a thermophilic cyanobacterium, *Synechococcus vulcanus* with unusual allosteric properties. Plant and Cell Physiology **43:** 159-169

Chen Z, Bommareddy RR, Frank D, Rappert S, Zeng A-P (2014) Deregulation of feedback Inhibition of phosphoenolpyruvate carboxylase for improved lysine production in *Corynebacterium glutamicum*. Applied and Environmental Microbiology **80:** 1388-1393

Chollet R, Vidal J, O'Leary MH (1996) Phosphoenolpyruvate carboxylase: A ubiquitous, highly regulated enzyme in plants. Annual Review of Plant Physiology and Plant Molecular Biology **47:** 273-298

Christin P-A, Arakaki M, Osborne CP, Bräutigam A, Sage RF, Hibberd JM, Kelly S, Covshoff S, Wong GK-S, Hancock L, Edwards EJ (2014) Shared origins of a key enzyme during the evolution of C_4 and CAM metabolism. Journal of Experimental Botany **65:** 3609-3621

Christin P-A, Besnard G, Samaritani E, Duvall MR, Hodkinson TR, Savolainen V, Salamin N (2008) Oligocene CO_2 Decline Promoted C_4 Photosynthesis in Grasses. Current Biology **18:** 37-43

Christin P-A, Osborne CP, Chatelet DS, Columbus JT, Besnard G, Hodkinson TR, Garrison LM, Vorontsova MS, Edwards EJ (2013) Anatomical enablers and the evolution of C_4 photosynthesis in grasses. Proceedings of the National Academy of Sciences **110:** 1381-1386

Christin P-A, Salamin N, Savolainen V, Duvall MR, Besnard G (2007) C_4 photosynthesis evolved in grasses via parallel adaptive genetic changes. Current Biology **17:** 1241-1247

Conaty WC, Constable GA (2020) Factors responsible for yield improvement in new *Gossypium hirsutum* L. cotton cultivars. Field Crops Research **250:** 107780

Coombs J, Baldry CW, Bucke C (1973) The C_4 pathway in *Pennisetum purpureum*: I. The allosteric nature of PEP carboxylase. Planta **110:** 95-107

Cousins AB, Baroli I, Badger MR, Ivakov A, Lea PJ, Leegood RC, Von Caemmerer S (2007) The role of phosphoenolpyruvate carboxylase during C_4 photosynthetic isotope exchange and stomatal conductance. Plant Physiology **145:** 1006-1017

Cytiva (2020) Principles and methods: Size Exclusion Chromatography. *In*,

Danila F, Quick WP, White RG, Kelly S, von Caemmerer S, Furbank R (2018) Multiple mechanisms for enhanced plasmodesmata density in disparate subtypes of C_4 grasses. Journal of Experimental Botany **69:** 1135-1145

Danker T, Dreesen B, Offermann S, Horst I, Peterhänsel C (2008) Developmental information but not promoter activity controls the methylation state of histone H3 lysine 4 on two photosynthetic genes in maize. The Plant Journal **53:** 465-474

Davidi D, Shamshoum M, Guo Z, Bar-On YM, Prywes N, Oz A, Jablonska J, Flamholz A, Wernick DG, Antonovsky N, Pins B, Shachar L, Hochhauser D, Peleg Y, Albeck S, Sharon I, Mueller-Cajar O, Milo R (2020) Highly active rubiscos discovered by systematic interrogation of natural sequence diversity. The EMBO Journal **39:** e104081-n/a

De Souza AP, Burgess SJ, Doran L, Hansen J, Manukyan L, Maryn N, Gotarkar D, Leonelli L, Niyogi KK, Long SP (2022) Soybean photosynthesis and crop yield are improved by accelerating recovery from photoprotection. Science **377:** 851-854

Defelice MS (2002) Green Foxtail, *Setaria viridis* (L.) P. Beauv. Weed Technology **16:** 253-257

Del Prete S, De Luca V, Capasso C, Supuran CT, Carginale V (2016) Recombinant thermoactive phosphoenolpyruvate carboxylase (PEPC) from *Thermosynechococcus elongatus* and its coupling with mesophilic/thermophilic bacterial carbonic anhydrases (CAs) for the conversion of CO_2 to oxaloacetate. Bioorganic & Medicinal Chemistry **24:** 220-225

Dever LV, Bailey KJ, Leegood RC, Lea PJ (1997) Control of photosynthesis in *Amaranthus edulis* mutants with reduced amounts of PEP carboxylase. Functional Plant Biology **24:** 469

Dever LV, Blackwell RD, Fullwood NJ, Lacuesta M, Leegood RC, Onek LA, Pearson M, Lea PJ (1995) The isolation and characterization of mutants of the C_4 photosynthetic pathway. Journal of Experimental Botany **46:** 1363-1376

Dharmarajan L, Kraszewski JL, Mukhopadhyay B, Dunten PW (2011) Structure of an archaeal-type phosphoenolpyruvate carboxylase sensitive to inhibition by aspartate. Proteins, Structure, Function, and Bioinformatics **79:** 1820-1829

DiMario RJ, Cousins AB (2019) A single serine to alanine substitution decreases bicarbonate affinity of phosphoenolpyruvate carboxylase in C_4 *Flaveria trinervia*. Journal of Experimental Botany **70:** 995-1004

DiMario RJ, Kophs AN, Pathare VS, Schnable JC, Cousins AB (2021) Kinetic variation in grass phosphoenolpyruvate carboxylases provides opportunity to enhance C_4 photosynthetic efficiency. The Plant Journal **105:** 1677

Dong L-Y, Masuda T, Kawamura T, Hata S, Izui K (1998) Cloning, expression, and characterization of a root-form phosphoenolpyruvate carboxylase from *Zea mays*: Comparison with the C_4-form enzyme. Plant and Cell Physiology **39:** 865-873

Dong L, Patil S, Condon SA, Haas EJ, Chollet R (1999) The conserved C-terminal tetrapeptide of *Sorghum* C_4 phosphoenolpyruvate carboxylase is indispensable for maximal catalytic activity, but not for homotetramer formation. Archives of Biochemistry and Biophysics **371:** 124

Dong LY, Ueno Y, Hata S, Izui K (1997) Effects of site-directed mutagenesis of conserved lys606 residue on catalytic and regulatory functions of maize [*Zea mays*] C_4-form phosphoenolpyruvate carboxylase. Plant and Cell Physiology **38:** 1340-1345

Edwards EJ, Ogburn RM (2012) Angiosperm Responses to a Low-CO_2 World: CAM and C_4 Photosynthesis as Parallel Evolutionary Trajectories. International Journal of Plant Sciences **173:** 724-733

Ehleringer JR, Cerling TE, Helliker BR (1997) C_4 Photosynthesis, atmospheric CO_2, and climate. Oecologia **112:** 285-299

Ehleringer JR, Ehleringer JR, Sage RF, Sage RF, Flanagan LB, Flanagan LB, Pearcy RW, Pearcy RW (1991) Climate change and the evolution of C_4 photosynthesis. Trends in Ecology and Evolution **6:** 95-99

Ehleringer JR, Monson RK (1993) Evolutionary and ecological aspects of photosynthetic pathway variation. Annual Review of Ecology and Systematics **24:** 411-439

Ellis RP, Vogel JC, Fuls A (1980) Photosynthetic pathways and the geographical distribution of grasses in South West Africa/Namibia. South African Journal of Science **76:** 307-314

Endo T, Mihara Y, Furumoto T, Matsumura H, Kai Y, Izui K (2008) Maize C_4-form phosphoenolpyruvate carboxylase engineered to be functional in C_3 plants: mutations for diminished sensitivity to feedback inhibitors and for increased substrate affinity. Journal of Experimental Botany **59:** 1811-1818

Engelmann S, Bläsing OE, Gowik U, Svensson P, Westhoff P (2003) Molecular evolution of C_4 phosphoenolpyruvate carboxylase in the genus *Flaveria* — a gradual increase from C_3 to C_4 characteristics. Planta **217:** 717-725

Engelmann S, Bläsing OE, Westhoff P, Svensson P (2002) Serine 774 and amino acids 296 to 437 comprise the major C_4 determinants of the C_4 phosphoenolpyruvate carboxylase of *Flaveria trinervia*. FEBS letters **524:** 11-14

Engelmann S, Zogel C, Koczor M, Schlue U, Streubel M, Westhoff P (2008) Evolution of the C_4 phosphoenolpyruvate carboxylase promoter of the C_4 species *Flaveria trinervia*: the role of the proximal promoter region. BMC Plant Biology **8:** 4-4

Ermakova M, Danila FR, Furbank RT, Caemmerer S (2020) On the road to C_4 rice: advances and perspectives. The Plant Journal **101:** 940-950

Ettema TJG, Makarova KS, Jellema GL, Gierman HJ, Koonin EV, Huynen MA, de Vos WM, van der Oost J (2004) Identification and functional verification of archaeal-type phosphoenolpyruvate carboxylase, a missing link in archaeal central carbohydrate metabolism. Journal of Bacteriology **186:** 7754-7762

Evans JR (1989) Photosynthesis and nitrogen relationships in leaves of C_3 plants. Oecologia **78:** 9-19

Evans JR, Clarke VC (2019) The nitrogen cost of photosynthesis. Journal of Experimental Botany **70:** 7-15

Evans JR, Seemann JR (1984) Differences between wheat genotypes in specific activity of ribulose-1,5-bisphosphate carboxylase and the relationship to photosynthesis [*Triticum* and *Aegilops* spp.]. Plant Physiology **74:** 759-765

Fan Z, Li J, Lu M, Li X, Yin H (2013) Overexpression of phosphoenolpyruvate carboxylase from *Jatropha curcas* increases fatty acid accumulation in *Nicotiana tabacum*. Acta Physiologiae Plantarum **35:** 2269-2279

Farquhar GD, von Caemmerer S, Berry JA (1980) A biochemical model of photosynthetic CO_2 assimilation in leaves of C_3 species. Planta **149:** 78-90

Flamholz AI, Prywes N, Moran U, Davidi D, Bar-On YM, Oltrogge LM, Alves R, Savage D, Milo R (2019) Revisiting trade-offs between rubisco kinetic parameters. Biochemistry **58:** 3365-3376

Foley JA, Ramankutty N, Brauman KA, Cassidy ES, Gerber JS, Johnston M, Mueller ND, O'Connell C, Ray DK, West PC, Balzer C, Bennett EM, Carpenter SR, Hill J, Monfreda C, Polasky S, Rockström J, Sheehan J, Siebert S, Tilman D, Zaks DPM, Stockholms u, Stockholm Environment I, Stockholm Resilience C (2011) Solutions for a cultivated planet. Nature **478:** 337-342

Food and Agriculture Organization of the United Nations (FAO) (2020) FAOSTAT crops. *In*, Vol 2020

Frank J, Clarke RJ, Vater J, Holzwarth JF (2001) Influence of allosteric effectors on the kinetics and equilibrium binding of phosphoenolpyruvate (PEP) to phosphoenolpyruvate carboxylase (PEPC) from *Zea mays*. Biophysical Chemistry **92:** 53-64

Furbank RT (2011) Evolution of the C_4 photosynthetic mechanism: are there really three C_4 acid decarboxylation types? Journal of Experimental Botany **62:** 3103-3108

Furbank RT, Hatch MD (1987) Mechanism of C_4 photosynthesis: The size and composition of the inorganic carbon pool in bundle sheath cells. Plant Physiology **85:** 958-964

Furbank RT, Sharwood R, Estavillo GM, Silva-Perez V, Condon AG (2020) Photons to food: genetic improvement of cereal crop photosynthesis. Journal of Experimental Botany **71:** 2226-2238

Gao Y, Woo KC (1995) Site-directed mutagenesis of Lys600in phosphoenolpyruvate carboxylase of *Flaveria trinervia*: its roles in catalytic and regulatory functions. FEBS Letters **375:** 95-98

Gao Y, Woo KC (1996) Site-directed mutagenesis of *Flaveria trinervia* phosphoenolpyruvate carboxylase: Arg450 and Arg767 are essential for catalytic activity and Lys829 affects substrate binding. FEBS Letters **392:** 285-288

Gasteiger E, Hoogland C, Gattiker A, Duvaud Se, Wilkins MR, Appel RD, Bairoch A (2005) Protein identification and analysis tools on the ExPASy server. *In* JM Walker, ed, The Proteomics Protocols Handbook. Humana Press, Totowa, NJ, pp 571-607

Gehlen J, Panstruga R, Smets H, Merkelbach S, Kleines M, Porsch P, Fladung M, Becker I, Rademacher T, Haeusler RE, Hirsch HJ (1996) Effects of altered phosphoenolpyruvate carboxylase activities on transgenic C_3 plant *Solanum tuberosum*. Plant Molecular Biology **32:** 831-848

Ghannoum O, Evans J, Chow WS, Andrews T, Conroy JP, von Caemmerer S (2005) Faster Rubisco is the key to superior nitrogen-use efficiency in NADP-malic enzyme relative to NAD-malic enzyme C_4 grasses. Plant Physiology

Ghannoum O, Evans J, von Caemmerer S (2011) Chapter 8 Nitrogen and Water Use Efficiency of C_4 Plants. *In*, Vol 32, pp 129-146
Goatly MB, Smith H (1974) Differential properties of phosphoenolpyruvate carboxylase from etiolated and green sugar cane. Planta **117:** 67-73
Gold EW, Smith TE (1974) *Escherichia coli* phosphoenolpyruvate carboxylase: Effect of allosteric inhibitors on the kinetic parameters and sedimentation behavior. Archives of Biochemistry and Biophysics **164:** 447-455
Gowik U, Burscheidt J, Akyildiz M, Schlue U, Koczor M, Streubel M, Westhoff P (2004) cis-regulatory elements for mesophyll-specific gene expression in the C_4 plant *Flaveria trinervia*, the promoter of the C_4 phosphoenolpyruvate carboxylase gene. The Plant Cell **16:** 1077-1090
Gowik U, Engelmann S, Bläsing OE, Raghavendra AS, Westhoff P (2006) Evolution of C_4 phosphoenolpyruvate carboxylase in the genus *Alternanthera*: gene families and the enzymatic characteristics of the C_4 isozyme and its orthologues in C_3 and C_3/C_4 *Alternantheras*. Planta **223:** 359-368
Grass Phylogeny Working G, II (2012) New grass phylogeny resolves deep evolutionary relationships and discovers C4 origins. The New phytologist **193:** 304-312
Gurel S, Gurel E, Kaur R, Wong J, Meng L, Tan H-Q, Lemaux PG (2008) Efficient, reproducible *Agrobacterium*-mediated transformation of *sorghum* using heat treatment of immature embryos. Plant Cell Reports **28:** 429-444
Haberlandt GFJ (1914) Physiological Plant Anatomy Macmillan and Co., Limited, London
Hall NP, Kendall AC, Lea PJ, Turner JC, Wallsgrove RM (1987) Characteristics of a photorespiratory mutant of barley (*Hordeum vulgare* L.) deficient in phosphogly collate phosphatase. Photosynthesis Research **11:** 89-96
Hamel N, Simon J-P (2000) Molecular forms and kinetic properties of phosphoenolpyruvate carboxylase from barnyard grass (*Echinochloa crus-galli* (L.) Beauv.: Poaceae). Canadian Journal of Botany **78:** 619-628
Hatch M, Osmond C, Slatyer R (1971) Photosynthesis and Photorespiration. Wiley-Interscience, New York
Hatch MD (1987) C_4 photosynthesis: a unique blend of modified biochemistry, anatomy and ultrastructure. Biochimica et Biophysica Acta **895:** 81-106
Hatch MD (1992) C_4 photosynthesis: An unlikely process full of surprises. Plant and Cell Physiology **33:** 333-342
Hatch MD, Kagawa T, Craig S (1975) Subdivision of C_4-pathway species based on differing C_4 acid decarboxylating systems and ultrastructural features. Functional Plant Biology **2:** 111
Hatch MD, Slack CR (1966) Photosynthesis by sugar-cane leaves. A new carboxylation reaction and the pathway of sugar formation. The Biochemical Journal **101:** 103-111
Hauser T, Bhat JY, Miličić G, Wendler P, Hartl FU, Bracher A, Hayer-Hartl M (2015) Structure and mechanism of the Rubisco-assembly chaperone Raf1. Nature Structural & Molecular Biology **22:** 720-728
Häusler RE, Kleines M, Uhrig H, Hirsch H-J, Smets H (1999) Overexpression of phosphoenolpyruvate carboxylase from *Corynebacterium glutamicum* lowers the CO_2 compensation point (Γ) and enhances dark and light respiration in transgenic potato. Journal of Experimental Botany **50:** 1231-1242
Häusler RE, Rademacher T, Li J, Lipka V, Fischer KL, Schubert S, Kreuzaler F, Hirsch HJ (2001) Single and double overexpression of C_4-cycle genes had differential effects on the pattern of endogenous enzymes, attenuation of photorespiration and on contents of UV protectants in transgenic potato and tobacco plants. Journal of Experimental Botany **52:** 1785-1803
He S, Chou H-T, Matthies D, Wunder T, Meyer MT, Atkinson N, Martinez-Sanchez A, Jeffrey PD, Port SA, Patena W, He G, Chen VK, Hughson FM, McCormick AJ, Mueller-Cajar O, Engel BD, Yu Z, Jonikas MC (2020) The structural basis of Rubisco phase separation in the pyrenoid. Nature Plants **6:** 1480-1490
Heimann L, Horst I, Perduns R, Dreesen B, Offermann S, Peterhansel C (2013) A common histone modification code on C_4 genes in maize and its conservation in *Sorghum* and *Setaria italica*. Plant Physiology **162:** 456-469

Hibberd JM, Covshoff S (2010) The regulation of gene expression required for C_4 photosynthesis. Annual Review of Plant Biology **61:** 181-207
Hoban DJ, Lyric RM (1975) Phosphoenolpyruvate carboxylase of *Thiobacillus thioparus*. I. General properties. Canadian Journal of Biochemistry **53:** 875-880
Holaday AS, Black CC (1981) Comparative characterization of phosphoenolpyruvate carboxylase in C_3, C_4, and C_3-C_4 intermediate *Panicum* species. Plant Physiology **67:** 330-334
Hopp TP, Prickett KS, Price VL, Libby RT, March CJ, Pat Cerretti D, Urdal DL, Conlon PJ (1988) A short polypeptide marker sequence useful for recombinant protein identification and purification. Biotechnology **6:** 1204-1210
Huber SC, Edwards GE (1975) Inhibition of phosphoenolpyruvate carboxylase from C_4 plants by malate and aspartate. Canadian Journal of Botany **53:** 1925-1933
Huber SC, Sugiyama T (1986) Changes in sensitivity to effectors of maize leaf phosphoenolypyruvate carboxylase during light/dark transitions. Plant Physiology **81:** 674-677
Huber SC, Sugiyama T, Akazawa T (1986) Light modulation of maize leaf phosphoenolpyruvate carboxylase. Plant Physiology **82:** 550-554
Hudspeth RL, Grula JW, Edwards GE, Ku MSB (1992) Expression of maize phosphoenolpyruvate carboxylase in transgenic tobacco: effects on biochemistry and physiology. Plant Physiology **98:** 458-464
Iglesias AA, Gonzalez DH, Andreo CS (1986) Purification and molecular and kinetic properties of phosphoenolpyruvate carboxylase from *Amaranthus viridis* L. leaves. Planta **168:** 239-244
IPCC (2012) Managing the risks of extreme events and disasters to advance climate change adaption: special report of the Intergovernmental Panel on Climate Change. *In* CB Field, V Barros, TF Stocker, D Qin, DJ Dokken, KL Ebi, MD Mastrandrea, KJ Mach, G-K Plattner, SK Allen, M Tignor, PM Midgley, eds. Cambridge University Press, Cambridge, UK and New York, NY, USA
IPCC (2021) Climate Change 2021: The Physical Science Basis. Contribution of Working Group I to the Sixth Assessment Report of the Intergovernmental Panel on Climate Change. *In* V Masson-Delmotte, P Zhai, A Pirani, SL Connors, C Péan, S Berger, N Caud, Y Chen, L Goldfarb, MI Gomis, M Huang, K Leitzell, E Lonnoy, JBR Matthews, TK Maycock, T Waterfield, O Yelekçi, R Yu, B Zhou, eds. Cambridge University Press, Cambridge, United Kingdom and New York, NY, USA
Izui K (1970) Kinetic studies on the allosteric nature of phosphoenolpyruvate carboxylase from *Escherichia coli*. Journal of Biochemistry **68:** 227-238
Izui K, Matsumura H, Furumoto T, Kai Y (2004) Phosphoenolpyruvate carboxylase: a new era of structural biology. Annual Review of Plant Biology **55:** 69-84
Izui K, Taguchi M, Morikawa M, Katsuki H (1981) Regulation of *Escherichia coli* phosphoenolpyruvate carboxylase by multiple effectors *in vivo*. II. Kinetic studies with a reaction system containing physiological concentrations of ligands. Journal of Biochemistry **90:** 1321-1331
Jacobs B, Engelmann S, Westhoff P, Gowik UDO (2008) Evolution of C_4 phosphoenolpyruvate carboxylase in *Flaveria*: determinants for high tolerance towards the inhibitor L-malate. Plant, Cell and Environment **31:** 793-803
Janc JW, O'Leary MH, Cleland WW (1992) A kinetic investigation of phosphoenolpyruvate carboxylase from *Zea mays*. Biochemistry **31:** 6421-6426
Jeanneau M, Vidal J, Gousset-Dupont A, Lebouteiller B, Hodges M, Gerentes D, Perez P (2002) Manipulating PEPC levels in plants. Journal of Experimental Botany **53:** 1837-1845
Jenkins CLD (1989) Effects of the phosphoenolpyruvate carboxylase inhibitor 3,3-dichloro-2-(dihydroxyphosphinoylmethyl)propenoate on photosynthesis: C_4 selectivity and studies on C_4 photosynthesis. Plant Physiology **89:** 1231-1237
Jenkins CLD, Furbank RT, Hatch MD (1989) Mechanism of C_4 photosynthesis: A model describing the inorganic carbon pool in bundle sheath cells. Plant Physiology **91:** 1372-1381

Jiao J-a, Chollet R (1990) Regulatory phosphorylation of serine-15 in maize phosphoenolpyruvate carboxylase by a C_4-leaf protein-serine kinase. Archives of Biochemistry and Biophysics **283:** 300-305
Jiao JA, Chollet R (1988) Light/dark regulation of maize leaf phosphoenolpyruvate carboxylase by *in vivo* phosphorylation. Archives of Biochemistry and Biophysics **261:** 409-417
Jolliffe PA, Tregunna EB (1968) Effect of temperature, CO_2 concentration, and light intensity on oxygen inhibition of photosynthesis in wheat leaves. Plant Physiology **43:** 902-906
Jolliffe PA, Tregunna EB (1973) Environmental regulation of the oxygen effect on apparent photosynthesis in wheat. Canadian Journal of Botany **51:** 841-853
Jones R, Buchanan IC, Wilkins MB, Fewson CA, A. D. B M (1981) Phosphoenolpyruvate carboxylase from the crassulacean plant *Bryophyllum fedtschenkoi* Hamet et Perrier: Activity changes and kinetic behaviour in crude extracts. Journal of Experimental Botany **32:** 427-441
Jones R, Wilkins MB, Coggins JR, Fewson CA, Malcolm AD (1978) Phosphoenolpyruvate carboxylase from the crassulacean plant *Bryophyllum fedtschenkoi* Hamet et Perrier. Purification, molecular and kinetic properties. Biochemical Journal **175:** 391-406
Jordan DB, Chollet R (1983) Inhibition of ribulose bisphosphate carboxylase by substrate ribulose 1,5-bisphosphate. The Journal of Biological Chemistry **258:** 13752-13758
Jordan DB, Ogren WL (1984) The CO_2/O_2 specificity of ribulose 1,5-bisphosphate carboxylase/oxygenase: Dependence on ribulosebisphosphate concentration, pH and temperature. Planta **161:** 308-313
Kai Y, Matsumura H, Inoue T, Terada K, Nagara Y, Yoshinaga T, Kihara A, Tsumura K, Izui K (1999) Three-dimensional structure of phosphoenolpyruvate carboxylase: A proposed mechanism for allosteric inhibition. Proceedings of the National Academy of Sciences **96:** 823-828
Kai Y, Matsumura H, Izui K (2003) Phosphoenolpyruvate carboxylase: three-dimensional structure and molecular mechanisms. Archives of Biochemistry and Biophysics **414:** 170-179
Kanai R, Edwards G (1999) The biochemistry of C_4 photosynthesis. *In* R Sage, R Monson, eds, C4 Plant Biology. Academic Press, New York, pp 49-87
Kandoi D, Mohanty S, Govindjee, Tripathy BC (2016) Towards efficient photosynthesis: overexpression of Zea mays phosphoenolpyruvate carboxylase in Arabidopsis thaliana. Photosynthesis research **130:** 47-72
Kano-Murakami Y, Suzuki I, Sugiyama T, Matsuoka M (1991) Sequence-specific interactions of a maize factor with a GC-rich repeat in the phosphoenolpyruvate carboxylase gene. Molecular and General Genetics **225:** 203-208
Karabourniotis G, Manetas Y, Gavalas NA (1983) Photoregulation of phosphoenolpyruvate carboxylase in *Salsola soda* L. and other C_4 [four-carbon pathway] plants. Plant Physiology **73:** 735-739
Kawamitsu Y, Susumu H, Waichi A, Tomoshiro T (1985) Leaf interveinal distances corresponding to anatomical types in grasses. Plant and Cell Physiology **26:** 589-593
Kebeish R, Niessen M, Oksaksin M, Blume C, Peterhaensel C (2012) Constitutive and dark-induced expression of *Solanum tuberosum* phosphoenolpyruvate carboxylase enhances stomatal opening and photosynthetic performance of *Arabidopsis thaliana*. Biotechnology and Bioengineering **109:** 536-544
Keys AJ (1986) Rubisco: Its role in photorespiration. Philosophical Transactions of the Royal Society of London. Series B, Biological sciences **313:** 325-336
Kogami H, Shono M, Koike T, Yanagisawa S, Izui K, Sentoku N, Tanifuji S, Uchimiya H, Toki S (1994) Molecular and physiological evaluation of transgenic tobacco plants expressing a maize phosphoenolpyruvate carboxylase gene under the control of the cauliflower mosaic virus 35S promoter. Transgenic Research **3:** 287-296
Korasick DA, Tanner JJ (2018) Determination of protein oligomeric structure from small-angle X-ray scattering. Protein Science **27:** 814-824
Kortschak HP, Hartt CE, Burr GO (1965) Carbon dioxide fixation in sugarcane leaves. Plant Physiology **40:** 209-213

Kromdijk J, Głowacka K, Leonelli L, Gabilly ST, Iwai M, Niyogi KK, Long SP (2016) Improving photosynthesis and crop productivity by accelerating recovery from photoprotection. Science **354:** 857-861
Ku MSB, Agarie S, Nomura M, Fukayama H, Tsuchida H, Ono K, Hirose S, Toki S, Miyao M, Matsuoka M (1999) High-level expression of maize phosphoenolpyruvate carboxylase in transgenic rice plants. Nature Biotechnology **17:** 76-80
Ku MSB, Schmitt MR, Edwards GE (1979) Quantitative determination of RuBP carboxylase-oxygenase protein in leaves of several C_3 and C_4 plants. Journal of Experimental Botany **30:** 89-98
Kubien DS, Brown CM, Kane HJ (2011) Quantifying the Amount and Activity of Rubisco in Leaves. *In* R Carpentier, ed, Photosynthesis Research Protocols. Humana Press, Totowa, NJ, pp 349-362
Kung S (1976) Tobacco fraction 1 protein: a unique genetic marker. Science **191:** 429-434
Laing WA, Ogren WL, Hageman RH (1974) Regulation of soybean net photosynthetic CO_2 fixation by the interaction of CO_2, O_2, and ribulose 1,5-diphosphate carboxylase. Plant Physiology **54:** 678-685
Langdale JA (2011) C_4 cycles: Past, present, and future research on C_4 photosynthesis. The Plant Cell **23:** 3879-3892
Lara MV, Chuong SDX, Akhani H, Andreo CS, Edwards GE (2006) Species having C_4 single-cell-type photosynthesis in the Chenopodiaceae family evolved a photosynthetic phosphoenolpyruvate carboxylase like that of Kranz-type C_4 species. Plant Physiology **142:** 673-684
Law RD, Plaxton WC (1995) Purification and characterization of a novel phosphoenolpyruvate carboxylase from banana fruit. Biochemical Journal **307 (Pt 3):** 807-816
Lebouteiller B, Gousset-Dupont A, Pierre J-N, Bleton J, Tchapla A, Maucourt M, Moing A, Rolin D, Vidal J (2007) Physiological impacts of modulating phosphoenolpyruvate carboxylase levels in leaves and seeds of *Arabidopsis thaliana*. Plant Science **172:** 265-272
Leegood RC, Caemmerer Sv (1988) The relationship between contents of photosynthetic metabolites and the rate of photosynthetic carbon assimilation in leaves of Amaranthus edulis L. Planta **174:** 253-262
Li P, Brutnell TP (2011) *Setaria viridis* and *Setaria italica*, model genetic systems for the Panicoid grasses. Journal of Experimental Botany **62:** 3031-3037
Life Technologies Corporation (2012) Ni-NTA Purification System. *In*,
Lin MT, Hanson MR, Cornell Univ INY (2018) Red algal Rubisco fails to accumulate in transplastomic tobacco expressing *Griffithsia monilis* RbcL and RbcS genes. Plant Direct **2:** e00045-n/a
Link G, Coen DM, Bogorad L (1978) Differential expression of the gene for the large subunit of ribulose bisphosphate carboxylase in maize leaf cell types. Cell **15:** 725-731
Lloyd J, Farquhar GD (1994) ^{13}C discrimination during CO_2 assimilation by the terrestrial biosphere. Oecologia **99:** 201-215
Long SP (1999) Environmental responses. *In* RF Sage, RK Monson, eds, C_4 Plant Biology. Academic Press, San Diego, pp 215-249
Long SP (2014) We need winners in the race to increase photosynthesis in rice, whether from conventional breeding, biotechnology or both. Plant, Cell & Environment **37:** 19-21
Long Stephen P, Marshall-Colon A, Zhu X-G (2015) Meeting the global food demand of the future by engineering crop photosynthesis and yield potential. Cell **161:** 56-66
Long SP, Zhu XG, Naidu SL, Ort DR (2006) Can improvement in photosynthesis increase crop yields? Plant, Cell & Environment **29:** 315-330
Lorimer GH, Badger MR, Andrews TJ (1976) The activation of ribulose-1,5-bisphosphate carboxylase by carbon dioxide and magnesium ions. Equilibria, kinetics, a suggested mechanism, and physiological implications. Biochemistry **15:** 529-536
Ludwig M (2016) The roles of organic acids in C_4 photosynthesis. Frontiers in Plant Science **7:** 647-647
Mann CC (1999) Genetic engineers aim to soup up crop photosynthesis. Science **283:** 314-316

Martins PK, Nakayama TJ, Ribeiro AP, Cunha BADBd, Nepomuceno AL, Harmon FG, Kobayashi AK, Molinari HBC (2015) *Setaria viridis* floral-dip: A simple and rapid *Agrobacterium*-mediated transformation method. Biotechnology Reports **6:** 61-63

Martins PK, Ribeiro AP, Cunha BADBd, Kobayashi AK, Molinari HBC (2015) A simple and highly efficient *Agrobacterium*-mediated transformation protocol for *Setaria viridis*. Biotechnology Reports **6:** 41-44

Maruyama H, Easterday RL, Chang HC, Lane MD (1966) The enzymatic carboxylation of phosphoenolpyruvate. I. Purification and properties of phosphoenolpyruvate carboxylase. The Journal of Biological Chemistry **241:** 2405-2412

Matsumura H, Terada M, Shirakata S, Inoue T, Yoshinaga T, Izui K, Kai Y (1999) Plausible phosphoenolpyruvate binding site revealed by 2.6 Å structure of Mn^{2+}-bound phosphoenolpyruvate carboxylase from *Escherichia coli*. FEBS Letters **458:** 93-96

Matsumura H, Xie Y, Shirakata S, Inoue T, Yoshinaga T, Ueno Y, Izui K, Kai Y (2002) Crystal structures of C_4 form maize and quaternary complex of *E. coli* phosphoenolpyruvate carboxylases. Structure **10:** 1721-1730

McDaniel HG, Siu PM (1972) Purification and characterization of phosphoenolpyruvate carboxylase from *Plasmodium berghei*. Journal of Bacteriology **109:** 385-390

McNaughton GA, Fewson CA, Wilkins MB, Nimmo HG (1989) Purification, oligomerization state and malate sensitivity of maize leaf phosphoenolpyruvate carboxylase. Biochemical Journal **261:** 349-355

McNaughton GAL, Mackintosh C, Fewson CA, Wilkins MB, Nimmo HG (1991) Illumination increases the phosphorylation state of maize leaf phosphoenolpyruvate carboxylase by causing an increase in the activity of a protein kinase. Biochimica et Biophysica Acta **1093:** 189-195

Meyer CR, Willeford KO, Wedding RT (1991) Regulation of phosphoenolpyruvate carboxylase from *Crassula argentea*: effect of incubation with ligands and dilution on oligomeric state, activity, and allosteric properties. Archives of Biochemistry and Biophysics **288:** 343-349

Miziorko HM, Nowak T, Mildvan AS (1974) Spinach leaf phosphoenolpyruvate carboxylase: Purification, properties, and kinetic studies. Archives of Biochemistry and Biophysics **163:** 378-389

Monteith JL, Moss CJ (1977) Climate and the efficiency of crop production in Britain [and discussion]. Philosophical Transactions of the Royal Society of London. Series B, Biological Sciences **281:** 277-294

Mueller-Cajar O, Stotz M, Wendler P, Ulrich Hartl F, Bracher A, Hayer-Hartl M (2011) Structure and function of the AAA+ protein CbbX, a red-type Rubisco activase. Nature **479:** 194-199

Mukerji SK (1977) Corn leaf phosphoenolpyruvate carboxylases: Purification and properties of two isoenzymes. Archives of Biochemistry and Biophysics **182:** 343-351

Mukerji SK, Ting IP (1971) Phosphoenolpyruvate carboxylase isoenzymes: Separation and properties of three forms from cotton leaf tissue. Archives of Biochemistry and Biophysics **143:** 297-317

Nakamoto H, Ku MSB, Edwards GE (1983) Photosynthetic characteristics of C_3–C_4 intermediate *Flaveria* species II. Kinetic properties of phosphoenolpyruvate carboxylase from C_3, C_4 and C_3–C_4 intermediate species. Plant and Cell Physiology **24:** 1387-1393

Nakamura Y, Gojobori T, Ikemura T (2000) Codon usage tabulated from international DNA sequence databases: status for the year 2000. Nucleic Acids Research **28:** 292-292

Nguyen DQ, Van Eck J, Eamens AL, Grof CPL (2020) Robust and reproducible *Agrobacterium*-mediated transformation system of the C_4 genetic model species *Setaria viridis*. Frontiers in Plant Science **11**

Nimmo GA, McNaughton GAL, Fewson CA, Wilkins MB, Nimmo HG (1987) Changes in the kinetic properties and phosphorylation state of phosphoenolpyruvate carboxylase in *Zea mays* leaves in reponse to light and dark. FEBS Letters **213:** 18-22

Nimmo GA, Nimmo HG, Hamilton ID, Fewson CA, Wilkins MB (1986) Purification of the phosphorylated night form and dephosphorylated day form of phosphoenolpyruvate carboxylase from *Bryophyllum fedtschenkoi*. Biochemical Journal **239:** 213-220

Nishikido T, Takanashi H (1973) Glycine activation of PEP carboxylase from monocotyledoneous C_4 plants. Biochemical and Biophysical Research Communications **53:** 126-133
Nott DL, Osmond CB (1982) Purification and properties of phosphopyruvate carboxylase from plants with crassulacean acid metabolism. Functional Plant Biology **9:** 409-422
Novagen Ni-NTA His•Bind Resins. *In*,
O'Leary B, Park J, Plaxton WC (2011) The remarkable diversity of plant PEPC (phosphoenolpyruvate carboxylase): recent insights into the physiological functions and post-translational controls of non-photosynthetic PEPCs. The Biochemical Journal **436:** 15-34
O'Leary MH (1982) Phosphoenolpyruvate carboxylase: An enzymologist's view. Annual Review of Plant Physiology **33:** 297-315
O'Leary MH, Rife JE, Slater JD (1981) Kinetic and isotope effect studies of maize phosphoenolpyruvate carboxylase. Biochemistry **20:** 7308-7314
Offermann S, Danker T, Dreymüller D, Kalamajka R, Töpsch S, Weyand K, Peterhänsel C (2006) Illumination is necessary and sufficient to induce histone acetylation independent of transcriptional activity at the C_4-specific phosphoenolpyruvate carboxylase promoter in maize. Plant Physiology **141:** 1078-1088
Offermann S, Dreesen B, Horst I, Danker T, Jaskiewicz M, Peterhansel C (2008) Developmental and environmental signals induce distinct histone acetylation profiles on distal and proximal promoter elements of the C_4-pepc gene in maize. Genetics **179:** 1891-1901
Outlaw WH, Du Z, Xia Meng F, Aghoram K, Riddle KA, Chollet R (2002) Requirements for activation of the signal-transduction network that leads to regulatory phosphorylation of leaf guard-cell phosphoenolpyruvate carboxylase during fusicoccin-stimulated stomatal opening. Archives of Biochemistry and Biophysics **407:** 63-71
Owttrim GW, Colman B (1986) Purification and characterization of phosphoenolpyruvate carboxylase from a cyanobacterium. Journal of Bacteriology **168:** 207-212
Park S, Lee W, Kim H, Pack SP, Lee J (2015) Characterization of phosphoenolpyruvate carboxylase from *Oceanimonas smirnovii* in *Escherichia coli*. Applied Biochemistry and Biotechnology **177:** 217-225
Parry MAJ, Andralojc PJ, Khan S, Lea PJ, Keys AJ (2002) Rubisco activity: Effects of drought stress. Annals of Botany **89:** 833-839
Parry MAJ, Madgwick PJ, Carvalho JFC, Andralojc PJ (2007) Prospects for increasing photosynthesis by overcoming the limitations of Rubisco. The Journal of Agricultural Science **145:** 31
Parvathi K, Bhagwat AS, Ueno Y, Izui K, Raghavendra AS (2000) Illumination increases the affinity of phosphoenolpyruvate carboxylase to bicarbonate in leaves of a C_4 plant, *Amaranthus hypochondriacus*. Plant and Cell Physiology **41:** 905-910
Patel HM, Kraszewski JL, Mukhopadhyay B (2004) The phosphoenolpyruvate carboxylase from *Methanothermobacter thermautotrophicus* has a novel structure. Journal of Bacteriology **186:** 5129-5137
Paulus JK, Niehus C, Groth G (2013) Evolution of C_4 phosphoenolpyruvate carboxylase: Enhanced feedback inhibitor tolerance is determined by a single residue. Molecular Plant **6:** 1996-1999
Paulus JK, Schlieper D, Groth G (2013) Greater efficiency of photosynthetic carbon fixation due to single amino-acid substitution. Nature Communications **4:** 1518-1518
Peterson-Forbrook DS, Hilton MT, Tichacek L, Henderson JN, Bui HQ, Wachter RM, Arizona State Univ TAZ (2017) Nucleotide dependence of subunit rearrangements in short-form Rubisco activase from spinach. Biochemistry **56:** 4906-4921
Pierre J-N, Prieto J-L, Gadal P, Vidal J (2004) *In situ* C_4 phosphoenolpyruvate carboxylase activity and kinetic properties in isolated *Digitaria sanguinalis* mesophyll cells. Photosynthesis Research **79:** 349-355
Pinto H, Sharwood RE, Tissue DT, Ghannoum O (2014) Photosynthesis of C_3, C_3-C_4, and C_4 grasses at glacial CO_2. Journal of Experimental Botany **65:** 3669-3681
Podesta FE, Andreo CS (1989) Maize leaf phosphoenolpyruvate carboxylase, oligomeric state and activity in the presence of glycerol. Plant Physiology **90:** 427-433

Portis AR, Jr., Salvucci ME, Ogren WL (1986) Activation of ribulosebisphosphate carboxylase/oxygenase at physiological CO_2 and ribulosebisphosphate concentrations by rubisco activase. Plant Physiology **82:** 967-971
QIAGEN (2011) Ni-NTA superflow cartridge handbook. *In*,
Qin N, Xu W, Hu L, Li Y, Wang H, Qi X, Fang Y, Hua X (2016) Drought tolerance and proteomics studies of transgenic wheat containing the maize C_4 phosphoenolpyruvate carboxylase (PEPC) gene. Protoplasma **253:** 1503-1512
Rademacher T, Häusler RE, Hirsch HJ, Zhang L, Lipka V, Weier D, Kreuzaler F, Peterhänsel C (2002) An engineered phosphoenolpyruvate carboxylase redirects carbon and nitrogen flow in transgenic potato plants. The Plant Journal **32:** 25-39
Raghavendra AS, Das VSR (1975) Malonate-inhibition of allosteric phosphoenolpyruvate carboxylase from *Setaria italica*. Biochemical and Biophysical Research Communications **66:** 160-165
Raghavendra AS, Vallejos RH (1980) Regulation of phosphoenolpyruvate carboxylase in C_4 plants: Inhibition by pyrophosphate of the enzyme from *Amaranthus viridis*. Archives of Biochemistry and Biophysics **201:** 356-358
Raines CA (2011) Increasing photosynthetic carbon assimilation in C_3 plants to improve crop yield: Current and future strategies. Plant Physiology **155:** 36-42
Ray DK, Mueller ND, West PC, Foley JA (2013) Yield trends are insufficient to double global crop production by 2050. Plos One **8**
Reeves G, Grangé-Guermente MJ, Hibberd JM (2017) Regulatory gateways for cell-specific gene expression in C_4 leaves with Kranz anatomy. Journal of Experimental Botany **68:** 107-116
Rivoal J, Dunford R, Plaxton WC, Turpin DH (1996) Purification and properties of four phosphoenolpyruvate carboxylase isoforms from the green alga *Selenastrum minutum*: evidence that association of the 102-kDa catalytic subunit with unrelated polypeptides may modify the physical and kinetic properties of the enzyme. Archives of Biochemistry and Biophysics **332:** 47-57
Rivoal J, Plaxton WC, Turpin DH (1998) Purification and characterization of high- and low-molecular-mass isoforms of phosphoenolpyruvate carboxylase from *Chlamydomonas reinhardtii*. Kinetic, structural and immunological evidence that the green algal enzyme is distinct from the prokaryotic and higher plant enzymes. Biochemical Journal **331 (Pt 1):** 201-209
Ruiz-Ballesta I, Feria A-B, Ni H, She Y-M, Plaxton WC, Echevarría C (2014) *In vivo* monoubiquitination of anaplerotic phosphoenolpyruvate carboxylase occurs at Lys624 in germinating *Sorghum* seeds. Journal of Experimental Botany **65:** 443-451
Sage R, Li M, Monson R (1999) The Taxonomic Distribution of C_4 Photosynthesis. *In* R Sage, R Monson, eds, C_4 Plant Biology. Academic Press, San Diego, California, pp 551-584
Sage RF (2004) The evolution of C_4 photosynthesis. The New Phytologist **161:** 341-370
Sage RF (2016) A portrait of the C_4 photosynthetic family on the 50th anniversary of its discovery: species number, evolutionary lineages, and Hall of Fame. Journal of Experimental Botany **67:** 4039-4056
Sage RF, Pearcy RW (1987) The nitrogen use efficiency of C_3 and C_4 plants: I. Leaf nitrogen, growth, and biomass partitioning in in *Chenopodium album* (L.) and *Amaranthus retroflexus* (L.). Plant Physiology **84:** 954-958
Sage RF, Pearcy RW (1987) The nitrogen use efficiency of C_3 and C_4 plants: II. Leaf nitrogen effects on the gas exchange characteristics of *Chenopodium album* (L.) and *Amaranthus retroflexus* (L.). Plant Physiology **84:** 959-963
Sage RF, Sage RF (1999) C_4 Plant Biology. Elsevier Science & Technology, San Diego
Sage RF, Sage TL, Kocacinar F (2012) Photorespiration and the evolution of C_4 photosynthesis. Annual Review of Plant Biology **63:** 19
Sako Y, Takai K, Nishizaka T, Ishida Y (1997) Biochemical relationship of phosphoenolpyruvate carboxylases (PEPCs) from thermophilic archaea. FEMS Microbiology Letters **153:** 159-165
Sako Y, Takai K, Uchida A, Ishida Y (1996) Purification and characterization of phosphoenolpyruvate carboxylase from the hyperthermophilic archaeon *Methanothermus sociabilis*. FEBS Letters **392:** 148-152

Salesse-Smith CE, Sharwood RE, Busch FA, Kromdijk J, Bardal V, Stern DB (2018) Overexpression of Rubisco subunits with RAF1 increases Rubisco content in maize. Nature Plants **4:** 802-810

Samaras Y, Manetas Y, Gavalas NA (1988) Effects of temperature and photosynthetic inhibitors on light activation of C_4-phosphoenolpyruvate carboxylase. Photosynthesis Research **16:** 233-242

Sambrook J, Maniatis T, Fritsch EF (1989) Molecular cloning: a laboratory manual, Ed 2nd. Cold Spring Harbor Laboratory, Cold Spring Harbor, N.Y

Savir Y, Noor E, Milo R, Tlusty T (2010) Cross-species analysis traces adaptation of Rubisco toward optimality in a low-dimensional landscape. Proceedings of the National Academy of Sciences **107:** 3475-3480

Serban AJ, Breen IL, Bui HQ, Levitus M, Wachter RM, Arizona State Univ TAZ (2018) Assembly–disassembly is coupled to the ATPase cycle of tobacco Rubisco activase. The Journal of Biological Chemistry **293:** 19451-19465

Shane MW, Fedosejevs ET, Plaxton WC (2013) Reciprocal control of anaplerotic phosphoenolpyruvate carboxylase by *in vivo* monoubiquitination and phosphorylation in developing proteoid roots of phosphate-deficient harsh hakea. Plant Physiology **161:** 1634-1644

Sharkey TD (1988) Estimating the rate of photorespiration in leaves. Physiologia Plantarum **73:** 147-152

Sharwood RE (2017) Engineering chloroplasts to improve Rubisco catalysis: prospects for translating improvements into food and fiber crops. New Phytologist **213:** 494-510

Sharwood RE, Ghannoum O, Kapralov MV, Gunn LH, Whitney SM (2016) Temperature responses of Rubisco from Paniceae grasses provide opportunities for improving C_3 photosynthesis. Nature Plants **2:** 16186

Sharwood RE, Quick WP, Sargent D, Estavillo GM, Silva-Perez V, Furbank RT (2022) Mining for allelic gold: finding genetic variation in photosynthetic traits in crops and wild relatives. Journal of Experimental Botany **73:** 3085-3108

Sharwood RE, Sonawane BV, Ghannoum O, Whitney SM (2016) Improved analysis of C_4 and C_3 photosynthesis via refined *in vitro* assays of their carbon fixation biochemistry. Journal of Experimental Botany **67:** 3137-3148

Shen WJ, Chen GX, Xu JG, Jiang Y, Liu L, Gao ZP, Ma J, Chen X, Chen TH, Lv CF (2015) Overexpression of maize phosphoenolpyruvate carboxylase improves drought tolerance in rice by stabilization the function and structure of thylakoid membrane. Photosynthetica **53:** 436-446

Shylajanaciyar M, Dineshbabu G, Rajalakshmi R, Subramanian G, Prabaharan D, Uma L (2015) Analysis and elucidation of phosphoenolpyruvate carboxylase in cyanobacteria. The Protein Journal **34:** 73-81

South PF, Cavanagh AP, Lopez-Calcagno PE, Raines CA, Ort DR (2018) Optimizing photorespiration for improved crop productivity. Journal of Integrative Plant Biology **60:** 1217-1230

Stiborová M, Leblová S (1986) Stucture of phosphoenolpyruvate carboxylase from maize leaves. FEBS Letters **205:** 32-34

Suzuki I, Werkman CH (1957) Phosphoenolpyruvate carboxylase in extracts of *Thiobacillus thiooxidans*, a chemoautotrophic bacterium. Archives of Biochemistry and Biophysics **72:** 514-515

Svensson P, Bläsing OE, Westhoff P (1997) Evolution of the enzymatic characteristics of C_4 phosphoenolpyruvate carboxylase: a comparison of the orthologous PPCA phosphoenolpyruvate carboxylases of *Flaveria trinervia* (C_4) and *Flaveria pringlei* (C_3). European Journal of Biochemistry **246:** 452-460

Svensson P, Bläsing OE, Westhoff P (2003) Evolution of C4 phosphoenolpyruvate carboxylase. Archives of Biochemistry and Biophysics **414:** 180-188

Takahashi-Terada A, Kotera M, Ohshima K, Furumoto T, Matsumura H, Kai Y, Izui K (2005) Maize phosphoenolpyruvate carboxylase. Mutations at the putative binding site for glucose 6-phosphate caused desensitization and abolished responsiveness to regulatory phosphorylation. The Journal of Biological Chemistry **280:** 11798-11806

Takai K, Sako Y, Uchida A, Ishida Y (1997) Extremely thermostable phosphoenolpyruvate carboxylase from an extreme thermophile, *Rhodothermus obamensis*. Journal of Biochemistry **122:** 32-40
Taniguchi M, Izawa K, Ku MSB, Lin J-H, Saito H, Ishida Y, Ohta S, Komari T, Matsuoka M, Sugiyama T (2000) Binding of cell type-specific nuclear proteins to the 5′-flanking region of maize C_4 phosphoenolpyruvate carboxylase gene confers its differential transcription in mesophyll cells. Plant Molecular Biology **44:** 543-557
Taniguchi Y, Ohkawa H, Masumoto C, Fukuda T, Tamai T, Lee K, Sudoh S, Tsuchida H, Sasaki H, Fukayama H, Miyao M (2008) Overproduction of C_4 photosynthetic enzymes in transgenic rice plants: an approach to introduce the C_4-like photosynthetic pathway into rice. Journal of Experimental Botany **59:** 1799-1809
Tashian RE (1989) The carbonic anhydrases: Widening perspectives on their evolution, expression and function. BioEssays **10:** 186-192
Tashima M, Yabiku T, Ueno O (2021) *Coleataenia prionitis*, a C_4-like species in the Poaceae. Photosynthesis Research **147:** 211-227
Taub DR (2000) Climate and the U.S. distribution of C_4 grass subfamilies and decarboxylation variants of C_4 photosynthesis. American Journal of Botany **87:** 1211-1215
Terada K, Izui K (1991) Site-directed mutagenesis of the conserved histidine residue of phosphoenolpyruvate carboxylase. His138 is essential for the second partial reaction. European Journal of Biochemistry/FEBS **202:** 797
Terada K, Murata T, Izui K (1991) Site-directed mutagenesis of phosphoenolpyruvate carboxylase from *E. coli*: the role of His579 in the catalytic and regulatory functions. Journal of Biochemistry **109:** 49
Teraoka H, Izui K, Katsuki H (1972) Phosphoenolpyruvate carboxylase of *Escherichia coli*: Alteration of allosteric properties by photooxidation. Archives of Biochemistry and Biophysics **152:** 821-827
Tilman D, Balzer C, Hill J, Befort BL (2011) Global food demand and the sustainable intensification of agriculture. Proceedings of the National Academy of Sciences of the United States of America **108:** 20260-20264
Ting IP, Osmond CB (1973a) Activation of plant p-enolpyruvate carboxylases by glucose-6-phosphate: A particular role in crassulacean acid metabolism. Plant Science Letters **1:** 123-128
Ting IP, Osmond CB (1973b) Multiple forms of plant phosphoenolpyruvate carboxylase associated with different metabolic pathways. Plant Physiology **51:** 448-453
Ting IP, Osmond CB (1973c) Photosynthetic phosphoenolpyruvate carboxylases: characteristics of alloenzymes from leaves of C_3 and C_4 plants. Plant Physiology **51:** 439-447
Tolbert NE (1971) Microbodies: peroxisomes and glyoxysomes. Annual Review of Plant Physiology **22:** 45-74
Tovar-Méndez A, Mújica-Jiménez C, Muñoz-Clares RA (2000) Physiological implications of the kinetics of maize leaf phosphoenolpyruvate carboxylase. Plant Physiology **123:** 149-160
Tsai Y-CC, Lapina MC, Bhushan S, Mueller-Cajar O (2015) Identification and characterization of multiple rubisco activases in chemoautotrophic bacteria. Nature Communications **6:** 8883-8883
Uedan K, Sugiyama T (1976) Purification and Characterization of Phosphoenolpyruvate Carboxylase from Maize Leaves. Plant physiology (Bethesda) **57:** 906-910
Uhrig RG, She Y-M, Leach CA, Plaxton WC (2008) Regulatory monoubiquitination of phosphoenolpyruvate carboxylase in germinating castor oil seeds. The Journal of Biological Chemistry **283:** 29650-29657
United Nations DoEaSA, Population Division (2019) World Population Prospects 2019: Highlights. *In*,
Van Eck J (2018) The status of *Setaria viridis* transformation: *Agrobacterium*-mediated to floral dip. Frontiers in Plant Science **9:** 652-652
Van Eck J, Swartwood K (2015) *Setaria viridis*. Methods Mol Biol **1223:** 57-67
Van Eck J, Swartwood K, Pidgeon K, Maxson-Stein K (2017) *Agrobacterium tumefaciens*-mediated transformation of *Setaria viridis*. *In* A Doust, X Diao, eds, Genetics and

Genomics of Setaria. Plant Genetics and Genomics: Crops and Models, Vol 19. Springer, Cham
Vidal J, Chollet R (1997) Regulatory phosphorylation of C_4 PEP carboxylase. Trends in Plant Science **2:** 230-237
von Caemmerer S (2000) Biochemical models of leaf photosynthesis. CSIRO Publishing, Collingwood, Australia
von Caemmerer S, Edwards GE, Koteyeva N, Cousins AB (2014) Single cell C_4 photosynthesis in aquatic and terrestrial plants: A gas exchange perspective. Aquatic Botany **118:** 71-80
von Caemmerer S, Evans JR (2010) Enhancing C_3 photosynthesis. Plant Physiology **154:** 589-592
von Caemmerer S, Furbank RT (2016) Strategies for improving C_4 photosynthesis. Current Opinion in Plant Biology **31:** 125-134
von Caemmerer S, Quick WP, Furbank RT (2012) The development of C_4 rice: current progress and future challenges. Science **336:** 1671-1672
Wagner R, Gonzalez DH, Podesta FE, Andreo CS (1987) Changes in the quaternary structure of phosphoenolpyruvate carboxylase induced by ionic strength affect its catalytic activity. European Journal of Biochemistry **164:** 661-666
Walker BJ, VanLoocke A, Bernacchi CJ, Ort DR (2016) The costs of photorespiration to food production now and in the future. Annual Review of Plant Biology **67:** 107-129
Walker GH, Ku MSB, Edwards GE (1986) Catalytic activity of maize leaf phosphoenolpyruvate carboxylase in relation to oligomerization. Plant Physiology **80:** 848-855
Wang H, Yan X, Aigner H, Bracher A, Nguyen ND, Hee WY, Long BM, Price GD, Hartl FU, Hayer-Hartl M (2019) Rubisco condensate formation by CcmM in β-carboxysome biogenesis. Nature **566:** 131-135
Wang L, Czedik-Eysenberg A, Mertz RA, Si Y, Tohge T, Nunes-Nesi A, Arrivault S, Dedow LK, Bryant DW, Zhou W, Xu J, Weissmann S, Studer A, Li P, Zhang C, LaRue T, Shao Y, Ding Z, Sun Q, Patel RV, Turgeon R, Zhu X, Provart NJ, Mockler TC, Fernie AR, Stitt M, Liu P, Brutnell TP (2014) Comparative analyses of C_4 and C_3 photosynthesis in developing leaves of maize and rice. Nature Biotechnology **32:** 1158-1165
Wang Q, Serban AJ, Wachter RM, Moerner WE (2018) Single-molecule diffusometry reveals the nucleotide-dependent oligomerization pathways of *Nicotiana tabacum* Rubisco activase. The Journal of Chemical Physics **148:** 123319-123319
Wang Y, Bräutigam A, Weber APM, Zhu X-G, X Energy LLCRMD (2014) Three distinct biochemical subtypes of C_4 photosynthesis? A modelling analysis. Journal of Experimental Botany **65:** 3567-3578
Wedding RT, O'Brien CE, Kline K (1994) Oligomerization and the affinity of maize phosphoenolpyruvate carboxylase for its substrate. Plant Physiology **104:** 613-616
Weigel D, Glazebrook J (2006) Transformation of *Agrobacterium* using the freeze-thaw method. Cold Spring Harbor Protocols **2006:** pdb.prot4666-pdb.prot4666
Weiss T, Wang C, Kang X, Zhao H, Elena Gamo M, Starker CG, Crisp PA, Zhou P, Springer NM, Voytas DF, Zhang F, Donald Danforth Plant Science Center SLMO (2020) Optimization of multiplexed CRISPR/Cas9 system for highly efficient genome editing in *Setaria viridis*. The Plant Journal **104:** 828-838
Westhoff P, Gowik UDO (2004) Evolution of C_4 phosphoenolpyruvate carboxylase. Genes and proteins: a case study with the genus *Flaveria*. Annals of Botany **93:** 13-23
Westhoff P, Svensson P, Ernst K, Bläsing O, Burscheidt J, Stockhaus J (1997) Molecular evolution of C_4 phosphoenolpyruvate carboxylase in the genus *Flaveria*. Functional Plant Biology **24:** 429
Whitney SM, Baldet P, Hudson GS, Andrews TJ (2001) Form I Rubiscos from non-green algae are expressed abundantly but not assembled in tobacco chloroplasts. The Plant Journal **26:** 535-547
Whitney SM, Sharwood RE (2008) Construction of a tobacco master line to improve Rubisco engineering in chloroplasts. Journal of Experimental Botany **59:** 1909-1921
Willeford KO, Wedding RT (1992) Oligomerization and regulation of higher plant phosphoenolpyruvate carboxylase. Plant Physiology **99:** 755-758

Willeford KO, Wu MX, Meyer CR, Wedding RT (1990) The role of oligomerization in regulation of maize phosphoenolpyruvate carboxylase activity. Influence of Mg-PEP and malate on the oligomeric equilibrium of PEP carboxylase. Biochemical and Biophysical Research Communications **168:** 778-785

Windhövel A, Hein I, Dabrowa R, Stockhaus J (2001) Characterization of a novel class of plant homeodomain proteins that bind to the C_4 phosphoenolpyruvate carboxylase gene of *Flaveria trinervia*. Plant Molecular Biology **45:** 201-214

Wingler A, Lea PJ, Quick WP, Leegood RC (2000) Photorespiration: metabolic pathways and their role in stress protection. Philosophical Transactions of the Royal Society of London. Series B: Biological Sciences **355:** 1517-1529

Wohl RC, Markus G (1972) Phosphoenolpyruvate carboxylase of *Escherichia coli*. The Journal of Biological Chemistry **247:** 5785-5792

Wu M-X, Wedding RT (1985) Regulation of phosphoenolpyruvate carboxylase from *Crassula* by interconversion of oligomeric forms. Archives of Biochemistry and Biophysics **240:** 655-662

Wu MX, Meyer CR, Willeford KO, Weeding RT (1990) Regulation of the aggregation state of maize phosphoenolpyruvate carboxylase: evidence from dynamic light-scattering measurements. Archives of Biochemistry and Biophysics **281:** 324-329

Wu MX, Wedding RT (1985) Diurnal regulation of phosphoenolpyruvate carboxylase from *Crassula*. Plant Physiology **77:** 667-675

Wu MX, Wedding RT (1987) Regulation of phosphoenolpyruvate carboxylase from *Crassula argentea*. Further evidence on the dimer-tetramer interconversion. Plant Physiology **84:** 1080-1083

Wunder T, Cheng SLH, Lai S-K, Li H-Y, Mueller-Cajar O (2018) The phase separation underlying the pyrenoid-based microalgal Rubisco supercharger. Nature Communications **9:** 5076-5010

Xia L, Cao W (2013) Physiological and metabolic enzymes activity changes in transgenic rice plants with increased phosphoenolpyruvate carboxylase activity during the flowering stage. Acta Physiologiae Plantarum **35:** 1503-1512

Yanagisawa S (2000) Dof1 and Dof2 transcription factors are associated with expression of multiple genes involved in carbon metabolism in maize. The Plant Journal **21:** 281-288

Yanagisawa S, Sheen J (1998) Involvement of maize Dof zinc finger proteins in tissue-specific and light-regulated gene expression. The Plant Cell **10:** 75-89

Yang J, Yan R, Roy A, Xu D, Poisson J, Zhang Y (2015) The I-TASSER Suite: protein structure and function prediction. Nature Methods **12:** 7-8

Yang J, Zhang Y (2015) I-TASSER server: new development for protein structure and function predictions. Nucleic Acids Research **43:** W174-W181

Yano M, Terada K, Umiji K, Izui K (1995) Catalytic role of an arginine residue in the highly conserved and unique sequence of phosphoenolpyruvate carboxylase. Journal of Biochemistry **117:** 1196

Yu L, Sivitz IW (2020) Oxaloacetate mediates mitochondrial metabolism and function. Current Metabolomics and Systems Biology **7:** 11-23

Zang K, Wang H, Hartl FU, Hayer-Hartl M (2021) Scaffolding protein CcmM directs multiprotein phase separation in β-carboxysome biogenesis. Nature Structural & Molecular Biology **28:** 909-922

Zelitch I (1973) Plant productivity and the control of photorespiration. Proceedings of the National Academy of Sciences **70:** 579-584

Zhang H, Xu W, Wang H, Hu L, Li Y, Qi X, Zhang L, Li C, Hua X (2014) Pyramiding expression of maize genes encoding phosphoenolpyruvate carboxylase (PEPC) and pyruvate orthophosphate dikinase (PPDK) synergistically improve the photosynthetic characteristics of transgenic wheat. Protoplasma **251:** 1163-1173

Zhang X-Q, Li B, Chollet R (1995) *In vivo* regulatory phosphorylation of soybean nodule phosphoenolpyruvate carboxylase. Plant Physiology **108:** 1561-1568

Zhou Y, Whitney S (2019) Directed evolution of an improved Rubisco; *in vitro* analyses to decipher fact from fiction. International Journal of Molecular Sciences **20:** 5019

Zhu X-G, Long SP, Ort DR (2010) Improving photosynthetic efficiency for greater yield. Annual Review of Plant Biology **61:** 235-261

Ziska LH, Bunce JA, Shimono H, Gealy DR, Baker JT, Paul CDN, Reynolds MP, Krishna SVJ, Zhu C, Howden M, Wilson LT (2012) Food security and climate change: on the potential to adapt global crop production by active selection to rising atmospheric carbon dioxide. Proceedings: Biological Sciences **279:** 4097-4105

Appendices

Appendix 1: Meta-analysis of phosphoenolpyruvate carboxylase carboxylation kinetics data

Phosphoenolpyruvate carboxylase (plant, bacterial and archaeal species) carboxylation kinetics data from published research papers. Available information regarding K_mPEP, K_mMg^{2+}, $K_mHCO_3^-$, V_{max}, k_{cat}, and pH and temperature optimums has been included. C_4 plant species subtype information is indicated (Sage and Sage, 1999). Archaeal species are indicated by grey shading, bacterial species are indicated by purple shading, CAM species are indicated by yellow shading, C_3 species are indicated by green shading, C_3-C_4 intermediate and C_4-like species are indicated by white shading, single-celled C_4 species are indicated by brown shading, NAD-ME species are indicated by orange shading, NADP-ME species are indicated by blue shading, and PEPCK species are indicated by pink shading.

		PEPC carboxylation kinetics									
		K_mPEP (mM)			K_m Mg^{2+}	$K_m$$HCO_3^-$		V_{max} or k_{cat}		Notes	Reference
	Species	+ G6P or other activator where mentioned	- G6P	+ inhibitor		+ G6P	- G6P	+ G6P or other activator where mentioned	- G6P		
Archaea	*Clostridium perfringens*		0.06 (pH 7.2; 37 °C)						V_{max}: 40 µmol min^{-1} mg^{-1} (37 °C)		(Dharmarajan et al., 2011)
	Methanothermobacter thermautotrophicus		0.46 (pH 8.0, 50 °C)				1.8 mM (pH 8.0, 50 °C)			Optimum temperature: 62 °C Optimum pH: 6.8	(Patel et al., 2004)
	Methanothermus sociabilis		1.3 (pH 8.5, 85 °C)							Optimum temperature: 85 °C Optimum pH: 8.5 Retained 80% of activity after incubation for 2 hours at 80 °C; no loss of activity after incubation for 2 hours at 75 °C. Known activators (acetyl-CoA, glucose-6-phosphate, fructose 1,6-diphosphate) had no effect on enzyme activity.	(Sako et al., 1996)
	Sulfolobus solfataricus		0.09 (pH 8.0, 80 °C)						2.1 U mg^{-1} (pH 8.0, 80 °C)	Optimum pH: 8.0	(Ettema et al., 2004)
	Sulfolobus acidocaldarius		0.2 (pH 8.0, 80 °C)							Optimum temperature: 90 °C Optimum pH: 8.0 Not activated by G6P No loss of activity after incubation for 2 hours at 80 °C	(Sako et al., 1997)
Bacteria											
Bacteria	*Anabaena* sp BDU 41811		0.10784 (pH 7.5, 30 °C)						V_{max}: 0.242 unit mg^{-1} crude protein (pH 7.5, 30 °C)		(Shylajanaciyar et al., 2015)

Bacteria	*Chlamydomonas reinhardtii*	**2 mM glutamine** PEPC1: 0.28 (pH 7.4, 25 °C) 0.11 (pH 8.4, 25 °C) PEPC2: 0.15 (pH 7.4, 25 °C) 0.09 (pH 8.4, 25 °C) **2 mM dihydroxyacetone phosphate** PEPC1: 0.31 (pH 7.4, 25 °C)0.21 (pH 8.4, 25 °C) PEPC2: 0.23 (pH 7.4, 25 °C) 0.11 (pH 8.4, 25 °C)	PEPC1: 0.64 (pH 7.4, 25 °C) 0.24 (pH 8.4, 25 °C) PEPC2: 0.37 (pH 7.4, 25 °C) 0.10 (pH 8.4, 25 °C)	**2 mM 2-oxoglutarate** PEPC1: 0.76 (pH 7.4, 25 °C) 0.53 (pH 8.4, 25 °C) PEPC2 0.68 (pH 7.4, 25 °C) 0.27 (pH 8.4, 25 °C) **2 mM Glu** PEPC1: 1.21 (pH 7.4, 25 °C) 0.38 (pH 8.4, 25 °C) PEPC2: 0.58 (pH 7.4, 25 °C) 0.27 (pH 8.4, 25 °C) **2 mM Asp** PEPC1: 0.88 (pH 7.4, 25 °C) 0.38 (pH 8.4, 25 °C) PEPC2: 0.43 (pH 7.4, 25 °C) 0.36 (pH 8.4, 25 °C) **2 mM malate** PEPC1: 0.92 (pH 7.4, 25 °C) 0.80 (pH 8.4, 25 °C) PEPC2: 0.62 (pH 7.4, 25 °C) 0.23 (pH 8.4, 25 °C)						PEPC1 and PEPC2 isoforms isolated from *C. reinhardtii* PEPC2 = major polypeptide chain (100kDa), several associated polypeptides (50-70 kDa) PEPC1 optimum pH: 8.8 PEPC2 optimum pH: 8.1 Isoforms are activated by glutamine and dihydroxyacetone phosphate.	(Rivoal et al., 1998)

		PEPC carboxylation kinetics									
		K_mPEP (mM)			K_m Mg^{2+}	$K_m HCO_3^-$		V_{max} or k_{cat}		Notes	Reference
	Species	+ G6P or other activator where mentioned	- G6P	+ inhibitor		+ G6P	- G6P	+ G6P or other activator where mentioned	- G6P		
Bacteria	*Coccochloris peniocystis*		0.6 (30 °C, pH 8.0)		0.27 mM (30 °C, pH 8.0)		0.8 mM (30 °C, pH 8.0)		V_{max}: 8.84 µmol/mg of protein per min (30 °C, pH 8.0).	Optimum temperature: 40 °C Optimum pH: 8.0	(Owttrim and Colman, 1986)
	Escherichia coli	2.0 mM Acetyl-CoA 1.4 (pH 8.5, 25 °C) Saturating Acetyl-CoA: 0.6 (pH 8.5, 25 °C)	200 (pH 8.5, 25 °C)					2.0 mM Acetyl CoA V_{max}: 1.50 ΔA_{340}/min	V_{max}: 1.54 ΔA_{340}/min		(Wohl and Markus, 1972)
	Escherichia coli	0.4 mM Acetyl-CoA 1.5 (pH 7.3) 0.2 mM Acetyl-CoA + 2 mM fructose-1,6-bisphosphate 0.25	15 (pH 7.3)							Activator: Acetyl-CoA, and fructose 1,6-bisphosphate (only when present in combination with Acetyl-CoA)	(Izui et al., 1981)
			32 (30 °C, pH 8.5)								(Teraoka et al., 1972)
		2 mM Acetyl-CoA 0.16 (pH 8.5; 30 °C)	16.0 (pH 8.5; 30 °C)		2 mM Acetyl CoA 0.20 (pH 8.5; 30 °C)	2 mM Acetyl CoA 0.15 (pH 8.5; 30 °C)		2 mM Acetyl CoA 154 U/mg (pH 8.5; 30 °C)	V_{max}: 43.3 U/mg (pH 8.5; 30 °C)		(Terada and Izui, 1991)
	Myxosarcina sp BDU 60881		0.01334 (pH 7.5; 30 °C)						V_{max}: 0.159 unit per mg of crude protein (pH 7.5; 30 °C)		(Shylajanaciyar et al., 2015)
	Nostoc calcicola BDU 40302		0.05126 (pH 7.5; 30 °C)						V_{max}: 0.205 unit per mg of crude protein (pH 7.5; 30 °C)		(Shylajanaciyar et al., 2015)
	Oceanimonas smirnovii		1.22				0.139 mM		V_{max}: 21.8 U/mg protein		(Park et al., 2015)

		PEPC carboxylation kinetics									
		K_mPEP (mM)			K_m Mg^{2+}	$K_m HCO_3^-$		V_{max} or k_{cat}		Notes	Reference
	Species	+ G6P or other activator where mentioned	- G6P	+ inhibitor		+ G6P	- G6P	+ G6P or other activator where mentioned	- G6P		
Bacteria	*Oscillatoria willei* BDU 130791		0.03644 (pH 7.5; 30 °C)						V_{max}: 0.216 unit per mg of crude protein (pH 7.5; 30 °C)		(Shylajanaciyar et al., 2015)
	Phormidium valderianum BDU 30711		0.03608 (pH 7.5; 30 °C)						V_{max}: 0.247 unit per mg of crude protein (pH 7.5; 30 °C)		(Shylajanaciyar et al., 2015)
	Rhodothermus obamensis Thermophilic				K_m Mg^{2+} 0.25 mM K_m Mn^{2+} 0.1 mM			Relative activity of PEPC enzyme: **Acetyl-CoA** 143.2% (1mM) 155.8% (2mM) 157.1% (5mM) **F-1,6-P2** 126.6% (2mM) 141.8% (5mM) 143.7% (10mM)	V_{max}: 100 µmol NADH/min per mg (pH 8.0)	Optimum temperature: 75 °C pH optimum: 8.0 Activated by fructose 1,6-bisphosphate and acetyl-CoA. Effectors affected the thermophilicity and thermostability of the enzyme.	(Takai et al., 1997)

Bacteria	*Selenastrum minutum* Fresh water green alga	**dihydroxyacetone phosphate** PEPC1 3.20 (pH 7.4, 25 °C) 0.68 (pH 8.4, 25 °C) PEPC2: 0.72 (pH 7.4, 25 °C) 0.25 (pH 8.4, 25 °C) PEPC3: 1.81 (pH 7.4, 25 °C) 0.25 (pH 8.4, 25 °C) PEPC4: pH 8.4 0.21 (pH 8.4, 25 °C) **Glutamine** PEPC1: 2.33 (pH 7.4, 25 °C) 0.32 (pH 8.4, 25 °C) PEPC2: 0.65 (pH 7.4, 25 °C) 0.23 (pH 8.4, 25 °C) PEPC3 0.58 (pH 7.4, 25 °C) 0.19 (pH 8.4, 25 °C) PEPC4: 0.26 (pH 8.4, 25 °C)	PEPC1: 9.29 (pH 7.4, 25 °C) 1.56 (pH 8.4, 25 °C) PEPC2: 0.87 (pH 7.4, 25 °C) 0.3 (pH 8.4, 25 °C) PEPC3: 0.72 (pH 7.4, 25 °C) 0.28 (pH 8.4, 25 °C) PEPC4: 0.86 (pH 7.4, 25 °C) 0.31 (pH 8.4, 25 °C)	**2 mM malate** PEPC1: 11.7 (pH 7.4, 25 °C) 4.69 (pH 8.4, 25 °C) PEPC2: 1.10 (pH 7.4, 25 °C) 0.26 (pH 8.4, 25 °C) PEPC3 1.06 (pH 7.4, 25 °C) 0.33 (pH 8.4, 25 °C) PEPC4: 0.29 (pH 8.4, 25 °C) **2 mM aspartate** PEPC1: 18.0 (pH 7.4, 25 °C) 2.51 (pH 8.4, 25 °C) PEPC2: 2.23 (pH 7.4, 25 °C) 0.30 (pH 8.4, 25 °C) PEPC3: 2.11 (pH 7.4, 25 °C) 0.28 (pH 8.4, 25 °C) PEPC4: 0.35 (pH 8.4, 25 °C) **Glu** PEPC1: 15.7 (pH 7.4, 25 °C) 2.50 (pH 8.4, 25 °C) PEPC2:					V_{max}: PEPC1 32.6 U/mg PEPC2 26.6 U/mg PEPC3 26.4 U/mg PEPC4 14.2 U/mg	Four PEPC isoforms: PEPC1, PEPC2, PEPC3, PEPC4. PEPC1 starts lose activity at 30 °C and is completely denatured at 53 °C. PEPC2, PEPC3, and PEPC4 remain fairly stable up to 53°C and then rapidly denature between 53 °C and 65 °C.	(Rivoal et al., 1996)

		PEPC carboxylation kinetics									
		K_mPEP (mM)			K_m Mg^{2+}	$K_m HCO_3^-$		V_{max} or k_{cat}		Notes	Reference
	Species	+ G6P or other activator where mentioned	- G6P	+ inhibitor		+ G6P	- G6P	+ G6P or other activator where mentioned	- G6P		
				2.66 (pH 7.4, 25 °C) 0.36 (pH 8.4, 25 °C) PEPC3: 2.54 (pH 7.4, 25 °C) 0.33 (pH 8.4, 25 °C) PEPC4: 0.30 (pH 8.4, 25 °C)							
Bacteria	*Synechococcus elongatus* BDU 30312		0.01313 (pH 7.5; 30 °C)						V_{max}: 0.101 unit per mg of crude protein (pH 7.5; 30 °C)		(Shylajanaciyar et al., 2015)
	Synechoccus vulcans Thermphilic cyanobacterium		0.58 (pH 7.5) 0.53 (pH 9.0)		0.45 mM (pH 7.5) 0.30 mM (pH 9.0)		0.48 mM (pH 7.5)		V_{max}: 17.30 unit mg^{-1} (pH 7.5) 25.30 unit mg^{-1} (pH 9.0)	Retained full activity after incubation at 50 °C for 50 mins. Optimum temp: 42 °C (pH 7.5) Optimum pH: 9.0 (30°C) Activated by fructose 1,6-bisphosphate and slightly stimulated by 3-PGA, G6P, G1P, Glu and Gln. Acetyl CoA has no effect.	(Chen et al., 2002)
	Thermobacillus thiooxidans						1.2 mM (pH 7.4; 30 °C)				(Suzuki and Werkman, 1957)
	Thermosynechococcus elongatus		0.55 (pH 8.5; 25 °C)						V_{max}: 22.5 unit mg^{-1} (pH 8.5; 25 °C)	Full activity at 40 °C, 84 % activity at 50 °C and 71 % activity at 60 °C.	(Del Prete et al., 2016)
	Thiobacillus novellus	0.1 mM Acetyl-CoA 0.64 (pH 8.0; 22 °C)			0.11 mM (pH 8.0; 22 °C)				V_{max}: 60 µmol/min/mg protein (pH 8.0; 22 °C)	pH optimum: 8.0 Acteyl-CoA is a potent activator	(Charles and Sykora, 1992)
	Thiobacillus thioparus		0.44 (pH 7.3)		0.37 mM (pH 7.3)		0.89 mM (pH 7.3)		V_{max}: 0.320 units/mg	No allosteric activators apart from dioxane.	(Hoban and Lyric, 1975)

		PEPC carboxylation kinetics									
		K_mPEP (mM)			K_m Mg^{2+}	$K_m HCO_3^-$		V_{max} or k_{cat}		Notes	Reference
	Species	+ G6P or other activator where mentioned	- G6P	+ inhibitor		+ G6P	- G6P	+ G6P or other activator where mentioned	- G6P		
Bacteria	*Plasmodium berghei*		2.6 (pH 7.8; 25 °C)		1.3 mM (pH 7.8)		2 mM (pH 7.8)			Acetyl-CoA and fructose 1,6-diphosphate had no effect on activity. PH optimum: 7.4	(McDaniel and Siu, 1972)
Plants											
Plants	*Bryophyllum fedtschenkoi* CAM species		0.7 (pH 7.8, 25 °C) 1.7 (pH 7.8, 11 °C) 2.4 (pH 7.8, 40 °C)						V_{max}: 26 units/mg of protein (pH 7.8, 25 °C)	Relatively small variations in V_{max} between pH 5.5 and 9.0. Double optimum at pH 5.6 and 7.8. Inactivated between 30 and 45 °C	(Jones et al., 1978)
	Bryophyllum pinnatum CAM species		0.14						V_{max}: 4.1 µmoles per minute per mg of chlorophyll (pH 7.4)		(Ting and Osmond, 1973b)
	Bryophyllum tubiflorum CAM species		0.22						V_{max}: 20.2 µmoles per minute per mg of chlorophyll (pH 7.4)		(Ting and Osmond, 1973b)
	Kalanchoe daigremontiana CAM species		0.13 (pH 7.4)						V_{max}: 12.5 µmoles per minute per mg of chlorophyll (pH 7.4)		(Ting and Osmond, 1973b)
							16.2 µM (pH 6.2; 10 °C) 11 µM (pH 7.5; 10 °C) 20 µM (pH 8.0; 10 °C)				(Nott and Osmond, 1982)
	Optunia inermis CAM species		0.12 (pH 7.4)						V_{max}: 14.9 µmoles per minute per mg of chlorophyll (pH 7.4)		(Ting and Osmond, 1973b)

		PEPC carboxylation kinetics									
		K_mPEP (mM)			K_m Mg^{2+}	$K_m HCO_3^-$		V_{max} or k_{cat}		Notes	Reference
	Species	+ G6P or other activator where mentioned	- G6P	+ inhibitor		+ G6P	- G6P	+ G6P or other activator where mentioned	- G6P		
Plants	*Sedum praealtum* CAM species		0.33 (pH 7.4)						V_{max}: 39.6 µmoles per minute per mg of chlorophyll (pH 7.4)		(Ting and Osmond, 1973b)
	Alternanthera sessilis C_3 species	0.013 (25 °C)	0.036 (25 °C)					V_{max}: 17.4 µmol min^{-1} mg^{-1} (25 °C) k_{cat}: 20 s^{-1} (25 °C)	V_{max}: 12 µmol min^{-1} mg^{-1} (25 °C) k_{cat}: 22 s^{-1} (25 °C)		(Gowik et al., 2006)
	Arachis hypogaea C_3 species		0.3 – 0.4 (pH 7.9; 30 °C)		0.5 – 0.6 mM (pH 7.9; 30 °C)		0.31 mM (pH 7.9; 30 °C)				(Maruyama et al., 1966)
	Atriplex hastata C_3 species		0.08 (pH 7.8; 30 °C)		0.017 mM (pH 7.8; 30 °C)		0.018 mM (pH 7.8; 30 °C)		V_{max}: 1.48 µmoles per minute per mg of chlorophyll (pH 7.8; 30 °C)		(Ting and Osmond, 1973c)
	Atriplex patula C_3 species		0.11 (pH 7.4)						V_{max}: 0.92 µmoles per minute per mg of chlorophyll (pH 7.4)		(Ting and Osmond, 1973b)
	Avena sativa C_3 species							5 mM Glycine Activation of PEPC (% activity compared to control) 108 %			(Nishikido and Takanashi, 1973)
	Flaveria cronquistii C_3 species	0.008 (pH 8.0; 25 °C)	0.013 (pH 8.0; 25 °C)								(Bauwe and Chollet, 1986)
		5 mM G6P 0.04 (pH 7.0; 25 °C) 0.08 (pH 8.0; 25 °C)	0.32 (pH 7.0; 25 °C) 0.13 (pH 8.0; 25 °C)					5 mM G6P 12 µmol·mg Chl^{-1}·hr^{-1} (pH 7.0; 25 °C) 19 µmol·mg Chl^{-1}·hr^{-1} (pH 8.0; 25 °C)	V_{max}: 12 µmol·mg Chl^{-1}·hr^{-1} (pH 7.0; 25 °C) 17 µmol·mg Chl^{-1}·hr^{-1} (pH 8.0; 25 °C)		(Nakamoto et al., 1983)

		PEPC carboxylation kinetics									
		K_mPEP (mM)			K_m Mg^{2+}	$K_mHCO_3^-$		V_{max} or k_{cat}		Notes	Reference
	Species	+ G6P or other activator where mentioned	- G6P	+ inhibitor		+ G6P	- G6P	+ G6P or other activator where mentioned	- G6P		
Plants	*Flaveria pringlei* C_3 species	5 mM G6P 0.017 (pH 8.0; 25 °C) 0.015 (pH 7.6; 25 °C)	0.029 (pH 8.0; 25 °C) 0.041 (pH 7.6; 25 °C)					5 mM G6P V_{max}: 32 U/mg (pH 8.0; 25 °C) 26 U/mg (pH 7.6; 25 °C)	V_{max}: 31 U/mg (pH 8.0; 25 °C) 24 U/mg (pH 7.6; 25 °C)		(Engelmann et al., 2003)
		0.019 (pH 8.0; 25 °C)	0.029 (pH 8.0; 25 °C)					V_{max}: 32 U/mg (pH 8.0; 25 °C) k_{cat}: 60 s^{-1} (pH 8.0; 25 °C)	V_{max}: 28 U/mg (pH 8.0; 25 °C) k_{cat}: 51 s^{-1} (pH 8.0; 25 °C)		(Bläsing et al., 2000)
		5 mM G6P 0.021 (pH 8.0; 25 °C)	0.061 (pH 8.0; 25 °C)						V_{max}: 27 U/mg protein (pH 8.0; 25 °C)		(Svensson et al., 1997)
						64.0 µM (pH 7.6; 30 °C)		V_{max}: 5.1 µmol mg $protein^{-1}$ min^{-1} (pH 7.6; 30 °C)			(DiMario and Cousins, 2019)
		0.020	0.060								(Westhoff et al., 1997)
		5 mM G6P 0.019 (pH 8.0; 25 °C) 0.016(pH 7.6; 25 °C)	0.029 (pH 8.0; 25 °C) 0.038 (pH 7.6; 25 °C)					5 mM G6P V_{max}: 32 U/mg (pH 8.0; 25 °C) 28 U/mg (pH 7.6; 25 °C) k_{cat}: 60 s^{-1} (pH 8.0; 25 °C) 51 s^{-1} (pH 7.6; 25 °C)	V_{max}: 28 U/mg (pH 8.0; 25 °C) 24 U/mg (pH 7.6; 25 °C) k_{cat}: 51 s^{-1} (pH 8.0; 25 °C) 44 s^{-1} (pH 7.6; 25 °C)		(Bläsing et al., 2002)
			0.039 (pH 7.6; 25°C)								(Jacobs et al., 2008)
	Gossipium hirsutum C_3 species		0.18 (pH 7.8; 30 °C)		0.180 mM (pH 7.8; 30 °C)				V_{max}: 1.15 µmoles per minute per mg of chlorophyll (pH 7.8; 30 °C)		(Ting and Osmond, 1973c)

		PEPC carboxylation kinetics									
		K_mPEP (mM)			K_m Mg^{2+}	$K_m HCO_3^-$		V_{max} or k_{cat}		Notes	Reference
	Species	+ G6P or other activator where mentioned	- G6P	+ inhibitor		+ G6P	- G6P	+ G6P or other activator where mentioned	- G6P		
Plants			PCI: 0.0368 PCII: 0.057 PCIII: 0.0407 (pH 8.5 [PEP] in the range 0.05 – 2.5 mM)		PCI: 0.0095 mM PCII: 0.0735 mM PCIII: 0.125 mM (pH 8.5)		PCI: 144 µM PCII: 53.4 µM PCIII: 55.5 µM (pH 8.5)			Isolated three isozymes of PEPC (PCI, PCII, and PCIII) from cotton leaf PCI pH optimum: 7.7 PCII pH optimum: 8.5 PCIII pH optimum: 8.5	(Mukerji and Ting, 1971)
	Helianthus annus C_3 species		0.11 (pH 7.8; 30 °C)		0.11 mM (pH 7.8; 30 °C)				V_{max}: 1.10 µmoles per minute per mg of chlorophyll (pH 7.8; 30 °C)		(Ting and Osmond, 1973c)
	Hordeum vulgare C_3 species							5 mM Glycine Inhibition of PEPC (% activity compared to control) 90.0 %			(Nishikido and Takanashi, 1973)
	Musa cavendishii L. Heterotetramer Banana C_3 species	0.030 (pH 7.0; 30 °C)	0.140 (pH 7.0; 30 °C) 0.078 (pH 8.0; 30 °C)				pH 8.0 0.064 mM	1 mM G6P V_{max}: 28 units/mg of protein (pH 7.0; 30 °C)	V_{max}: 16 units/mg of protein (pH 7.0; 30 °C) 31 units/mg of protein (pH 8.0; 30 °C)		(Law and Plaxton, 1995)
	Nicotiana glutinosa C_3 species		0.08 (pH 7.8; 30 °C)						V_{max}: 2.72 µmoles per minute per mg of chlorophyll (pH 7.8; 30 °C)		(Ting and Osmond, 1973c)
	Nicotiana tabacum C_3 species							5 mM Glycine Inhibition of PEPC (% activity compared to control) 88.1 %			(Nishikido and Takanashi, 1973)

		PEPC carboxylation kinetics									
		K_mPEP (mM)			K_m Mg^{2+}	$K_m HCO_3^-$		V_{max} or k_{cat}		Notes	Reference
	Species	+ G6P or other activator where mentioned	- G6P	+ inhibitor		+ G6P	- G6P	+ G6P or other activator where mentioned	- G6P		
Plants	*Oryza sativa* C_3 species							5 mM Glycine Activation of PEPC (% activity compared to control) 102 %			(Nishikido and Takanashi, 1973)
	Panicum laxum C_3 species		0.06 (pH 8.3; 30 °C) 0.16 (pH 7.3; 30 °C)				0.4 – 0.8 mM (30 °C)		V_{max}: 21-39 µmol CO_2/mg Chl·h (30 °C) V_{max}: 21 µmol CO_2/mg Chl·h (pH 8.3; 30 °C) 23 µmol CO_2/mg Chl·h (pH 7.3; 30 °C)	No activation by G6P was observed in the range of 0.1 – 5 mM G6P	(Holaday and Black, 1981)
	Phaseolus vulgaris C_3 species		0.30 (pH 7.8; 30 °C)		0.128 mM (pH 7.8; 30 °C)				V_{max}: 1.52 µmoles per minute per mg of chlorophyll (pH 7.8; 30 °C)		(Ting and Osmond, 1973c)
	Phytolacca americana C_3 species							5 mM Glycine Activation of PEPC (% activity compared to control) 100 %			(Nishikido and Takanashi, 1973)
	Spinacea oleracea (spinach) C_3 species		0.108 mM (pH 7.5; 25 °C)		K_mMn^{2+}: 0.037 mM (pH 7.5; 25 °C), K_mMg^{2+}: 0.079 mM (pH 7.5; 25 °C)		0.11 mM (pH 7.5; 25 °C)				(Miziorko et al., 1974)
			0.13 (pH 7.8; 30 °C)						V_{max}: 1.54 µmoles per minute per mg of chlorophyll (pH 7.8; 30 °C)		(Ting and Osmond, 1973c)

		PEPC carboxylation kinetics									
		K_mPEP (mM)			K_m Mg^{2+}	$K_m HCO_3^-$		V_{max} or k_{cat}		Notes	Reference
	Species	+ G6P or other activator where mentioned	- G6P	+ inhibitor		+ G6P	- G6P	+ G6P or other activator where mentioned	- G6P		
Plants								5 mM Glycine Inhibition of PEPC (% activity compared to control) 94.5 %			(Nishikido and Takanashi, 1973)
	Suaeda linifolia C_3 species		0.05 (pH 8.0; 20 % glycerol)						V_{max}: 0.09 units/mg protein (pH 8.0; 20 % glycerol)		(Lara et al., 2006)
	Triticum aestivum C_3 species							5 mM Glycine Inhibition of PEPC (% activity compared to control) 94.7 %			(Nishikido and Takanashi, 1973)
	Triticum vulgare C_3 species		0.09 (pH 7.8; 30 °C)		0.053 mM (pH 7.8; 30 °C)				V_{max}: 0.82 µmoles per minute per mg of chlorophyll (pH 7.8; 30 °C)		(Ting and Osmond, 1973c)
	Vicia faba C_3 species		0.11 (pH 7.8; 30 °C)		0.095 mM (pH 7.8; 30 °C)				V_{max}: 1.63 µmoles per minute per mg of chlorophyll (pH 7.8; 30 °C)		(Ting and Osmond, 1973c)
	Alternanthera tenella C_3-C_4 intermediate species	0.025 (25 °C)	0.042 (25 °C)					V_{max}: 18 µmol min^{-1} mg^{-1} (25 °C) k_{cat}: 33 s^{-1} (25 °C)	V_{max}: 17.64 µmol min^{-1} mg^{-1} (25 °C) k_{cat}: 33 s^{-1} (25 °C		(Gowik et al., 2006)
	Coleataenia prionitis (Formerly *Panicum prionitis*) C_3-C_4 intermediate species		0.22 (pH 8.3; 30 °C) 0.93 (pH 7.3; 30 °C)				0.3 mM (30 °C)		V_{max}: 1374 µmol CO_2/mg Chl·h (30 °C) V_{max}: 952 µmol CO_2/mg Chl·h (pH 8.3; 30 °C) 1176 µmol CO_2/mg Chl·h (pH 7.3; 30 °C)	No activation by G6P was observed in the range of 0.1 – 5 mM G6P	(Holaday and Black, 1981) (Tashima et al., 2021)

		PEPC carboxylation kinetics									
		K_mPEP (mM)			K_m Mg^{2+}	$K_m HCO_3^-$		V_{max} or k_{cat}		Notes	Reference
	Species	+ G6P or other activator where mentioned	- G6P	+ inhibitor		+ G6P	- G6P	+ G6P or other activator where mentioned	- G6P		
Plants	*Flaveria anomala* C_3-C_4 intermediate species		0.015 (pH 8.0; 25 °C)								(Bauwe and Chollet, 1986)
	Flaveria chloraefolia C_3-C_4 intermediate species	0.008 (pH 8.0; 25 °C)	0.006 (pH 8.0; 25 °C)								(Bauwe and Chollet, 1986)
	Flaveria floridana C_3-C_4 intermediate species	0.009 (pH 8.0; 25 °C)	0.013 (pH 8.0; 25 °C)								(Bauwe and Chollet, 1986)
	Flaveria linearis C_3-C_4 intermediate species		0.012 (pH 8.0; 25 °C)								(Bauwe and Chollet, 1986)
		5 mM G6P 0.14 (pH 7.0; 25 °C) 0.19 (pH 8.0; 25 °C)	0.50 (pH 7.0; 25 °C) 0.83 (pH 8.0; 25 °C)					5 mM G6P V_{max}: 204 µmol·mg Chl^{-1}·hr^{-1} (pH 7.0; 25 °C) 204 µmol·mg Chl^{-1}·hr^{-1} (pH 8.0; 25 °C)	V_{max}: 187 µmol·mg Chl^{-1}·hr^{-1} (pH 7.0; 25 °C) 204 µmol·mg Chl^{-1}·hr^{-1} (pH 8.0; 25 °C)		(Nakamoto et al., 1983)
	Flaveria pubescens C_3-C_4 intermediate species	5 mM G6P 0.020 (pH 8.0; 25 °C) 0.014 (pH 7.6; 25 °C)	0.053 (pH 8.0; 25 °C) 0.060 (pH 7.6; 25 °C)					5 mM G6P V_{max}: 26 U/mg (pH 8.0; 25 °C) 22 U/mg (pH 7.6; 25 °C)	V_{max}: 25 U/mg (pH 8.0; 25 °C) 20 U/mg (pH 7.6; 25 °C)		(Engelmann et al., 2003)
		5 mM G6P 0.09 (pH 7.0; 25 °C)	0.42 (pH 7.0; 25 °C) 0.19 (pH 8.0; 25 °C)					5 mM G6P 385 µmol·mg Chl^{-1}·hr^{-1} (pH 7.0; 25 °C)	V_{max}: 364 µmol·mg Chl^{-1}·hr^{-1} (pH 7.0; 25 °C) 513 µmol·mg Chl^{-1}·hr^{-1} (pH 8.0; 25 °C)		(Nakamoto et al., 1983)
		0.008 (pH 8.0; 25 °C)	0.014 (pH 8.0; 25 °C)								(Bauwe and Chollet, 1986)
	Panicum decipens C_3-C_4 intermediate species		0.09 (pH 8.3; 30 °C)						V_{max}: 61 µmol CO_2/mg Chl·h (pH 8.3; 30 °C)	No activation by G6P was observed in the range of 0.1 – 5 mM G6P	(Holaday and Black, 1981)

		PEPC carboxylation kinetics									
		K_mPEP (mM)			K_m Mg^{2+}	$K_m HCO_3^-$		V_{max} or k_{cat}		Notes	Reference
	Species	+ G6P or other activator where mentioned	- G6P	+ inhibitor		+ G6P	- G6P	+ G6P or other activator where mentioned	- G6P		
Plants	*Panicum miliodes* C_3-C_4 intermediate species		0.9-1.10) 0.07 (pH 8.3; 30 °C) 0.24 (pH 7.3; 30 °C)				0.4 – 0.8 mM (30 °C)		V_{max}: 57-69 µmol CO_2/mg Chl·h (30 °C) V_{max}: 75 µmol CO_2/mg Chl·h (pH 8.3; 30 °C) 73 µmol CO_2/mg Chl·h (pH 7.3; 30 °C)	No activation by G6P was observed in the range of 0.1 – 5 mM G6P	(Holaday and Black, 1981)
	Panicum schenckii C_3-C_4 intermediate species		0.07 (pH 8.3; 30 °C)						V_{max}: 66 µmol CO_2/mg Chl·h (pH 8.3; 30 °C)	No activation by G6P was observed in the range of 0.1 – 5 mM G6P	(Holaday and Black, 1981)
	Flaveria brownii C_4-like species	5 mM G6P 0.017 (pH 8.0; 25 °C) 0.015 (pH 7.6; 25 °C)	0.108 (pH 8.0; 25 °C) 0.128 (pH 7.6; 25 °C)					5 mM G6P V_{max}: 27 U/mg (pH 8.0; 25 °C) 21 U/mg (pH 7.6; 25 °C)	V_{max}: 26 U/mg (pH 8.0; 25 °C) 18 U/mg (pH 7.6; 25 °C)		(Engelmann et al., 2003)
		0.029 (pH 8.0; 25 °C)	0.088 (pH 8.0; 25 °C)								(Bauwe and Chollet, 1986)
	Bienertia sinuspersici Single-cell C_4 species		0.06 (pH 8.0; 20 % glycerol)						V_{max}: 1.96 units/mg protein (pH 8.0; 20 % glycerol)		(Lara et al., 2006)
	Suaeda aralocaspica Single-cell C_4 species		0.10 (pH 8.0; 20 % glycerol)						V_{max}: 1.67 units/mg protein (pH 8.0; 20 % glycerol)		(Lara et al., 2006)
	Amaranthus edulis (NAD-ME) C_4 species		0.19 (pH 7.8; 30 °C)		0.21 mM (pH 7.8; 30 °C)				V_{max}: 38.5 µmoles per minute per mg of chlorophyll (pH 7.8; 30 °C)		(Ting and Osmond, 1973c)

		PEPC carboxylation kinetics									
		K_mPEP (mM)			K_m Mg^{2+}	$K_m HCO_3^-$		V_{max} or k_{cat}		Notes	Reference
	Species	+ G6P or other activator where mentioned	- G6P	+ inhibitor		+ G6P	- G6P	+ G6P or other activator where mentioned	- G6P		
Plants	*Amaranthus hypochondriacus* (NAD-ME) C_4 species						IL: 0.011 mM (pH 7.3; 30 °C) D-AL: 0.031 mM (pH 7.3; 30 °C)		V_{max}: IL: 0.64 µmol min^{-1} (mg protein)$^{-1}$ (pH 7.3; 30 °C) D-AL: 0.16 µmol min^{-1} (mg protein)$^{-1}$ (pH 7.3; 30 °C)	Illuminated leaves = IL Dark-adapted leaves = D-AL	(Parvathi et al., 2000)
	Amaranthus palmeri (NAD-ME) C_4 species		0.19 (pH 7.8; 30 °C)		0.18 mM (pH 7.8; 30 °C)				V_{max}: 19.2 µmoles per minute per mg of chlorophyll (pH 7.8; 30 °C)		(Ting and Osmond, 1973c)
	Amaranthus retroflexus (NAD-ME) C_4 species							5 mM Glycine Activation of PEPC (% activity compared to control) 108 %			(Nishikido and Takanashi, 1973)
	Amaranthus tricolor (NAD-ME) C_4 species							5 mM Glycine Activation of PEPC (% activity compared to control) 103 %			(Nishikido and Takanashi, 1973)
	Amaranthus viridis (NAD-ME) C_4 species		0.29 (pH 8.0; 30 °C)				0.17 mM (pH 8.0; 30 °C)		17.1 µmol·(mg protein)$^{-1}$·min^{-1} (pH 8.0; 30 °C)	Activated by G6P	(Iglesias et al., 1986)
			0.35 (pH 8.0; 30 °C)		0.22 mM (pH 8.0; 30 °C)						(Raghavendra and Vallejos, 1980)
	Atriplex nummularia (NAD-ME) C_4 species		0.63 (pH 7.8; 30 °C)		0.50 mM (pH 7.8; 30 °C)				V_{max}: 39.6 µmoles per minute per mg of chlorophyll (pH 7.8; 30 °C)		(Ting and Osmond, 1973c)

		PEPC carboxylation kinetics									
		K_mPEP (mM)			K_m Mg^{2+}	$K_m HCO_3^-$		V_{max} or k_{cat}		Notes	Reference
	Species	+ G6P or other activator where mentioned	- G6P	+ inhibitor		+ G6P	- G6P	+ G6P or other activator where mentioned	- G6P		
Plants	*Atriplex rosea* (NAD-ME) C_4 species		0.62 (pH 7.4)						V_{max}: 39.0 µmoles per minute per mg of chlorophyll (pH 7.4)		(Ting and Osmond, 1973b)
	Atriplex spongiosa (NAD-ME) C_4 species	2 mM G6P 0.12 (pH 7.8; 30 °C)	0.49 (pH 7.8; 30 °C)		0.33 mM (pH 7.8; 30 °C)		0.022 mM (pH 7.8; 30 °C)		V_{max}: 38.0 µmoles per minute per mg of chlorophyll (pH 7.8; 30 °C)		(Ting and Osmond, 1973c)
		2 mM G6P 0.13 (pH 7.8)	0.48 (pH 7.8)								(Ting and Osmond, 1973a)
	Eleusine coracana (NAD-ME) C_4 species						26 µM (pH 8.0; 30 °C)				(Bauwe, 1986)
	Eleusine indica (NAD-ME) C_4 species						24 µM (pH 8.0; 30 °C)				(Bauwe, 1986)
	Panicum miliaceum (NAD-ME) C_4 species		1.40 (pH 7.8; 30 °C)		0.95 mM(pH 7.8; 30 °C)				V_{max}: 13.0 µmoles per minute per mg of chlorophyll (pH 7.8; 30 °C)		(Ting and Osmond, 1973c)
	Portulaca oleracea (NAD-ME) C_4 species							5 mM Glycine Inhibition of PEPC (% activity compared to control) 90.8 %			(Nishikido and Takanashi, 1973)
	Suaeda eltonica (NAD-ME) C_4 species		0.09 (pH 8.0; 20 % glycerol)						V_{max}: 0.83 units/mg protein (pH 8.0; 20 % glycerol)		(Lara et al., 2006)
	Alternanthera pungens (NADP-ME) C_4 species	0.020 (25 °C)	0.157 (25 °C)					V_{max}: 21.36 µmol min^{-1} mg^{-1} (25 °C) k_{cat}: 38 s^{-1} (25 °C)	V_{max}: 21 µmol min^{-1} mg^{-1} (25 °C) k_{cat}: 38 s^{-1} (25 °C)		(Gowik et al., 2006)

		PEPC carboxylation kinetics									
		K_mPEP (mM)			K_m Mg^{2+}	$K_m HCO_3^-$		V_{max} or k_{cat}		Notes	Reference
	Species	+ G6P or other activator where mentioned	- G6P	+ inhibitor		+ G6P	- G6P	+ G6P or other activator where mentioned	- G6P		
Plants	*Digitaria sanguinalis* (NADP-ME) C_4 species		*In situ*: 0.4 (pH 7.3; 30 °C) *In vitro*: 0.6 (pH 7.3; 30 °C)							*In situ* = from darkened leaves *In vitro* = enzyme extracted *in vitro*.	(Pierre et al., 2004)
		2 mM G6P 0.40 (pH 7.6; 37 °C)	0.75 (pH 7.6; 37 °C)	1 mM malate 1.23 (pH 7.6; 37 °C) 1 mM aspartate 1.42 (pH 7.6; 37 °C)							(Huber and Edwards, 1975)
	Echinochloa cruz-galli (NADP-ME) C_4 species		0.77 (pH 8.3; 30 °C)								(Hamel and Simon, 2000)
	Flaveria australasica (NADP-ME) C_4 species	0.055 (pH 8.0; 25 °C)	0.187 (pH 8.0; 25 °C)								(Bauwe and Chollet, 1986)
	Flaveria trinervia (NADP-ME) C_4 species	5 mM G6P 0.053 (pH 8.0; 25 °C) 0.141 (pH 7.6; 25 °C)	0.269 (pH 8.0; 25 °C) 0.393 (pH 7.6; 25 °C)					5 mM G6P V_{max}: 27 U/mg (pH 8.0; 25 °C) 24 U/mg (pH 7.6; 25 °C)	V_{max}: 26 U/mg (pH 8.0; 25 °C) 24 U/mg (pH 7.6; 25 °C)		(Engelmann et al., 2003)
		5 mM G6P 0.362 (pH 8.0; 25 °C)	0.652 (pH 8.0; 25 °C)						V_{max}: 29 U/mg protein (pH 8.0; 25 °C)		(Svensson et al., 1997)
		0.047 (pH 8.0; 25 °C)	0.215 (pH 8.0; 25 °C)								(Bauwe and Chollet, 1986)
						26.6 µM (pH 7.6; 30 °C)		V_{max}: 8.1 µmol mg $protein^{-1}$ min^{-1} (pH 7.6; 30 °C)			(DiMario and Cousins, 2019)
		0.360	0.650								(Westhoff et al., 1997)

		PEPC carboxylation kinetics									
		K_mPEP (mM)			K_m Mg^{2+}	$K_m HCO_3^-$		V_{max} or k_{cat}		Notes	Reference
	Species	+ G6P or other activator where mentioned	- G6P	+ inhibitor		+ G6P	- G6P	+ G6P or other activator where mentioned	- G6P		
Plants		5 mM G6P 0.058 (pH 8.0; 25 °C) 0.096(pH 7.6; 25 °C)	0.278 (pH 8.0; 25 °C) 0.375 (pH 7.6; 25 °C)					5 mM G6P V_{max}: 30 U/mg (pH 8.0; 25 °C) 29 U/mg (pH 7.6; 25 °C) k_{cat}: 55 s^{-1} (pH 8.0; 25 °C) 52 s^{-1} (pH 7.6; 25 °C)	V_{max}: 27 U/mg (pH 8.0; 25 °C) 26 U/mg (pH 7.6; 25 °C) k_{cat}: 49 s^{-1} (pH 8.0; 25 °C) 48 s^{-1} (pH 7.6; 25 °C)		(Bläsing et al., 2002)
		0.058 (pH 8.0; 25 °C)	0.278 (pH 8.0; 25 °C)					V_{max}: 30 U/mg (pH 8.0; 25 °C) k_{cat}: 55 s^{-1} (pH 8.0; 25 °C)	V_{max}: 27 U/mg (pH 8.0; 25 °C) k_{cat}: 49 s^{-1} (pH 8.0; 25 °C)		(Bläsing et al., 2000)
			0.76 (pH 7.3; 30°C) 0.44 (pH 8.0; 30°C)		0.95 mM (pH 7.3; 30°C) 0.18 mM (pH 8.0; 30°C)		0.072 mM (pH 7.3; 30°C) 0.081 mM (pH 8.0; 30°C)		V_{max}: 11.36 U mg^{-1} protein min^{-1} (pH 7.3; 30°C) 11.98 U mg^{-1} protein min^{-1} (pH 8.0; 30°C)		(Gao and Woo, 1996)
			0.313 (pH 7.6; 25°C)								(Jacobs et al., 2008)
	Gomphrena globosa (NADP-ME) C_4 species						27 µM (pH 8.0; 30 °C)				(Bauwe, 1986)
	Haloxylon persicum (NADP-ME) C_4 species		0.12 (pH 8.0; 20 % glycerol)						V_{max}: 1.27 units/mg protein (pH 8.0; 20 % glycerol)		(Lara et al., 2006)
	Miscanthus sinensis (NADP-ME) C_4 species							5 mM Glycine Activation of PEPC (% activity compared to control) 164 %			(Nishikido and Takanashi, 1973)

		PEPC carboxylation kinetics									
		K_mPEP (mM)			K_m Mg^{2+}	$K_m HCO_3^-$		V_{max} or k_{cat}		Notes	Reference
	Species	+ G6P or other activator where mentioned	- G6P	+ inhibitor		+ G6P	- G6P	+ G6P or other activator where mentioned	- G6P		
Plants	*Pennisetum purpureum* (NADP-ME) C_4 species				0.14 mM (pH 8.0; 27 °C) 5 mM G6P 0.4 mM (pH 8.0; 27 °C)	0.8 mM (pH 8.0; 27 °C)	2 mM (pH 8.0; 27 °C)				(Coombs et al., 1973)
	Saccharum officinarum (NADP-ME) C_4 species		0.80 (pH 7.8; 30 °C)		1.00 mM (pH 7.8; 30 °C)				V_{max}: 50.0 µmoles per minute per mg of chlorophyll (pH 7.8; 30 °C)		(Ting and Osmond, 1973c)
								5 mM Glycine Activation of PEPC (% activity compared to control) 139 %			(Nishikido and Takanashi, 1973)
	Saccharum hybrid		2.9 (pH 7.7)		0.27 (pH 7.7)						(Goatly and Smith, 1974)
	Salsola richteri (NADP-ME) C_4 species		0.21 (pH 8.0; 20 % glycerol)						V_{max}: 0.93 units/mg protein (pH 8.0; 20 % glycerol)		(Lara et al., 2006)
	Setaria italica (NADP-ME) C_4 species		0.53 (pH 8.0; 30 °C)								(Raghavendra and Das, 1975)
	Setaria verticillata (NADP-ME) C_4 species		1.9 (pH 7.2; 30 °C)								(Samaras et al., 1988)
	Setaria viridis (NADP-ME) C_4 species						60.2 µM (25 °C)		V_{max}: 450 µmol HCO_3^- m^{-2} s^{-1} (25 °C)		(Boyd et al., 2015)
	Sorghum bicolor (NADP-ME) C_4 species		0.63 (pH 7.8; 30 °C)		0.50 mM (pH 7.8; 30 °C)				V_{max}: 25.6 µmoles per minute per mg of chlorophyll (pH 7.8; 30 °C)		(Ting and Osmond, 1973c)

		PEPC carboxylation kinetics									
		K_mPEP (mM)			K_m Mg^{2+}	$K_m HCO_3^-$		V_{max} or k_{cat}		Notes	Reference
	Species	+ G6P or other activator where mentioned	- G6P	+ inhibitor		+ G6P	- G6P	+ G6P or other activator where mentioned	- G6P		
Plants								5 mM Glycine Activation of PEPC (% activity compared to control) 183 %			(Nishikido and Takanashi, 1973)
	Zea mays (NADP-ME) C_4 species		1.48 mM (pH 7.3; 30 °C) 0.59 mM (pH 9.0; 30 °C)		1.79 mM (pH 7.3; 30 °C) 0.58 mM (pH 9.0; 30 °C)		0.12 mM (pH 7.3; 30 °C) 0.10 mM (pH 9.0; 30 °C)		V_{max}: 18.20 unit mg^{-1} (pH 7.0; 30 °C) 23.00 unit mg^{-1} (pH 9.0; 30 °C)		(Dong et al., 1998)
			0.35 (pH 7.8; 30 °C)		0.46 mM (pH 7.8; 30 °C)				V_{max}: 12.9 µmoles per minute per mg of chlorophyll (pH 7.8; 30 °C)		(Ting and Osmond, 1973c)
	Zea mays (NADP-ME) C_4 species	0.089 mM (25 °C)	0.93 mM (25 °C)					V_{max}: increased 56 % in the presence of G6P (25 °C)			(Bandarian et al., 1992)
			0.34 mM (pH 7.4)						V_{max}: 19.2 9 µmoles per minute per g of fresh weight (pH 7.4)		(Ting and Osmond, 1973b)
	Zea mays (NADP-ME) C_4 species	0.53 (pH 7.0, 25 °C) 0.14 (pH 8.0, 25 °C)	7.9 (pH 7.0, 25 °C) 0.94 (pH 8.0, 25 °C)					V_{max}: 15.1 µM PEP min^{-1} mg^{-1} (pH 7.0, 25 °C) 27.05 µM PEP min^{-1} mg^{-1} (pH 8.0, 25 °C)	V_{max}: 16.4 µM PEP min^{-1} mg^{-1} (pH 7.0, 25 °C) 25.1 µM PEP min^{-1} mg^{-1} (pH 8.0, 25 °C)		(Frank et al., 2001)
		5 mM G6P: 0.49 (pH 7.3)	1.92 (pH 7.3)		1.75 mM (pH 7.3)			V_{max}: 16.6 U mg^{-1} protein (pH 7.3)			(Endo et al., 2008)

		PEPC carboxylation kinetics									
		K_mPEP (mM)			K_m Mg^{2+}	$K_m HCO_3^-$		V_{max} or k_{cat}		Notes	Reference
	Species	+ G6P or other activator where mentioned	- G6P	+ inhibitor		+ G6P	- G6P	+ G6P or other activator where mentioned	- G6P		
Plants			3.6 mM (pH 7.8; 26 °C)				0.18 mM (pH 7.8; 26 °C)				(Janc et al., 1992)
	Zea mays (NADP-ME) C_4 species	5 mM G6P 0.6 (pH 7.0; 22 °C)	2.6 (pH 7.0; 22 °C) 1.16 (pH 8.0; 22 °C)					V_{max}: 245.2 munits (pH 7.0; 22 °C)	V_{max}: 80.6 munits (pH 7.0; 22 °C) 193.6 (pH 8.0; 22 °C)		(Uedan and Sugiyama, 1976)
			PCI: 0.1 (pH 8.5) PCII: 0.047 (pH 8.5)		PCI: 0.032 mM (pH 8.5) PCII: 0.015 mM (pH 8.5)		PCI: 1.45 mM (pH 8.5) PCII: 1.28 (pH 8.5)			Two isozymes were isolated, PCI and PCII Temperature optimum: PCI: 40 °C	(Mukerji, 1977)
		5 mM G6P Phosphorylated: 0.4 (pH 7.3; 30 °C) Non-phosphorylated: 1.1 (pH 7.3; 30 °C)	Phosphorylated: 0.5 (pH 7.3; 30 °C) Non-phosphorylated: 1.8 (pH 7.3; 30 °C)					5 mM G6P Phosphorylated: V_{max}: 26.4 units mg^{-1} (pH 7.3; 30 °C) Non-phosphorylated: V_{max}: 31.9 units mg^{-1} (pH 7.3; 30 °C)	Phosphorylated: V_{max}: 18.0 units mg^{-1} (pH 7.3; 30 °C) Non-phosphorylated: V_{max}: 19.8 units mg^{-1} (pH 7.3; 30 °C)		(Takahashi-Terada et al., 2005)
							27 µM (pH 8.0; 30 °C)				(Bauwe, 1986)
								5 mM Glycine Activation of PEPC (% activity compared to control) 161 %			(Nishikido and Takanashi, 1973)
					3.3 mM (pH 8.0; 25 °C)				V_{max}: 8.2 µM/min (pH 8.0; 25 °C)		(O'Leary et al., 1981)

		PEPC carboxylation kinetics									
		K_mPEP (mM)			K_m Mg^{2+}	$K_m HCO_3^-$		V_{max} or k_{cat}		Notes	Reference
	Species	+ G6P or other activator where mentioned	- G6P	+ inhibitor		+ G6P	- G6P	+ G6P or other activator where mentioned	- G6P		
Plants	*Chloris gayana* (PEPCK) C_4 species		0.73 (pH 7.8; 30 °C)		0.14 mM (pH 7.8; 30 °C)				V_{max}: 15.6 µmoles per minute per mg of chlorophyll (pH 7.8; 30 °C)		(Ting and Osmond, 1973c)
	Panicum maximum (PEPCK) C_4 species		0.53 (pH 7.8; 30 °C)		0.07 mM (pH 7.8; 30 °C)				V_{max}: 37.6 µmoles per minute per mg of chlorophyll (pH 7.8; 30 °C)		(Ting and Osmond, 1973c)
							27 µM (pH 8.0; 30 °C)				(Bauwe, 1986)

Appendix 2: Meta-analysis of phosphoenolpyruvate carboxylase inhibition kinetics data

Phosphoenolpyruvate carboxylase (plant, bacterial and archaeal species) inhibition kinetics data from published research papers. Available information regarding K_i of inhibitors malate and aspartate, IC_{50} of inhibitors malate and aspartate, and other inhibitor data has been included. C_4 plant species subtype information is indicated (Sage and Sage, 1999). Archaeal species are indicated by grey shading, bacterial species are indicated by purple shading, CAM species are indicated by yellow shading, C_3 species are indicated by green shading, C_3-C_4 intermediate and C_4-like species are indicated by white shading, single-celled C_4 species are indicated by brown shading, NAD-ME species are indicated by orange shading, NADP-ME species are indicated by blue shading, and PEPCK species are indicated by pink shading.

		PEPC inhibition kinetics			
		Inhibition by L-malate and/or L-aspartate		Notes	Reference
	Species	**+ G6P or other activator where mentioned**	**- G6P**		
Archaea	*Clostridium perfringens*		K_i aspartate: 0.2 mM (pH 7.2; 37 °C)		(Dharmarajan et al., 2011)
	Methanothermobacter thermautotrophicus		Inhibition by aspartate observed	Highly inhibited by NaCl and KCl	(Patel et al., 2004)
	Methanothermus sociabilis	L-aspartate, and L-malate had no effect on enzyme activity.		Strong sensitivity to oxygen	(Sako et al., 1996)
	Sulfolobus solfataricus	Inhibited by malate and aspartate			(Ettema et al., 2004)
	Sulfolobus acidocaldarius		I_{50} malate: 10 mM I_{50} aspartate: 1.2 mM (pH 8.0, 80 °C)		(Sako et al., 1997)
Bacteria					
Bacteria	*Anabaena* sp BDU 41811		51 % inhibition by 1 mM aspartate		(Shylajanaciyar et al., 2015)
	Chlamydomonas reinhardtii			PEPC1 and PEPC2 isoforms isolated from *C. reinhardtii* Isoforms are inhibited by malate, aspartate glutamate, and 2-oxoglutarate.	(Rivoal et al., 1998)
	Coccochloris peniocystis		K_i OAA: 5 mM (30 °C, pH 8.0) Inhibited by malate (90%), aspartate (25%) and OAA (70%)		(Owttrim and Colman, 1986)
	Escherichia coli	1 mM acetyl CoA $I_{0.5}$ malate: 2.2 mM (20 °C) K_i malate: 0.23 mM (20 °C) $I_{0.5}$ aspartate: 3.5 mM (20 °C) K_i aspartate: 0.31 mM (20 °C)			(Gold and Smith, 1974)
		0.4 mM Acetyl-CoA $I_{0.5}$ malate: 0.14 mM $I_{0.5}$ aspartate: 0.13 mM Acetyl CoA + 2 mM fructose-1,6-bisphosphate $I_{0.5}$ malate: 0.52 mM $I_{0.5}$ aspartate: 0.51 mM		Malate and aspartate severely inhibited the enzyme	(Izui et al., 1981)

		PEPC inhibition kinetics			
		Inhibition by L-malate and/or L-aspartate		Notes	Reference
	Species	+ G6P or other activator where mentioned	- G6P		
Bacteria	*Escherichia coli*		K_i-aspartate: 0.2 mM (30 °C, pH 8.5)		(Teraoka et al., 1972)
		1 mM acetyl-CoA $I_{0.5}$ malate: 1.8 mM (pH 8.5) $I_{0.5}$ aspartate: 1.7 mM (pH 8.5)			(Endo et al., 2008)
	Myxosarcina sp BDU 60881		4.18 % inhibition by 1 mM aspartate (pH 7.5; 30 °C)		(Shylajanaciyar et al., 2015)
	Nostoc calcicola BDU 40302		41.28 % inhibition by 1 mM aspartate (pH 7.5; 30 °C)		(Shylajanaciyar et al., 2015)
	Oscillatoria willei BDU 130791		26.75 % inhibition by 1 mM aspartate (pH 7.5; 30 °C)		(Shylajanaciyar et al., 2015)
	Phormidium valderianum BDU 30711		26.02 % inhibition by 1 mM aspartate (pH 7.5; 30 °C)		(Shylajanaciyar et al., 2015)
	Rhodothermus obamensis Thermophilic		I_{50} malate: 0.3 mM 100% inhibition: 2.0 mM malate I_{50}-aspartate: 0.7 mM 100% inhibition: 2.5 mM aspartate	Inhibited by aspartate and malate. Effectors affected the thermophilicity and thermostability of the enzyme.	(Takai et al., 1997)
	Synechococcus elongatus BDU 30312		2.76 % inhibition by 1 mM aspartate (pH 7.5; 30 °C)		(Shylajanaciyar et al., 2015)
	Synechoccus vulcans Thermphilic cyanobacterium 1,011 AA, 116.4 kDa	At pH 7.5 G6P alleviated inhibition by aspartate.	K_i aspartate: 0.025 mM (pH 9.0, 30 °C) 2 mM (pH 9.0, 30 °C) Relative activity of PEPC (pH 7.5, 30 °C): 10 mM malate: 96.6 % 10 mM aspartate: 37.1% 10 mM 3-PGA: 192.0 % 10 mM G1P: 167.0 % 10 mM G6P 140% 10 mM F-1,6-P_2: 564.0%	Inhibited by aspartate	(Chen et al., 2002)

		PEPC inhibition kinetics			
		Inhibition by L-malate and/or L-aspartate		Notes	Reference
	Species	+ G6P or other activator where mentioned	- G6P		
Bacteria	*Thiobacillus novellus*		20 mM malate: 100 % inhibition 3.0 mM OAA: 100% inhibition Aspartate: little effect on enzyme activity.		(Charles and Sykora, 1992)
	Thiobacillus thioparus	K_i malate: 1 mM K_i aspartate: 1 mM			(Hoban and Lyric, 1975)
	Plasmodium berghei	I_{50} chloroquine: 0.18 mM Change from the initial rate OAA: -30 %		Aspartate had no effect on activity.	(McDaniel and Siu, 1972)
Plants					
Plants	*Bryophyllum fedtschenkoi* CAM species		I_{50} malate: 13 mM (pH 7.8, 25 °C)		(Jones et al., 1978)
			I_{50} malate: 0.3 mM (pH 7.0; 25 °C)		(Jones et al., 1981)
	Kalanchoe daigremontiana CAM species		K_i-malate: 0.3 mM (pH 6.2) 6.6 mM (pH 8.0)		(Nott and Osmond, 1982)
	Atriplex hastata C_3 species			Inhibited by citrate and pyruvate.	(Ting and Osmond, 1973c)
	Avena sativa C_3 species		5 mM malate Inhibition of PEPC (% activity compared to control) 25.7 %		(Nishikido and Takanashi, 1973)
	Flaveria pringlei C_3 species	5 mM G6P K_i-malate 1.4 mM (pH 7.6; 25 °C)	K_i-malate 0.2 (pH 7.6; 25 °C)		(Engelmann et al., 2003)
	Flaveria pringlei C_3 species		$I_{0.5}$ malate: 0.08 mM (pH 7.6; 25 °C)		(Svensson et al., 1997)
			$I_{0.5}$ malate: 0.08 mM		(Westhoff et al., 1997)
			$I_{0.5}$ malate: 0.57 mM (pH 7.6; 25 °C)		(Bläsing et al., 2002)
			IC_{50} malate: 2.6 mM (pH 7.6; 25°C)		(Paulus et al., 2013)
			IC_{50} malate: 2.9 mM (pH 7.6; 25°C)		(Paulus et al., 2013)
		IC_{50} malate: 5.5 mM (pH 7.6; 25°C)	IC_{50} malate: 1.1 mM (pH 7.6; 25°C)		(Jacobs et al., 2008)

		PEPC inhibition kinetics			
		Inhibition by L-malate and/or L-aspartate		Notes	Reference
	Species	+ G6P or other activator where mentioned	- G6P		
Plants	*Gossipium hirsutum* C_3 species		Relative activity when 5mM of metabolites are present. L-malate: PCI: 0.94 PCII: 0.39 PCIII: 0.88 L-aspartate: PCI: 0.99 PCII: 2.14 PCIII: 1.10 Pyruvate: PCI: 1.06 PCII: 0.11 PCIII: 0.80 Citrate: PCI: 1.12 PCII: 0.78 PCIII: 0.83	Isolated three isozymes of PEPC (PCI, PCII, and PCIII) from cotton leaf	(Mukerji and Ting, 1971)
	Hordeum vulgare C_3 species		5 mM malate Inhibition of PEPC (% activity compared to control) 35.2 %		(Nishikido and Takanashi, 1973)
	Musa cavendishii L. Banana C_3 species		I_{50}-malate: 0.015 mM (pH 7.0; 30 °C) 8.0 mM (pH 8.0; 30 °C) I_{50}-aspartate: 0.054 mM (pH 7.0; 30 °C) No effect (pH 8.0; 30 °C)		(Law and Plaxton, 1995)
	Nicotiana tabacum C_3 species		5 mM malate Inhibition of PEPC (% activity compared to control) 0 %		(Nishikido and Takanashi, 1973)
	Oryza sativa C_3 species		5 mM malate Inhibition of PEPC (% activity compared to control) 19.5 %		(Nishikido and Takanashi, 1973)
	Phytolacca americana C_3 species		5 mM malate Inhibition of PEPC (% activity compared to control) 8.3 %		(Nishikido and Takanashi, 1973)
	Spinacea oleracea (spinach)			Inhibitors: L-phospholactate, D-phospholactate and phosphoglycolate (PEP analogs)	(Miziorko et al., 1974)

		PEPC inhibition kinetics			
		Inhibition by L-malate and/or L-aspartate		Notes	Reference
	Species	+ G6P or other activator where mentioned	- G6P		
Plants	C_3 species		5 mM malate Inhibition of PEPC (% activity compared to control) 20.8 %		(Nishikido and Takanashi, 1973)
	Suaeda linifolia C_3 species		I_{50}-malate 3.93 mM (pH 7.2, 0.1 mM PEP)		(Lara et al., 2006)
	Triticum aestivum C_3 species		Inhibition of PEPC (% of control) 1 mM malate: 94 % (pH 7.6; 37 °C) 5mM malate: 91 % (pH 7.6; 37 °C) 1 mM aspartate: 91 % (pH 7.6; 37 °C) 5 mM aspartate: 85 % (pH 7.6; 37 °C)		(Huber and Edwards, 1975)
			5 mM malate Inhibition of PEPC (% activity compared to control) 21.3 %		(Nishikido and Takanashi, 1973)
	Flaveria pubescens C_3-C_4 intermediate species	5 mM G6P K_i-malate 1.2 mM (pH 7.6; 25 °C)	K_i-malate 0.6 (pH 7.6; 25 °C)		(Engelmann et al., 2003)
	Flaveria brownii C_4-like species	5 mM G6P K_i-malate 1.1 mM (pH 7.6; 25 °C)	K_i-malate 1.5 (pH 7.6; 25 °C)		(Engelmann et al., 2003)
	Bienertia sinuspersici Single-cell C_4 species		I_{50}-malate 2.22 mM (pH 7.2, 0.1 mM PEP)		(Lara et al., 2006)
	Suaeda aralocaspica Single-cell C_4 species		I_{50}-malate 0.69 mM (pH 7.2, 0.1 mM PEP)		(Lara et al., 2006)
	Amaranthus hypochondriacus (NAD-ME) C_4 species		K_I malate: IL: 0.24 mM (pH 7.3; 30 °C) D-AL: 0.07 mM (pH 7.3; 30 °C)	Illuminated leaves = IL Dark-adapted leaves = D-AL	(Parvathi et al., 2000)
	Amaranthus retroflexus (NAD-ME) C_4 species		5 mM malate Inhibition of PEPC (% activity compared to control) 26.0 %		(Nishikido and Takanashi, 1973)
	Amaranthus tricolor (NAD-ME) C_4 species		5 mM malate Inhibition of PEPC (% activity compared to control) 42.7 %		(Nishikido and Takanashi, 1973)

		PEPC inhibition kinetics			
		Inhibition by L-malate and/or L-aspartate		Notes	Reference
	Species	+ G6P or other activator where mentioned	- G6P		
Plants	*Amaranthus viridis* (NAD-ME) C_4 species		I_{50}: I_{50} Aspartate: 2.0 mM (pH 7.0; 30 °C) >20 mM (pH 8.0; 30 °C) I_{50} Malate: 2.5 mM (pH 7.0; 30 °C) 10 mM (pH 8.0; 30 °C) I_{50} OAA: 1.0 mM (pH 7.0; 30 °C) 0.5 mM (pH 8.0; 30 °C) I_{50} Pyruvate: >20 mM (pH 7.0; 30 °C) 5.0 mM (pH 8.0; 30 °C)		(Iglesias et al., 1986)
	Atriplex spongiosa (NAD-ME) C_4 species			Inhibited by citrate and pyruvate.	(Ting and Osmond, 1973c)
	Eleusine indica (NAD-ME) C_4 species		Inhibition of PEPC (% of control) 1 mM malate: 56 % (pH 7.6; 37 °C) 5mM malate: 26 % (pH 7.6; 37 °C) 1 mM aspartate: 81 % (pH 7.6; 37 °C) 5 mM aspartate: 59 % (pH 7.6; 37 °C)		(Huber and Edwards, 1975)
	Panicum miliaceum (NAD-ME) C_4 species		Inhibition of PEPC (% of control) 1 mM malate: 62 % (pH 7.6; 37 °C) 5mM malate: 25 % (pH 7.6; 37 °C) 1 mM aspartate: 75 % (pH 7.6; 37 °C) 5 mM aspartate: 41 % (pH 7.6; 37 °C)		(Huber and Edwards, 1975)
	Portulaca oleracea (NAD-ME) C_4 species		5 mM malate Inhibition of PEPC (% activity compared to control) 33.2 %		(Nishikido and Takanashi, 1973)
	Suaeda eltonica (NAD-ME) C_4 species		I_{50}-malate 0.89 mM (pH 7.2, 0.1 mM PEP)		(Lara et al., 2006)

		PEPC inhibition kinetics			
		Inhibition by L-malate and/or L-aspartate		Notes	Reference
	Species	+ G6P or other activator where mentioned	- G6P		
Plants	*Digitaria sanguinalis* (NADP-ME) C_4 species	IC_{50} : *In situ*: 22 mM (pH 7.3; 30 °C) *In vitro*: 4 mM(pH 7.3; 30 °C)	IC_{50} : *In situ*: 8 mM (pH 7.3; 30 °C) *In vitro*: 1.5 mM (pH 7.3; 30 °C)	*In situ* = from darkened leaves *In vitro* = enzyme extracted *in vitro*.	(Pierre et al., 2004)
	Digitaria sanguinalis (NADP-ME) C_4 species		Inhibition of PEPC (% of control) 1 mM malate: 66 % (pH 7.6; 37 °C) 1 mM aspartate: 70 % (pH 7.6; 37 °C)	Total inhibition at 10 mM malate Total inhibition at 10 mM aspartate	(Huber and Edwards, 1975)
	Flaveria trinervia (NADP-ME) C_4 species	5 mM G6P K_i-malate 0.8 mM (pH 7.6; 25 °C)	K_i-malate 2.5 (pH 7.6; 25 °C)		(Engelmann et al., 2003)
			$I_{0.5}$ malate: 1.2 mM (pH 7.6; 25 °C)		(Svensson et al., 1997)
			$I_{0.5}$ malate: 1.2 mM		(Westhoff et al., 1997)
			$I_{0.5}$ malate: 9.4 mM (pH 7.6; 25 °C)		(Bläsing et al., 2002)
			IC_{50} malate: 8.7 mM (pH 7.6; 25°C)		(Paulus et al., 2013)
			IC_{50} malate: 8.4 mM (pH 7.6; 25°C)		(Paulus et al., 2013)
		IC_{50} malate: 6.5 mM (pH 7.6; 25°C)	IC_{50} malate: 8.2 mM (pH 7.6; 25°C)		(Jacobs et al., 2008)
	Haloxylon persicum (NADP-ME) C_4 species		I_{50}-malate 1.91 mM (pH 7.2, 0.1 mM PEP)		(Lara et al., 2006)
	Miscanthus sinensis (NADP-ME) C_4 species		5 mM malate Inhibition of PEPC (% activity compared to control) 26.0 %		(Nishikido and Takanashi, 1973)
	Pennisetum purpureum (NADP-ME) C_4 species			Malate was a less effective inhibitor than OAA	(Coombs et al., 1973)
	Saccharum officinarum (NADP-ME) C_4 species		5 mM malate Inhibition of PEPC (% activity compared to control) 17.7 %		(Nishikido and Takanashi, 1973)
	Salsola richteri (NADP-ME) C_4 species		I_{50}-malate 2.17 mM (pH 7.2, 0.1 mM PEP)		(Lara et al., 2006)

		PEPC inhibition kinetics			
		Inhibition by L-malate and/or L-aspartate		Notes	Reference
	Species	+ G6P or other activator where mentioned	- G6P		
Plants	*Setaria italica* (NADP-ME) C_4 species		K_i malate: 5 mM (pH 8.0; 30 °C) K_i OAA: 1 mM (pH 8.0; 30 °C) K_i malonate: 2.15 mM (pH 8.0; 30 °C)		(Raghavendra and Das, 1975)
	Sorghum bicolor (NADP-ME) C_4 species		5 mM malate Inhibition of PEPC (% activity compared to control) 35.2 %		(Nishikido and Takanashi, 1973)
	Zea mays (NADP-ME) C_4 species	10 mM G6P $I_{0.5}$ L malate: 10 mM (pH 7.3, 30 °C)	$I_{0.5}$ L malate: 0.82 mM (pH 7.3, 30 °C)		(Dong et al., 1998)
		5 mM G6P: K_i malate: 0.95 mM (illuminated leaves) 0.32 mM (darkened leaves) (pH 7.0) Dimer/tetramer form had no effect on K_i			(McNaughton et al., 1989)
			Inhibition of PEPC (% of control) 1 mM malate: 58 % (pH 7.6; 37 °C) 5mM malate: 27 % (pH 7.6; 37 °C) 1 mM aspartate: 45 % (pH 7.6; 37 °C) 5 mM aspartate: 34 % (pH 7.6; 37 °C)		(Huber and Edwards, 1975)
			2 mM L-malate: K_mPEP: 37.1 mM; V_{max}: 11.4 µM PEP min^{-1} mg^{-1} (pH 7.0, 25 °C) K_mPEP: 1.06 mM; V_{max}: 19.4 µM PEP min^{-1} mg^{-1} (pH 8.0, 25 °C) 2 mM L-aspartate: K_mPEP: 59.4 mM; V_{max}: 10.8 µM PEP min^{-1} mg^{-1} (pH 7.0, 25 °C) K_mPEP: 0.89 mM; V_{max}: 16.8 µM PEP min^{-1} mg^{-1} (pH 8.0, 25 °C)		(Frank et al., 2001)
			$I_{0.5}$ malate: 1.60 mM (pH 7.3) $I_{0.5}$ aspartate: 0.74 mM (pH 7.3)		(Endo et al., 2008)

		PEPC inhibition kinetics			
		Inhibition by L-malate and/or L-aspartate		Notes	Reference
	Species	+ G6P or other activator where mentioned	- G6P		
Plants	*Zea mays* (NADP-ME) C_4 species	5 mM G6P $I_{0.5}$ malate Phosphorylated: ` 10.2 mM (pH 7.3; 30 °C) Non-phosphorylated: 6.6 mM (pH 7.3; 30 °C)	$I_{0.5}$ malate: Phosphorylated: 8.1 mM (pH 7.3; 30 °C) Non-phosphorylated: 1.8 mM (pH 7.3; 30 °C)		(Takahashi-Terada et al., 2005)
			5 mM malate Inhibition of PEPC (% activity compared to control) 25.5 %		(Nishikido and Takanashi, 1973)
	Panicum maximum (PEPCK) C_4 species		Inhibition of PEPC (% of control) 1 mM malate: 71 % (pH 7.6; 37 °C) 5mM malate: 54 % (pH 7.6; 37 °C) 1 mM aspartate: 61 % (pH 7.6; 37 °C) 5 mM aspartate: 56 % (pH 7.6; 37 °C)		(Huber and Edwards, 1975)
	Urochloa panicoides (PEPCK) C_4 species		Inhibition of PEPC (% of control) 1 mM malate: 78 % (pH 7.6; 37 °C) 5mM malate: 38 % (pH 7.6; 37 °C) 1 mM aspartate: 77 % (pH 7.6; 37 °C) 5 mM aspartate: 68 % (pH 7.6; 37 °C)		(Huber and Edwards, 1975)

Appendix 3: Alignment of seven *Setaria viridis* PEPC, *Sorghum bicolor* PEPC and codon modified PEPC sequences.

Alignment of the seven *Setaria viridis* PEPC sequences (Sevir.4G143500.1, Sevir.1G020600.1, Sevir.2G179400.1, Sevir.5G328100.2, Sevir.5G328100.1, Sevir.5G145500.1, and Sevir.5G072900.1), the original *S. bicolor* PEPC sequence and the codon modified *S. bicolor* PEPC sequence. The codons of the *Setaria viridis* PEPCs were used as a guide for the selection of the codon for each amino acid in codon modified PEPC of *S. bicolor*. Where possible, a codon that was not used in one of the seven *S. viridis* PEPC sequences was selected. Where possible the rough ratio of codons used in the *S. bicolor* codon modified PEPC was kept the same as in *Setaria viridis* Rubisco activase (Figure 5.9).

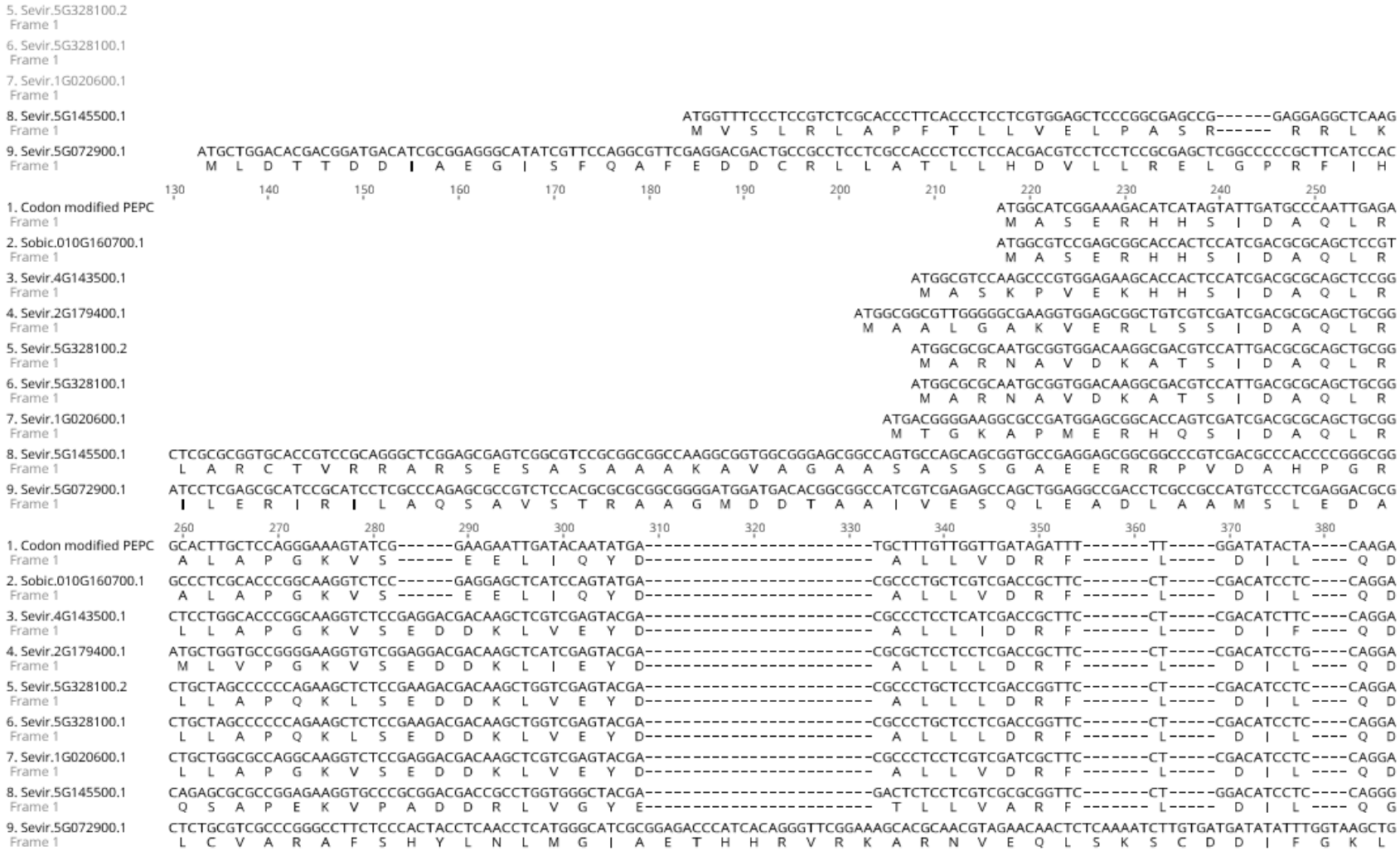
5. Sevir.5G328100.2
Frame 1
6. Sevir.5G328100.1
Frame 1
7. Sevir.1G020600.1
Frame 1
8. Sevir.5G145500.1
Frame 1
ATGGTTTCCCTCCGTCTCGCACCCTTCACCCTCCTCGTGGAGCTCCCGGCGAGCCG------GAGGAGGCTCAAG
M V S L R L A P F T L L V E L P A S R------ R R L K
9. Sevir.5G072900.1
Frame 1
ATGCTGGACACGACGGATGACATCGCGGAGGGCATATCGTTCCAGGCGTTCGAGGACGACTGCCGCCTCCTCGCCACCCTCCTCCACGACGTCCTCCTCCGCGAGCTCGGCCCCCGCTTCATCCAC
M L D T T D D I A E G I S F Q A F E D D C R L L A T L L H D V L L R E L G P R F I H
130
140
150
160
170
180
190
200
210
220
230
240
250
1. Codon modified PEPC
Frame 1
ATGGCATCGGAAAGACATCATAGTATTGATGCCCAATTGAGA
M A S E R H H S I D A Q L R
2. Sobic.010G160700.1
Frame 1
ATGGCGTCCGAGCGGCACCACTCCATCGACGCGCAGCTCCGT
M A S E R H H S I D A Q L R
3. Sevir.4G143500.1
Frame 1
ATGGCGTCCAAGCCCGTGGAGAAGCACCACTCCATCGACGCGCAGCTCCGG
M A S K P V E K H H S I D A Q L R
4. Sevir.2G179400.1
Frame 1
ATGGCGGCGTTGGGGGCGAAGGTGGAGCGGCTGTCGTCGATCGACGCGCAGCTGCGG
M A A L G A K V E R L S S I D A Q L R
5. Sevir.5G328100.2
Frame 1
ATGGCGCGCAATGCGGTGGACAAGGCGACGTCCATTGACGCGCAGCTGCGG
M A R N A V D K A T S I D A Q L R
6. Sevir.5G328100.1
Frame 1
ATGGCGCGCAATGCGGTGGACAAGGCGACGTCCATTGACGCGCAGCTGCGG
M A R N A V D K A T S I D A Q L R
7. Sevir.1G020600.1
Frame 1
ATGACGGGGAAGGCGCCGATGGAGCGGCACCAGTCGATCGACGCGCAGCTGCGG
M T G K A P M E R H Q S I D A Q L R
8. Sevir.5G145500.1
Frame 1
CTCGCGCGGTGCACCGTCCGCAGGGCTCGGAGCGAGTCGGCGTCCGCGGCGGCCAAGGCGGTGGCGGGAGCGGCCAGTGCCAGCAGCGGTGCCGAGGAGCGGCGGCCCGTCGACGCCCACCCCGGGCGG
L A R C T V R R A R S E S A S A A A K A V A G A A S A S S G A E E R R P V D A H P G R
9. Sevir.5G072900.1
Frame 1
ATCCTCGAGCGCATCCGCATCCTCGCCCAGAGCGCCGTCTCCACGCGCGCGGCGGGGATGGATGACACGGCGGCCATCGTCGAGAGCCAGCTGGAGGCCGACCTCGCCGCCATGTCCCTCGAGGACGCG
I L E R I R I L A Q S A V S T R A A G M D D T A A I V E S Q L E A D L A A M S L E D A
260
270
280
290
300
310
320
330
340
350
360
370
380
1. Codon modified PEPC
Frame 1
GCACTTGCTCCAGGGAAAGTATCG------GAAGAATTGATACAATATGA----------TGCTTTGTTGGTTGATAGATTT-------TT-----GGATATACTA----CAAGA
A L A P G K V S ------ E E L I Q Y D---------- A L L V D R F ------- L----- D I L ---- Q D
2. Sobic.010G160700.1
Frame 1
GCCCTCGCACCCGGCAAGGTCTCC------GAGGAGCTCATCCAGTATGA----------CGCCCTGCTCGTCGACCGCTTC-------CT-----CGACATCCTC----CAGGA
A L A P G K V S ------ E E L I Q Y D---------- A L L V D R F ------- L----- D I L ---- Q D
3. Sevir.4G143500.1
Frame 1
CTCCTGGCACCCGGCAAGGTCTCCGAGGACGACAAGCTCGTCGAGTACGA----------CGCCCTCCTCATCGACCGCTTC-------CT-----CGACATCTTC----CAGGA
L L A P G K V S E D D K L V E Y D---------- A L L I D R F ------- L----- D I F ---- Q D
4. Sevir.2G179400.1
Frame 1
ATGCTGGTGCCGGGGAAGGTGTCGGAGGACGACAAGCTCATCGAGTACGA----------CGCGCTCCTCCTCGACCGCTTC-------CT-----CGACATCCTG----CAGGA
M L V P G K V S E D D K L I E Y D---------- A L L L D R F ------- L----- D I L ---- Q D
5. Sevir.5G328100.2
Frame 1
CTGCTAGCCCCCCAGAAGCTCTCCGAAGACGACAAGCTGGTCGAGTACGA----------CGCCCTGCTCCTCGACCGGTTC-------CT-----CGACATCCTC----CAGGA
L L A P Q K L S E D D K L V E Y D---------- A L L L D R F ------- L----- D I L ---- Q D
6. Sevir.5G328100.1
Frame 1
CTGCTAGCCCCCCAGAAGCTCTCCGAAGACGACAAGCTGGTCGAGTACGA----------CGCCCTGCTCCTCGACCGGTTC-------CT-----CGACATCCTC----CAGGA
L L A P Q K L S E D D K L V E Y D---------- A L L L D R F ------- L----- D I L ---- Q D
7. Sevir.1G020600.1
Frame 1
CTGCTGGCGCCAGGCAAGGTCTCCGAGGACGACAAGCTCGTCGAGTACGA----------CGCCCTCCTCGTCGATCGCTTC-------CT-----CGACATCCTC----CAGGA
L L A P G K V S E D D K L V E Y D---------- A L L V D R F ------- L----- D I L ---- Q D
8. Sevir.5G145500.1
Frame 1
CAGAGCGCGCCGGAGAAGGTGCCCGCGGACGACCGCCTGGTGGGCTACGA----------GACTCTCCTCGTCGCGCGGTTC-------CT-----GGACATCCTC----CAGGG
Q S A P E K V P A D D R L V G Y E---------- T L L V A R F ------- L----- D I L ---- Q G
9. Sevir.5G072900.1
Frame 1
CTCTGCGTCGCCCGGGCCTTCTCCCACTACCTCAACCTCATGGGCATCGCGGAGACCCATCACAGGGTTCGGAAAGCACGCAACGTAGAACAACTCTCAAAATCTTGTGATGATATATTTGGTAAGCTG
L C V A R A F S H Y L N L M G I A E T H H R V R K A R N V E Q L S K S C D D I F G K L

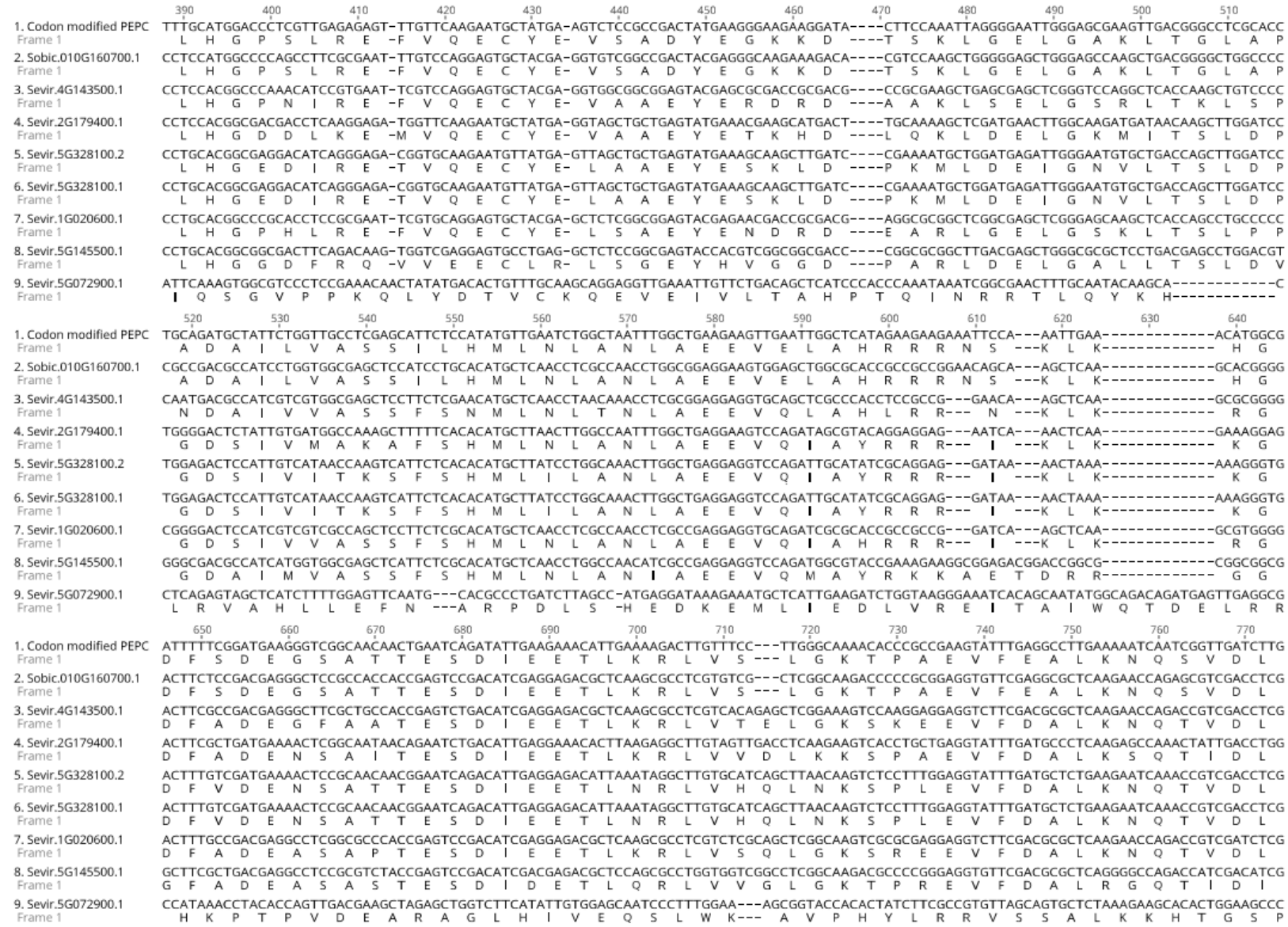
390 400 410 420 430 440 450 460 470 480 490 500 510
1. Codon modified PEPC
Frame 1
TTTGCATGGACCCTCGTTGAGAGAGT-TTGTTCAAGAATGCTATGA-AGTCTCCGCCGACTATGAAGGGAAGAAGGATA----CTTCCAAATTAGGGGAATTGGGAGCGAAGTTGACGGGCCTCGCACC
L H G P S L R E -F V Q E C Y E- V S A D Y E G K K D ----T S K L G E L G A K L T G L A P
2. Sobic.010G160700.1
CCTCCATGGCCCCAGCCTTCGCGAAT-TTGTCCAGGAGTGCTACGA-GGTGTCGGCCGACTACGAGGGCAAGAAAGACA----CGTCCAAGCTGGGGGAGCTGGGAGCCAAGCTGACGGGGCTGGCCCC
L H G P S L R E -F V Q E C Y E- V S A D Y E G K K D ----T S K L G E L G A K L T G L A P
3. Sevir.4G143500.1
CCTCCACGGCCCAAACATCCGTGAAT-TCGTCCAGGAGTGCTACGA-GGTGGCGGCGGAGTACGAGCGCGACCGCGACG----CCGCGAAGCTGAGCGAGCTCGGGTCCAGGCTCACCAAGCTGTCCCC
L H G P N I R E -F V Q E C Y E- V A A E Y E R D R D ----A A K L S E L G S R L T K L S P
4. Sevir.2G179400.1
CCTCCACGGCGACGACCTCAAGGAGA-TGGTTCAAGAATGCTATGA-GGTAGCTGCTGAGTATGAAACGAAGCATGACT----TGCAAAAGCTCGATGAACTTGGCAAGATGATAACAAGCTTGGATCC
L H G D D L K E -M V Q E C Y E- V A A E Y E T K H D ----L Q K L D E L G K M I T S L D P
5. Sevir.5G328100.2
CCTGCACGGCGAGGACATCAGGGAGA-CGGTGCAAGAATGTTATGA-GTTAGCTGCTGAGTATGAAAGCAAGCTTGATC----CGAAAATGCTGGATGAGATTGGGAATGTGCTGACCAGCTTGGATCC
L H G E D I R E -T V Q E C Y E- L A A E Y E S K L D ----P K M L D E I G N V L T S L D P
6. Sevir.5G328100.1
CCTGCACGGCGAGGACATCAGGGAGA-CGGTGCAAGAATGTTATGA-GTTAGCTGCTGAGTATGAAAGCAAGCTTGATC----CGAAAATGCTGGATGAGATTGGGAATGTGCTGACCAGCTTGGATCC
L H G E D I R E -T V Q E C Y E- L A A E Y E S K L D ----P K M L D E I G N V L T S L D P
7. Sevir.1G020600.1
CCTGCACGGCCCGCACCTCCGCGAAT-TCGTGCAGGAGTGCTACGA-GCTCTCGGCGGAGTACGAGAACGACCGCGACG----AGGCGCGGCTCGGCGAGCTCGGGAGCAAGCTCACCAGCCTGCCCCC
L H G P H L R E -F V Q E C Y E- L S A E Y E N D R D ----E A R L G E L G S K L T S L P P
8. Sevir.5G145500.1
CCTGCACGGCGGCGACTTCAGACAAG-TGGTCGAGGAGTGCCTGAG-GCTCTCCGGCGAGTACCACGTCGGCGGCGACC----CGGCGCGGCTTGACGAGCTGGGCGCGCTCCTGACGAGCCTGGACGT
L H G G D F R Q -V V E E C L R- L S G E Y H V G G D ----P A R L D E L G A L L T S L D V
9. Sevir.5G072900.1
ATTCAAAGTGGCGTCCCTCCGAAACAACTATATGACACTGTTTGCAAGCAGGAGGTTGAAATTGTTCTGACAGCTCATCCCACCCAAATAAATCGGCGAACTTTGCAATACAAGCA----------C
I Q S G V P P K Q L Y D T V C K Q E V E I V L T A H P T Q I N R R T L Q Y K H----------
520 530 540 550 560 570 580 590 600 610 620 630 640
1. Codon modified PEPC
Frame 1
TGCAGATGCTATTCTGGTTGCCTCGAGCATTCTCCATATGTTGAATCTGGCTAATTTGGCTGAAGAAGTTGAATTGGCTCATAGAAGAAGAAATTCCA---AATTGAA----------ACATGGCG
A D A I L V A S S I L H M L N L A N L A E E V E L A H R R R N S ---K L K---------- H G
2. Sobic.010G160700.1
CGCCGACGCCATCCTGGTGGCGAGCTCCATCCTGCACATGCTCAACCTCGCCAACCTGGCGGAGGAAGTGGAGCTGGCGCACCGCCGCCGGAACAGCA---AGCTCAA----------GCACGGGG
A D A I L V A S S I L H M L N L A N L A E E V E L A H R R R N S ---K L K---------- H G
3. Sevir.4G143500.1
CAATGACGCCATCGTCGTGGCGAGCTCCTTCTCGAACATGCTCAACCTAACAAACCTCGCGGAGGAGGTGCAGCTCGCCCACCTCCGCCG---GAACA---AGCTCAA----------GCGCGGGG
N D A I V V A S S F S N M L N L T N L A E E V Q L A H L R R--- N ---K L K---------- R G
4. Sevir.2G179400.1
TGGGGACTCTATTGTGATGGCCAAAGCTTTTTCACACATGCTTAACTTGGCCAATTTGGCTGAGGAAGTCCAGATAGCGTACAGGAGGAG---AATCA---AACTCAA----------GAAAGGAG
G D S I V M A K A F S H M L N L A N L A E E V Q I A Y R R R--- I ---K L K---------- K G
5. Sevir.5G328100.2
TGGAGACTCCATTGTCATAACCAAGTCATTCTCACACATGCTTATCCTGGCAAACTTGGCTGAGGAGGTCCAGATTGCATATCGCAGGAG---GATAA---AACTAAA----------AAAGGGTG
G D S I V I T K S F S H M L I L A N L A E E V Q I A Y R R R--- I ---K L K---------- K G
6. Sevir.5G328100.1
TGGAGACTCCATTGTCATAACCAAGTCATTCTCACACATGCTTATCCTGGCAAACTTGGCTGAGGAGGTCCAGATTGCATATCGCAGGAG---GATAA---AACTAAA----------AAAGGGTG
G D S I V I T K S F S H M L I L A N L A E E V Q I A Y R R R--- I ---K L K---------- K G
7. Sevir.1G020600.1
CGGGGACTCCATCGTCGTCGCCAGCTCCTTCTCGCACATGCTCAACCTCGCCAACCTCGCCGAGGAGGTGCAGATCGCGCACCGCCGCCG---GATCA---AGCTCAA----------GCGTGGGG
G D S I V V A S S F S H M L N L A N L A E E V Q I A H R R R--- I ---K L K---------- R G
8. Sevir.5G145500.1
GGGCGACGCCATCATGGTGGCGAGCTCATTCTCGCACATGCTCAACCTGGCCAACATCGCCGAGGAGGTCCAGATGGCGTACCGAAAGAAGGCGGAGACGGACCGGCG----------CGGCGGCG
G D A I M V A S S F S H M L N L A N I A E E V Q M A Y R K K A E T D R R---------- G G
9. Sevir.5G072900.1
CTCAGAGTAGCTCATCTTTTGGAGTTCAATG---CACGCCCTGATCTTAGCC-ATGAGGATAAAGAAATGCTCATTGAAGATCTGGTAAGGGAAATCACAGCAATATGGCAGACAGATGAGTTGAGGCG
L R V A H L L E F N ---A R P D L S -H E D K E M L I E D L V R E I T A I W Q T D E L R R
650 660 670 680 690 700 710 720 730 740 750 760 770
1. Codon modified PEPC
Frame 1
ATTTTTCGGATGAAGGGTCGGCAACAACTGAATCAGATATTGAAGAAACATTGAAAAGACTTGTTTCC---TTGGGCAAAACACCCGCCGAAGTATTTGAGGCCTTGAAAAATCAATCGGTTGATCTTG
D F S D E G S A T T E S D I E E T L K R L V S ---L G K T P A E V F E A L K N Q S V D L
2. Sobic.010G160700.1
ACTTCTCCGACGAGGGCTCCGCCACCACCGAGTCCGACATCGAGGAGACGCTCAAGCGCCTCGTGTCG---CTCGGCAAGACCCCCGCGGAGGTGTTCGAGGCGCTCAAGAACCAGAGCGTCGACCTCG
D F S D E G S A T T E S D I E E T L K R L V S ---L G K T P A E V F E A L K N Q S V D L
3. Sevir.4G143500.1
ACTTCGCCGACGAGGGCTTCGCTGCCACCGAGTCTGACATCGAGGAGACGCTCAAGCGCCTCGTCACAGAGCTCGGAAAGTCCAAGGAGGAGGTCTTCGACGCGCTCAAGAACCAGACCGTCGACCTCG
D F A D E G F A A T E S D I E E T L K R L V T E L G K S K E E V F D A L K N Q T V D L
4. Sevir.2G179400.1
ACTTCGCTGATGAAAACTCGGCAATAACAGAATCTGACATTGAGGAAACACTTAAGAGGCTTGTAGTTGACCTCAAGAAGTCACCTGCTGAGGTATTTGATGCCCTCAAGAGCCAAACTATTGACCTGG
D F A D E N S A I T E S D I E E T L K R L V V D L K K S P A E V F D A L K S Q T I D L
5. Sevir.5G328100.2
ACTTTGTCGATGAAAACTCCGCAACAACGGAATCAGACATTGAGGAGACATTAAATAGGCTTGTGCATCAGCTTAACAAGTCTCCTTTGGAGGTATTTGATGCTCTGAAGAATCAAACCGTCGACCTCG
D F V D E N S A T T E S D I E E T L N R L V H Q L N K S P L E V F D A L K N Q T V D L
6. Sevir.5G328100.1
ACTTTGTCGATGAAAACTCCGCAACAACGGAATCAGACATTGAGGAGACATTAAATAGGCTTGTGCATCAGCTTAACAAGTCTCCTTTGGAGGTATTTGATGCTCTGAAGAATCAAACCGTCGACCTCG
D F V D E N S A T T E S D I E E T L N R L V H Q L N K S P L E V F D A L K N Q T V D L
7. Sevir.1G020600.1
ACTTTGCCGACGAGGCCTCGGCGCCCACCGAGTCCGACATCGAGGAGACGCTCAAGCGCCTCGTCTCGCAGCTCGGCAAGTCGCGCGAGGAGGTCTTCGACGCGCTCAAGAACCAGACCGTCGATCTCG
D F A D E A S A P T E S D I E E T L K R L V S Q L G K S R E E V F D A L K N Q T V D L
8. Sevir.5G145500.1
GCTTCGCTGACGAGGCCTCCGCGTCTACCGAGTCCGACATCGACGAGACGCTCCAGCGCCTGGTGGTCGGCCTCGGCAAGACGCCCCGGGAGGTGTTCGACGCGCTCAGGGGCCAGACCATCGACATCG
G F A D E A S A S T E S D I D E T L Q R L V V G L G K T P R E V F D A L R G Q T I D I
9. Sevir.5G072900.1
CCATAAACCTACACCAGTTGACGAAGCTAGAGCTGGTCTTCATATTGTGGAGCAATCCCTTTGGAA---AGCGGTACCACACTATCTTCGCCGTGTTAGCAGTGCTCTAAAGAAGCACACTGGAAGCCC
H K P T P V D E A R A G L H I V E Q S L W K--- A V P H Y L R R V S S A L K K H T G S P

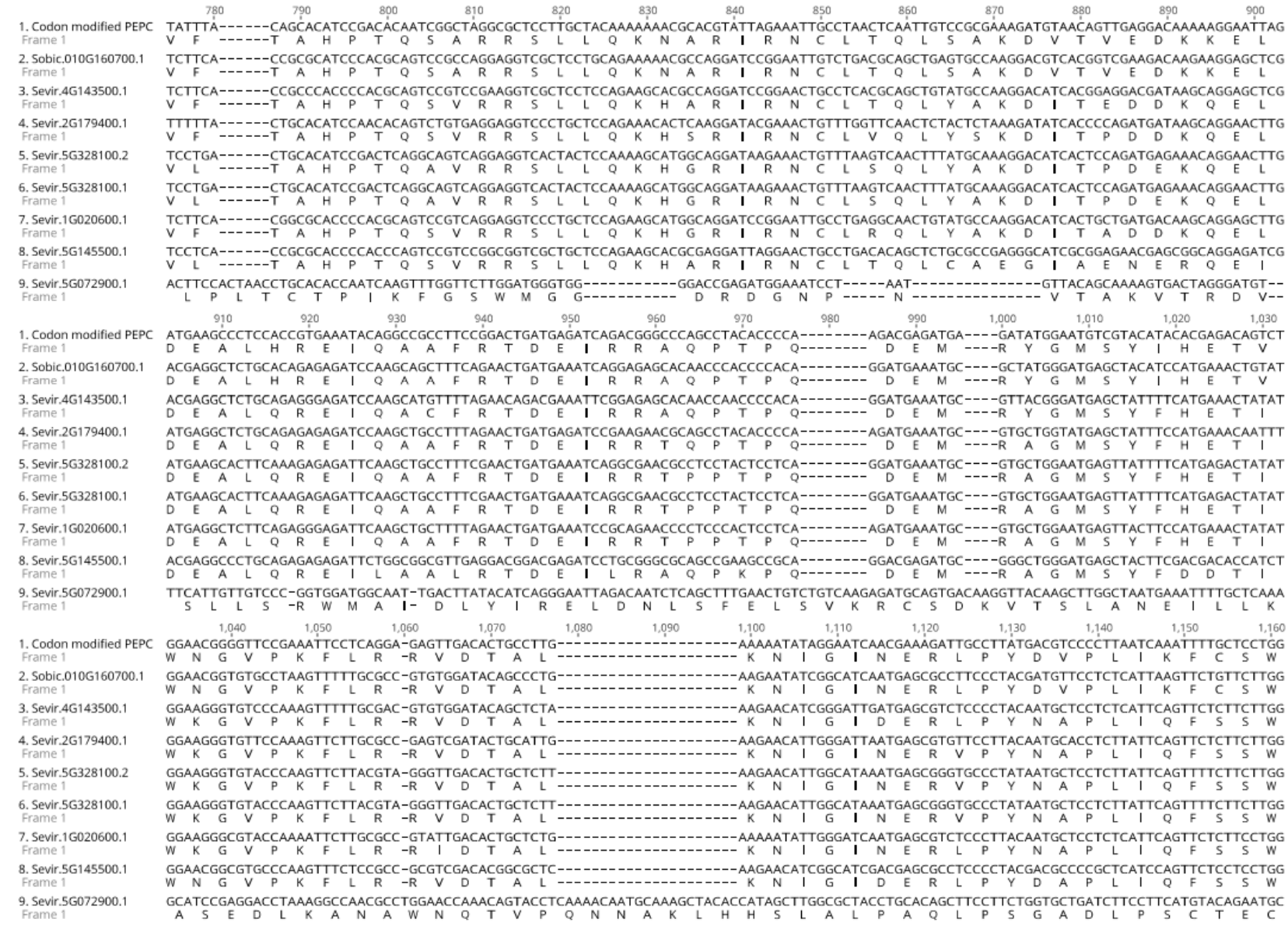
780 790 800 810 820 830 840 850 860 870 880 890 900
1. Codon modified PEPC
Frame 1
2. Sobic.010G160700.1
Frame 1
3. Sevir.4G143500.1
Frame 1
4. Sevir.2G179400.1
Frame 1
5. Sevir.5G328100.2
Frame 1
6. Sevir.5G328100.1
Frame 1
7. Sevir.1G020600.1
Frame 1
8. Sevir.5G145500.1
Frame 1
9. Sevir.5G072900.1
Frame 1
910 920 930 940 950 960 970 980 990 1,000 1,010 1,020 1,030
1. Codon modified PEPC
Frame 1
2. Sobic.010G160700.1
Frame 1
3. Sevir.4G143500.1
Frame 1
4. Sevir.2G179400.1
Frame 1
5. Sevir.5G328100.2
Frame 1
6. Sevir.5G328100.1
Frame 1
7. Sevir.1G020600.1
Frame 1
8. Sevir.5G145500.1
Frame 1
9. Sevir.5G072900.1
Frame 1
1,040 1,050 1,060 1,070 1,080 1,090 1,100 1,110 1,120 1,130 1,140 1,150 1,160
1. Codon modified PEPC
Frame 1
2. Sobic.010G160700.1
Frame 1
3. Sevir.4G143500.1
Frame 1
4. Sevir.2G179400.1
Frame 1
5. Sevir.5G328100.2
Frame 1
6. Sevir.5G328100.1
Frame 1
7. Sevir.1G020600.1
Frame 1
8. Sevir.5G145500.1
Frame 1
9. Sevir.5G072900.1
Frame 1

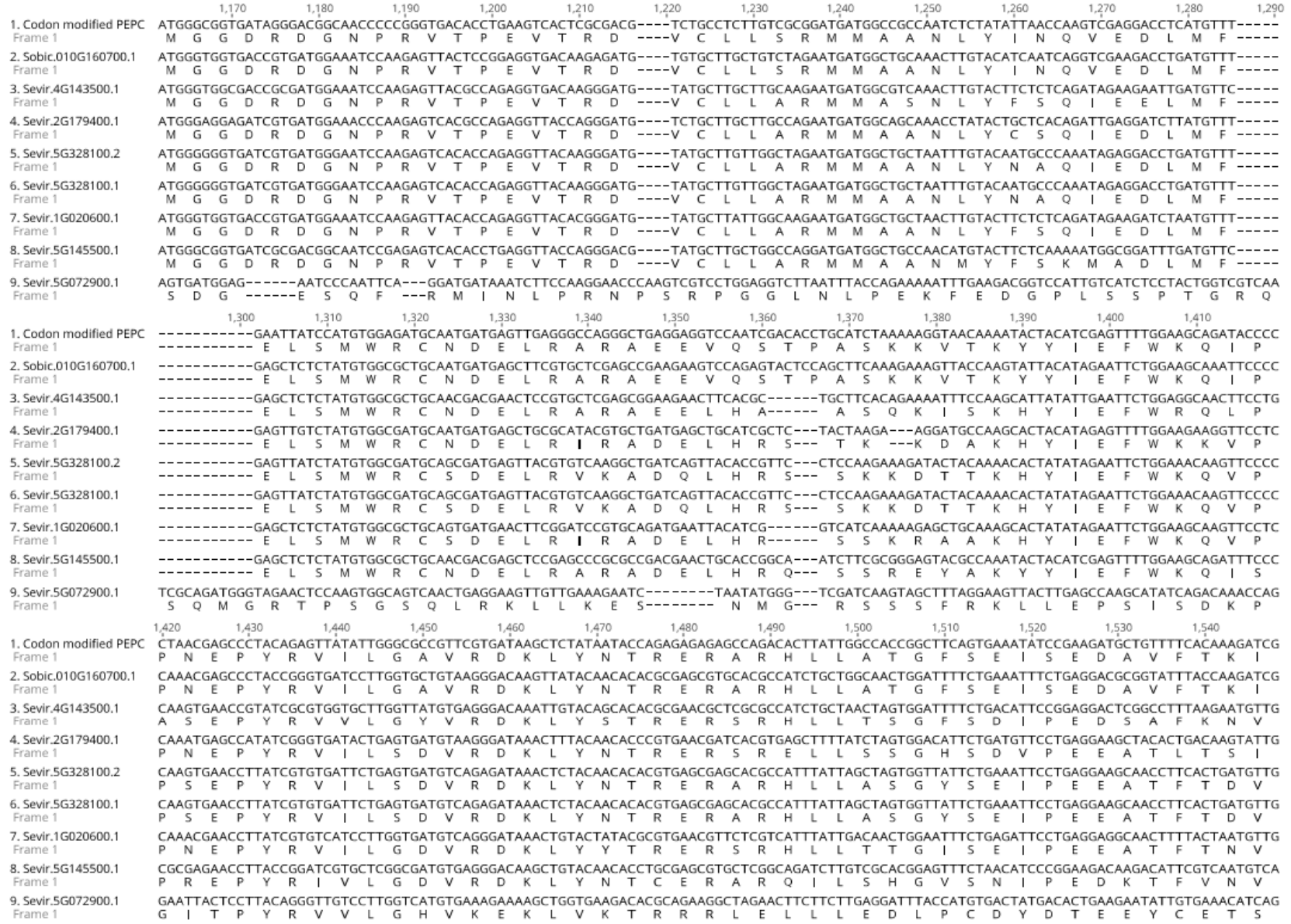
1,170 1,180 1,190 1,200 1,210 1,220 1,230 1,240 1,250 1,260 1,270 1,280 1,290
1. Codon modified PEPC
Frame 1
ATGGGCGGTGATAGGGACGGCAACCCCCGGGTGACACCTGAAGTCACTCGCGACG----TCTGCCTCTTGTCGCGGATGATGGCCGCCAATCTCTATATTAACCAAGTCGAGGACCTCATGTTT-----
M G G D R D G N P R V T P E V T R D ----V C L L S R M M A A N L Y I N Q V E D L M F -----
2. Sobic.010G160700.1
Frame 1
ATGGGTGGTGACCGTGATGGAAATCCAAGAGTTACTCCGGAGGTGACAAGAGATG----TGTGCTTGCTGTCTAGAATGATGGCTGCAAACTTGTACATCAATCAGGTCGAAGACCTGATGTTT-----
M G G D R D G N P R V T P E V T R D ----V C L L S R M M A A N L Y I N Q V E D L M F -----
3. Sevir.4G143500.1
Frame 1
ATGGGTGGCGACCGCGATGGAAATCCAAGAGTTACGCCAGAGGTGACAAGGGATG----TATGCTTGCTTGCAAGAATGATGGCGTCAAACTTGTACTTCTCTCAGATAGAAGAATTGATGTTC-----
M G G D R D G N P R V T P E V T R D ----V C L L A R M M A S N L Y F S Q I E E L M F -----
4. Sevir.2G179400.1
Frame 1
ATGGGAGGAGATCGTGATGGAAACCCAAGAGTCACGCCAGAGGTTACCAGGGATG----TCTGCTTGCTTGCCAGAATGATGGCAGCAAACCTATACTGCTCACAGATTGAGGATCTTATGTTT-----
M G G D R D G N P R V T P E V T R D ----V C L L A R M M A A N L Y C S Q I E D L M F -----
5. Sevir.5G328100.2
Frame 1
ATGGGGGGTGATCGTGATGGGAATCCAAGAGTCACACCAGAGGTTACAAGGGATG----TATGCTTGTTGGCTAGAATGATGGCTGCTAATTTGTACAATGCCCAAATAGAGGACCTGATGTTT-----
M G G D R D G N P R V T P E V T R D ----V C L L A R M M A A N L Y N A Q I E D L M F -----
6. Sevir.5G328100.1
Frame 1
ATGGGGGGTGATCGTGATGGGAATCCAAGAGTCACACCAGAGGTTACAAGGGATG----TATGCTTGTTGGCTAGAATGATGGCTGCTAATTTGTACAATGCCCAAATAGAGGACCTGATGTTT-----
M G G D R D G N P R V T P E V T R D ----V C L L A R M M A A N L Y N A Q I E D L M F -----
7. Sevir.1G020600.1
Frame 1
ATGGGTGGTGACCGTGATGGAAATCCAAGAGTTACACCAGAGGTTACACGGGATG----TATGCTTATTGGCAAGAATGATGGCTGCTAACTTGTACTTCTCTCAGATAGAAGATCTAATGTTT-----
M G G D R D G N P R V T P E V T R D ----V C L L A R M M A A N L Y F S Q I E D L M F -----
8. Sevir.5G145500.1
Frame 1
ATGGGCGGTGATCGCGACGGCAATCCGAGAGTCACACCTGAGGTTACCAGGGACG----TATGCTTGCTGGCCAGGATGATGGCTGCCAACATGTACTTCTCAAAAATGGCGGATTTGATGTTC-----
M G G D R D G N P R V T P E V T R D ----V C L L A R M M A A N M Y F S K M A A D L M F -----
9. Sevir.5G072900.1
Frame 1
AGTGATGGAG------AATCCCAATTCA---GGATGATAAATCTTCCAAGGAACCCAAGTCGTCCTGGAGGTCTTAATTTACCAGAAAAATTTGAAGACGGTCCATTGTCATCTCCTACTGGTCGTCAA
S D G ------E S Q F ---R M I N L P R N P S R P G G L N L P E K F E D G P L S S P T G R Q
1,300 1,310 1,320 1,330 1,340 1,350 1,360 1,370 1,380 1,390 1,400 1,410
1. Codon modified PEPC
Frame 1
----------GAATTATCCATGTGGAGATGCAATGATGAGTTGAGGGCCAGGGCTGAGGAGGTCCAATCGACACCTGCATCTAAAAAGGTAACAAAATACTACATCGAGTTTTGGAAGCAGATACCCC
---------- E L S M W R C N D E L R A R A E E V Q S T P A S K K V T K Y Y I E F W K Q I P
2. Sobic.010G160700.1
Frame 1
----------GAGCTCTCTATGTGGCGCTGCAATGATGAGCTTCGTGCTCGAGCCGAAGAAGTCCAGAGTACTCCAGCTTCAAAGAAAGTTACCAAGTATTACATAGAATTCTGGAAGCAAATTCCCC
---------- E L S M W R C N D E L R A R A E E V Q S T P A S K K V T K Y Y I E F W K Q I P
3. Sevir.4G143500.1
Frame 1
----------GAGCTCTCTATGTGGCGCTGCAACGACGAACTCCGTGCTCGAGCGGAAGAACTTCACGC------TGCTTCACAGAAAATTTCCAAGCATTATATTGAATTCTGGAGGCAACTTCCTG
---------- E L S M W R C N D E L R A R A E E L H A------ A S Q K I S K H Y I E F W R Q L P
4. Sevir.2G179400.1
Frame 1
----------GAGTTGTCTATGTGGCGATGCAATGATGAGCTGCGCATACGTGCTGATGAGCTGCATCGCTC---TACTAAGA---AGGATGCCAAGCACTACATAGAGTTTTGGAAGAAGGTTCCTC
---------- E L S M W R C N D E L R I R A D E L H R S--- T K ---K D A K H Y I E F W K K V P
5. Sevir.5G328100.2
Frame 1
----------GAGTTATCTATGTGGCGATGCAGCGATGAGTTACGTGTCAAGGCTGATCAGTTACACCGTTC---CTCCAAGAAAGATACTACAAAACACTATATAGAATTCTGGAAACAAGTTCCCC
---------- E L S M W R C S D E L R V K A D Q L H R S--- S K K D T T K H Y I E F W K Q V P
6. Sevir.5G328100.1
Frame 1
----------GAGTTATCTATGTGGCGATGCAGCGATGAGTTACGTGTCAAGGCTGATCAGTTACACCGTTC---CTCCAAGAAAGATACTACAAAACACTATATAGAATTCTGGAAACAAGTTCCCC
---------- E L S M W R C S D E L R V K A D Q L H R S--- S K K D T T K H Y I E F W K Q V P
7. Sevir.1G020600.1
Frame 1
----------GAGCTCTCTATGTGGCGCTGCAGTGATGAACTTCGGATCCGTGCAGATGAATTACATCG------GTCATCAAAAAGAGCTGCAAAGCACTATATAGAATTCTGGAAGCAAGTTCCTC
---------- E L S M W R C S D E L R I R A D E L H R------ S S K R A A K H Y I E F W K Q V P
8. Sevir.5G145500.1
Frame 1
----------GAGCTCTCTATGTGGCGCTGCAACGACGAGCTCCGAGCCCGCGCCGACGAACTGCACCGGCA---ATCTTCGCGGGAGTACGCCAAATACTACATCGAGTTTTGGAAGCAGATTTCCC
---------- E L S M W R C N D E L R A R A D E L H R Q--- S S R E Y A K Y Y I E F W K Q I S
9. Sevir.5G072900.1
Frame 1
TCGCAGATGGGTAGAACTCCAAGTGGCAGTCAACTGAGGAAGTTGTTGAAAGAATC--------TAATATGGG---TCGATCAAGTAGCTTTAGGAAGTTACTTGAGCCAAGCATATCAGACAAACCAG
S Q M G R T P S G S Q L R K L L K E S-------- N M G--- R S S S F R K L L E P S I S D K P
1,420 1,430 1,440 1,450 1,460 1,470 1,480 1,490 1,500 1,510 1,520 1,530 1,540
1. Codon modified PEPC
Frame 1
CTAACGAGCCCTACAGAGTTATATTGGGCGCCGTTCGTGATAAGCTCTATAATACCAGAGAGAGAGCCAGACACTTATTGGCCACCGGCTTCAGTGAAATATCCGAAGATGCTGTTTTCACAAAGATCG
P N E P Y R V I L G A V R D K L Y N T R E R A R H L L A T G F S E I S E D A V F T K I
2. Sobic.010G160700.1
Frame 1
CAAACGAGCCCTACCGGGTGATCCTTGGTGCTGTAAGGGACAAGTTATACAACACACGCGAGCGTGCACGCCATCTGCTGGCAACTGGATTTTCTGAAATTTCTGAGGACGCGGTATTTACCAAGATCG
P N E P Y R V I L G A V R D K L Y N T R E R A R H L L A T G F S E I S E D A V F T K I
3. Sevir.4G143500.1
Frame 1
CAAGTGAACCGTATCGCGTGGTGCTTGGTTATGTGAGGGACAAATTGTACAGCACACGCGAACGCTCGCGCCATCTGCTAACTAGTGGATTTTCTGACATTCCGGAGGACTCGGCCTTTAAGAATGTTG
A S E P Y R V V L G Y V R D K L Y S T R E R S R H L L T S G F S D I P E D S A F K N V
4. Sevir.2G179400.1
Frame 1
CAAATGAGCCATATCGGGTGATACTGAGTGATGTAAGGGATAAACTTTACAACACCCGTGAACGATCACGTGAGCTTTTATCTAGTGGACATTCTGATGTTCCTGAGGAAGCTACACTGACAAGTATTG
P N E P Y R V I L S D V R D K L Y N T R E R S R E L L S S G H S D V P E E A T L T S I
5. Sevir.5G328100.2
Frame 1
CAAGTGAACCTTATCGTGTGATTCTGAGTGATGTCAGAGATAAACTCTACAACACACGTGAGCGAGCACGCCATTTATTAGCTAGTGGTTATTCTGAAATTCCTGAGGAAGCAACCTTCACTGATGTTG
P S E P Y R V I L S D V R D K L Y N T R E R A R H L L A S G Y S E I P E E A T F T D V
6. Sevir.5G328100.1
Frame 1
CAAGTGAACCTTATCGTGTGATTCTGAGTGATGTCAGAGATAAACTCTACAACACACGTGAGCGAGCACGCCATTTATTAGCTAGTGGTTATTCTGAAATTCCTGAGGAAGCAACCTTCACTGATGTTG
P S E P Y R V I L S D V R D K L Y N T R E R A R H L L A S G Y S E I P E E A T F T D V
7. Sevir.1G020600.1
Frame 1
CAAACGAACCTTATCGTGTCATCCTTGGTGATGTCAGGGATAAACTGTACTATACGCGTGAACGTTCTCGTCATTTATTGACAACTGGAATTTCTGAGATTCCTGAGGAGGCAACTTTTACTAATGTTG
P N E P Y R V I L G D V R D K L Y Y T R E R S R H L L T T G I S E I P E E A T F T N V
8. Sevir.5G145500.1
Frame 1
CGCGAGAACCTTACCGGATCGTGCTCGGCGATGTGAGGGACAAGCTGTACAACACCTGCGAGCGTGCTCGGCAGATCTTGTCGCACGGAGTTTCTAACATCCCGGAAGACAAGACATTCGTCAATGTCA
P R E P Y R I V L G D V R D K L Y N T C E R A R Q I L S H G V S N I P E D K T F V N V
9. Sevir.5G072900.1
Frame 1
GAATTACTCCTTACAGGGTTGTCCTTGGTCATGTGAAAGAAAAGCTGGTGAAGACACGCAGAAGGCTAGAACTTCTTCTTGAGGATTTACCATGTGACTATGACACTGAAGAATATTGTGAAACATCAG
G I T P Y R V V L G H V K E K L V K T R R R L E L L L E D L P C D Y D T E E Y C E T S

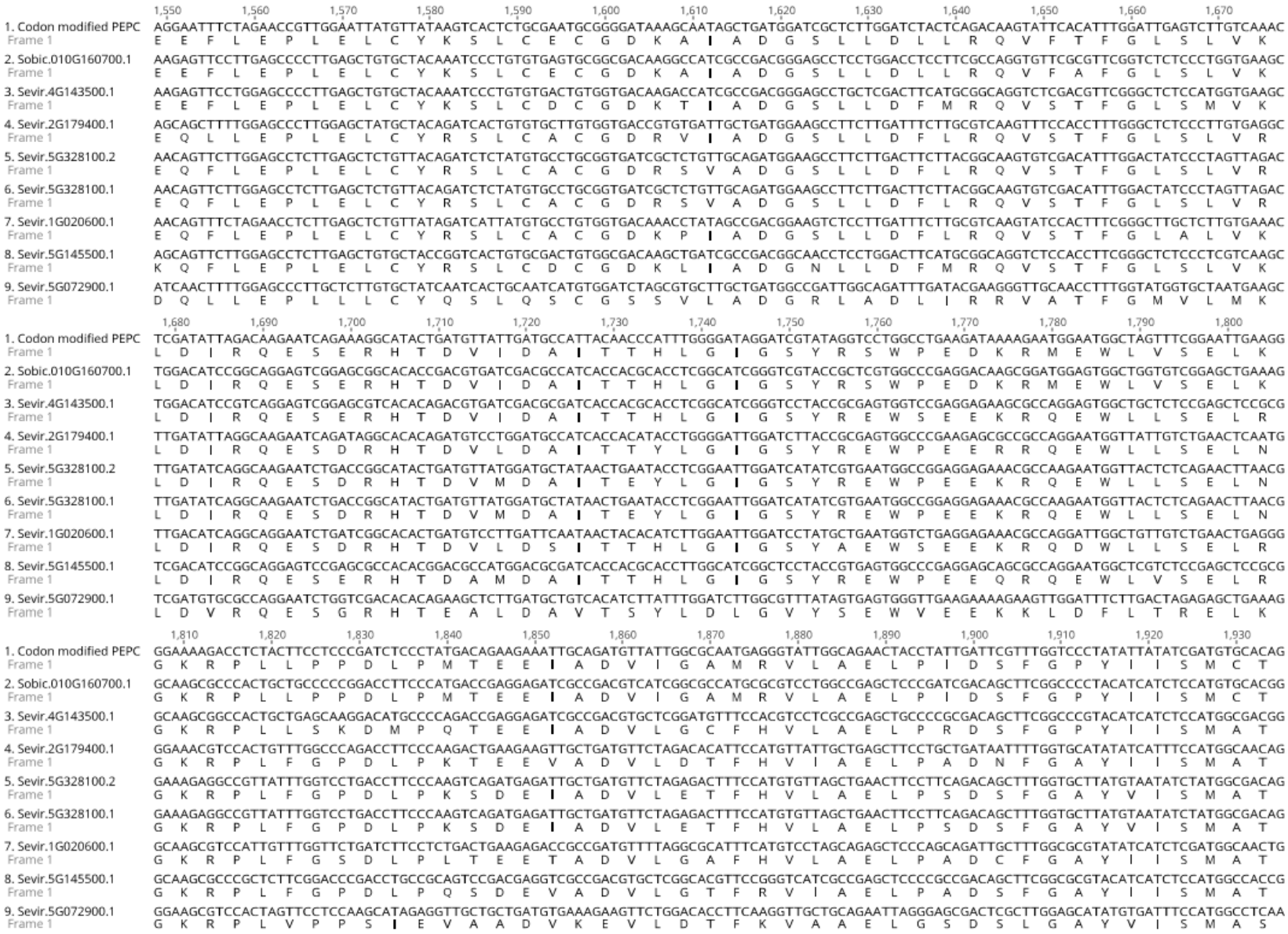
1,550 1,560 1,570 1,580 1,590 1,600 1,610 1,620 1,630 1,640 1,650 1,660 1,670
1. Codon modified PEPC
AGGAATTTCTAGAACCGTTGGAATTATGTTATAAGTCACTCTGCGAATGCGGGGATAAAGCAATAGCTGATGGATCGCTCTTGGATCTACTCAGACAAGTATTCACATTTGGATTGAGTCTTGTCAAAC
Frame 1
E E F L E P L E L C Y K S L C E C G D K A I A D G S L L D L L R Q V F T F G L S L V K
2. Sobic.010G160700.1
AAGAGTTCCTTGAGCCCCTTGAGCTGTGCTACAAATCCCTGTGTGAGTGCGGCGACAAGGCCATCGCCGACGGGAGCCTCCTGGACCTCCTTCGCCAGGTGTTCGCGTTCGGTCTCTCCCTGGTGAAGC
Frame 1
E E F L E P L E L C Y K S L C E C G D K A I A D G S L L D L L R Q V F A F G L S L V K
3. Sevir.4G143500.1
AAGAGTTCCTGGAGCCCCTTGAGCTGTGCTACAAATCCCTGTGTGACTGTGGTGACAAGACCATCGCCGACGGGAGCCTGCTCGACTTCATGCGGCAGGTCTCGACGTTCGGGCTCTCCATGGTGAAGC
Frame 1
E E F L E P L E L C Y K S L C D C G D K T I A D G S L L D F M R Q V S T F G L S M V K
4. Sevir.2G179400.1
AGCAGCTTTTGGAGCCCTTGGAGCTATGCTACAGATCACTGTGTGCTTGTGGTGACCGTGTGATTGCTGATGGAAGCCTTCTTGATTTCTTGCGTCAAGTTTCCACCTTTGGGCTCTCCCTTGTGAGGC
Frame 1
E Q L L E P L E L C Y R S L C A C G D R V I A D G S L L D F L R Q V S T F G L S L V R
5. Sevir.5G328100.2
AACAGTTCTTGGAGCCTCTTGAGCTCTGTTACAGATCTCTATGTGCCTGCGGTGATCGCTCTGTTGCAGATGGAAGCCTTCTTGACTTCTTACGGCAAGTGTCGACATTTGGACTATCCCTAGTTAGAC
Frame 1
E Q F L E P L E L C Y R S L C A C G D R S V A D G S L L D F L R Q V S T F G L S L V R
6. Sevir.5G328100.1
AACAGTTCTTGGAGCCTCTTGAGCTCTGTTACAGATCTCTATGTGCCTGCGGTGATCGCTCTGTTGCAGATGGAAGCCTTCTTGACTTCTTACGGCAAGTGTCGACATTTGGACTATCCCTAGTTAGAC
Frame 1
E Q F L E P L E L C Y R S L C A C G D R S V A D G S L L D F L R Q V S T F G L S L V R
7. Sevir.1G020600.1
AACAGTTTCTAGAACCTCTTGAGCTCTGTTATAGATCATTATGTGCCTGTGGTGACAAACCTATAGCCGACGGAAGTCTCCTTGATTTCTTGCGTCAAGTATCCACTTTCGGGCTTGCTCTTGTGAAAC
Frame 1
E Q F L E P L E L C Y R S L C A C G D K P I A D G S L L D F L R Q V S T F G L A L V K
8. Sevir.5G145500.1
AGCAGTTCTTGGAGCCTCTTGAGCTGTGCTACCGGTCACTGTGCGACTGTGGCGACAAGCTGATCGCCGACGGCAACCTCCTGGACTTCATGCGGCAGGTCTCCACCTTCGGGCTCTCCCTCGTCAAGC
Frame 1
K Q F L E P L E L C Y R S L C D C G D K L I A D G N L L D F M R Q V S T F G L S L V K
9. Sevir.5G072900.1
ATCAACTTTTGGAGCCCTTGCTCTTGTGCTATCAATCACTGCAATCATGTGGATCTAGCGTGCTTGCTGATGGCCGATTGGCAGATTTGATACGAAGGGTTGCAACCTTTGGTATGGTGCTAATGAAGC
Frame 1
D Q L L E P L L L C Y Q S L Q S C G S S V L A D G R L A D L I R R V A T F G M V L M K
1,680 1,690 1,700 1,710 1,720 1,730 1,740 1,750 1,760 1,770 1,780 1,790 1,800
1. Codon modified PEPC
TCGATATTAGACAAGAATCAGAAAGGCATACTGATGTTATTGATGCCATTACAACCCATTTGGGGATAGGATCGTATAGGTCCTGGCCTGAAGATAAAAGAATGGAATGGCTAGTTTCGGAATTGAAGG
Frame 1
L D I R Q E S E R H T D V I D A I T T H L G I G S Y R S W P E D K R M E W L V S E L K
2. Sobic.010G160700.1
TGGACATCCGGCAGGAGTCGGAGCGGCACACCGACGTGATCGACGCCATCACCACGCACCTCGGCATCGGGTCGTACCGCTCGTGGCCCGAGGACAAGCGGATGGAGTGGCTGGTGTCGGAGCTGAAAG
Frame 1
L D I R Q E S E R H T D V I D A I T T H L G I G S Y R S W P E D K R M E W L V S E L K
3. Sevir.4G143500.1
TGGACATCCGTCAGGAGTCGGAGCGTCACACAGACGTGATCGACGCGATCACCACGCACCTCGGCATCGGGTCCTACCGCGAGTGGTCCGAGGAGAAGCGCCAGGAGTGGCTGCTCTCCGAGCTCCGCG
Frame 1
L D I R Q E S E R H T D V I D A I T T H L G I G S Y R E W S E E K R Q E W L L S E L R
4. Sevir.2G179400.1
TTGATATTAGGCAAGAATCAGATAGGCACACAGATGTCCTGGATGCCATCACCACATACCTGGGGATTGGATCTTACCGCGAGTGGCCCGAAGAGCGCCGCCAGGAATGGTTATTGTCTGAACTCAATG
Frame 1
L D I R Q E S D R H T D V L D A I T T Y L G I G S Y R E W P E E R R Q E W L L S E L N
5. Sevir.5G328100.2
TTGATATCAGGCAAGAATCTGACCGGCATACTGATGTTATGGATGCTATAACTGAATACCTCGGAATTGGATCATATCGTGAATGGCCGGAGGAGAAACGCCAAGAATGGTTACTCTCAGAACTTAACG
Frame 1
L D I R Q E S D R H T D V M D A I T E Y L G I G S Y R E W P E E K R Q E W L L S E L N
6. Sevir.5G328100.1
TTGATATCAGGCAAGAATCTGACCGGCATACTGATGTTATGGATGCTATAACTGAATACCTCGGAATTGGATCATATCGTGAATGGCCGGAGGAGAAACGCCAAGAATGGTTACTCTCAGAACTTAACG
Frame 1
L D I R Q E S D R H T D V M D A I T E Y L G I G S Y R E W P E E K R Q E W L L S E L N
7. Sevir.1G020600.1
TTGACATCAGGCAGGAATCTGATCGGCACACTGATGTCCTTGATTCAATAACTACACATCTTGGAATTGGATCCTATGCTGAATGGTCTGAGGAGAAACGCCAGGATTGGCTGTTGTCTGAACTGAGGG
Frame 1
L D I R Q E S D R H T D V L D S I T T H L G I G S Y A E W S E E K R Q D W L L S E L R
8. Sevir.5G145500.1
TCGACATCCGGCAGGAGTCCGAGCGCCACACGGACGCCATGGACGCGATCACCACGCACCTTGGCATCGGCTCCTACCGTGAGTGGCCCGAGGAGCAGCGCCAGGAATGGCTCGTCTCCGAGCTCCGCG
Frame 1
L D I R Q E S E R H T D A M D A I T T H L G I G S Y R E W P E E Q R Q E W L V S E L R
9. Sevir.5G072900.1
TCGATGTGCGCCAGGAATCTGGTCGACACACAGAAGCTCTTGATGCTGTCACATCTTATTTGGATCTTGGCGTTTATAGTGAGTGGGTTGAAGAAAAGAAGTTGGATTTCTTGACTAGAGAGCTGAAAG
Frame 1
L D V R Q E S G R H T E A L D A V T S Y L D L G V Y S E W V E E K K L D F L T R E L K
1,810 1,820 1,830 1,840 1,850 1,860 1,870 1,880 1,890 1,900 1,910 1,920 1,930
1. Codon modified PEPC
GGAAAAGACCTCTACTTCCTCCCGATCTCCCTATGACAGAAGAAATTGCAGATGTTATTGGCGCAATGAGGGTATTGGCAGAACTACCTATTGATTCGTTTGGTCCCTATATTATATCGATGTGCACAG
Frame 1
G K R P L L P P D L P M T E E I A D V I G A M R V L A E L P I D S F G P Y I I S M C T
2. Sobic.010G160700.1
GCAAGCGCCCACTGCTGCCCCCGGACCTTCCCATGACCGAGGAGATCGCCGACGTCATCGGCGCCATGCGCGTCCTGGCCGAGCTCCCGATCGACAGCTTCGGCCCCTACATCATCTCCATGTGCACGG
Frame 1
G K R P L L P P D L P M T E E I A D V I G A M R V L A E L P I D S F G P Y I I S M C T
3. Sevir.4G143500.1
GCAAGCGGCCACTGCTGAGCAAGGACATGCCCCAGACCGAGGAGATCGCCGACGTGCTCGGATGTTTCCACGTCCTCGCCGAGCTGCCCCGCGACAGCTTCGGCCCGTACATCATCTCCATGGCGACGG
Frame 1
G K R P L L S K D M P Q T E E I A D V L G C F H V L A E L P R D S F G P Y I I S M A T
4. Sevir.2G179400.1
GGAAACGTCCACTGTTTGGCCCAGACCTTCCCAAGACTGAAGAAGTTGCTGATGTTCTAGACACATTCCATGTTATTGCTGAGCTTCCTGCTGATAATTTTGGTGCATATATCATTTCCATGGCAACAG
Frame 1
G K R P L F G P D L P K T E E V A D V L D T F H V I A E L P A D N F G A Y I I S M A T
5. Sevir.5G328100.2
GAAAGAGGCCGTTATTTGGTCCTGACCTTCCCAAGTCAGATGAGATTGCTGATGTTCTAGAGACTTTCCATGTGTTAGCTGAACTTCCTTCAGACAGCTTTGGTGCTTATGTAATATCTATGGCGACAG
Frame 1
G K R P L F G P D L P K S D E I A D V L E T F H V L A E L P S D S F G A Y V I S M A T
6. Sevir.5G328100.1
GAAAGAGGCCGTTATTTGGTCCTGACCTTCCCAAGTCAGATGAGATTGCTGATGTTCTAGAGACTTTCCATGTGTTAGCTGAACTTCCTTCAGACAGCTTTGGTGCTTATGTAATATCTATGGCGACAG
Frame 1
G K R P L F G P D L P K S D E I A D V L E T F H V L A E L P S D S F G A Y V I S M A T
7. Sevir.1G020600.1
GCAAGCGTCCATTGTTTGGTTCTGATCTTCCTCTGACTGAAGAGACCGCCGATGTTTTAGGCGCATTTCATGTCCTAGCAGAGCTCCCAGCAGATTGCTTTGGCGCGTATATCATCTCGATGGCAACTG
Frame 1
G K R P L F G S D L P L T E E T A D V L G A F H V L A E L P A D C F G A Y I I S M A T
8. Sevir.5G145500.1
GCAAGCGCCCGCTCTTCGGACCCGACCTGCCGCAGTCCGACGAGGTCGCCGACGTGCTCGGCACGTTCCGGGTCATCGCCGAGCTCCCCGCCGACAGCTTCGGCGCGTACATCATCTCCATGGCCACCG
Frame 1
G K R P L F G P D L P Q S D E V A D V L G T F R V I A E L P A D S F G A Y I I S M A T
9. Sevir.5G072900.1
GGAAGCGTCCACTAGTTCCTCCAAGCATAGAGGTTGCTGCTGATGTGAAAGAAGTTCTGGACACCTTCAAGGTTGCTGCAGAATTAGGGAGCGACTCGCTTGGAGCATATGTGATTTCCATGGCCTCAA
Frame 1
G K R P L V P P S I E V A A D V K E V L D T F K V A A E L G S D S L G A Y V I S M A S

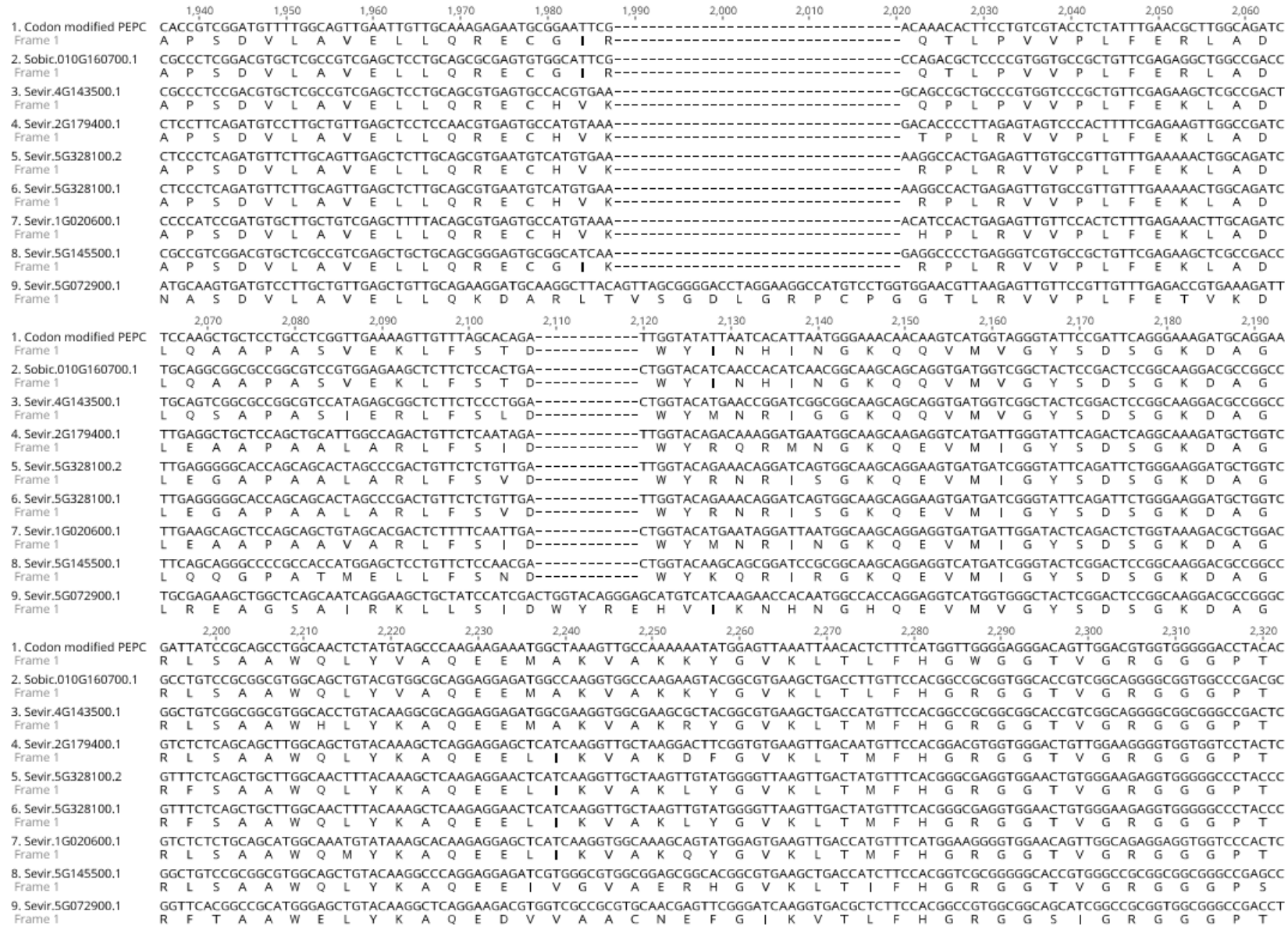
1,940 1,950 1,960 1,970 1,980 1,990 2,000 2,010 2,020 2,030 2,040 2,050 2,060
1. Codon modified PEPC
Frame 1
2. Sobic.010G160700.1
3. Sevir.4G143500.1
4. Sevir.2G179400.1
5. Sevir.5G328100.2
6. Sevir.5G328100.1
7. Sevir.1G020600.1
8. Sevir.5G145500.1
9. Sevir.5G072900.1
2,070 2,080 2,090 2,100 2,110 2,120 2,130 2,140 2,150 2,160 2,170 2,180 2,190
2,200 2,210 2,220 2,230 2,240 2,250 2,260 2,270 2,280 2,290 2,300 2,310 2,320

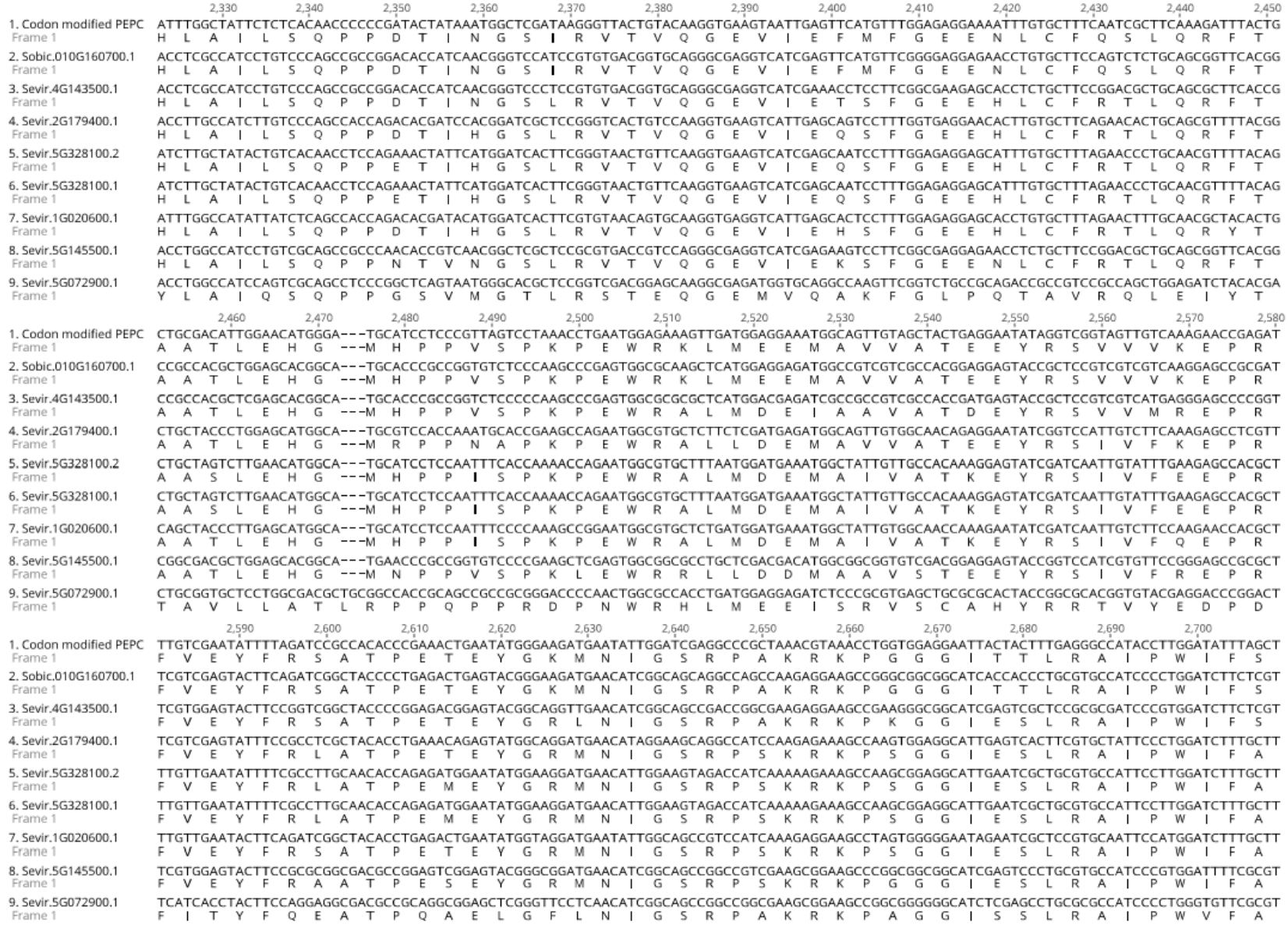
2,330 2,340 2,350 2,360 2,370 2,380 2,390 2,400 2,410 2,420 2,430 2,440 2,450
1. Codon modified PEPC
ATTTGGCTATTCTCTCACAACCCCCCGATACTATAAATGGCTCGATAAGGGTTACTGTACAAGGTGAAGTAATTGAGTTCATGTTTGGAGAGGAAAATTTGTGCTTTCAATCGCTTCAAAGATTTACTG
Frame 1
H L A I L S Q P P D T I N G S I R V T V Q G E V I E F M F G E E N L C F Q S L Q R F T
2. Sobic.010G160700.1
ACCTCGCCATCCTGTCCCAGCCGCCGGACACCATCAACGGGTCCATCCGTGTGACGGTGCAGGGCGAGGTCATCGAGTTCATGTTCGGGGAGGAGAACCTGTGCTTCCAGTCTCTGCAGCGGTTCACGG
Frame 1
H L A I L S Q P P D T I N G S I R V T V Q G E V I E F M F G E E N L C F Q S L Q R F T
3. Sevir.4G143500.1
ACCTCGCCATCCTGTCCCAGCCGCCGGACACCATCAACGGGTCCCTCCGTGTGACGGTGCAGGGCGAGGTCATCGAAACCTCCTTCGGCGAAGAGCACCTCTGCTTCCGGACGCTGCAGCGCTTCACCG
Frame 1
H L A I L S Q P P D T I N G S L R V T V Q G E V I E T S F G E E H L C F R T L Q R F T
4. Sevir.2G179400.1
ACCTTGCCATCTTGTCCCAGCCACCAGACACGATCCACGGATCGCTCCGGGTCACTGTCCAAGGTGAAGTCATTGAGCAGTCCTTTGGTGAGGAACACTTGTGCTTCAGAACACTGCAGCGTTTTACGG
Frame 1
H L A I L S Q P P D T I H G S L R V T V Q G E V I E Q S F G E E H L C F R T L Q R F T
5. Sevir.5G328100.2
ATCTTGCTATACTGTCACAACCTCCAGAAACTATTCATGGATCACTTCGGGTAACTGTTCAAGGTGAAGTCATCGAGCAATCCTTTGGAGAGGAGCATTTGTGCTTTAGAACCCTGCAACGTTTTACAG
Frame 1
H L A I L S Q P P E T I H G S L R V T V Q G E V I E Q S F G E E H L C F R T L Q R F T
6. Sevir.5G328100.1
ATCTTGCTATACTGTCACAACCTCCAGAAACTATTCATGGATCACTTCGGGTAACTGTTCAAGGTGAAGTCATCGAGCAATCCTTTGGAGAGGAGCATTTGTGCTTTAGAACCCTGCAACGTTTTACAG
Frame 1
H L A I L S Q P P E T I H G S L R V T V Q G E V I E Q S F G E E H L C F R T L Q R F T
7. Sevir.1G020600.1
ATTTGGCCATATTATCTCAGCCACCAGACACGATACATGGATCACTTCGTGTAACAGTGCAAGGTGAGGTCATTGAGCACTCCTTTGGAGAGGAGCACCTGTGCTTTAGAACTTTGCAACGCTACACTG
Frame 1
H L A I L S Q P P D T I H G S L R V T V Q G E V I E H S F G E E H L C F R T L Q R Y T
8. Sevir.5G145500.1
ACCTGGCCATCCTGTCGCAGCCGCCCAACACCGTCAACGGCTCGCTCCGCGTGACCGTCCAGGGCGAGGTCATCGAGAAGTCCTTCGGCGAGGAGAACCTCTGCTTCCGGACGCTGCAGCGGTTCACGG
Frame 1
H L A I L S Q P P N T V N G S L R V T V Q G E V I E K S F G E E N L C F R T L Q R F T
9. Sevir.5G072900.1
ACCTGGCCATCCAGTCGCAGCCTCCCGGCTCAGTAATGGGCACGCTCCGGTCGACGGAGCAAGGCGAGATGGTGCAGGCCAAGTTCGGTCTGCCGCAGACCGCCGTCCGCCAGCTGGAGATCTACACGA
Frame 1
Y L A I Q S Q P P G S V M G T L R S T E Q G E M V Q A K F G L P Q T A V R Q L E I Y T
2,460 2,470 2,480 2,490 2,500 2,510 2,520 2,530 2,540 2,550 2,560 2,570 2,580
1. Codon modified PEPC
CTGCGACATTGGAACATGGGA---TGCATCCTCCCGTTAGTCCTAAACCTGAATGGAGAAAGTTGATGGAGGAAATGGCAGTTGTAGCTACTGAGGAATATAGGTCGGTAGTTGTCAAAGAACCGAGAT
Frame 1
A A T L E H G ---M H P P V S P K P E W R K L M E E M A V V A T E E Y R S V V V K E P R
2. Sobic.010G160700.1
CCGCCACGCTGGAGCACGGCA---TGCACCCGCCGGTGTCTCCCAAGCCCGAGTGGCGCAAGCTCATGGAGGAGATGGCCGTCGTCGCCACGGAGGAGTACCGCTCCGTCGTCGTCAAGGAGCCGCGAT
Frame 1
A A T L E H G ---M H P P V S P K P E W R K L M E E M A V V A T E E Y R S V V V K E P R
3. Sevir.4G143500.1
CCGCCACGCTCGAGCACGGCA---TGCACCCGCCGGTCTCCCCCAAGCCCGAGTGGCGCGCGCTCATGGACGAGATCGCCGCCGTCCGCCACCGATGAGTACCGCTCCGTCGTCATGAGGGAGCCCCGGT
Frame 1
A A T L E H G ---M H P P V S P K P E W R A L M D E I A A V A T D E Y R S V V M R E P R
4. Sevir.2G179400.1
CTGCTACCCTGGAGCATGGCA---TGCGTCCACCAAATGCACCGAAGCCAGAATGGCGTGCTCTTCTCGATGAGATGGCAGTTGTGGCAACAGAGGAATATCGGTCCATTGTCTTCAAAGAGCCTCGTT
Frame 1
A A T L E H G ---M R P P N A P K P E W R A L L D E M A V V A T E E Y R S I V F K E P R
5. Sevir.5G328100.2
CTGCTAGTCTTGAACATGGCA---TGCATCCTCCAATTTCACCAAAACCAGAATGGCGTGCTTTAATGGATGAAATGGCTATTGTTGCCACAAAGGAGTATCGATCAATTGTATTTGAAGAGCCACGCT
Frame 1
A A S L E H G ---M H P P I S P K P E W R A L M D E M A I V A T K E Y R S I V F E E P R
6. Sevir.5G328100.1
CTGCTAGTCTTGAACATGGCA---TGCATCCTCCAATTTCACCAAAACCAGAATGGCGTGCTTTAATGGATGAAATGGCTATTGTTGCCACAAAGGAGTATCGATCAATTGTATTTGAAGAGCCACGCT
Frame 1
A A S L E H G ---M H P P I S P K P E W R A L M D E M A I V A T K E Y R S I V F E E P R
7. Sevir.1G020600.1
CAGCTACCCTTGAGCATGGCA---TGCATCCTCCAAATTTCCCCAAAGCCGGAATGGCGTGCTCTGATGGATGAAATGGCTATTGTGGCAACCAAAGAATATCGATCAATTGTCTTCCAAGAACCACGCT
Frame 1
A A T L E H G ---M H P P I S P K P E W R A L M D E M A I V A T K E Y R S I V F Q E P R
8. Sevir.5G145500.1
CGGCGACGCTGGAGCACGGCA---TGAACCCGCCGGTGTCCCCGAAGCTCGAGTGGCGGCGCCTGCTCGACGACATGGCGGCGGTGTCGACGGAGGAGTACCGGTCCATCGTGTTCCGGGAGCCGCGCT
Frame 1
A A T L E H G ---M N P P V S P K L E W R R L L D D M A A V S T E E Y R S I V F R E P R
9. Sevir.5G072900.1
CTGCGGTGCTCCTGGCGACGCTGCGGCCACCGCAGCCGCCGCGGGACCCCAACTGGCGCCACCTGATGGAGGAGATCTCCCCGCGTGAGCTGCGCGCACTACCGGCGCACGGTGTACGAGGACCCGGACT
Frame 1
T A V L L A T L R P P Q P P R D P N W R H L M E E I S R V S C A H Y R R T V Y E D P D
2,590 2,600 2,610 2,620 2,630 2,640 2,650 2,660 2,670 2,680 2,690 2,700
1. Codon modified PEPC
TTGTCGAATATTTTAGATCCGCCACACCCGAAACTGAATATGGGAAGATGAATATTGGATCGAGGCCCGCTAAACGTAAACCTGGTGGAGGAATTACTACTTTGAGGGCCATACCTTGGATATTTAGCT
Frame 1
F V E Y F R S A T P E T E Y G K M N I G S R P A K R K P G G G I T T L R A I P W I F S
2. Sobic.010G160700.1
TCGTCGAGTACTTCAGATCGGCTACCCCTGAGACTGAGTACGGGAAGATGAACATCGGCAGCAGGCCAGCCAAGAGGAAGCCGGGCGGCGGCATCACCACCCTGCGTGCCATCCCCTGGATCTTCTCGT
Frame 1
F V E Y F R S A T P E T E Y G K M N I G S R P A K R K P G G G I T T L R A I P W I F S
3. Sevir.4G143500.1
TCGTGGAGTACTTCCGGTCGGCTACCCCGGAGACGGAGTACGGCAGGTTGAACATCGGCAGCCGACCGGCGAAGAGGAAGCCGAAGGGCGGCATCGAGTCGCTCCGCGCGATCCCGTGGATCTTCTCGT
Frame 1
F V E Y F R S A T P E T E Y G R L N I G S R P A K R K P K G G I E S L R A I P W I F S
4. Sevir.2G179400.1
TCGTCGAGTATTTCCGCCTCGCTACACCTGAAACAGAGTATGGCAGGATGAACATAGGAAGCAGGCCATCCAAGAGAAAGCCAAGTGGAGGCATTGAGTCACTTCGTGCTATTCCCTGGATCTTTGCTT
Frame 1
F V E Y F R L A T P E T E Y G R M N I G S R P S K R K P S G G I E S L R A I P W I F A
5. Sevir.5G328100.2
TTGTTGAATATTTTCGCCTTGCAACACCAGAGATGGAATATGGAAGGATGAACATTGGAAGTAGACCATCAAAAAGAAAGCCAAGCGGAGGCATTGAATCGCTGCGTGCCATTCCTTGGATCTTTGCTT
Frame 1
F V E Y F R L A T P E M E Y G R M N I G S R P S K R K P S G G I E S L R A I P W I F A
6. Sevir.5G328100.1
TTGTTGAATATTTTCGCCTTGCAACACCAGAGATGGAATATGGAAGGATGAACATTGGAAGTAGACCATCAAAAAGAAAGCCAAGCGGAGGCATTGAATCGCTGCGTGCCATTCCTTGGATCTTTGCTT
Frame 1
F V E Y F R L A T P E M E Y G R M N I G S R P S K R K P S G G I E S L R A I P W I F A
7. Sevir.1G020600.1
TTGTTGAATACTTCAGATCGGCTACACCTGAGACTGAATATGGTAGGATGAATATTGGCAGCCGTCCATCAAAGAGGAAGCCTAGTGGGGGAATAGAATCGCTCCGTGCAATTCCATGGATCTTTGCTT
Frame 1
F V E Y F R S A T P E T E Y G R M N I G S R P S K R K P S G G I E S L R A I P W I F A
8. Sevir.5G145500.1
TCGTGGAGTACTTCCGCGCGGCGACGCCGGAGTCGGAGTACGGGCGGATGAACATCGGCAGCCGGCCGTCGAAGCGGAAGCCCGGCGGCGGCATCGAGTCCCTGCGTGCCATCCCGTGGATTTTCGCGT
Frame 1
F V E Y F R A A T P E S E Y G R M N I G S R P S K R K P G G G I E S L R A I P W I F A
9. Sevir.5G072900.1
TCATCACCTACTTCCAGGAGGCGACGCCGCAGGCGGAGCTCGGGTTCCTCAACATCGGCAGCCGGCCGGCGAAGCGGAAGCCGGCGGGGGGCATCTCGAGCCTGCGCGCCATCCCCTGGGTGTTCGCGT
Frame 1
F I T Y F Q E A T P Q A E L G F L N I G S R P A K R K P A G G I S S L R A I P W V F A


2,710 2,720 2,730 2,740 2,750 2,760 2,770 2,780 2,790 2,800 2,810 2,820 2,830
1. Codon modified PEPC
Frame 1
2. Sobic.010G160700.1
3. Sevir.4G143500.1
4. Sevir.2G179400.1
5. Sevir.5G328100.2
6. Sevir.5G328100.1
7. Sevir.1G020600.1
8. Sevir.5G145500.1
9. Sevir.5G072900.1
2,840 2,850 2,860 2,870 2,880 2,890 2,900 2,910 2,920 2,930 2,940 2,950 2,960
2,970 2,980 2,990 3,000 3,010 3,020 3,030 3,040 3,050 3,060 3,070 3,080 3,090

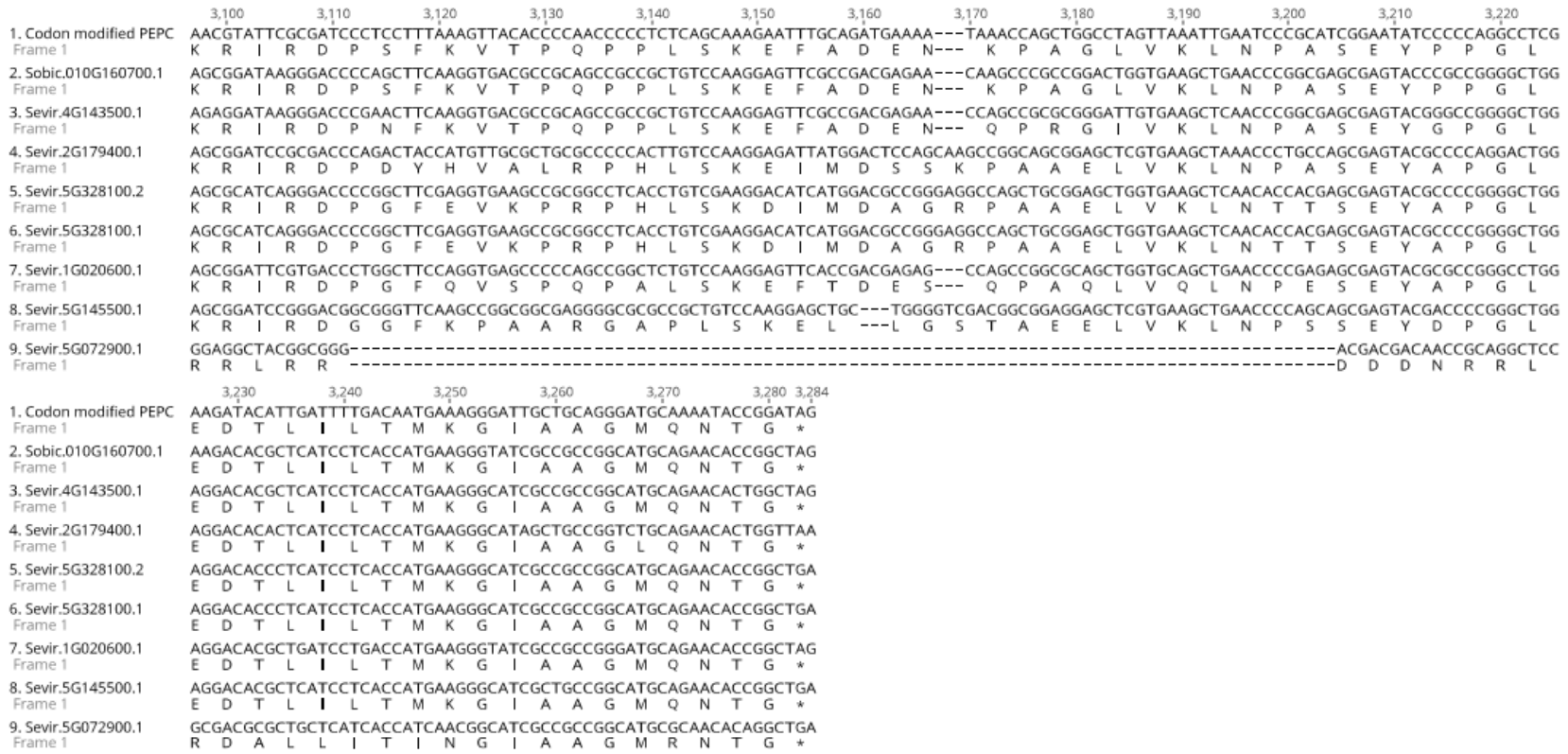
3,100 3,110 3,120 3,130 3,140 3,150 3,160 3,170 3,180 3,190 3,200 3,210 3,220
1. Codon modified PEPC
AACGTATTCGCGATCCCTCCTTTAAAGTTACACCCCAACCCCCTCTCAGCAAAGAATTTGCAGATGAAAA---TAAACCAGCTGGCCTAGTTAAATTGAATCCCGCATCGGAATATCCCCCAGGCCTCG
Frame 1
K R I R D P S F K V T P Q P P L S K E F A D E N--- K P A G L V K L N P A S E Y P P G L
2. Sobic.010G160700.1
AGCGGATAAGGGACCCCAGCTTCAAGGTGACGCCGCAGCCGCCGCTGTCCAAGGAGTTCGCCGACGAGAA---CAAGCCCGCCGGACTGGTGAAGCTGAACCCGGCGAGCGAGTACCCGCCGGGGCTGG
Frame 1
K R I R D P S F K V T P Q P P L S K E F A D E N--- K P A G L V K L N P A S E Y P P G L
3. Sevir.4G143500.1
AGAGGATAAGGGACCCGAACTTCAAGGTGACGCCGCAGCCGCCGCTGTCCAAGGAGTTCGCCGACGAGAA---CCAGCCGCGCGGGATTGTGAAGCTCAACCCGGCGAGCGAGTACGGGCCGGGGCTGG
Frame 1
K R I R D P N F K V T P Q P P L S K E F A D E N--- Q P R G I V K L N P A S E Y G P G L
4. Sevir.2G179400.1
AGCGGATCCGCGACCCAGACTACCATGTTGCGCTGCGCCCCCACTTGTCCAAGGAGATTATGGACTCCAGCAAGCCGGCAGCGGAGCTCGTGAAGCTAAACCCTGCCAGCGAGTACGCCCCAGGACTGG
Frame 1
K R I R D P D Y H V A L R P H L S K E I M D S S K P A A E L V K L N P A S E Y A P G L
5. Sevir.5G328100.2
AGCGCATCAGGGACCCCGGCTTCGAGGTGAAGCCGCGGCCTCACCTGTCGAAGGACATCATGGACGCCGGGAGGCCAGCTGCGGAGCTGGTGAAGCTCAACACCACGAGCGAGTACGCCCCGGGGCTGG
Frame 1
K R I R D P G F E V K P R P H L S K D I M D A G R P A A E L V K L N T T S E Y A P G L
6. Sevir.5G328100.1
AGCGCATCAGGGACCCCGGCTTCGAGGTGAAGCCGCGGCCTCACCTGTCGAAGGACATCATGGACGCCGGGAGGCCAGCTGCGGAGCTGGTGAAGCTCAACACCACGAGCGAGTACGCCCCGGGGCTGG
Frame 1
K R I R D P G F E V K P R P H L S K D I M D A G R P A A E L V K L N T T S E Y A P G L
7. Sevir.1G020600.1
AGCGGATTCGTGACCCTGGCTTCCAGGTGAGCCCCCAGCCGGCTCTGTCCAAGGAGTTCACCGACGAGAG---CCAGCCGGCGCAGCTGGTGCAGCTGAACCCCGAGAGCGAGTACGCGCCGGGCCTGG
Frame 1
K R I R D P G F Q V S P Q P A L S K E F T D E S--- Q P A Q L V Q L N P E S E Y A P G L
8. Sevir.5G145500.1
AGCGGATCCGGGACGGCGGGTTCAAGCCGGCGGCGAGGGGCGCGCCGCTGTCCAAGGAGCTGC---TGGGGTCGACGGCGGAGGAGCTCGTGAAGCTGAACCCCAGCAGCGAGTACGACCCCGGGCTGG
Frame 1
K R I R D G G F K P A A R G A P L S K E L ---L G S T A E E L V K L N P S S E Y D P G L
9. Sevir.5G072900.1
GGAGGCTACGGCGGG----------ACGACGACAACCGCAGGCTCC
Frame 1
R R L R R ----------D D D N R R L
3,230 3,240 3,250 3,260 3,270 3,280 3,284
1. Codon modified PEPC
AAGATACATTGATTTTGACAATGAAAGGGATTGCTGCAGGGATGCAAAATACCGGATAG
Frame 1
E D T L I L T M K G I A A G M Q N T G *
2. Sobic.010G160700.1
AAGACACGCTCATCCTCACCATGAAGGGTATCGCCGCCGGCATGCAGAACACCGGCTAG
Frame 1
E D T L I L T M K G I A A G M Q N T G *
3. Sevir.4G143500.1
AGGACACGCTCATCCTCACCATGAAGGGCATCGCCGCCGGCATGCAGAACACTGGCTAG
Frame 1
E D T L I L T M K G I A A G M Q N T G *
4. Sevir.2G179400.1
AGGACACACTCATCCTCACCATGAAGGGCATAGCTGCCGGTCTGCAGAACACTGGTTAA
Frame 1
E D T L I L T M K G I A A G L Q N T G *
5. Sevir.5G328100.2
AGGACACCCTCATCCTCACCATGAAGGGCATCGCCGCCGGCATGCAGAACACCGGCTGA
Frame 1
E D T L I L T M K G I A A G M Q N T G *
6. Sevir.5G328100.1
AGGACACCCTCATCCTCACCATGAAGGGCATCGCCGCCGGCATGCAGAACACCGGCTGA
Frame 1
E D T L I L T M K G I A A G M Q N T G *
7. Sevir.1G020600.1
AGGACACGCTGATCCTGACCATGAAGGGTATCGCCGCCGGGATGCAGAACACCGGCTAG
Frame 1
E D T L I L T M K G I A A G M Q N T G *
8. Sevir.5G145500.1
AGGACACGCTCATCCTCACCATGAAGGGCATCGCTGCCGGCATGCAGAACACCGGCTGA
Frame 1
E D T L I L T M K G I A A G M Q N T G *
9. Sevir.5G072900.1
GCGACGCGCTGCTCATCACCATCAACGGCATCGCCGCCGGCATGCGCAACACAGGCTGA
Frame 1
R D A L L I T I N G I A A G M R N T G *